

The fate of nitrogen during hydrothermal liquefaction of sewage sludge

zur Erlangung des akademischen Grades eines

DOKTORS DER INGENIEURWISSENSCHAFTEN (DR.-ING.)

von der KIT-Fakultät für Chemieingenieurwesen und Verfahrenstechnik des

Karlsruher Instituts für Technologie (KIT)

genehmigte

DISSERTATION

von

M.Sc. Yujie Fan
aus Nanyang, China

Tag der mündlichen Prüfung: 14.09.2020

Erstgutachter: Prof. Dr. Nicolaus Dahmen

Zweitgutachterin: Prof. Dr. Andrea Kruse, Universität Hohenheim

DECLARATION

The candidate declares that this thesis represents her own work which has been written independently by herself, without the use of other documents or sources beyond those stated in the references. The candidate confirms that appropriate citation has been given within the thesis where reference has been made to the work of others.

The following, jointly authored publications are part of this thesis:

1. **Y. Fan**; F.G. Fonseca; A. Hoffmann; M. Gong; U. Hornung; N. Dahmen. Energy valorization of integrating lipid extraction and hydrothermal liquefaction of lipid-extracted sewage sludge” (Journal of Cleaner Production.2020 **under review**)
2. **Fan, Y.**; Hornung, U.; Raffelt, K.; Dahmen, N., The influence of lipids on the fate of nitrogen during hydrothermal liquefaction of protein-containing biomass. *Journal of Analytical and Applied Pyrolysis* **2020**, *147*, 104798.
3. **Fan, Y.**; Hornung, U.; Dahmen, N.; Kruse, A., Hydrothermal liquefaction of protein-containing biomass: study of model compounds for Maillard reactions. *Biomass Conversion and Biorefinery* **2018**, *8*, (4), 909-923.
4. **Y. Fan**; U. Hornung; N. Dahmen; Kruse, A. *Formation of N-Containing Heterocycles from Hydrothermal Liquefaction of Model Compounds and Sewage Sludge*, 26th European Biomass Conference and Exhibition, 2018; 2018.
5. Wang, C.; **Fan, Y.**; Hornung, U.; Zhu, W.; Dahmen, N., Char and tar formation during hydrothermal treatment of sewage sludge in subcritical and supercritical water: Effect of organic matter composition and experiments with model compounds. *Journal of Cleaner Production* **2020**, *242*, 118586.

Details of contributions from the candidate and co-authors are listed below:

1. The candidate performed part of the experimental work, analysis and write up. F.G. Fonseca contributed data analysis and writing, A. Hoffmann performed most of the experiments. Dr. Gong contributed introduction writing, Dr. Hornung and Prof. Dahmen contributed critical revision, proof reading.
2. The candidate performed the experimental work, analysis and write up. Dr. Hornung, Dr. Klaus and Prof. Dahmen contributed with comments, guidance and proof reading.
3. The candidate performed the experimental work, analysis and write up. Prof. Kruse contributed discussion writing, guidance and proof reading. Dr. Hornung and Prof. Dahmen contributed critical revision, proof reading.
4. The candidate performed the majority of experimental work, analysis and write up. Prof. Kruse contributed discussion writing, guidance and proof reading. Dr. Hornung and Prof. Dahmen contributed critical revision, proof reading.

5. Dr. Wang performed the majority of experimental work, analysis and wrote up, the candidate performed the miority of experimental work and provided guidance, Dr. Hornung, Prof. Zhu and Prof. Dahmen contributed critical revision, proof reading.

ACKNOWLEDGMENTS

Time flies. It feels like yesterday was October 10, 2016, when after a sleepless night I had to say goodbye to the place I had lived in for four years. I would like to take this opportunity to express my deepest appreciation to everyone who has helped and supported me during this beautiful journey in Germany. It was their great support, encouragement, and motivation that made my work and life in Germany go much better than I had expected.

First, I would like to express my deepest appreciation to my supervisor, Prof. Nicolaus Dahmen, for allowing me to work in his research group. Owing to the numerous times he provided me with helpful advice and motivation, I now feel more confident than ever in my work.

Likewise, I would like to express my sincere gratitude to Prof. Andrea Kruse, for offering me this precious opportunity to take up Ph.D. studies in Germany. I am extremely grateful for her constructive guidance and patience over the past four years.

I would like to thank Dr. Ursel Hornung, for offering me the chance to work on this fascinating research topic, and for her tremendous support. Owing to her kindness and motivating encouragement, I have enjoyed precious experiences during my work in Germany.

Secondly, I would like to express my gratefulness to the staff who worked with me: Birgit Rolli, Alexandra Böhm, Sonja Habicht, Veronika Holderied, Armin Lautenbach, Thomas Tietz, Hermann Köhler, Matthias Pagel, and Christoph Seeger. Thank you for continuously supporting and helping me with invaluable analyses and your professional experience. Among these, special appreciation goes to Birgit, Alex, and Armin, for making me feel so comfortable and cared for in this working group.

Furthermore, I would like to thank my colleagues and friends in IKFT, for the supportive and joyful working atmosphere. I would like to specifically name Dr. Klaus Raffelt, Dr. Bingfeng Guo, Clarissa Baehr, Frederico Gomes Fonseca, Joscha Zimmermann, Jessica Heinrich, Dr. Chiara Boscagli, Dr. Sheng Wang, Dr. Karla Herrera Delgado, Jessica Maier, Teresa Franzen, Janine Bürchner, Caroline Schmitt, Ewelina Kaczowka, Roland Fritz, Dr. Marcus Breunig, David Steinbach, Dr. Julia Schuler, Dr. Axel Funke, Dr. Farah Obeid, Claudia Prestigiacomo, Nina Schmitt, Dr. Silke Behrens, Dr. Thomas Zevaco, Si Chen, Bing Wang, Eugen Aschenbrenner, and Maximilian Wörner.

In addition, I would like to sincerely thank my laboratory partners Alexander Hoffmann, Leif Meyer, and Carsten Unglaub, who either worked with me on student theses or contributed in their role of research assistants. Besides, I would like to thank the colleagues from the University of Hohenheim: Lin Du, Zebin Cao, Muhammad Jamal Alhndi, Gero Becher, and Dominik Wüst for several productive discussions and much appreciated support with analytics.

Special thanks to my great friends Jingwei, Yang, Hongyan Wang, Xinshuang Ge, Xiaojing Liu, Pengchao Sun, Ruijie Tan, and Ningyi, Li. They contributed to making my life in Germany full of joy and happiness. Special gratitude goes to Yang Jing and Xin Wang, who always stand behind and support me.

Last but not least, I would like to pay special thanks to the China Scholarship Council for all the support provided during my stay in Germany. I would like to express my gratitude to my lovely family. Thank you very much for your everlasting support and your confidence in every choice I have made in my whole life.

.
.

LIST OF PUBLICATIONS

Peer-reviewed original research papers

Y. Fan; F.G. Fonseca; A. Hoffmann; M. Gong; U. Hornung; N. Dahmen. Energy valorization of integrating lipid extraction and hydrothermal liquefaction of lipid-extracted sewage sludge” (Journal of Cleaner Production **2020**, **under review**)

Fan, Y.; Hornung, U.; Raffelt, K.; Dahmen, N., The influence of lipids on the fate of nitrogen during hydrothermal liquefaction of protein-containing biomass. *Journal of Analytical and Applied Pyrolysis* **2020**, *147*, 104798.

Fan, Y.; Hornung, U.; Dahmen, N.; Kruse, A., Hydrothermal liquefaction of protein-containing biomass: study of model compounds for Maillard reactions. *Biomass Conversion and Biorefinery* **2018**, *8*, (4), 909-923.

Y. Fan; U. Hornung; N. Dahmen; Kruse, A. Formation of N-Containing Heterocycles from Hydrothermal Liquefaction of Model Compounds and Sewage Sludge, 26th European Biomass Conference and Exhibition **2018**.

Wang, C.; **Fan, Y.**; Hornung, U.; Zhu, W.; Dahmen, N., Char and tar formation during hydrothermal treatment of sewage sludge in subcritical and supercritical water: Effect of organic matter composition and experiments with model compounds. *Journal of Cleaner Production* **2020**, *242*, 118586.

Conference oral /poster presentation

Y. Fan; U. Hornung; N. Dahmen; Kruse, A. The influence of lipids on the fate of nitrogen during hydrothermal liquefaction of protein-containing biomass. Oral presentation at ECI-Pyroliq 2019: Pyrolysis and Liquefaction of Biomass and Wastes in Ireland, 2019.

Y. Fan; U. Hornung; N. Dahmen; Kruse, A. Formation of N-Containing Heterocycles from Hydrothermal Liquefaction of Model Compounds and Sewage Sludge. Poster presentation at 26th European Biomass Conference and Exhibition in Denmark, 2018.

List of publications

Y. Fan; U. Hornung; N. Dahmen; Kruse, A. The fate of nitrogen during catalytic hydrothermal liquefaction of sewage sludge. Poster presentation at DBFZ: Fachforum Hydrothermale Prozesse in Germany, 2018.

Y. Fan; U. Hornung; N. Dahmen; Kruse, A. Hydrothermal liquefaction of biomass to bio-oil: study of model compounds for the influence of Maillard reaction during the process. Poster presentation at 2nd Bioeconomy Congress in Germany, 2017.

ABSTRACT

Worldwide economic and social development has led to an increasing production of sewage sludge (SS). Concerns about environmental and ecological issues, as well as a gradually broadening sense of sustainable development, raise awareness of and investments into waste reduction aspects. Previous reports show that landfilling, composting, and combustion do not only waste material but also create environmental problems. This creates a need to substitute traditional ways of disposal, for which a multitude of technologies have been proposed. Besides, initiatives for the reduction of CO₂ emissions are driving society to find alternative sources to supply an ever-increasing demand for fuel products, providing an opportunity to view sewage sludge as a source of carbon and energy rather than labelled waste.

In recent decades, hydrothermal liquefaction (HTL) has been suggested as a cost-effective and eco-friendly solution for the valorization of SS in the fields of waste management and renewable energy production. Without the need for pre-drying, which can be observed in competing technologies such as pyrolysis and incineration, HTL allows for the production of liquid biocrude at elevated temperatures and heating rates, with relatively short reaction times. However, SS is a protein-rich feedstock, leading to an inevitable presence of N-containing compounds in the formed biocrude, thus preventing fuel standards from being met and preventing the integration into refineries for further processing. Developing economic potential for SS-derived biocrude requires an in-depth investigation of the fate of nitrogen during liquefaction, and a special focus on the formation of N-containing compounds.

A detailed characterization of the distribution of N across the products from HTL of SS is investigated in the context of this doctoral thesis. The products are subjected to coupled analyses, including elemental content, GC-MS, TGA, FTIR and NMR addressing different properties. The results of this characterization are used for mass balance calculations and reaction chemistry throughout the thesis.

HTL of SS for biocrude production is investigated in both batch units and a continuous flow plant. Processing at elevated temperatures (< 300 °C) results in a lower yield of biocrude with higher N content, with a substantial contribution from the interaction between carbohydrates and proteins in the feedstock. Higher temperatures favour the

decarboxylation of lipids to produce better biocrude quality with less heteroatoms. The received digested sludge (dry matter of 21.25 wt.%) could be easily processed as feedstock for biocrude in a batch system. More than 50 wt.% of the feedstock N content is recovered in the aqueous phase, and a higher fraction of N is distributed into the biocrude rather than into the solid residue with increasing temperature. In batch operation, maximal biocrude yields of 22.05 wt.% with a heating value of 37.1 MJ/kg are achieved at 350 °C with a residence time of 20 min, but also contain relatively high amounts of nitrogen at 6.0 wt.%.

The feasible implementation of continuous flow processing has shown significant dependency on the properties of the feedstock due to issues with its pumpability. In a house-built continuous flow plant (2 kg/h), a mixed sludge comprised of primary and secondary sludge (10 wt.% (db.)) mixed with KOH (10 wt.% (db.)) was used successfully. The mass recovery reached 80 %, with a biocrude yield of 30.84 wt.% (N content 3.90 wt.%), at 350 °C with a retention time of 8 min. Comparable results were also achieved using batch units under the same conditions: a slightly higher biocrude yield (33.1 wt.%) with an N content (4.25 wt.%). N-containing compounds identified in the biocrude mostly consisted of N-heterocycles, including pyrazines, pyrroles and indoles, cyclic amines, and fatty acid amides.

Model compounds of protein, carbohydrates, and lipids are processed under hydrothermal conditions on their own as well as in mixtures, taking a closer look on the characteristics of the produced biocrude. The focus is again on the fate of N and the reaction pathways involved in biocrude formation. Furthermore, the effect of lipids in the reaction mixture is investigated. Here, the organic solvent (dichloromethane) extracts unconverted lipids into the biocrude phase, apparently increasing the yield. Only higher temperatures seem to increase the conversion of lipids into biocrude through the formation of alkanes and alkenes by decarboxylation, which is a favourable reaction to improve the quality. Amidation reactions between lipids and proteins during HTL also increase the yields but introduce undesirable N in the form of amides. Carbohydrates (lactose) mainly undergo carbonization to produce hydro-char with a yield of up to 65.1 wt.%, while the yield of biocrude at 350 °C is merely 7.3 wt.%. HTL of an isolated amino acid (lysine) led to a higher biocrude yield, with the formation of amines and amides by cyclization and dimerization. Maillard reactions (MRs) occurring between proteins and carbohydrates affect the mechanistic reaction in biocrude formation. On the one hand, MRs improve the

biocrude yield by inhibiting carbonization and transferring more carbon into the oil phase. On the other hand, they compete with amidation reactions, producing N-containing heterocycles instead of fatty acid amides; the former are regarded as more problematic N-species in terms of cost in upgrading the biocrude.

The systematic investigation of the influence of MRs under different HTL conditions is explored in greater detail, with a focus on the formation of typical N-containing compounds. Results revealed that typical Maillard reaction products are formed at 150 °C during the heat-up period of HTL; then reached a maximum at 250 °C in less than 10 min. The polymerization of these products most likely occurs at higher temperatures and longer reaction times, resulting in the formation of macromolecular chemicals.

Based on the synergistic effects of the interactions mentioned above, an innovative integration of lipid extraction of sewage sludge and HTL of the extracted sewage sludge (LESS) is explored in order to maximize energy valorization. Values of 98 % energy recovery and 35 wt.% (daf.) of liquid fuel-like products can be achieved by integrating lipid extraction and HTL of the lipid-extracted residual. The energy demand of the combined process is highly dependent on the drying step required for conventional lipid extraction. However, recent advances in the field may allow for the attainment of high energetic efficiencies.

Overall, the results presented throughout this work agree with published literature, in the sense that HTL is a promising and energetically efficient processing technique to valorise sewage sludge to produce value-added biofuels. As the individual biochemical components of this feedstock significantly affect the product distribution due to chemical interactions, especially with regard to nitrogen distribution, downstream processing is inevitable, either through upgrading and refining or via extraction for the production of renewable platform chemicals.

ZUSAMMENFASSUNG

Die weltweite wirtschaftliche und soziale Entwicklung hat zu einer Ausweitung der Produktion von Klärschlamm (SS) geführt. Achtsamkeit in Bezug auf ökologische und umweltspezifische Fragen sowie ein sukzessive voranschreitendes Engagement für nachhaltige Entwicklung fördern die Aufmerksamkeit sowie Investitionen bezüglich einer weitgehenden Emissions- und Abfallreduzierung. Frühere Berichte zeigen, dass Deponierung, Kompostierung und Verbrennung nicht nur Material verschwenden, sondern auch Umweltprobleme verursachen. Es besteht daher die Notwendigkeit, traditionelle Entsorgungsmethoden zu ersetzen, für die bisher eine Vielzahl von Technologien vorgeschlagen wurden. Darüber hinaus versuchen die Initiativen zur Reduzierung der CO₂-Emissionen in der Gesellschaft alternative Quellen zu finden, die die weiterhin steigende Nachfrage am Kraftstoffprodukten befriedigen und die Möglichkeit bieten, Klärschlamm nicht als gekennzeichneten Abfall, sondern als Kohlenstoff- und Energiequelle zu betrachten.

In den letzten Jahrzehnten wurde die hydrothermale Verflüssigung (HTL) als kostengünstige und umweltfreundliche Lösung für die Verwertung von SS in den Bereichen Abfallwirtschaft und Erzeugung erneuerbarer Energien vorgeschlagen. Ohne die Notwendigkeit einer Vortrocknung, die bei konkurrierenden Technologien wie Pyrolyse und Verbrennung beobachtet werden kann, ermöglicht HTL die Herstellung von flüssigem Bio-Rohöl bei geringen Temperaturen und Heizraten bei kürzerer Reaktionszeit. SS ist jedoch ein proteinreiches Ausgangsmaterial, das unvermeidlich zu N-haltigen Verbindungen im produzierten Bio-Rohöl führt und somit die Einhaltung der Kraftstoffstandards bzw. die Integration in Raffinerien zur weiteren Verarbeitung behindert. Die Entwicklung des wirtschaftlichen Potenzials für aus SS gewonnenes Bio-Rohöl erfordert eine genauere Untersuchung der Stickstoffsinken während der Verflüssigung, im speziellen auf die Bildung von N-haltigen Verbindungen.

Im Rahmen dieser Doktorarbeit wurde eine detaillierte Charakterisierung der Verteilung von N über die Produkte von HTL von SS untersucht. Die Produkte wurden gekoppelten Analysen unterzogen, die sich mit Eigenschaften wie Elementar-, GC-MS-, TGA-, FTIR- und NMR-Eigenschaften befassten. Die Ergebnisse dieser Charakterisierung werden in der gesamten Arbeit für die Berechnung von Massenbilanzen und die Betrachtung

chemischer Reaktionen verwendet.

Die HTL von SS für die Bio-Rohölproduktion wurde sowohl in Batch-Reaktoren als auch in einer kontinuierlichen Pilotanlage untersucht. Das Verfahren bei warmen Bedingungen (< 300 °C) führt zu einer geringeren Ausbeute an Bio-Rohöl mit höherem N-Gehalt, wobei Kohlenhydrate und Proteine im Ausgangsmaterial eine wesentliche Rolle spielen. Höhere Temperaturen begünstigen die Produktion von Bio-Rohöl von besserer Qualität mit einer geringeren Anzahl an Heteroatomen, was hauptsächlich auf den Lipidgehalt zurückzuführen ist. Der verwendete Faulschlamm (Trockenmasse von 21,25 Gew.-%) ließ sich ohne Probleme als Ausgangsmaterial für Bio-Rohöl im Batch-Reaktor verarbeiten. Mehr als 50 Gew.-% des N-Gehalts im Ausgangsmaterial werden in der wässrigen Phase zurückgewonnen. Mit zunehmender Temperatur findet sich im Bio-Rohöl ein höherer N-Anteil als im festen Rückstand wieder. Im Batch-Betrieb wurden maximale Bio-Rohölausbeuten von 22,05 Gew.-% mit einem Heizwert von 37,1 MJ/kg bei 350 °C und einer Reaktionszeit von 20 min erreicht, wobei diese aber auch signifikante Mengen an Stickstoff von 6,0 Gew.-% enthalten.

Die realisierbare Implementierung einer kontinuierlichen Flussverarbeitung hat aufgrund von Problemen mit der Pumpbarkeit eine signifikante Abhängigkeit von den Eigenschaften des Ausgangsmaterials gezeigt. In einer hausgemachten Pilotanlage (2 kg/h) war ein Mischschlamm aus Primär- und Sekundärschlamm (10 Gew.% (db.)), gemischt mit KOH (10 Gew.% (db.)) erfolgreich. Die Massenerückgewinnung erreichte 80 % bei einer Bio-Rohölausbeute von 30,84 Gew.% (N-Gehalt 3,90 Gew.%) bei 350 °C mit einer Retentionszeit von 8 min. Vergleichbare Ergebnisse wurden auch unter Verwendung von Chargeneinheiten unter den gleichen Bedingungen erzielt: Eine geringfügig höhere Bio-Rohölausbeute (33,1 Gew.%) mit einem N-Gehalt von 4,25 Gew.%. N-haltige Verbindungen, die im Bio-Rohöl identifiziert wurden, bestehen hauptsächlich aus N-Heterocyclen, einschließlich Pyrazinen, Pyrrolen und Indolen, cyclischen Aminen und Fettsäureamiden.

Modellverbindungen, bestehend aus Protein, Kohlenhydraten und Fettsäure, wurden einzeln und in Gemischen unter hydrothermalen Bedingungen verarbeitet, um die Eigenschaften des hergestellten Bio-Rohöls zu beleuchten. Der Schwerpunkt lag wieder auf dem Verbleib von N und den Reaktionswegen für die Bildung von Bio-Rohöl. Die Wirkung von Fettsäuren in der Reaktionsmischung wurde untersucht, wobei das organische Lösungsmittel (Dichlormethan) nicht umgewandelte Fettsäuren ins Bio-Rohöl

extrahiert und somit die Ausbeute nur scheinbar erhöht. Höhere Temperaturen scheinen die Umwandlung von Fettsäuren in Bio-Rohöl durch die Bildung von Alkanen und Alkenen durch Decarboxylierung zu erhöhen, was eine präferierte Reaktion zur Verbesserung der Qualität darstellt. Die Amidierung zwischen Fettsäuren und Proteinen während der HTL erhöht ebenfalls die Bio-Rohölausbeuten, führt jedoch zu unerwünschtem N in Form von Amiden. Kohlenhydrate (Lactose) werden hauptsächlich karbonisiert, um Hydrokohle mit einer Ausbeute von bis zu 65,1 Gew.% zu erzeugen, während die Ausbeute an Bio-Rohöl bei 350 °C nur 7,3 Gew.% beträgt. HTL unter Verwendung einer isolierten Aminosäure (Lysin) führte zu einer höheren Bio-Rohölausbeute unter Bildung von Aminen und Amiden durch Cyclisierung und Dimerisierung. Maillard-Reaktionen (MRs) zwischen Proteinen und Kohlenhydraten beeinflussen die Reaktionswege bei der Bildung von Bio-Rohöl. Einerseits verbessern MRs die Bio-Rohöl-Ausbeute, indem sie die Karbonisierung hemmen und somit mehr Kohlenstoff in die Ölphase überführen. Andererseits konkurrieren sie mit Amidierungsreaktionen und produzieren N-haltige Heterocyclen anstelle von Fettsäureamiden; erstere werden als problematische N-Spezies in Bezug auf die Kosten bei der Aufbereitung des Bio-Rohöls angesehen.

Die systematische Untersuchung des Einflusses von MRs unter verschiedenen HTL-Bedingungen wurde eingehender untersucht, wobei der Schwerpunkt auf der Bildung typischer N-haltiger Verbindungen lag. Die Ergebnisse zeigten, dass Maillard-Reaktionsprodukte während der Aufheizperiode von HTL bei 150 °C gebildet wurden; sie erreichen 250 °C dann in weniger als 10 min. Die Polymerisation dieser Produkte erfolgt höchstwahrscheinlich bei höheren Temperaturen und längeren Reaktionszeiten, was zur Bildung makromolekularer Chemikalien führt.

Basierend auf den synergistischen Effekten der oben genannten Wechselwirkungen wird eine neuartige Integration der Fettextraktion von Klärschlamm und der HTL des extrahierten Klärschlammes (LESS) untersucht, um die Energieverwertung zu maximieren. Energierückgewinnungswerte von 98 % und 35 Gew.-% (daf.) Flüssigbrennstoff-ähnlicher Produkte können durch Integration der Lipidextraktion und der HTL des lipidextrahierten Rests erreicht werden. Der Energiebedarf des kombinierten Verfahrens hängt jedoch stark vom bisher erforderlichen Trocknungsschritt der herkömmlichen Lipidextraktion ab. Jüngste Fortschritte auf diesem Gebiet könnten jedoch hohe energetische Wirkungsgrade ermöglichen.

Insgesamt stimmen die in dieser Arbeit vorgestellten Ergebnisse mit der veröffentlichten Literatur in dem Sinne überein, dass HTL ein vielversprechender und energieeffizienter Prozess zur Verwertung von Klärschlamm ist, um neuartige Biokraftstoffe herzustellen. Einzelne biochemische Komponenten des Ausgangsmaterials beeinflussen die Produktverteilung aufgrund chemischer Wechselwirkungen erheblich, insbesondere im Hinblick auf die Stickstoffverteilung. Daher ist ein nachgeschalteter Aufwertungsprozess unverzichtbar, entweder durch Aufbereitung und Raffination oder durch Extraktion zur Herstellung von Chemikalien für erneuerbare Plattformen.

LIST OF ABBREVIATIONS

A	Ash
db.	Dry basis
AQ	Aqueous phase
BC	Biocrude
C	Carbon
daf.	Dry ash free basis
DCM	Dichloromethane
DKP	Octahydrodipyrido[1,2-a:1',2'-d]pyrazine-6,12(2H,6aH)-dione
DTG	Derivative thermogravimetry
ECR	Energy consumption ratio
ED	Energy demand
ER	Energy recovery
FAMEs	Fatty acid methyl ester
FFAs	Free fatty acids
FID	Flame ionization detector
FTIR	Fourier-transform infrared spectroscopy
GC	Gas Chromatography
GC-MS	Gas chromatography-mass spectrometry
H	Hydrogen
HCW	Hot Compressed Water
HHVs	Higher heating values
HMF	Hydroxymethylfurfural
HPLC	High-performance liquid chromatography
HTC	Hydrothermal carbonization
HTL	Hydrothermal liquefaction
ICP-OES	Inductively coupled plasma optical emission spectroscopy
IKFT	Institute for catalytic research and technology
KIT	Karlsruher Institut für Technologie
Lac	Lactose

List of abbreviations

LESS	Lipids extracted sewage sludge
Lys	Lysine
N	Nitrogen
NH ₄ ⁺	Ammonium
NMR	Nuclear magnetic resonance
O	Oxygen
OM	Organic Mass
P	Phosphor
RT	Retention Time
S	Sulphur
SCWG	Supercritical water gasification
SR	Solid residue
SS	Sewage Sludge
TAN	Total Acid Number
TC	Total carbon
TCR	Thermocatalytic Reforming
TGA	Thermogravimetric analysis
THF	Tetrahydrofuran
TIC	Total inorganic carbon
TNb	Total nitrogen bound
TOC	Total organic carbon
Vol%.	Volume Percentage
WC	Wood Chips
WP	Wood Pellets
Wt.%	Weight Percentage
WWTP	Waste Water Treatment Plant
XPS	X-ray photoelectron spectroscopy

LIST OF FIGURES

Figure 1-1 Flow chart of wastewater treatment and sludge generation, adapted from [1, 6]	1
Figure 1-2 Potential sewage sludge to resource and energy recovery routes	10
Figure 3-1 Micro-autoclaves used for batch HTL process	43
Figure 3-2 Heating devices for batch HTL (a) GC-oven; (b) fluidized sand bath.....	44
Figure 3-3 Gas collection system.....	44
Figure 3-4 Procedures for product separation and extraction from batch HTL process.	45
Figure 3-5 (a) Schematic flow of the continuous Process (b) continuous reactor.....	46
Figure 4-1 (a) mass balance and (b) carbon (C) balance of products from HTL of SS at different conditions	54
Figure 4-2 Gas yields from HTL SS at different temperatures.....	55
Figure 4-3 Evolution of N 1s XPS spectra for original sewage sludge and solid residue derived from HTL at different conditions.....	60
Figure 4-4 The concentration of total Nitrogen, ammonium, nitrite and nitrate in the aqueous phase from HTL at different temperatures.....	62
Figure 4-5 N distribution of HTL products from SS at different temperatures	63
Figure 5-1 The flow chart of procedures for product separation and extraction from continuous and batch HTL process.....	68
Figure 5-2 Controlled evaporation system to collect evaporated solvents with volatiles	69
Figure 5-3 GC-MS total ion chromatograms of volatiles in the collect solvent from continuous flow HTL of sewage sludge at a concentration of 10 wt.%	74
Figure 5-4 Comparison the yields of products from batch and continuous flow HTL experiments with a loading of 10 wt.% at 350 °C for 8 min, (a) on dry basis;(b) on dry ash free basis.....	75
Figure 5-5 The comparison of GC-MS total ion chromatograms of biocrude from batch and continuous flow HTL of sewage sludge at 350 °C with 8 min	77
Figure 5-6 The comparison of component fractions in biocrude obtained from batch and continuous flow HTL of sewage sludge at a concentration of 10 wt.% under 350 at 350 °C with 8 min	78

List of figures

Figure 6-1 (a) products yields; (b) PA concentration in the bio-crude; (c) PA conversion efficiency; (d) TOC concentration in the aqueous phase from HTL of PA at different temperatures	85
Figure 6-2 Biocrude yields from HTL of model compounds at three different temperatures (biocrude from lysine mixed with PA at 250 °C were not collected).....	87
Figure 6-3 Mixed samples from HTL of palmitic acid and lysine at 250 °C.....	88
Figure 6-4 Comparison of N content (represented by data points) and N distribution (represented by bars) in the biocrude obtained from (a) lysine; (b) lysine mixed with lactose; (c) lysine mixed with palmitic acid; (d) ternary mixture at different temperatures	89
Figure 6-5 Yields of palmitic acid in the biocrude obtained from HTL of model compounds at different temperatures (biocrude from lysine mixed with PA at 250 °C were not collected).....	90
Figure 6-6 Comparison of compounds identified by GC-MS analysis of biocrude from HTL of model compounds at 300 °C (20 min) based on fraction distribution	93
Figure 6-7 Key N-containing compounds in the biocrude obtained from HTL of model compounds (a) single lysine; (b) lysine and lactose mixtures; (c) lysine and palmitic acid; (d) ternary mixture	95
Figure 6-8 Reaction network for the N-containing compounds obtained from HTL of model substances (the up and down arrows represent the increase and decrease in efficiency, respectively).....	97
Figure 6-9 (a) N distribution to different product phases; (b) NH ₄ ⁺ -N distribution to aqueous phase.....	97
Figure 7-1 Biocrude and solid residue yields from HTL of binary mixture at 300 °C for 20 min for different initial mass ratio of lysine to mixture	101
Figure 7-2 C distribution in different phases from HTL of binary mixture at 300 °C and 20 min for different initial mass ratio of lysine to mixture	102
Figure 7-3 (a) N content in the biocrude and (b) N distribution in different phases from HTL of binary mixture at 300 °C and 20 min for different initial mass ratio of lysine to mixture	104
Figure 7-4 Total N concentration and ammonium in the aqueous phase from HTL of binary mixture at 300 °C and 20 min for different initial mass ratio of lysine to mixture	105

Figure 7-5 Chromatograms obtained from GCMS analysis of biocrude from HTL of model compounds under 300 °C with 20 min	106
Figure 7-6 Comparison of compounds identified by GC-MS analysis of bio-oil from HTL of model compounds at 300 °C (20 min) based on fraction distribution relative peak area	107
Figure 7-7 FT-IR spectra of bio-crudes from HTL of model compounds at 300 °C with 20 min	109
Figure 7-8 ¹ H NMR spectra of bio-oils from HTL of model compounds at 300 °C with 20 min	110
Figure 7-9 Key N-containing compounds in the biocrude from HTL of binary mixture at 300 °C and 20 min for different initial mass ratio of lysine to mixture.....	110
Figure 7-10 Biocrude yields obtained from HTL of the individual model compounds and their binary mixtures at different temperature	112
Figure 7-11 Effects of heating rate on the yields of biocrude (a) and solid residue (b) obtained from HTL of model compounds at 250 °C and 300 °C for 20 min	113
Figure 7-12 Effects of heating rate on the N content in the biocrude obtained from HTL of model compounds at 250 °C and 300 °C for 20 min.....	114
Figure 7-13 The temporal variation of biocrude and solid residue yields from HTL of model substances at 250 and 300 °C (a) lactose; (b) lysine; (c) binary mixture	115
Figure 7-13 The temporal variation of biocrude and solid residue yields from HTL of model substances at 250 and 300 °C: (a) lactose, (b) lysine, (c) binary mixture	115
Figure 7-14 The temporal variation of sugars and lysine in the aqueous phase after HTL of model substances at 250 and 300 °C (a) lactose; (b) lysine	117
Figure 7-15 The temporal variation of total organic carbon and inorganic carbon in the aqueous phase after HTL of model substances at 250 and 300 °C (a) lactose; (b) lysine; (c) binary mixture	118
Figure 7-16 The temporal variation of HMF in the aqueous phase after HTL of model substances at 250 and 300 °C (a) lactose	119
Figure 7-17 The temporal variation of N content in the biocrude after HTL of model substances at 250 and 300 °C (a) lysine; (b) binary mixture	120
Figure 7-18 The temporal variation of key components in the biocrude after HTL of model substances at 250 and 300 °C (a) lactose; (b) lysine; (c) binary mixture; (d) binary mixture	121

Figure 7-19 Biocrude yields (a) and key compounds in the biocrude (b) from HTL of binary mixture during heating period.....	123
Figure 7-20 Possible reaction pathways during the HTL of lactose	124
Figure 7-21 Proposed mechanisms of reaction pathways during HTL of model mixtures	126
Figure 8-1 FAMES analysis of biodiesel obtained from the in-situ transesterification of SS	134
Figure 8-2 Comparison between HTL of SS and LESS at different temperatures, the yield of the aqueous phase was determined as the difference between unity and the sum of the yields of bio-crude, solid residue, and bio-gas fractions.....	136
Figure 8-3 Total organic carbon concentration (a) and ammonium concentration (b) in the aqueous phase from HTL of SS and LESS	137
Figure 8-4 Chemical groups represented in biocrude obtained from HTL of SS and LESS under different temperatures	139
Figure 8-5 Block flow diagram of combined lipid extraction, HTL and methanolysis for FAME production.....	140
Figure A-1 Raw sewage sludge (a) and pre-treated sewage sludge (b)	168
Figure A-2 The yields of biocrude obtained from catalytic HTL of raw sludge and treated sludge at 300 °C	168
Figure A-3 Overview XPS spectra, the Auger peaks and the most intense peaks of the silver tape (zoom in region with low binding energies).....	169
Figure A-4 Evolution of O 1s (a) and C 2s (b) XPS spectra for raw sludge and solid residue derived from HTL at 300 °C	169
Figure A-5 Surface elemental composition (%) evaluated by XPS for raw sludge sample and solid residue from HTL of sewage sludge at different temperatures.....	170
Figure A-6 N 1s XPS spectra for solid residue derived from HTL of model system ...	171
Figure A-7 TGA (a) and DTG (b) curve of analysis of products from HTL of lysine and lactose mixture at 300 °C	171
Figure A-8 TGA and DTG curves of biocrude from HTL of (a) SS and (b) LESS at different temperatures.....	174

LIST OF TABLES

Table 1-1 General overview for hydrothermal liquefaction of sewage sludge (Part 1/2)	18
Table 1-2 Comparison of the selected properties of HTL-derived biocrude and upgrading crude from sewage sludge	24
Table 1-3 The main drawbacks of biocrude with their effects and possible solutions	25
Table 4-1 Characterization of sewage sludge sample used in this study	52
Table 4-2 Elemental composition and high heating values in the obtained bio-crude	56
Table 4-3 Identified main components of biocrude obtained from HTL of SS at 300 °C and relative percentage in the total ion chromatogram (RT: retention time)	57
Table 4-4 Elemental composition and high heating values in the solid residue	59
Table 4-5 The deconvolution results (% normalized peak intensities) of XPS for the solid residue from HTL of SS under three temperatures	60
Table 5-1 Characterization of sewage sludge sample used in this study	69
Table 5-2 Mass balance and the yields (wt.%) of products from continuous process at 350 °C with 8 min	70
Table 5-3 Carbon and nitrogen distribution (CD/ND, wt.%) of products from continuous process at 350 °C with 8 min	71
Table 5-4 Identified main components with relative area percentage in the total ion chromatogram of biocrude obtained from continuous flow HTL of SS at 350 °C with 8 min (RT: retention time)	72
Table 5-5 Identified main components with relative area percentage in the total ion chromatogram of volatiles in the collect solvent collected solvent obtained from continuous flow HTL of SS at 350 °C with 8 min (RT: retention time)	74
Table 5-6 The comparison of elemental content and heating values in the biocrude obtained from batch and continuous HTL of sludge at 350 °C with 8 min	76
Table 5-7 The different components identified by GC-MS of the biocrude from continuous flow HTL of SS at 350 °C with 8 min (RT: retention time)	78
Table 5-8 The comparison of nutrients recovery (wt.%) in the aqueous phase from batch and continuous HTL of sludge at 350 °C with 8 min	79
Table 5-9 characterization of solid residue from batch and continuous HTL of sludge at	

List of tables

350 °C with 8 min	80
Table 5-10 The comparison of Elemental distributions (wt.%) across various products from batch and continuous HTL of sludge at 350 °C with 8 min	80
Table 6-1 Elemental content in the biocrude and solid residue from HTL of palmitic acid at three temperatures	86
Table 6-2 Identified main components with relative area in the total ion chromatogram of biocrude obtained from HTL of model substances at 300 °C for 20 min	91
Table 7-1 HMF concentration in the aqueous phase from HTL of model compounds at 200 °C with 20 min	103
Table 7-2 Identified main components of biocrude and relative percentage in the total ion chromatogram. (HTL of lactose at 300 °C for 20 min).....	107
Table 8-1 Characterization of sewage sludge and lipid-extracted sludge	133
Table 8-2 Summary of lipid extraction from published sources	133
Table 8-3 Elemental distribution (wt.%) of various products at various conditions.....	136
Table 8-4 Elemental composition (atomic ratio), higher heating value (MJ/kg) of biocrude and solid residue.....	138
Table 8-5 Boiling point distribution of biocrude from HTL of SS and LESS	140
Table 8-6 Comparing the Mass yields of lipid extraction and HTL and their combination. Values in brackets correspond to the HHV of the product in (MJ/kg).....	141
Table 8-7 Energy requirements (MJ/kg) for different steps of the integrated process (without considering heat recovery).....	141
Table 8-8 Estimation of the Energy Recovery (ER) and Energy Consumption Ratio (ECR), as well as the Energy Demand (ED) of HTL and combined processes. Value assuming a FAME yield of 8.5 wt.% of the dry sludge.	144
Table A-0-1 Identified main components of biocrude and relative percentage in the total ion chromatogram	172
Table A-0-2 Ash compositions (wt.%) of solid residue from HTL of SS and LESS at different temperatures.....	174

TABLE OF CONTENTS

DECLARATION	I
ACKNOWLEDGMENTS	I
LIST OF PUBLICATIONS	I
ABSTRACT.....	III
ZUSAMMENFASSUNG.....	VII
LIST OF ABBREVIATIONS	XI
LIST OF FIGURES	XIII
LIST OF TABLES	XVII
1 Chapter 1 Introduction	1
1.1 State of the art: Sewage sludge production	1
1.2 State of the art: Sewage sludge treatment	2
1.2.1 Valorization waste sludge to a resource	2
1.2.2 Valorization waste sludge to energy recovery	4
1.3 State of the art: HTL of sewage sludge	10
1.3.1 Fundamentals of hydrothermal liquefaction	10
1.3.2 Process parameters.....	12
1.3.3 Pre-treatment.....	20
1.3.4 Co-liquefaction	21
1.3.5 Post-treatment	22
1.3.6 Continuous HTL process	29
1.4 State of the art: the fate of nitrogen during HTL of sewage sludge	31
1.4.1 Nitrogen issues in HTL of sewage sludge	32
1.4.2 Nitrogen containing model substances	33
1.5 Conclusion and further research.....	34
2 Chapter 2 The aim and outline of this thesis.....	37
3 Chapter 3 Methodology	41
3.1 Characterization of sewage sludge.....	41

Table of contents

3.1.1	Proximate and ultimate analysis.....	41
3.1.2	Organic components.....	41
3.2	Chemicals	42
3.3	Hydrothermal liquefaction process.....	43
3.3.1	Batch process.....	43
3.3.2	Continuous process	45
3.4	Products analysis	47
3.4.1	Gas analysis.....	47
3.4.2	Biocrude analysis	47
3.4.3	Aqueous phase analysis.....	48
3.4.4	Solid residue analysis	49
3.5	Data interpretation	49
4	Chapter 4 HTL of sewage sludge via batch process	51
4.1	Introduction	51
4.2	Methodology.....	51
4.2.1	Materials.....	51
4.2.2	Pretreatment of sludge.....	51
4.2.3	HTL procedure	52
4.3	HTL of sewage sludge	52
4.3.1	Feedstock characterization	52
4.3.2	The influence of pre-treatment.....	52
4.3.3	Product yields.....	53
4.3.4	Characterization of Bio-crude	56
4.3.5	Characterization of solid residue.....	58
4.3.6	Characterization of aqueous phase	61
4.3.7	Nitrogen distribution	62
4.4	Conclusion.....	63
5	Chapter 5 HTL of sewage sludge via continuous processing	65
5.1	Introduction	65
5.2	Methodology.....	66
5.2.1	Materials.....	66

5.2.2	Continuous procedure	66
5.3	Results and discussion.....	69
5.3.1	Characterization of feedstock	69
5.3.2	Mass balance.....	69
5.3.3	Characterization of products	71
5.3.4	Comparison between continuous and batch HTL.....	74
5.4	Conclusion.....	81
6	Chapter 6 HTL of model substances: Effects of lipids	83
6.1	Introduction.....	83
6.1	Methodology	84
6.1.1	Materials	84
6.1.2	HTL procedure.....	84
6.2	Results and discussion.....	84
6.2.1	HTL conversion of single lipid	84
6.2.2	Biocrude products from HTL of mixture.....	86
6.2.3	N content in the biocrude.....	88
6.2.4	Chemical compositions in the bio-crude	90
6.2.5	Nitrogen distribution.....	97
6.3	Conclusion.....	98
7	Chapter 7 HTL of model substances: Maillard reactions	99
7.1	Introduction	99
7.2	Methodology	99
7.2.1	Materials	99
7.2.2	Hydrothermal liquefaction procedure.....	99
7.3	Results and Discussion.....	100
7.3.1	The effects of carbohydrates-to-proteins ratio.....	100
7.3.2	The effects of temperatures.....	111
7.3.3	The effects of heating rate.....	112
7.3.4	The effects of residence time	114
7.3.5	Reaction pathways	123
7.4	Conclusion.....	127

Table of contents

8	Chapter 8 Energy valorization of integrating lipid extraction and hydrothermal liquefaction of lipid-extracted sewage sludge	129
8.1	Introduction	129
8.2	Methodology.....	130
8.2.1	Materials.....	130
8.2.2	Lipid quantification	130
8.2.3	HTL procedure	131
8.2.4	Data interpretation.....	131
8.3	Results and discussion	132
8.3.1	Feedstock characterization	132
8.3.2	Lipid extraction from sewage sludge	134
8.3.3	HTL conversion.....	134
8.3.4	Carbon and nitrogen balance.....	135
8.3.5	Energy content of the products.....	137
8.3.6	Biocrude composition	138
8.3.7	Integration of lipid extraction and HTL of LESS.....	140
8.4	Conclusion.....	145
9	Chapter 9 Conclusion & Outlook.....	146
9.1	Conclusion.....	146
9.2	Outlook	149
	References	152
	Appendix	168

Chapter 1 Introduction

1.1 State of the art: Sewage sludge production

Sewage sludge (SS) is a by-product of wastewater treatment plants (WWTP), and is generated in large quantities during waste water treatment. With the rapidly increasing urban population, urbanization growth, and demand for better treatment of sewage, there is a drastic increase in SS generation. Recently, the annual SS production has been estimated at 20 million tons (dry matter), 10 million tons and 49 trillion litres in China, Europe and the United States, respectively [1-3]. The ever-increasing amount of SS has intensified environmental challenges, including waste management and pollution issues. An advancement in sustainable treatment of sewage sludge has become an urgent concern globally [4, 5].

Sewage sludge is the solid, semisolid, or slurry residual material that commonly classified as primary and secondary sludge. The production of sewage sludge from WWTP is shown in Figure 1-1. Primary sludge is generated from chemical precipitation, sedimentation, while secondary sludge is the activated waste from biological treatment processes. Reducing its volume to decrease the storage cost and stabilizing its organic materials to decrease associated risks are the two basic goals of treating sludge before final disposal.

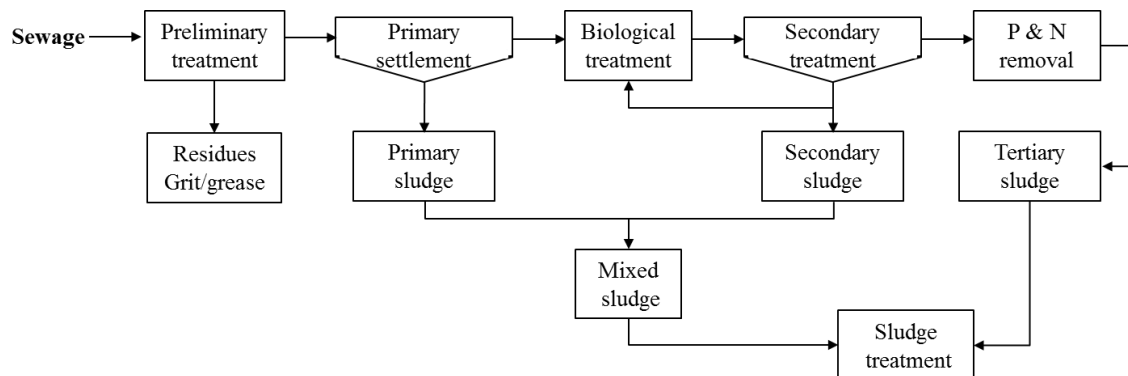


Figure 1-1 Flow chart of wastewater treatment and sludge generation, adapted from [1, 6]

Thickening is usually the first step to handle thin sludge in WWTPs. The sewage sludge is thickened in a gravity thickener to reduce the total volume to less than half the original volume. Dissolved air flotation is an alternative process that can be used to effectively carry the solids to the surface. After thickening, the sludge enters a biological digestion

process, in which the organic solids are decomposed into stable substances. The remaining digested sludge is then dewatered before final disposal [7, 8]. Using sludge-drying beds is the most common but extremely time-consuming way to complete this process. In order to speed up these processes, WWTPs also employ alternative processes including centrifugation, rotary drum vacuum filtration, and belt filter pressing. Sludge conditioning is preceded by adding chemicals to coagulate solids and improve drainability [9]. In most cases, dewatered sludge contains as much as 80 wt.% water [10]. Sewage sludge is composed of inorganic compounds, a large amount of nutrients, organic chemicals, as well as pathogens. Rulkens [11] categorized the composition of sewage sludge into six groups of components: (1) non-toxic organic carbon compounds (approximately 60 % on a dry basis); (2) nitrogen- and phosphorous-containing components, (3) toxic inorganic (e.g. Zn, Pb, Cu, Cr, Ni, Cd, Hg, and As) and organic pollutants (e.g. polychlorinated biphenyls, polycyclic aromatic hydrocarbons); (4) pathogens and other microbiological pollutants; (5) inorganic compounds, such as silicates, aluminates, and calcium- and magnesium-containing compounds, and (6) water. Therefore, it is extremely important to properly treat such sludge in order to minimize its environmental and social impact. A review of different approaches used in sewage sludge treatment is classified in the term of valorisation of waste into resources and energy recovery. General potential routes of various treatments of sewage sludge are summarized and displayed at the end of section 1.2.2.

1.2 State of the art: Sewage sludge treatment

1.2.1 Valorization waste sludge to a resource

The use of wastewater sludge as a source for resource recovery is a good alternative to its conventional management considering the circular economy principles.

Landfilling

Landfilling is the traditional way to treat sewage sludge. Primarily, the application of sewage sludge to agricultural land is generally considered to be the “Best Practical Environmental Option” because the nitrogen (N) phosphorus (P) and potassium (K) contents of sludge provide high fertilizer value and the organic matter acts as a useful organic amendment in the remediation of contaminated sites [12]. On the other hand, recycled sewage sludge is considered a potential source of soil contamination by organic

and inorganic pollutants and pathogens. These are not allowed to be spread on land where crops are grown for human consumption.

Current sludge to landfill methods generally suggest to mix the concentrated sludge with other solid waste in municipal landfills. However, a number of factors make land-spreading of sewage sludge increasingly difficult. For example, the transport times and distances between utilities producing sludge and suitable agricultural land are generally increasing, which increases costs. Considering the difficulties associated with construction and the instability of landfill slopes, landfill operators are also increasingly reluctant to accept sludge material in the slurry state [13]. Taking into account the increasingly stringent laws applicable to the design and operation of new landfills, as well as the costs for the construction and operation of landfills, the amount of sewage sludge being stored is decreasing.

Composting

Composting is the main biological stabilization process for the agricultural use of sewage sludge. The biological process can convert nitrogen from unstable ammonia to a stable organic form of nitrogen, destroy pathogens and reduce waste [14]. The fertilization by sludge compost improves the chemical properties of soil. However, similar to landfilling, compost unfortunately contains unfavourable pollutants such as heavy metals and toxic chemicals. When compost is used as fertilizer, the pollutants can accumulate in the soil and enter the food chain via crop plants. The environmental and health hazards caused by compost fertilizer are difficult to determine because the interactions and transformation processes of compost pollutants are often unknown. Moreover, the dewatering of sludge is an important factor when looking at composting. Composting of any material generally requires a moisture content of less than 60 % (wet weight basis) and a bulk density of less than 650 – 700 kg/m³, which is generally achieved by adding amendments and bulkers [15, 16].

Conversion the sludge into adsorbents

Due to the carbonaceous structure of sewage sludge, it has been considered a potential feedstock to produce activated carbon by chemical activation and carbonization [17] of the dried sludge. Thus, the modified sludge can be used as low-cost adsorbents to remove heavy metals and organic pollutants from water and soil [18]. Pre-drying has a positive effect on the porosity of the sludge-based char, especially on the Brunauer-Emmett-Teller (BET) surface area, where the highest BET surface areas attained through carbonization

(at 900 °C for 62 min) of sewage sludge alone were 359 m²/g [19].

However, the properties of the adsorbents have been shown to be heavily dependent upon both the production/conversion method and the nature of the sludge. Chemical activation using alkali metal hydroxide reagents, especially KOH, was found to be the most effective technique for producing a high BET surface area, with areas in excess of 1800 m²/g being reported. On the other hand, carbonization and physical activation did not yield high surface areas as a consequence of the high inorganic content of the sludge [20].

Phosphorous recovery

P is an essential element of human nutrition, which cannot be replaced by any alternatives. The demand for P is inevitably increasing because of the world's growing population. However, the global reserves of high-grade phosphate rock are declining. At current rates of consumption, it is estimated that all reserves with economical exploitation potential will be exhausted in less than 100 years [21]. Therefore, phosphorus recovery from waste streams is extremely significant. Since one of the major components of P transformation is sewage production and treatment, sewage sludge (typically 1.4 wt.% P) [22] is a potential resource to recover P. With the proper infrastructure, P may be efficiently recovered through the precipitation of struvite crystals (ammonium magnesium phosphate) that can be applied directly to farm fields [23].

According to a study for the European Commission, around 41 % of P in municipal sewage sludge is currently recovered and reused in agriculture, so the potential for P recovery from sewage sludge would be 297 kt/a of P for the EU27. In China, the total P concentration in municipal sewage sludge varies significantly, from a 2.2 to 51.3 g/kg, which is estimated to amount to 167,634 Mg/year [24]. The maximum recovery potential from the sludge phase without extraction is 20 %, and for recovery by sludge leaching, a maximal P recovery rate of 70 % can be achieved at high chemical and/or energy cost. However, it may be assumed that the availability of P for plant uptake is low as most of the P in the recycled sludge will be in the form of aluminium and iron salts [25, 26].

1.2.2 Valorization waste sludge to energy recovery

In order to meet the globally growing energy demand and to support climate mitigation strategies, energy recovery from common waste has seen increasing attention, including the disposal of sewage sludge. Owing to its volatile organic contents ranging from 21 to

48 wt.%, the reported energy content of dried sewage sludge varies between 11 and 22 MJ/Kg [2], which indicates comparable calorific values in comparison to various biomass samples. Consequently, energy recovery from sludge is regarded as the most attractive method for valorisation. The energy obtained from waste sludge may be a sustainable solution to fulfil future energy requirements. The energy conversion technologies in focus, which have been widely investigated, including incineration, convert waste into heat/or electricity, anaerobic digestion provides biogas, as well as thermochemical conversion generates biofuels.

Incineration

Incineration is the most popular sludge disposal method in Europe, the USA and Japan, allowing to reduce its volume and making disposal more economical [27]. During incineration, organic matter is combusted to CO₂ and other trace gases and water is removed as vapor, leaving inert ash. The process cannot be considered a complete disposal option because significant quantities of inorganic incinerated sewage sludge ash remain. Sewage sludge mono-incineration facilities are operated at temperatures ranging from 850 to 950 °C; temperatures below 850 °C can result in odour emission, and temperatures above 950 °C cause ash sintering. Sewage sludge can also be incinerated in power plants, in a process known as co-incineration. This process is mainly carried out at coal-fired power plants, waste incineration plants and cement plants [28].

However, a high content of water in sewage sludge limits its normal fuel combustion. Combustion requires further drying of the dewatered sludge to reduce the moisture content to less than 50 wt.% before being fed into the reactor [2]. The water content consumes heat as it is vaporized. Sewage sludge typically has to contain at least 28–33 wt.% solids to burn without external heat and to maintain the incineration process [12, 29]. When pre-drying to higher solids content is required, the benefit in energy output must be balanced against the energy input. In addition, air pollution control is a very important consideration when sewage sludge is incinerated. Appropriate air-cleaning devices such as scrubbers and filters must be used. Another major disadvantage of using the incinerated ash in construction materials (sintered materials, cements), in general, is a loss of potentially valuable P as sewage sludge ash is promising P-rich residue.

Anaerobic digestion

Unlike composting and incineration, anaerobic digestion (AD) can avoid drying

procedures in disposing sewage sludge. As a cost-effective process for the conversion of sludge into renewable energy, AD, which is a biological conversion method, is widely used due to its ability to utilize organic matter for the production of biogas (CH_4) [30, 31]. The AD process consists of three steps: firstly, organic chemicals like polysaccharides, proteins, and fats are hydrolysed by extracellular enzymes, followed by acidification to convert the hydrolysis products into substances with lower molecular weights like hydrogen, formate, acetate, and higher molecular-weight volatile fatty acids. Finally, methane and carbon dioxide are generated from the intermediates generated in the second step. Currently, AD of sewage sludge is mainly applied in large and medium-sized WWTP. The vast majority of anaerobic processes applied in practice are mesophilic. However, the digestion time is quite long with 7 days to 5 weeks of fermentation time. With the standard digestion process, the conversion efficiency is usually low, around 40 – 70 % of organic compounds remain after the process, and only approximately 20 – 30 % of the organic matter is mineralized [2, 11]. The methane yield obtained from sludge varies between 80 – 377 mL/g of organic matter depending on the feedstock, the number of digestion days, the process temperature and the pre-treatment processes used [32, 33]. A substantial improvement of biogas can be achieved by applying suitable physical, chemical, thermal, mechanical, or biological pre-treatment technologies. The potential of the various pre-treatment processes to increase the anaerobic biodegradation rate and to produce higher yields of biogas is substantial.

Biodiesel

Biodiesel production has become increasingly significant in recent years. However, due to the high cost of conventional feedstock for biodiesel production, the lack of agricultural land for growing biodiesel feedstock and the associated impact on food prices, biodiesel expansion has been limited [34, 35]. Sewage sludge is considered a cost-effective alternative for raw biodiesel materials because it is consistently and readily available and it contains a considerable amount of lipids, typically in the range of 20 wt.% (daf.) [36]. The lipids fraction in SS is always characterized as oils, greases, fats, and long-chain fatty acids. The average yield of methyl esters from the SS lipids is 24 %, the total average of saturated fatty acids reaches as high as 55 % [37, 38].

Lipids can be extracted from raw sludge before the extracted lipids are converted into biodiesel by esterification and/or transesterification. Biodiesel can also be produced using in-situ transesterification of dried sludge [39]. Besides, this technology has been

developed from dry-extraction to liquid-liquid extraction, which is much more favourable for scaled-up production due to the unnecessary cost for pre-drying. The free fatty acids (FFAs) extracted from SS were predominantly in the range of C10 to C18, mainly containing methyl esters of palmitic acid (C16:0), palmitoleic acid (C16:1), stearic acid (C18:0), oleic acid (C18:1) and linoleic acid (C18:2), which is a good fit for the production of methyl esters [38]. However, lipid extraction from sludge is also expensive and requires large volumes of organic solvent and acid catalysts, and the exploration of achievable solvent reuse and promising catalysts can significantly improve the economic efficiency.

Thermochemical conversion

During the last decade, the thermochemical conversion process is considered one of the most promising technologies to produce renewable energy and valuable products from waste residues. Thermochemical technology can convert or reform organic matter into syngas, liquid bio-oil and solid residue. Thermochemical processes can be classified depending on the processing temperature and pressure, yielding different product distributions. There are four main process alternatives available: pyrolysis, gasification, hydrothermal liquefaction and carbonization [6, 40]. The selection of a conversion method can be influenced by the nature and quantity of biomass feedstock, targeted energy, and economic considerations.

Pyrolysis

Pyrolysis is the thermal decomposition of biomass in an inert atmosphere, the operating temperature ranges from 300 to 900 °C, degrading the chemical molecules of the biomass into bio-oil, fixed carbon, ash and gases [4]. The pyrolysis process produces liquid fuel known as pyrolysis oil that can be a substitute for fuel oil. The advantage of liquid fuel that is being produced by pyrolysis can be easily stored and transported [6]. There are three types of pyrolysis processes that differ based on operation conditions, namely slow, fast and flash pyrolysis. Accordingly, the composition of products varies. Slow pyrolysis involves a decomposition process that produces char at low temperatures. Fast pyrolysis produces bio-oil at temperature above 500 °C, with a high heating rate (> 200 °C/s) in a short time (< 2 s). In flash pyrolysis, the retention time is extremely short. Currently, fast pyrolysis is seeing increased attention due to the high bio-oil yield up to 75 wt.% [41, 42]. Karaca et al. [43] investigated higher-temperature pyrolysis of sewage sludge at 450 – 850 °C, and found that around 74 % of energy could be recovered as syngas and

tar at 850 °C. Bio-oils have been successfully tested in engines, turbines, and boilers, and have been upgraded to high-quality hydrocarbon fuels, although at presently unacceptable energetic and financial expense. However, pyro-oil has a high viscosity and is rich in oxygen, so the improvement of pyro-oil quality is necessary. Compared to established fast pyrolysis technologies, thermo-catalytic reforming (TCR[®]) is a proven integrated approach to an intermediate pyrolysis and reforming process for converting sewage sludge and residues for the production of high-quality oil, hydrogen-rich syngas, and char without volatiles [44-46]. The typical TCR[®] oil includes a low content of heterogeneous atoms, it can be easily upgraded to generate CO₂-neutral fuels, meeting the EN standards for fossil diesel and gasoline. TCR[®] gases can be used for upgrading the TCR[®] oil due to the high hydrogen content (up to 50 vol.%).

In addition, sludge has a high water content and much of the energy contained in the dry solids is consumed for drying. In terms of energy efficiency, pre-drying process stills limit the application of this thermal conversion.

Hydrothermal gasification

Gasification is the thermochemical process through which the carbonaceous content of the fuel is converted to combustible gas and ash. The syngas comprises of hydrogen (H₂), carbon monoxide (CO), carbon dioxide (CO₂), methane, and higher hydrocarbons. H₂ has been reported as the most promising product in terms of the clean combustible efficiency [10, 47]. This process involves temperature ranges from 400 to 1400 °C, with pressures up to 40 MPa. To achieve high yields, fast heat-up to high temperatures is necessary. Unlike pyrolysis, gasification can also happen in the presence of water without a pre-drying process, which is called supercritical gasification (SCWG). Gong et al. [10] have investigated direct gasification of 10 kinds of different dewatered sewage sludges at 400 °C over 30 min, and found that all sludges can be gasified to produce H₂, ranging from 0.06 to 0.87 mol/kg (ash-free dry basis). Regarding the relatively low H₂ yields at lower temperatures, suitable additives have been used as catalysts to accelerate the gasification reaction. For example, the addition of formic acid can dramatically improve the H₂ yields to up to 10.07 mol/kg (ash-free dry basis) [48]. However, SCWG has been getting less attention in the last decade, the high temperature and heat recovery make the choice of reactor material challenging, and high ash content conversely inhibits complete SCWG [40, 49].

Hydrothermal Carbonization

In contrast, hydrothermal carbonization and liquefaction processes at temperatures and pressures near and below the critical point (374.2 °C and 22.1 MPa, respectively) provide an excellent opportunity for processing sewage sludge with high water contents. Water in the sludge is utilized as a reaction medium, acting as a solvent and catalytic reagent [49]. Hydrothermal carbonization (HTC) is a process for converting wet sludge to a carbon-rich material with a heating value like that of lignite, often called hydro-char. As a carbon-rich compound, hydro-char can also be added to soils as a conditioner. Typical reaction conditions are in the range of 180 – 220 °C with reaction times from 30 min to several hours [50]. Primary sewage sludge was carried out by HTC at temperatures from 140 to 200 °C in 15 – 240 min, the carbon content in hydro-char is increased to 72 % and then decreased to 62 % with high heating values (HHVs) from 17 to 19 MJ/kg, which can be used as low-grade coal [51]. In addition, the P has been largely recovered from hydro-char obtained from HTC of digested sewage sludge [52]. Challenges are that the hydro-char is not stable in soil, fresh material is phytotoxic and fossil coal is too cheap compared to the HTC production costs. However, a drastic increase of research in this field with regard to no-fuel applications of hydro-char as new materials, being applied as super-capacitors or electrode materials for e-mobility, has recently been seen [53].

At elevated temperature, Hydrothermal Liquefaction (HTL) therefore stands out as a promising technology as it is able to convert high-moisture feedstocks to a liquid bio-crude with high energy density in water medium, which could be further refined into transportation fuels. This technology will be reviewed in the following section.

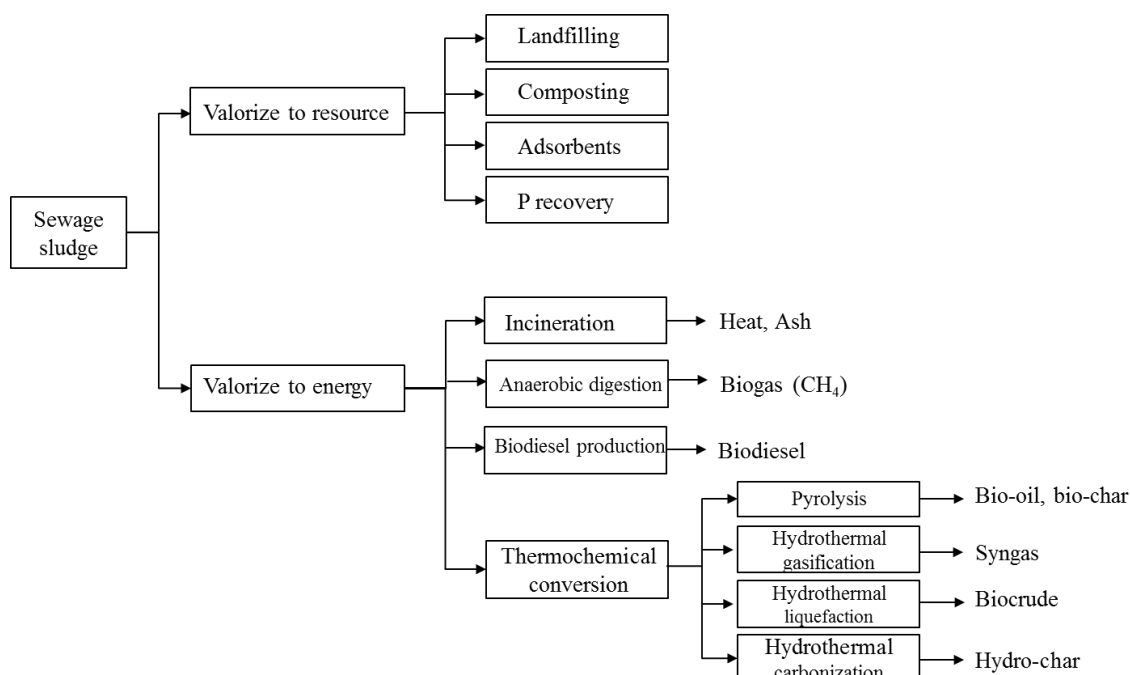


Figure 1-2 Potential sewage sludge to resource and energy recovery routes

1.3 State of the art: HTL of sewage sludge

1.3.1 Fundamentals of hydrothermal liquefaction

HTL is a thermochemical process in which biomass is decomposed and transformed to liquid, solid and gas fractions in subcritical or supercritical water, sometimes in the presence of organic solvents and/or catalysts [37]. HTL is also recognized as hydrous pyrolysis that utilizes subcritical water, the typical processing medium temperature ranges from 250 °C to 370 °C, while the operating pressure is between 4 and 22 MPa. The wet feedstocks and a supplementary amount of water are generally kept in the range 1:10 – 1:5 (biomass: water/weight ratio) [54, 55]. When the temperature and pressure are close to the critical point (374 °C, 22 MPa), the physical-chemical properties of water change significantly, including density, dielectric constant, and permittivity, etc. Water, being highly compressed, is still maintained in a liquid state but has a relatively higher ionic product and lower relative permittivity than at ambient conditions [11]. The combination of elevated pressure and temperature leads to a decrease in density, the hydrogen bonds of water become weaker, and the solubility of non-polar organic compounds increases. The water ions in such conditions can facilitate the decomposition of biopolymers in biomass to further form liquid (bio-crude oil and water-soluble product), gaseous and solid fractions.

Main reaction pathways

Owing to the complex composition of biomass, it is very difficult to identify the reaction pathways of these compounds found in the biocrude. Some of the compounds could originate from the raw feedstocks, while others could be converted through various reactions such as hydrolysis (e.g. hydrolysis of esters to form carboxylic acids and alcohols, hydrolysis of nitriles to form the corresponding amides), depolymerization, decomposition and recombination of reactive fragments. In detail, when HTL occurs at lower temperature, the hydrolysis firstly occurs to reduce the organic content in the biomass, by converting organic matter to dissoluble intermediates such as 5-hydroxymethylfurfural (HMF) and furfural. Hot compressed water breaks the bonds of biomass materials at heteroatom sites and hydrolyses the fragments. The hydrolysis of polysaccharides and proteins begins to occur around 190 °C, hemicellulose and lignin are dissolved into their liquid phase at 220 °C, the decomposition of remaining lignocellulose takes place at higher temperatures [56, 57]. Lipids or fats split into glycerol and fatty acids at 220 °C via a cleavage reaction [85]. When the temperature increases, the decomposition of the monomers takes place by cleavage, dehydration, reverse-aldol defragmentation, decarboxylation and deamination to reactive intermediates, involving the loss of H₂O, CO₂ and NH₃. Dehydration can remove oxygen heteroatoms in the form of H₂O. Decarboxylation is the thermal cracking of long chain carboxylic acids, which releases CO₂ and reduces the chain size.

Deamination of free amino acids leads to the production of ammonia. As a result, the macromolecules are hydrolysed to macro form polar oligomers and monomers. The majority of the degradation products such as polar organic molecules, glycolaldehydes, phenols and organic acids are highly soluble in water. At higher temperatures, hydrolysed and depolymerized reactive fragments and products usually undergo secondary reactions to generate biocrude, aqueous phase, solid organic products and gases. Major reactions among these are recombination, rearrangement, cyclization, condensation and repolymerization. The water-soluble intermediates are playing an extremely significant role in the distribution of end products and are highly dependent on the reaction conditions. At slower heating rates, which mean longer reaction times at lower temperatures, the polymerization and carbonization occur to generate hydro-char, which is barely converted into oily products [58]. On the other hand, those water-soluble organic compounds are converted to heavy oil via a dehydration reaction. With increasing

temperatures, usually above 350 °C, bio-oils are levelled off and then slightly decreased at the expense of higher-molecular compounds in the solid residue formed by condensation and cyclization reaction of water soluble products, as well as the hydrocarbon gases generated by cracking reaction [49, 59, 60].

Generally, the HTL process utilizes biomass or waste with a high moisture content to minimize the cost of a drying or dewatering phase. Hence, feedstocks with varied moisture content, for instance algae-based, woody and waste-based biomass, are suitable for biocrude production. Sewage sludge appears to be suitable feedstock for HTL due to its constituents that mainly comprise of proteins (~ 40 wt.%), lipids (~10 – 25 wt.%), carbohydrates (~14 wt.%), and ash (~ 30 – 50 wt.%) [61, 62]. Owing to its volatile organic content, which is reported to be between 21 and 48 wt.% in available literature, the energy of dried sewage sludge ranges from 11 to 22 MJ/Kg, suggesting calorific values that are comparable to various biomasses [2]. Sewage sludge is a promising feedstock for the HTL process as it is readily available in large volumes. In addition, it is reported that compared to dry sludge, exploiting wet sludge can decrease the consumption of energy by 30 % [63, 64].

1.3.2 Process parameters

In the HTL process, the common target product is liquid biocrude, which can be used as a promising candidate for transportation fuel. The objective of HTL is to obtain high-yield biocrude of good quality.

The yields of biocrude from sewage sludge are influenced by operation parameters and the type of catalysts and solvents. From previous studies of sewage sludge using HTL, the biocrude produced varies from 10 to 48 wt.% [65-67]. Unlike petroleum, biocrude is a complex mixture of nitrogenated and oxygenated compounds with a wide range of molar mass. Its quality can be characterized by its HHVs, viscosity, density, acidity, stability, molar mass distribution, O/C or H/C ratios and chemical compositions in biocrude. Additionally, more than 50 % of the oxygen in biomass can be removed, resulting in biocrude with a higher heating value between 30 and 40 MJ/kg. The production of biocrude from HTL of sewage sludge has been extensively investigated in literature under different operative conditions. A detailed general summary of key research on HTL of sewage sludge is provided in Table 1-1. The parameters that mainly influence this process were revealed to be temperature, residence time, pressure, the

addition of catalysts, biomass to water ratio and others.

Temperature

Even though many factors can affect the results of the HTL, it is generally accepted that temperature plays the dominant role in the yields of biocrude. The temperature referred to in literature varies from 200 to 450 °C [55, 60, 68]. An increase in HTL temperature favours organic compound hydrolysis and the production of oligomers and monomers through condensation, dehydration, and decarboxylation reactions. At a temperature of 250 °C or higher, proteins, carbohydrates, cellulose, hemicellulose, and lignin degrade, being gradually transformed into bio-crude. While lipids, which are mostly non-polar compounds with aliphatic characteristics, are, in a chemically sense, referred to as water-insoluble compounds at ambient conditions. Higher temperatures (> 300 °C) are usually required to achieve a cracking reaction [69, 70]. The suggestable temperature for hydrothermal liquefaction can be set at around 300 °C, a lower temperature is favourable for the production of bio-char, and a higher temperature is favourable for the production of gases. After reaching a maximum for the crude yield, any further increase in temperature inhibits sewage sludge liquefaction. When the temperature is sufficiently larger than the activation energies for the bond cleavage, extensive gasification and depolymerization will occur. The secondary decompositions become active, which leads to the formation of gases and the occurrence of biocrude cracking reactions to form light gas species. The recombination of free radical reactions results in char formation due to their high concentrations [59].

Residence time

The effects of residence time on the HTL process have been widely investigated in the range between 0 and 480 min [67, 71, 72]. Dote's group [66, 73-76] firstly investigated the influence of the residence time on biocrude yields obtained through HTL of several kinds of sewage sludge. Results showed that no marked differences in the yields of oils were observed at different holding time. Zhuang et al. [72] reported similar findings that a prolonged duration time from 60 to 480 min at 300 °C had a slight effect on the yield of biocrude. In terms of the product yields and the energy cost, the typical residence times are located in the range between 5 and 30 min. The increase in residence time leads to higher biocrude yields. However, beyond a certain threshold, which produces maximum crude yields, any further increase in the reaction time leads to the opposite results as self-condensation reactions enhance the formation of char via the repolymerization of

monomers and the biocrude decomposition. In general, the rate of hydrolysis and decomposition is relatively fast in supercritical processes, the short residence times are expected to degrade organic compounds effectively.

Pressure

Pressure is another parameter to impact the conversion efficiency of HTL of sewage sludge. Pressure maintains single-phase media for subcritical and supercritical liquefaction, the rate of hydrolysis and biomass dissolution can be controlled. However, once supercritical conditions for liquefaction are achieved, the influence of pressure on the biocrude yields is insignificant. Malins et al. [68] observed that the increase in pressure (2 – 11 MPa) has a negligible influence on the biocrude yield during thermochemical hydro-liquefaction of wet sewage sludge, and energy recovery and total conversion were relatively similar. Qian et al. [65] also found that the biocrude yield changes very little as the pressure rises from 25 to 40 MPa, which suggests that once the critical pressure of water (22.1 MPa) has been reached, the pressure has less effect on the bio-crude yield. This is because in the supercritical zone, the impact of pressure on the properties of water or the solvent medium is very small. As a matter of fact, few publications that investigate pressure can be found in the fields of HTL of either sewage sludge or other biomass.

Catalysts

According to the researches summarized above and listed in Table 1-1, the yields of biocrude obtained from HTL of SS are relatively low under optimized conditions. In order to achieve the higher conversion efficiency of waste into energies, catalysts are often applied in the HTL process. Catalysts are frequently used to improve the biocrude yields via the suppression of char formation. Catalysts can reduce the condensation and/or repolymerization reactions of the intermediate products formed by the decomposition of biomass, leading to higher biocrude and a lower solid residue yield [77, 78].

It is well-known that alkali salts have a positive influence on hydrothermal processes. These are typically water-soluble inorganic compounds, often called homogeneous catalysts, in the form of alkali salts such as Na_2CO_3 or KOH [78-83]. These catalysts increase the pH of the reaction medium, thereby inhibiting dehydration of the feedstock monomers. Usually, dehydration may result in unsaturated compounds which further polymerize into char.

Whereas heterogeneous catalysts like Ni-containing catalysts have so far been utilized in

HTL less frequently, they are widely used in supercritical gasification of biomass [62, 84, 85]. Previous studies on HTL of biomass in the presence of potential heterogeneous catalysts are rare, mostly applied in algal biomass. Jena et al. [86] firstly investigated the catalytic effects of NiO on HTL of algae, the added NiO decreased oil yields but led to a higher fraction of C in the gaseous products. Later on, Duan et al. [82] explored the application of six different heterogeneous catalysts (Pd/C, Pt/C, Ru/C, Ni/SiO₂-Al₂O₃, CoMo/ γ -Al₂O₃) on the biocrude from HTL of algae, and all tested catalysts produced higher yields of bio-crude, but the quality heavily depends on the catalysts. Xu et al. [87] tested heterogeneous catalysts (Pt/C, Ru/C, or Pt/C + Ru/C) on the water-soluble and water-insoluble biocrude from HTL of algae, and Pt/C has been proven to promote the formation of low-boiling-point compounds. There is limited information available on the catalytic liquefaction of SS with the application of heterogeneous catalysts. Qian et al. [65] reported that MoO₃-CoO/ γ -Al₂O₃ and Ru/C significantly decrease the biocrude yield when their loadings are 50 wt.% of the dried sludge. In addition, the loading of catalysts has been illustrated by previous research. Suzuki et al. [66] and Malins et al. [68] discovered that even 5 wt.% loading of Na₂CO₃ could decrease the yield of biocrude from HTL of sewage sludge.

Other parameters

Temperature, residence time, pressure, and catalysts are not the only parameters influencing the HTL process. The type of feedstock [54, 60, 88, 89], heating rate [65, 90, 91], feedstock particle size [59, 92] and solvent density [59, 65, 93] also have influences on product formation. Heterogeneity in feedstock leads to the modification of biocrude products in the yields and quality, mostly due to the proportion of different chemical constituents like proteins, carbohydrates and lipids reacting differently to hydrothermal temperature variations. Regarding sewage sludge as feedstock, Suzuki et al. [66] compared the HTL efficiency of different kinds of sludge in 1988 and observed that raw primary sludge or raw mixed sludge is the optimum feedstock for liquid oil products in terms of yield. However, the elemental compositions and heating values are independent on the nature of the individual sludge. In general, high or fast heating rates influence the rate of feedstock degradation and devolatilization. Fast heating rates may lead to the formation of highly reactive intermediate species, resulting in the reactive interaction among different produced intermediates during short residence times. Slow heating rates usually lead to char residue formation. Moreover, the liquid oil yield is not very sensitive

to large variations in high heating rates. Therefore, moderate heating rates may be enough to produce high bio-crude yields, meanwhile, to overcome the heat transfer limitations [59].

It is expected that the reduction in particle size can achieve better homogeneity of complex real feedstock and achieve a higher degree of hydrolysis and fragmentation. In terms of HTL of sewage sludge, most research so far has been performed in a lab scale, the sludge samples were directly treated with a series of pre-treatments including drying, mechanical pulverization, sieving and then drying again to obtain uniform feedstock. Then they were re-mixed with water to adjust the mixture content based on the designed concentration. The sieved fine particles are usually in a range of 40 – 150 mesh, with the absolute loading of dry sludge from 0.07 – 50 g [3, 65, 68, 94, 95]. In some cases, sewage sludge was used directly as received raw sludge [56, 96]. There is no comparable research to be found that reveals the influence of the sludge particle size on the biocrude yields during HTL. One research can be referred from Zhang et al. [32]: they observed the effect of three different particles sizes (1 in, 2 mm and 0.5 mm) on the liquid oil yield in HTL of grass perennials, and found that particle size reduction did not improve the liquid oil yield at 350 °C, indicating that HTL is relatively insensitive to the size of particles. It is also true that the reduction of biomass particle size is a costly process that consumes additional energy. Hence, an optimum particle size is required to achieve high HTL efficiency at low grinding cost.

Regarding the solvent application, unlike woody or algal biomass [97-101], the high frequency solvent applied in HTL of sewage sludge is water, very few involved alcohol as a co-solvent, such as ethanol or methanol mixed with water [67, 102-104]. It is important to note that the critical points of ethanol (240.75 °C, 6.14 MPa) and methanol (239.45 °C, 8.09 MPa) are much lower than those of water (373.95 °C, 22.06 MPa) [55], accordingly, they also have a lower dielectric constant and boiling point compared to water. But these alcohol solvents are mutually soluble with the target product biocrude, which makes the separation of biocrude solvent extremely difficult.

The mass ratio of biomass to water is also considered a key parameter in HTL. In general, a high moisture content results in increasing biocrude yields, most likely due to the faster sewage sludge hydrolysis reaction associated with improved solubility of the organic fragments. At lower water to sludge dry mass ratios, the relative interactions among molecules and water become less active, which can suppress the dissolution processes

and produce solid residues. However, increasing water content does not always yield high bio-crude amounts. Qian et al. [65] determined the influence of water content ranging from 75 to 97.2 wt.% in the HTL products, and they observed the maximum biocrude yields were obtained at 85 wt.% water content, the sufficient water content led to an decrease in biocrude with an increase in water-soluble products and gas.

Chapter 1 Introduction

Table 1-1 General overview for hydrothermal liquefaction of sewage sludge (Part 1/2)

Categories	Water (wt.%)	Ash (wt%)	Biochemical composition (wt.%) ^a				Temp (°C)	P (MPa)	Time (min)	Catalyst	Reactor	Solvent	Crude yields (wt.%)	HHV (MJ/kg)	Crude composition	Observations	Ref.
			Protein	Fat	CHs ^b	Fiber											
Mixture of primary and waste-activated Sludge	75	16	30	13	24	33	250 -	9-18	0-120	Na ₂ CO ₃	Autoclave 300 mL	DCM	19.5-50		Hydrocarbon, ester, ketone, alcohol, aldehyde, benzene, phenol, O&N-containing compounds	The yield of heavy oils depends on the reaction temperature; the operating pressure and holding time have no influence on the yield of heavy oils.	[73]
Digested sludge	80.9	43.1	51.1	7.5	35.8	5.6							25			Raw primary sludge or mixed sludge is the most suitable kind of sludge for HTL.	
Waste activated sludge	81.9	29.5	59.5	2.7	31.4	6.0	300	12	0	Na ₂ CO ₃	Autoclave 300 mL	DCM	35	> 33		The nature of the sludge has no significant influence on the elemental compositions and heating values.	[66]
Raw primary sludge	79.9	25.9	44.3	16.4	26.5	12.7							44				
Raw mixed sludge	74.1	45.5	45.5	14.4	22.7	17.4							42			Catalyst loading also has no significant influence on the properties of the heavy oils.	
Dewatered sewage sludge	90						350 400			SS-based activated carbons	Autoclave 300 mL	DCM	14.96-30	37-39	N-containing species, phenol and phenolic compounds, esters, alcohols, hydrocarbons and acids	350 °C with SSAC-550 favoured the oil yield and decrease of heavy metals.	[94]
Sewage sludge	80.5	36.68					200 to 350	2-11	10-100	Na ₂ CO ₃ Raney nickel, FeSO ₄ , MoS ₂	Autoclave 500 mL	DCM	38.9-47.8	31.42-35	Derivatives of cholestane, heterocyclic and carboxylic derivatives (amides and esters)	High yield of bio-oil, energy recovery, total conversion was reached using weight ratio of SS to water 1/5, 5.0 mpa initial H ₂ pressure, residence time 40 min, 5 wt.% of FeSO ₄ , at 300 °C.	[68]

Table 1-1 General overview for hydrothermal liquefaction of sewage sludge (Part 2/2)

Categories	Water (wt.%)	Ash (wt%)	Biochemical composition (wt.%) ^a				Temp (°C)	P (mpa)	Time (min)	Catalyst	Reactor	Solvent	Crude yields (wt.%)	HHV (MJ/kg)	Oil Composition	Observations	Ref.	
			Protein	Fat	CHs ^b	Fiber												
Sewage sludge	85	10.3						400	22	60	K ₂ CO ₃ , Na ₂ CO ₃ , HCOOH, CH ₃ COOH, MoO ₃ - CoO/γ - Al ₂ O ₃ Ru/C	Mini reactor 4.1mL	DCM Ketone, Hexane, Xylenes, chloroform, Methanol, ethanol, Acetone	12-27	35-40	Long-chain aliphatic hydrocarbon, Aliphatic acids	Highest biocrude yield and energy recovery achieved with DCM. Fast HTL produces biocrude with higher H/C and lower N/C ratio. Additives (K ₂ CO ₃ , Na ₂ CO ₃ , MoO ₃ -CoO/γ - Al ₂ O ₃ and Ru/C) decrease the biocrude yield.	[61, 65]
Dewatered sewage sludge	77.87	56.52					150-300			30-480		Tubular reactor 250 mL	DCM			Most of N in SS was converted into liquid, gas and oil products; besides, heterocycle-N became dominant in solid phase.	[72]	
Secondary sewage sludge	84.52	23.01	37.84	8.01	31.14		210-330			0-30	CuSO ₄ , CoSO ₄ , FeSO ₄ , ZnSO ₄ , CuCl ₂ , Cu(NO ₃) ₂	Tubular reactor 600 mL	DCM	17.1-47.5		Esters, fatty acid amides, alkanes and O&N-containing compounds	The highest biocrude yield and HTL conversion was obtained at 270 °C, 30 min, an ethanol-water ratio of 1:1, and in the presence of CuSO ₄ as catalyst. N and S in biocrude were reduced by 55.0 % and 14.6 %, respectively.	[67]

^a: dry ash-free basis^b: Carbohydrates

It turned out that adjusting these reaction parameters can lead to higher biocrude yields with better quality. However, these methods are not always economic when a severe reaction environment and expensive catalysts are required. Thus, alternative approaches are highly recommended to improve HTL efficiency and to decrease the severity of reaction conditions. Recently, several studies were conducted in an attempt to improve HTL efficiency of sewage sludge by using various methods such as pre-treatment, co-liquefaction and post-treatment.

1.3.3 Pre-treatment

Lately, some physical and chemical methods for sewage sludge pre-treatment were studied. Kapusta [105] investigated the effects of ultrasound pre-treatment in HTL of municipal sewage sludge and found that the pre-treatment was beneficial for the biocrude production; a maximum increase of 19 % was achieved at 320 °C compared with untreated sludge. Chen et al. [106, 107] explored the influence of microwave power (180 – 900 W) on the yield and composition of bio-crude from HTL of SS, suggesting that increasing the microwave power can improve the biocrude yields by between 2 and 10 %. These physical pre-treatments possibly destroy microbial cell walls and the complex structure of sewage sludge effectively. This can increase the concentration of soluble proteins, carbohydrates and lipids to some extent, improving the disintegration [108-110].

The effects of inorganic (HCl, HNO₃ and H₂SO₄) and organic (HCOOH, CH₃COOH and HOCCOOH) acid pre-treatments in HTL of municipal secondary sludge were also investigated [95]. Acids have been proven to have a better performance for HTL efficiency in terms of an increase in biocrude yields with a higher relative content of hydrocarbons. There are also combinations of physical and chemical methods, like co-pre-treatment with subcritical water and mixed surfactants [102]. The results show that the contents of hydrocarbons and their derivatives increased by a factor of 11.5 with the addition of surfactants. The alkali-thermal pre-treatment has been widely applied in anaerobic digestion because it can effectively solubilize organic matter contained in sewage sludge [111, 112]. However, no publications can be found regarding the effects of the sole alkaline pre-treatment of bio-crude obtained from HTL of sludge. Theoretically, alkaline pre-treatment may not be useful for HTL, as most organic compounds in the SS would be dissolved into the aqueous phase.

In summary, from the perspective of mechanism, all these pre-treatments could change

the physical and chemical structures of organic components and efficiently break cell walls, thus facilitating the HTL conversion of sewage sludge. Considering the economic factors, any further pre-treatment would of course increase the overall process costs.

Pre-extraction

Pre-extraction is an integrated process associated with HTL that produces value-added chemicals and biofuel. As stated above, sewage sludge as well as other biomass mainly comprises of proteins, carbohydrates and lipids, which can be extracted efficiently [113-116]. Because each organic fraction accounts for less than half of the total organic matter, the residue of sewage sludge still has a large volume and needs to be utilized to achieve complete utilization. Pyrolysis of the residual sewage sludge from lipid and sugar extraction [116] and post-digestion of the residue from lipid-extracted sludge [117] have been successfully tested. No comparable studies have directly determined the potential efficiency of HTL processing of the residual sludge after preferred extraction, which may also be attractive due to its multiple fuel-like products. In the fields of algal studies, the interest in HTL of residue from extraction is increasing [118-121] and notable integrated outputs have been achieved. Therefore, it is worthy to investigate the HTL process of residual sludge after extraction.

1.3.4 Co-liquefaction

Recently, hydrothermal co-liquefaction of various feedstocks has attracted considerable research interest as it aims to increase biocrude yield with improving quality to make full use of the different kinds of biomass available [122-126]. One challenge in the production of qualified biocrude using sewage sludge is the high moisture content which is usually higher than 85 %. A co-liquefaction process can reduce the water content by introducing dry feedstocks or feedstocks with less moisture content, and hence modify the ratios of chemical constituents in the mixed feedstocks. The chemical interactions among biomass model components (cellulose, hemicellulose, protein, lipid and lignin) have been thoroughly investigated to reveal the origin of co-liquefaction effects such as synergistic, antagonistic or additive on biocrude, as well as including quantitative models for predicting product yield as a function of the biochemical composition of biomass feedstock [127-129].

Many research groups have investigated co-liquefaction of sewage sludge with other types of feedstocks. Zhang et al. [96] has determined the co-liquefaction of secondary sludge from pulp/paper mill sludge with waste newspaper under different conditions and

found that the optimum heavy oil yield attained was 26.9 wt.% at 300 °C in a mixture of 33 wt.% sludge and 67 wt.% waste newspaper. The synergistic effects on biocrude yield could be attributed to the presence of alkali and alkaline metal ions (Na, K, Ca, etc.) in paper sludge, which could positively catalyse newspaper to produce oily products. Primary sludge was co-liquefied with a biomass filter at 340 °C for 20 min by Biller et al. [130], and the increased dry matter content of filter cakes (~25 %) has been proven to increase the biocrude yields and energy efficiency in HTL of primary sludge. The observed synergistic effects on biocrude were proposed to the formation of NH_4^+ from the decomposition of proteins in sludge, enhancing the biocrude yield during co-liquefaction. Fox et al. [131] conducted the hydrothermal co-liquefaction of blended low-value food production waste and low-value municipal sewage sludge at 500 °C after pre-treatment in supercritical water at 200 °C. This blended waste processing provides recovered gases and liquid fuels containing 37.7 and 40.5 MJ/kg, respectively. Huang et al. [104] investigated the effects of process parameters on the yields/properties of bio-oil from hydrothermal co-liquefaction of sewage sludge and rice straw/wood sawdust. The introduction of rice straw/wood sawdust into the liquefaction of sludge improved the bio-oil quality through the reduction of the contents of nitrogen and sulphur, and enhanced the formation of phenolic compounds. Algal biomass was also co-liquefied with sewage sludge [132, 133]. The effects of temperature, feedstock ratio, and retention time were systemically studied and optimized for maximum biocrude yield. The distillation profile of biocrude was improved to contain 10.1 % and 23.9 % of heavy naphtha and kerosene, respectively.

Thus, hydrothermal co-liquefaction of sewage sludge with other types of biomass generally improved biocrude quality through synergistic effects, and the observed additive effects seem to be highly associated with the abundantly available alkaline metals in sludge. The major challenge in the study of co-liquefaction is identified as the understanding of co-liquefaction effects at a molecular level, as well as the remaining undesirable heteroatoms.

1.3.5 Post-treatment

According to the summarized literature on HTL of SS, the majority of studies were published on the production of biocrude and on energy recovery from the same. Despite all the promising approaches which have been proven to improve the HTL efficiency, some pending issues still exist within HTL. These need to be resolved before its

application on a commercial scale. The relatively low quality and heating value of the biocrude, the management of the aqueous phase and solid residue are the leading challenges related to HTL.

In HTL processing, the biocrude should be potentially utilized as drop-in fuel, which is functionally equivalent to petroleum fuels and is fully compatible with existing petroleum infrastructure. This functional equivalence implies that biocrude must meet existing standards with certain physico-chemical and bulk properties such as miscibility with petroleum fuels, compatibility with fuel performance specifications, good storability, transportability with existing logistics infrastructures and usability within existing engines (vehicles, jet planes, etc.). Chemically, a drop-in biofuel should have a low heteroatom content, low water solubility and a high degree of carbon bond saturation [134, 135]. However, the biocrude itself comes out higher in nitrogen and oxygen than most refinery streams. Biocrude is a complex mixture of several hundreds of organic compounds, chiefly containing acids, alcohols, aldehydes, esters, and N-containing compounds as shown in Table 1-1. Some are directly related to the undesirable properties of biofuel. Table 1-2 shows the physical properties of liquefaction-derived bio-oil from sewage sludge as well as heavy petroleum fuel oil [136].

Table 1-2 Comparison of the selected properties of HTL-derived biocrude and upgrading crude from sewage sludge

Properties	Heavy petroleum fuel [136, 137]	Digested sludge HTL-derived crude [138]	sludge catalytic HTL-derived crude [68]	Primary sludge HTL-derived crude [139, 140]	Hydrotreated HTL – derived oil [139, 140]
Acid value (mg KOH/g)TAN	N/D	N/D	N/D	65	<0.01
Density (g/cm ³)	0.94	0.91 at 50 °C		1 at 40 °C	0.79
Viscosity (cP)	180 at 40 °C	818.3 at 50 °C		571	2.5
HHV (MJ/kg)	40	36.14	31.42-35.76	37.8	N/D
Water content (wt.%)	0.1			13	<0.1
Ash content (wt.%)	0.1	N/D		0.33	N/D
Elemental composition (wt.%)					
C	85	72.51	66.03-71.09	77	84
H	11	9.44	8.45-10.29	10	15
O	1.0	11.09	12.99-17.90	8.4	1.2
N	0.3	6.96	4.25-6.31	4.3	0.05
S		N/D	1.15-1.58	0.63	23 ppm

N/D: Not determined

As presented in Table 1-2, biocrude derived from HTL of sewage sludge has comparable heating values to petroleum crude. However, some of its properties such as high water content, oxygen and nitrogen content, high viscosity and corrosiveness, make it a generally undesirable choice for fuel applications as meeting the direct application specifications for transportation fuel is a challenge. The effects of undesirable characteristics for fuel applications of HTL biocrude and their possible solutions have been summarized in Table 1-3.

Table 1-3 The main drawbacks of biocrude with their effects and possible solutions

Drawback	Effect	Solution
high water content	lowers calorific value, density, stability, and affects catalysts	Phase separation
high viscosity	equipment cost high pumping cost	Solvent addition, blending, hydro- cracking, Catalytic cracking
high acidity	leading to corrosion of pipes and containers lowers calorific value	Chemical extraction, esterification
high O content	non-miscibility with hydrocarbons, low stability	Hydrodeoxygenation
high N content	poisons the catalyst, fuel exhaust contains NO _x , foul odour	Hydrotreating Catalytic cracking
high S content	catalyst poisoning	Hydrotreating
high ash content	precipitation, corrosion, blocking	Hydrotreating Steam reforming
thermal and chemical instability	increased viscosity and stratification	Catalytic cracking

Therefore, upgrading of biocrude is inevitable to improve its quality using as liquid fuel. There are varieties of techniques for biocrude upgrading including physical and chemical methods.

Catalytic upgrading

Hydrotreating is an established refinery process to reduce N, O, and S atoms from oil. Catalytic hydrodenitrogenation (HDN), hydrodeoxygenation and hydrodesulfurization are required to remove the high nitrogen (0.3 – 8 wt.%), oxygen (5 –18 wt.%), and sulphur contents (0.5 – 1.0 wt.%) in the bio-oil produced in HTL of certain feedstocks. Oxygen is removed as water by catalytic reaction. Nitrogen and sulphur are also removed

as NH_3 and H_2S . The process typically needs hydrogen (35 – 200 bar H_2) and heterogeneous catalysts (e.g., sulphided Co–Mo, Ni–Mo), to upgrade raw biocrude at high temperatures (300 – 450 °C) [139, 141-143].

With hydrotreatment of the sludge-derived biocrude, an increase of the carbon content (77 – 84 %) and hydrogen content (10 – 15 %) in the hydrotreated oils was obtained, and a concurrent decrease in nitrogen (4.3 to < 0.05 %), oxygen (8.4 to 1.2 %), and sulphur (0.63 to 23 ppm) content indicate successful upgrading [139]. The moisture content, density, viscosity, and ash of the hydrotreated biocrude are lower than that of the raw biocrude. Hydrotreating has already been commercialized in oil refineries, however, two disadvantages still exist. One is the consumption of high-pressure H_2 , which requires the development of a sustainable hydrogen resource and a large investment into high-pressure equipment. The other is that the high coking reduces the catalyst lifetime by deactivation. Hydro-cracking is a thermal catalytic cracking process due to which hydrogenation accompanies cracking in the presence of H_2 . This method is less popular than hydrotreating. In hydrotreatment, H_2 is utilized to break C–N, C–O, and C–S bonds, while in hydro-cracking, H_2 is used to break C–C bonds, aiming to produce lighter products with improved properties. The process takes place at temperatures of more than 350 °C and at relatively high pressures of up to 14 MPa [142, 144]. This process is performed by dual-function catalysts, with at least one acidic function mainly promoting catalytic cracking and a second component promoting hydrogenation. Usually, silica-alumina or zeolite catalysts provide the cracking function, and platinum-tungsten oxide catalyse the reactions, or nickel provides the hydrogenation function. This process might be an effective way to break down heavy molecules into a large amount of light products. From an economical point of view, this causes higher process cost to reach more severe conditions such as higher temperatures and hydrogen pressures.

Others kinds of biocrude conditioning

Some alternative approaches for upgrading biocrude have been investigated. Polar solvents often use a solvent addition such as methanol, ethanol, ethyl acetate, or acetone. Reportedly, solvent addition reduces bio-oil viscosity due to physical dilution and a chemical reaction between solvent and bio-oil components that prevents further chain growth and ageing reactions [142, 145]. Esterification has been investigated as a technique for bio-oil upgrading due to the plentiful fatty acids fractions inside. In this reaction, fatty acids react with alcohol to form alkyl ester or biodiesel in the presence of

an acid catalyst, in order to decrease viscosity, density, acidity, oxygen content and water content [146]. Emulsification with other fuels such as biodiesel by using surfactants is a method for upgrading. This process does not require a chemical reaction, but it is also costly due to surfactant addition and high energy cost for high-volume production of emulsions [147]. Steam reformation of bio-oil is aimed at syngas production, which can then be converted into a range of fuels. Since Ni-based catalysts are commonly applied, the deactivation of catalysts due to coking is one of the major problems [148, 149]. None of these techniques have been deeply investigated concerning the upgrading of specific biocrude from HTL of sewage sludge.

Use of the aqueous phase

Despite all the promising approaches, which have been proven to improve HTL efficiency, several issues have limited its development beyond a laboratory scale, one of which is the limited energy efficiency. HTL cannot convert and transfer all the organics in the feedstock into biocrude, leaving abundant amounts of aqueous phase (AQ) products. The aqueous by-product of HTL contains significant amounts (20 – 50 %) of biogenic feed carbon, and identified compounds include organic acids, alcohols, aldehydes, ketones and nitrogen compounds, and up to 80 % of the nutrients from the feedstock are released into the aqueous phase [150-152]. The remaining organics in the aqueous phase have been employed as a nutrient source to cultivate aquatic species like algae [153-155]. The water phase was shown to be high in all required nutrients for algae growth, a suitable dilution is necessary to achieve optimum growing conditions, due to the potential toxic organics (furans, phenols, N-heterocyclic compounds and nickel). The main focus has been on nutrient recycling rather than carbon recovery. Compared to the biological approach, anaerobic conversion of the HTL aqueous phase has been recently studied as energy recovery along with its higher tolerance for the HTL aqueous phase and cost-effective conversion [156, 157]. Villamil et al. [158] have studied the mesophilic anaerobic co-digestion of the liquid fraction generated by hydrothermal conversion of dewatered waste activated sludge with primary sewage. Methane production decreased as the aqueous phase ratio increased, which can be attributed to the presence of recalcitrant compounds in the water phase, such as alkenes, phenolics, and other oxygen- and nitrogen-bearing aromatics, which are hard-to-degrade through anaerobic digestion. Consequently, between 33 and 64 % [156] of organics in the HTL aqueous phase remained in the anaerobic residue. However, it has also been reported that the aqueous phase can be toxic

to both mammalian cells and microorganisms, and contain ammonia and various organic compounds. Therefore, it suffers from a few setbacks, including a low degradation efficiency of organics (33 – 64 %) and high dilution rates (5 – 1000) [82]. Some algal biomass studies revealed that aqueous by-products can also be utilized to produce biogas through catalytic hydrothermal gasification or catalytic reforming [159-161], where high yields of hydrogen were produced with near complete gasification of the organics. The produced H₂ has a potential use for upgrading or partial upgrading of the biocrude. To my knowledge, there is no publication on gasification of the aqueous phase from HTL of sewage sludge, only one relative energy recovery from the aqueous phase has been conducted by Aalborg University [162]. The obtained results showed that energy recovery in the form of biocrude increased by 50 % through aqueous phase recirculation into the HTL process. However, the nitrogen content in the biocrude had approximately doubled after eight rounds of recycling. In addition, as mentioned before, the aqueous phase contains huge amounts of organic compounds, many of which are high-value chemicals, including saccharides, monosaccharides, lignin fragments, phenol derivatives, fatty acids, long chain alkanes, esters, ketones and aldehydes [152]. Thus, direct separation or extraction of certain chemicals from the aqueous phase could help achieve an efficient utilization of chemicals. Chromatographic separation with resins has been used to separate phenolic compounds, lignin fragments, furfural and 5-hydroxymethylfurfural [163], and membrane separation has been used to separate monosaccharides, acetic acid and aromatic compounds [164]. These methods are rarely applied as a post-treatment method for sewage sludge, probably due to the complicated composition of the water phase and the low concentration of valuable chemicals, resulting in the difficulty to extract a pure single component with high efficiency.

Solid residue application

Solid residue (SR), also called hydro-char, is often overlooked as a side-product although it is an organic fraction of char and other nutrient elements. Except biocrude and AQ obtained from HTL, the solid residue ranging from 17 – 45 wt.% is also a potential end product adding value to the production chain, improving the economic feasibility of the HTL process [165]. Sewage sludge has been considered an attractive secondary phosphate source, because the major part of the phosphate obtained from wastewater is transferred to sludge [8, 166, 167]. Ovsyannikova et al. [168] have systematically investigated the migration and transformation of P in primary sewage sludge through HTL.

Half of the phosphorus (46.8 wt.%) was distributed in the solid residue, phosphate was successfully recovered in the form of struvite, which can be further used as fertilizer. The nutrient recovery of N has gotten more attention recently, since the original sewage sludge possesses considerable amounts of N (2.4 – 9 wt.%) after hydrothermal conversion, and even most solid-N was converted into liquid and oil phase during the hydrothermal process, still resulting in around 10 % of N remaining in solid residue in the form of quaternary-N, pyrrole-N as well as pyridine-N. Thus, the N-rich solid residue might be candidates for the development of slow N-release fertilizers, since the mobilization of their N is expected to be sufficiently low to avoid fast N losses due to leaching or nitrification shortly after fertilizer application [72, 169, 170]. Even though, further studies have to be developed to analyse the effects on applying the solid residue as soil amendment / bio-remediation, owing to the toxic heavy metals as well as the harmful concentrated organic compounds such as polycyclic aromatic hydrocarbons [8]. Previous work has explored the transformation behaviours of heavy metals in sewage sludge during hydrothermal treatment [171], as well as the potential application of metals as a catalyst to improve the HTL efficiency [132, 172]. In addition, SR can be used as an adsorbent, due to its large surface area, porous structure, charged surface, and functional groups including carboxyl, hydroxyl, carbonyl and phenolic hydroxyl groups, to remedy the soils contaminated with organic compounds and heavy metals through adsorption [173].

1.3.6 Continuous HTL process

Although HTL has been widely investigated with promising results, it is still in an early stage of process development. Besides the incomplete understanding of HTL reaction mechanisms, the less competitive, low level biofuel, and the exploratory treatment of side-products, the application of economic, continuous HTL is less demonstrated. An investigation of continuous processing is required for transferring this technology into industrial scale-up. Dating back to 1992, a Japanese group successfully tested the continuous HTL of sewage sludge with a capacity of 500 kg/d at 270 – 300 °C and a holding time of 0 – 60 min, which ran for more than 700 h without any trouble [75, 174]. Organic matter in the sludge was converted into 40 – 53 wt.% heavy oil. After that, there was no literature available reporting on pilot scales of continuous HTL of sewage sludge until 2015, and only a few papers can be found in the field of gasification [175, 176]. Elliott et al. [161] reviewed and summarized the recent research in continuous-flow

process development for biomass HTL, mostly covering algal and woody biomasses. For example, a continuous flow pilot-scale HTL process was established at the Sydney University in Australia with a reactor of approximately 2 L to liquefy micro and macro algae [177, 178]. Lignocellulosic forest biomass has been tested with HydrofractionTM technology, which was developed by Steeper Energy ApS in collaboration with Aalborg University, achieving 45.3 wt.% oil yields with 85.6 % energy recovery [179]. Plastic waste also has been extensively processed by the demonstration plants based on Cat-HTRTM technology, which is a catalytic technology developed by the Licella company [180].

Regarding sewage sludge, although results from batch systems showed promising results for their application in continuous systems, less information is available in terms of pilot-scale continuous processes. The selection of sludge slurry is very important as the high concentration and ash content will significantly increase the operation cost and negatively impact the pumpability. High-pressure feeding systems for biomass slurries have been recognized as a process development issue. More investment into the preparation of feedstock, such as grinding for easier pumping, on the other hand, results in a high energy cost penalty. Pacific Northwest National Laboratory (PNNL) has reported 37 wt.% yields of biocrude achieved from 12 wt.% dry matter slurries in a continuously stirred-tank HTL system [140, 181]. The novel pilot-scale continuous HTL plant incorporated an oscillating flow technology, developed by Aarhus University in Denmark, and has processed algae and sewage sludge with a capacity of up to 100 L/h [182]. Average yields of 25 wt.% biocrude was obtained by HTL of 4 wt.% dry primary sludge slurry at 350 °C with a 5 h retention time. However, the much lower dry content limited energy recovery to 33 %, and around 20 wt.% biocrude was comprised of inorganic solids owing to the separation by gravity. It is accepted that higher dry matter concentration can yield more biocrude, but pumping and feeding solid suspensions can lead to major plugging issues. Therefore, finding efficient pumping systems is necessary to develop HTL on an industrial scale. In addition, the separation between aqueous phase, biocrude and solid phase is the major challenge for continuous HTL processes. The fact that the organic acids would catch water in the biocrude phase, while metals like silica and iron would precipitate into bi-crude, both leads to lower quality and causes new issues.

Nevertheless, one of the most obvious drawbacks of HTL technology is the high cost of the equipment necessary for industrial scale processes. Corrosion in the subcritical water

environment is a critical issue [88]. Despite the current economic and technical concerns, as well as the several identified commercialization bottlenecks, including expensive materials, recycling huge amounts of process chemicals, uncertain performance characteristics, and the lack of industry and product standards, a number of research groups in cooperation with the industry are working on the industrial and global commercial development of HTL. There are some examples of HTL demonstration plants under development or in commissioning, but limited information on reaction designs, operation conditions and capacities is available. For example, Southern Oil Refining Pty Ltd has been working on continuous processes for HTL of municipal wastewater sludge since 2019, in which the renewable crude oil is to be upgraded to renewable diesel (and potentially jet fuel). Genifuel, in collaboration with Metro Vancouver and PNNL, is developing a HTL pilot plant next to the local WWTP with the aim to dispose 2 dry tonnes of sludge per day [183].

1.4 State of the art: the fate of nitrogen during HTL of sewage sludge

A high nitrogen (N) content is considered a challenge to the use of HTL biocrude without any type of upgrading to meet industrial standards [72, 170]. Biocrude generally has a potentially high N content (0.3 – 8 %) depending on the feedstocks used [138]. N in biocrude is undesirable not only because of its lower heating value and the pollution of the atmosphere by NO_x emissions during combustion, but also leads to high viscosity and instability of biocrude due to cross-linking/oligomerization reactions, which affect its storage and transportation properties [72]. Furthermore, a reduction of this N content would decrease the cost of downstream processing, since N-containing heterocycles in the biocrude are more recalcitrant to hydrotreatment than compounds with aliphatic nitrogen or oxygen heteroatoms [184]. Cyclic nitrogen compounds are particularly problematic during upgrading since they require ring hydrogenation to weaken the C-N bond before cleavage. Additionally, their high basicity can lead to adhesion to acidic active catalyst sites, preventing further hydrotreatment reactions [185]. Therefore, it is necessary to understand the transformation and fate of the nitrogen-containing compounds during HTL of sewage sludge. Hence, the speciation of nitrogen compounds in the biocrude needs to be investigated in order to develop proper methods to upgrade the HTL biocrude.

1.4.1 Nitrogen issues in HTL of sewage sludge

The nitrogen content (2.4 – 9 wt.%) of sewage sludge is primarily present in the form of proteins, and to a lesser extent in the form of pyridine, pyrrole and inorganic compounds, ammonia, and nitrite nitrogen [72, 186, 187]. Trace amounts come from fatty acids and sugars [188]. The protein content in the sludge ranges between approximately 30 and 60 % [110, 113]. After the HTL process, the biocrude obtained from high-protein feedstocks, including sewage sludge, typically contains 3 – 7 wt.% of N content [189].

Early studies with a focus on the fate of N from hydrothermal treatment of different varieties of sewage sludge were performed by Dote et al. [76, 190]. The results showed biocrude yields of 40 wt.% with 5.8 – 6.1 wt.% N content, resulting in a high nitrogen distribution (ND, defined as the amount of N in the biocrude relative to the initial N mass in the feedstock). An increase from 9 to 20 wt.% of ND in the biocrude was observed when the temperature was increased from 200 to 300 °C. Later, Xu et al. [191] demonstrated the effects of alkaline metal catalysts on direct liquefaction of pulp/paper sludge, in which the N content in heavy oil was reduced from 3.9 to 3.4 wt.% in the presence of K_2CO_3 . A similar observation can be found in the latest work of Shah et al. [162], where no significant improvement in bio-crude yield was observed after the addition of K_2CO_3 , even with a higher N content (from 4.6 to 5.1 wt.%), due to the substantial amount of proteins (43 %) present in the sewage sludge. This is in great agreement with the highlight in the work of Hu et al. [192], that the alkali catalyst is not favourable for the conversion of high protein-containing feedstocks. Biocrude obtained by recycling the aqueous phase showed an increase of energy recovery by 50 %, whereas the N content in the biocrude was approximately doubled (4.3 to 7.1 wt.%) after eight rounds of recycling. They proposed the increased N content in the crude phase especially due to the accumulation of N-containing compounds. However, Zhang et al. [96] reported that HCOOH can have higher catalytic effects than KOH and FeS, and that the addition of HCOOH could improve the biocrude yield from 24.9 to 34.4 wt.% at 300 °C, without any clear effect on the CHN composition. Ross et al. [193] suggested that the decomposition of small chain organic acids can form carbon monoxide and in-situ hydrogen, which further acts as a proton donor to improve biocrude yield. However, the addition of acetic acid in HTL of sewage sludge resulted in a negligible increase (1.5 %) in biocrude yield but a higher increase (8 %) in N content [162]. Qian et al. [65] compared the influence of heating procedures on the biocrude compositions using isothermal (673 K,

60 min) and fast (773 K, 1 min) HTL of sewage sludge. Biocrude produced with fast HTL features a lower N/C ratio than that obtained with isothermal HTL, while a longer reaction time results in a higher concentration of N-containing compounds in the biocrude.

Considering the minor effects of different parameters on N removal efficiency, it is necessary to get an insight into the reaction mechanism of HTL of sewage sludge. During the hydrothermal conversion process, the peptide bonds in proteins hydrolyse quickly and release constituent amino acids, which can undergo decarboxylation to produce alkylamines and carbonic acid or deamination to form ammonia and organic acids. These products can recombine into aromatic ring structures and N-containing heterocycles. However, proteins are not alone in sewage sludge as they occur along with carbohydrates and sugars, indicating that a complicated cross-linked interaction will definitely occur during HTL to produce complex compounds in biocrude. Lastly, given the great motivation to better understand reactions occurring during hydrothermal liquefaction of sewage sludge, most studies described in the literature have been confined to model systems.

1.4.2 Nitrogen containing model substances

To evaluate the influence of the complex feedstock on the fate of N, most work so far has been focused on the HTL of various types of model substances. Dote et al. [190] used egg albumin (13.9 wt.% nitrogen content) as a model protein to quantify the distribution of nitrogen in bio-oil products. The results of this study revealed a lower ND in bio-oil derived from albumin (about 5 wt.% retained nitrogen relative to the input), compared to silage and sewage sludge (30 – 50 wt.% retained nitrogen), despite both of these starting materials having lower nitrogen contents than albumin (3.9 – 7.4 wt.%). Nineteen different kinds of amino acids were liquefied by HTL to determine the effects of properties of amino acids on N content in the bio-oil. Results demonstrated that the ND in the bio-oil was independent from the nitrogen content in the single amino acids [194]. Teri et al. [195] studied hydrothermal conversion of model compounds (corn starch, cellulose, soy protein, albumin, sunflower oil and castor oil) in a small scale system, and found that the measured bio-oil yields in these mixtures exceeded the mass-average yields calculated from the pure compound results, providing evidence that interactions induced by proteins/amino acids influence the bio-oil yield. However, less information is available on the interactions between model compounds. Posmanik et al. [127] performed HTL of

model compounds (starch, bovine serum albumin and linoleic acid and their binary and ternary mixtures) into bio-oil under different temperatures and retention times. The authors revealed the influence of interactions that occur between these different model compounds based on the change of yields, elemental compositions and HHVs of the bio-oil obtained from HTL. Still, there is little information on the chemical compositions of the bio-oil affected by the interactions. A deeper investigation is needed to understand their contribution to the bio-oil properties.

Maillard reactions have already been confirmed to occur in food chemistry at lower temperatures of about 150 °C, which is caused by the reaction of amino acid groups present in proteins with carbonyl groups present in reducing carbohydrates [196, 197]. During food preparation, hundreds of different flavour compounds attributed to Maillard reactions are created, determining the final flavour of the meal. Depending on the conditions, these compounds can undergo further decomposition into a huge number of different components. This type of reaction can be expected to occur during HTL as well [198]. Peterson et al. [199] determined the degradation kinetics of glucose and glycine during hydrothermal conversion. The results point to Maillard-type reactions which strongly affected the kinetics at 250 °C. However, this complex network of parallel and consecutive reactions, forming different polymers and co-polymers called melanoidins including some N-containing compounds and nitrogenous heterocycles, is poorly understood.

Furthermore, amide formation is also considered an undesired reaction as it contributes to the N content in the bio-oil and decreases the fatty acid yields [200, 201]. To some extent, this reaction can compete with MRs to modify the N content along with the specific N-containing compounds in the bio-oil. However, among the aforementioned hydrothermal reaction studies using model compounds, relatively limited information is available regarding the effects of interaction between lipids and proteins on the chemical components of the biocrude.

1.5 Conclusion and further research

The review provided above reveals the potential of waste sewage sludge as a valuable resource and energy feedstock. However, the complex composition of sewage sludge remains an important limitation due to the high moisture and ash content as well as the

presence of toxic heavy metals and organic contaminants, which influence the quality of final products, reduce the process efficiency, and increase the overall cost of the applied technology. High water content significantly limits the application in landfilling and composting as the sludge volume requires high capacity; incineration and pyrolysis require energy-intensive pre-drying to improve conversion efficiency. Currently, anaerobic digestion seems to be the most appealing process due to its lower capital costs and absence of drying requirements. Even though, low biogas production and process instability still constitute unsolved challenges. Taking the best advantage of higher water content, hydrothermal conversion is a promising technology to simultaneously achieve disposal and utilization.

Compared with hydrothermal gasification and carbonization, hydrothermal liquefaction has been drawing more attention in recent years. Without pre-drying, condensed liquid biocrude can be obtained at relatively low temperatures with reasonable reaction times. However, sewage sludge is a protein-rich waste, indicating the inevitable N-containing compounds must be converted into biocrude, which is considered a big challenge and makes it hard to meet fuel standards.

A considerable amount of work can be found on the improvement of the yields and quality of biocrude by adjusting the reaction parameters and introducing other feedstocks for co-liquefaction. However, these methods are not significantly effective in N reduction. Pre-/post treatments are inevitable in combination with HTL to improve the biocrude quality for fuel applications. Pre-treatment can facilitate HTL conversion of sewage sludge by changing the physical and chemical structures of organic components; post-treatment like catalytic upgrading for HDN could achieve desirable results, and the N content in the upgraded bio-oil can be effectively reduced to 0.1 wt.%. It is to be noted that these processes increase the complexity and investment costs. Therefore, the implementation of considered technologies associated with HTL for obtaining nitrogen-reduced biocrude is only appropriate and useful with a better understanding of the behaviour of N during HTL.

However, very little research actually focuses on the chemical behaviour of biocrude and N transformation during HTL of sewage sludge, and even less of it reveals the reaction pathways of N-containing compounds and the influence of various parameters and combined/integrated processing. A deeper investigation on the fate of N during HTL of sewage sludge contributes to an understanding of the entire reaction mechanism of HTL,

and studies of specific N-containing compounds formed during HTL can offer better mechanistic insights into N removal through post-treatment. A complete process chain including combined approaches can be theoretically recommended and practically examined.

Chapter 2 The aim and outline of this thesis

The overall aim of this thesis is to pave the way for the utilization of waste sewage sludge as an energy source through hydrothermal liquefaction, with the goal to concurrently solve growing environmental waste management issues and to produce alternative, renewable fuels. For fuel applications, the problematic N content in the biocrude derived from HTL of sewage sludge has to be significantly reduced. However, the reviewed work carried out so far has revealed the difficulty of N removal by the various approaches tested. Therefore, as a main goal, it is extremely significant to get a mechanistic insight into the N-containing compounds in the biocrude. Therefore, this has a focus on fundamental research, and specifically makes an effort to investigate the interactions between different organic compounds, such as amidation and Maillard reactions. Thus, a series of HTL experiments with sewage sludge and model substances has been conducted to determine the complex mechanism of reactions under different conditions. In order to achieve these aims, a number of objectives with associated goals are outlined below and have been investigated in this thesis.

Characterize the N content during conversion of sewage sludge to biocrude through HTL: the N content should be as low as possible to improve the biocrude quality for further fuel application. The investigation of the N behaviour in the different product phases during HTL of SS helps to understand the transformation of N into biocrude and to find optimized process conditions.

Achieve relevant results for the industry: the lab-scale experiments will be finally applied in an industrial scale for commercialization. The comparison between batch and continuous-flow processes will provide valuable information for the development of this technology.

Understand the reaction mechanism of N-containing compounds in the biocrude: the reaction pathways of problematic N-containing heterocycles should be understood as deeply as possible, offer a valuable mechanistic insight into the N issue during HTL of sewage sludge and fill the gap of overall reaction pathways in HTL of N-containing feedstocks.

Valorise sewage sludge through energy recovery: the energy recovery from SS should be as comprehensive as possible to achieve better energy efficiency for commercial

application. The synergistic effects on the integrated approaches should be estimated.

In this thesis, **Chapter 1** provides a review of available literature on the subject area covered within this thesis. HTL shows a promising opportunity for processing sewage sludge with respect to the utilization of water and the production of sustainable biofuel. A detailed study of the literature on HTL of sewage sludge with a specific focus on the fate of N was performed for the purpose of this thesis. The aim and outline was highlighted in **Chapter 2** in line with the conclusion of the introduction.

Chapter 3 describes the methodology used for most experiments. The main objective of this chapter is to describe the general methods applied in this thesis, trying to avoid repeated descriptions in the following chapters. Further, it is useful for readers who want to familiarize themselves with the analysis methods. The specific methodology, including the selected chemicals, is individually described in the following chapters.

Chapter 4 presents the transformation and behaviour of N during HTL batch processing under different temperatures. The objective of this work is to lay the foundation of the thesis, obtaining a general understanding of the biofuels produced through HTL of sewage sludge, with a special focus on the N-species in the biocrude.

Chapter 5 presents a systematic study of continuous flow HTL of sewage sludge under optimized conditions. These experiments help investigate the technical problems associated with practical feasibility by selecting a suitable type of sewage sludge with a certain slurry concentration and adjusting the separation procedure. The comparison of results obtained between batch and continuous HTL processes can help to fill the gap between lab-scale and pilot-scale applications.

Chapter 6 exhibits HTL of model substances under different conditions. The objective of this chapter is to firstly investigate the influence of lipids on the fate of N during HTL of mixtures and to reveal the mechanistic pathways of amide formation.

Chapter 7 outlines a more detailed mechanism of Maillard reactions during HTL of model carbohydrates and proteins. The intention of this work is to investigate the effects of heating rate and residence time on the fate of N during HTL, and to further elucidate the reaction scheme of Maillard reactions.

Chapter 8 outlines an integrated approach that combines lipid extraction with HTL of

lipid-extracted sludge to accomplish an alternative path to the complete valorisation of sewage sludge. Previous chapters have confirmed the high dependency of Maillard reactions and amidation on the temperature; it is therefore interesting to evaluate whether lipid-extracted sludge can be a potential feedstock for the production of fuel-like products, to estimate the coupling effect of lipids extraction and HTL of LESS, as well as to assess the energy efficiency of the combined approach.

Chapter 9 presents the overall conclusion and a brief outlook. Every though a specific conclusion is being given in each of the previous chapters, this is a comprehensive conclusion to summarize the whole work and to bring up the highlights to response **Chapter 2**. The limitations of the research performed in this thesis are identified and further work is proposed.

Chapter 3 Methodology

3.1 Characterization of sewage sludge

3.1.1 Proximate and ultimate analysis

In this work, two types of sewage sludge feedstocks were tested. One type of sludge was sourced from the wastewater treatment plant (WWTP) in Plieningen near Stuttgart in Germany. Municipal sewage from Stuttgart and suburb cities as well as sewage from the airport and the fair is treated in Plieningen's WWTP. Another type of sludge was collected from the Karlsruhe wastewater treatment plant in Germany, constituted by mixed primary and secondary sludge.

The sewage sludge was stored at -18 °C until used in experiments. The moisture content of the raw sludge was determined through weight loss due to drying at 105 °C for 24 h. The ash content was determined by weight loss due to drying in a muffle oven under atmospheric conditions at 550 °C for 5 h.

The elemental content in sewage sludge was measured using elemental analysis (Vario EL III, Elementar Analysensysteme GmbH, Hanau, Germany), with the O content being calculated by difference. The higher heating value (HHV; MJ/kg) was estimated using the modified Dulong's formula [127].

Metals in the bio-crude were analysed using an ICP-OES Spectrometer (Agilent Technologies 725, Australia) after dissolution in 5 mL conc. 37 % hydrochloric acid (HCl) and 2 mL conc. 65 % nitric acid (HNO₃).

3.1.2 Organic components

Protein quantification For protein analysis, the Kjeldahl method for organic nitrogen was used. It involves acid digestion of the organic solids followed by distillation and measurement of the released ammonia.

(The total Kjeldahl nitrogen (TKN) and ammonia nitrogen contents were measured by Buchi AutoKjeldahl Unit K-370 after mineralization with Buchi Digestion Unit k-435 (for TKN only). The organic nitrogen content was calculated by difference between TKN and ammonia nitrogen. The total nitrogen is the sum of nitrates, nitrites, ammonium, and organic nitrogen. Organic nitrogen is calculated by subtracting nitrogen oxides and ammonia from TN. Nitrogen oxides were measured with HACH LANGE kits, (nitrites and nitrates). The protein content is estimated under the assumption that 16.5 wt.% of

proteins contains nitrogen (or 6.25 g proteins g/N) [113, 202, 203].

Carbohydrates quantification For carbohydrate measurements, photometric estimation by the DuBois method was used after treating samples with phenol [202, 204]. Sample preparation was carried out by adding 0.5 g ground dry sewage sludge, which was mixed with 2.5 mL sulfuric acid (12 molar) at room temperature for 16 h. This was followed by heating in a boiling water bath for 5 h using hot oil and a heating plate; hydrolysis of carbohydrates occurred. Hydrolysed samples were diluted, neutralized by sodium hydroxide (6 molar) to a pH of 6.8 – 7. After diluting to a volume of 100 mL, 2 mL of diluted sample was mixed with 50 μ L of a phenol solution (80 wt.%) and 5 mL concentrated sulfuric acid. The mixtures were placed in a water bath at 30 °C for 20 min and were finally measured with a photometer at 490 nm wavelength.

Lipids quantification The extraction was carried out in a Soxhlet apparatus using hexane mixed with ethanol as a solvent [115, 117]. For practical operation, a common 30 mL Soxhlet apparatus was installed and equipped with a condenser on top and oil heating bath underneath. 5 g of dried sample were poured into the thimble and 90 mL of solvent mixture was placed in the still pot. While heating the oil, solvents evaporated and condensed again in the upper condenser. Liquids dropped back, filled the Soxhlet container and lipids were washed out. With the filled siphon, liquids are capable of leaving the chamber and are released to the initial lower solvent glass tube. Within a few minutes, one passage is passed through. Extraction is sustained for approx. 6 h. After extraction, the mixed solvent was removed using a rotary evaporator at 40°C under vacuum at 50 mbar. Then, the remnant lipid fraction was stored in a desiccator overnight and weighed the next day to determine the extraction yield.

3.2 Chemicals

The water used is distilled water. HPLC (High Performance Liquid Chromatography) grade dichloromethane (DCM) purchased from Sigma-Aldrich was used for biocrude recovery throughout the entire work on the thesis, except for the continuous HTL process in Chapter 5.

Other chemicals are either HPLC grade or analytical grade and will be specified in each chapter. HPLC grade tetrahydrofuran (THF) purchased from Sigma-Aldrich were used for the dilution of biocrude.

3.3 Hydrothermal liquefaction process

3.3.1 Batch process

The detailed preparation of feedstock and HTL reaction conditions is described in the different experimental set-ups for each chapter. Here, only the general method is introduced in the following.

The batch HTL process was performed in micro-autoclaves shown in Figure 3-1, with a volume of 24.5 mL, made of stainless steel (1.4571 Ti), which can withstand pressures of up to 40 MPa and a maximum temperature of 400 °C. The reactors were loaded with carefully weighed amounts of feedstocks. Micro-autoclaves were flushed to remove the undesired air and then pressurized to 2 MPa using nitrogen gas.



Figure 3-1 Micro-autoclaves used for batch HTL process

Heating was performed in a gas chromatography (GC) furnace (Hewlett Packard) or a fluidized sand bath (SBL2, Teche) and kept at the target temperature for the designed retention time. After the reaction, the autoclaves were taken out of the heating device and put in cold water to cool down and to stop the reaction. All the experiments were executed at least twice to achieve better reproducibility.

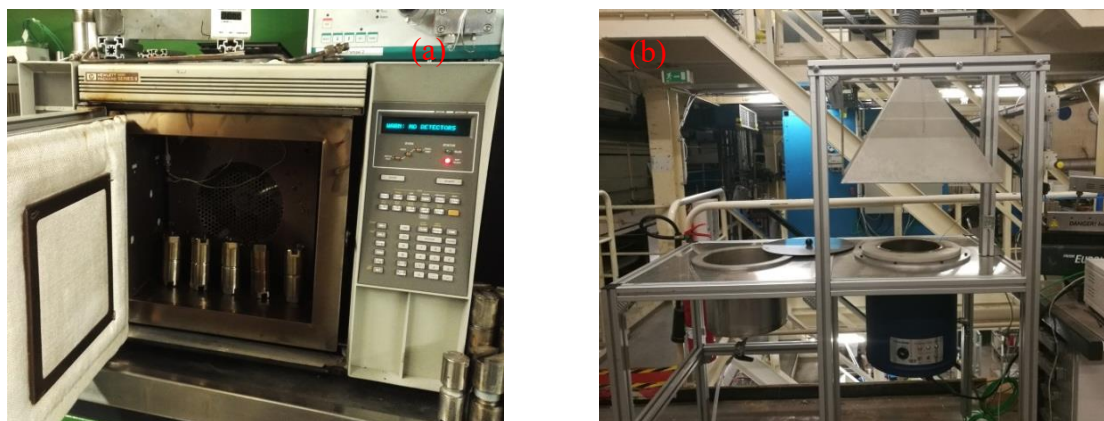


Figure 3-2 Heating devices for batch HTL (a) GC-oven; (b) fluidized sand bath

After the HTL reaction, the micro-autoclaves were opened in a gas-tight containment after being flushed with nitrogen. The amount of formed gas was measured by water displacement. Gas was collected for the gas chromatograph.



Figure 3-3 Gas collection system

The aqueous phase, biocrude and solid residue were washed with dichloromethane (DCM), then the mixed products were filtered by vacuum filtration using a Whatman nylon membrane (47 mm, 0.45 μm pore size). Part of the bio-crude and solid residue remained stuck to the micro-autoclave walls after the reaction, so the additional use of a solvent, DCM, was required to completely recover the products. The solid residue remaining in the filter was placed in an oven and dried overnight at 105 $^{\circ}\text{C}$ to determine its dry weight. The bi-phase mixture obtained (aqueous product plus bio-oil) was centrifuged and separated. The organic solvent was evaporated by flushing with nitrogen for 24 h. Once a constant weight had been achieved, it was recorded and considered the bio-oil mass. The flow chart of procedures for product separation and extraction is listed in Figure 3-4.

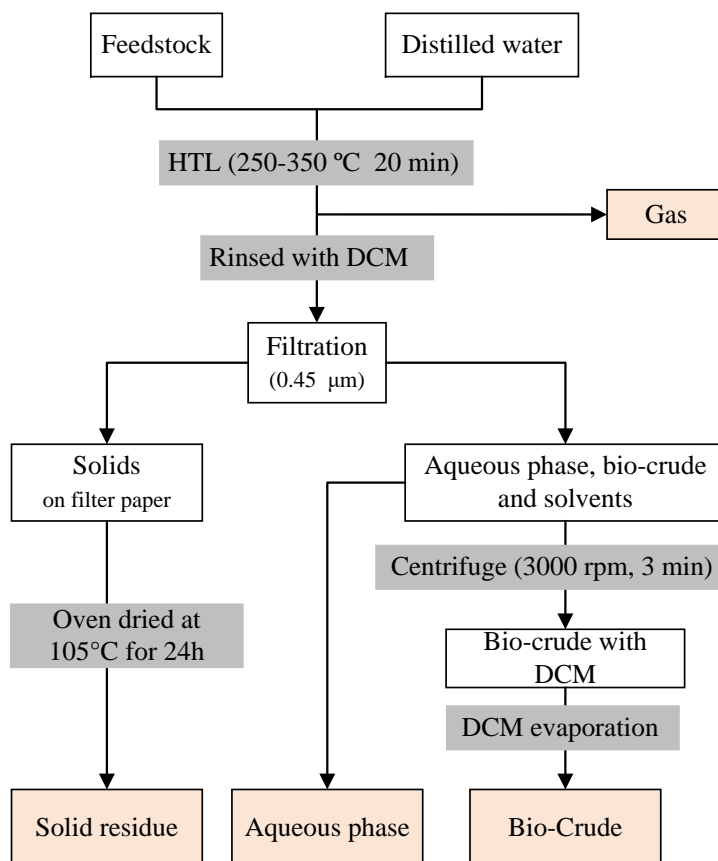


Figure 3-4 Procedures for product separation and extraction from batch HTL process

3.3.2 Continuous process

The continuous flow HTL plant was designed and built in-house at IKFT. The upper design temperature and pressure of the system are 450 °C and 350 bar, which fall in the sub-/supercritical range of water. The experimental work on the continuous flow hydrothermal reactor is described in detail in Chapter 5.

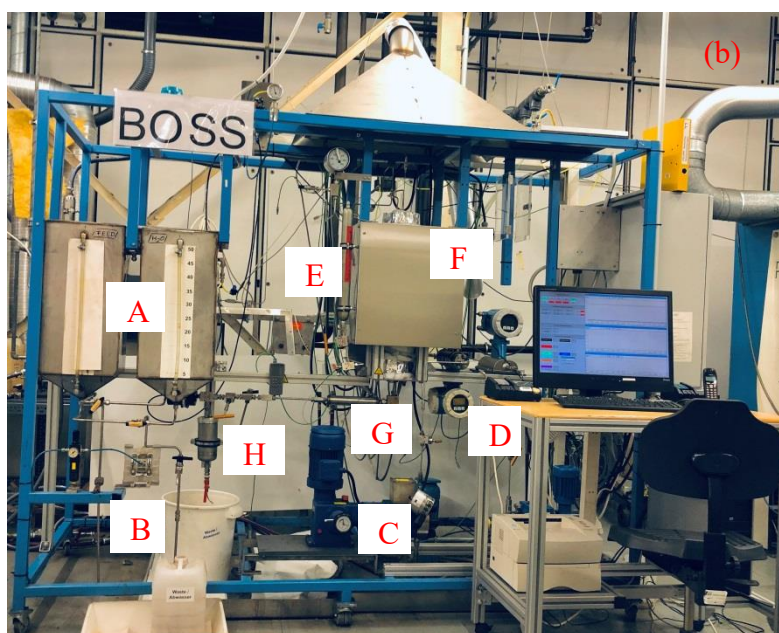
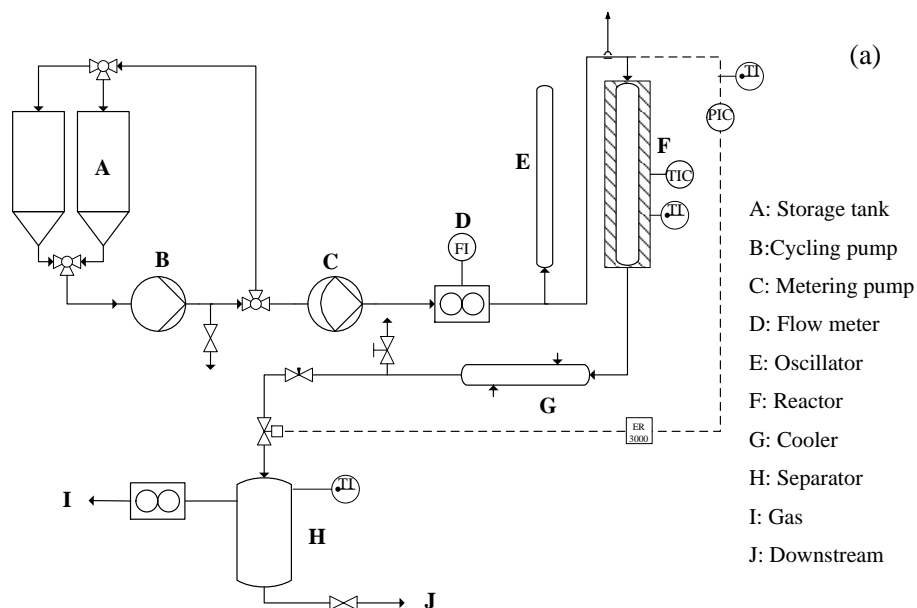


Figure 3-5 (a) Schematic flow of the continuous Process (b) continuous reactor

The process flow diagram of the plant is presented in

Figure 3-5. The continuous HTL plant is composed of: (1) two atmospheric-pressure storage tanks; (2) a recycle pump to recirculate the feed slurry and to avoid sedimentation problems; (3) a NOVADOS BRAN LUEBBE NP31 high-pressure metering pump, which is capable of delivering high viscosity fluids and slurries at up to 50 bar and flow rates of up to 15 L/h; (4) a PROMASS 80 F flowmeter to measure the actual slurry feed rate; (5) a vertical tubular reactor with an internal volume of 350 mL made of stainless steel 1.4571, the reactor was heated electrically by heating cartridges inserted into the wall of the

reactor; (6) a pressurized vessel located at the same length of the reactor to minimize the pressure oscillations inside the system during the experiments; (7) a cooling system connected with a water supply; (8) a pneumatic valve SITEC controlled by a Tescom ER 3000 is utilized in the process for pressure regulation; (9) a Ritter Gas Counter is able to measure the produced gas volume; (10) a vessel to collect downstream output. The entire plant is controlled via WinCC software supplied by Siemens. Process variables including temperature, pressure and flow rate are specified by the operators.

The plant can provide residence times between 50 seconds and 12 minutes. For this study, the flow rates were adjusted from 2 kg/h, leading to residence times within the reactor of 8 mins at a temperature of 350 °C. The plant was pre-heated by pumping water flux until the desired conditions were reached. In order to keep a constant slurry flow rate of 2 kg/h, the regulator of the piston stroke in the metering pump was regulated to 12 mm. When the fluid dynamics of the continuous plant were validated at 350 °C, the practical feasibility to pump sludge slurry was challenged. Though the metering pump is capable of delivering high-viscosity fluids and slurries, the nature of the suspended particles may bridge and plug the orifices and valves.

3.4 Products analysis

3.4.1 Gas analysis

The gas composition was measured by manually injecting 100 µL of the gas sample in an Agilent 7890A gas chromatograph (equipped with a 2 m Molsieve 5 Å and 2 m Porapak Q column). Detection succeeded via Flame Ionization Detection (FID) and Thermal Conductivity Detection (TCD). Detected gases were hydrogen, nitrogen, oxygen, carbon mono- and dioxide as well as C1-C4 gases.

3.4.2 Biocrude analysis

The C, H, and N contents were measured by the same CHNS-analyser for solid raw sewage sludge samples, with the O content being calculated by difference. The elemental measurements are checked for deviations by way of 10 measurements of one representative biocrude sample. The statistical errors of C, H, and N were 0.45, 3.03, and 0.69 %, respectively.

Qualitative analysis of biocrude was carried out using an Agilent 6890N gas chromatograph (GC) with an Agilent 5973 MSD mass spectrometry (MS) detector and a

DB-5 capillary column ($30 \times 0.25 \text{ mm} \times 0.25 \text{ }\mu\text{m}$) after diluting with THF (1:10 ml/ml) and filtering with a $0.20 \text{ }\mu\text{m}$ polytetrafluoroethylene (PTFE) filter. The substances were identified using the NIST library, considering only molecules with an identification probability of more than 80 %. The amount of the different compounds was estimated with the relative peak area percentage method.

The quantitative analysis of selected chemicals identified by GC-MS was measured by two GC-FID devices. Most non-polar chemicals were measured by GC-FID with an Agilent a DB-5 capillary column ($30 \times 0.25 \text{ mm} \times 0.25 \text{ }\mu\text{m}$). The GC oven column temperature was kept at $80 \text{ }^\circ\text{C}$ for 2 min, held at $175 \text{ }^\circ\text{C}$ for 5 min, after ramping at $5 \text{ }^\circ\text{C}/\text{min}$, and held at $250 \text{ }^\circ\text{C}$ for 8 min after ramping at $30 \text{ }^\circ\text{C}/\text{min}$. Organic acids were analysed by GC-FID with Restek-11023 Stabilwax-DA capillary column ($30 \times 0.25 \text{ mm} \times 0.25 \text{ }\mu\text{m}$). The GC oven column temperature was kept at $40 \text{ }^\circ\text{C}$ for 6 min, then increased to $225 \text{ }^\circ\text{C}$ for 0 min at $10 \text{ }^\circ\text{C}/\text{min}$, and held at $250 \text{ }^\circ\text{C}$ for 15 min after ramping at $30 \text{ }^\circ\text{C}/\text{min}$.

Thermal gravimetric analysis (TGA, SAT 409, Netzsch, Germany) was used to study the thermal stability and combustion behaviour with a heating rate of $10 \text{ K}/\text{min}$ and an N_2 flow rate of $50 \text{ mL}/\text{min}$.

The distribution of functional groups was measured by nuclear magnetic resonance (NMR) and Fourier Transform infrared spectroscopy (FT-IR) analysis. FT-IR was performed using a Varian 6600 Fourier Transform Infrared Spectroscopy over a range of $350 - 4000 \text{ cm}^{-1}$. $^1\text{H-NMR}$ spectra were measured with the following parameters: 90° pulse program ($4.95 \text{ }\mu\text{s}$), acquisition time 10 s, relaxation delay 1.0 s, number of scans 24, spectral width 3255.2 Hz and time domain 32 k. $^1\text{H-NMR}$ data was processed using MestReNova (version 9.0).

3.4.3 Aqueous phase analysis

The total carbon (TC), total inorganic carbon (TIC) and total nitrogen (TN) in the aqueous phase (AQ) were measured with a Dimatec® 2100 instrument. Ammonium (NH_4^+), nitrate (NO_3^-) and nitrite (NO_2^-) were investigated with a Metrohm 838 advanced sample processor device. Organic acids were analysed with an Aminex HPX-87H column (Biorad, Hercules, CA, USA). The mineral composition in the aqueous phase was analysed using an ICP-OES spectrometer (Agilent Technologies725, Australia) after dissolution in HCl and HNO_3 .

HPLC with a Lichrospher 100 RP-18 column (Merck, Darmstadt, Germany) was used to measure HMF in the aqueous phase.

The amino acids are separated and determined by ion exchange chromatography and ninhydrin post-column derivatization using an amino acid analyser (Biochrom 30, USA).

3.4.4 Solid residue analysis

Ash content, elemental composition and metals in the solid residue (SR) were measured using the same methods applied to raw sewage sludge in Section 3.1.1.

The crystalline structure was investigated by powder X-ray diffraction (XRD) using an X'Pert PRO MPD instrument (PANalytical GmbH) equipped with a copper anode (Cu $K\alpha$ 1.54060 Å). The sample was measured in a 2θ range between 5° and 120° for 2 h.

The solid residue surfaces were analysed using X-ray photoelectron spectroscopy (XPS). A layer of solid residue powder was uniformly glued on a silver tape and fixed in a molybdenum sample holder. The measurements were performed in an ultra-high vacuum chamber (base pressure $10 - 8$ Pa) equipped with an unmonochromated XR-50 Mg K alpha X-ray source and a Phoibos 150 analyser (manufacturer SPECS). The angle between the analyser and the X-ray source was 45° . The electrons originating from a sample were detected along the surface normal of the sample (sample area: 2 mm diameter); the energy scale was calibrated using the Ag 3d peak of a silver reference sample. Peak shifts due to charging effects were compensated using the flood gun FG 15/40 (SPECS). The chemical composition was quantified by the software Casa XPS.

3.5 Data interpretation

In this work, the uncertainty, namely the loss of recovery, is due to the remaining products stuck to the micro-autoclave walls after the reaction, and the loss of volatile compounds (during extraction solvent removal), water formation, and experimental errors. To confirm the reproducibility and comparability of results, experiments were carried out in duplicates. Each data point has been represented as the average of the two independent experiments, with an error corresponding to its standard deviation. In cases where the deviation between the two data sets was above 10 %, the experiment was repeated.

The yields (Y_i) of the different product fractions were calculated as the weight of the recovered mass of organic matter in the product (OM_i) related to the total mass of organic matter in the feedstock ($OM_{feed, daf.}$), see Eq. (3-1).

$$\text{Product Yields (wt. \%)} = \frac{OM_i}{OM_{feed}} \times 100 \quad (3-1)$$

The HTL conversion efficiency was calculated as the difference in feedstock mass (OM_{feed}) and solid residue (OM_{SR}) (assuming this to be unconverted feedstock) related to the feedstock mass (OM_{feed}), as shown in Eq. (3-2).

$$\text{HTL conversion efficiency (\%)} = \frac{OM_{feed} - OM_{SR}}{OM_{feed}} \times 100 \quad (3-2)$$

The elemental distribution, namely carbon distribution (CD) and nitrogen distribution (ND) are defined as the amount of an element in the product (m_{Ei}) relative to the amount in the SS product (m_{Ef}), see Eq. (3-3).

$$\text{Elemental Distribution (wt. \%)} = \frac{m_{Ei}}{m_{Ef}} \times 100 \quad (3-3)$$

The higher heating value (HHV; MJ/kg) was estimated using the modified Dulong's formula [127] as given in Eq. (3-4).

$$HHV(\text{MJ/kg}) = 0.0338 \times C + 1.428(H - O/8) \quad (3-4)$$

The energy recovery (ER) as the sum of the higher heating values (HHV_i) of the recovered fuel-like products (biocrude, bio-char) weighed by their yield Y_i^* relative to the value (HHV_{feed}) of the dry feedstock, Y_i^* , is the yield based on the dry basis, see Eq. (3-5).

$$ER (\%) = \frac{\sum (Y_i^* \times HHV_i)}{HHV_{feed}} \times 100 \quad (3-5)$$

Chapter 4 HTL of sewage sludge via batch process

4.1 Introduction

As stated in Chapter 1, hydrothermal liquefaction is considered an effective approach to produce the associated potential added-value products from sewage sludge. A large number of literatures published in recent decades are available. Previous studies have investigated the application of HTL technology for SS, under different conditions with or without catalysts. A controllable product quality is still hard to achieve. It is still considered a challenge to employ the biocrude without any type of upgrading, as meeting industrial standards proves difficult, for instance, due to the high N content [72, 170]. A reduction of this N content would decrease the cost of downstream processing, but the attainment of such a situation requires a deeper understanding of the fate of nitrogen during HTL.

In the current chapter, a systematic analysis of N behavior across different products is conducted, with the motivation to gain a general understanding of the fate of N during HTL of sewage sludge.

4.2 Methodology

4.2.1 Materials

The sewage sludge tested in this chapter was sourced from the WWTP in Plieningen near Stuttgart in Germany, and collected in the form of digested sludge. The chemicals are described in Section 0.

4.2.2 Pretreatment of sludge

As certain flaws regarding inhomogeneity of the RSS surfaced during the course of the experiments, efforts were made to homogenize the sludge. The frozen sludge from the freezer was first dewatered by freeze-drying at -82 °C and 30 mbar for three consecutive days (Christ Alpha 2-4 freeze-dryer), then the dried sludge was crushed in a mill (Fritsch Pulverisette 14, Germany) and filtered through a sieve (60 mesh). A certain amount of water was reintroduced and stirred to achieve the original water content.

4.2.3 HTL procedure

This HTL batch process was carried out in micro-autoclaves with a volume of 24.5 mL at designed temperature for 20 min. In this chapter, the experimental sets were heated with a GC oven. In order to keep the reaction pressure inside at 200 bar, the loading of raw sludge or prepared slurry was 14.7, 17.4 and 19.0 g at 250, 300 and 350 °C, respectively. Sample separation and analysis was the same procedure as described in Section 0.

4.3 HTL of sewage sludge

4.3.1 Feedstock characterization

The property of the sewage sludge originating from the WWTP is listed in Table 4-1. Protein was found to be the predominant fraction, accounting for 34.6 wt.%, which is within the range available in the literature (30 – 60 wt.%) [110, 113], including raw primary sludge [66], secondary sludge [67], and digested sludge [66]. The results were quite consistent after 5 runs with 10 parallel repetitions each. Lipids were found to be a minor component of sludge, constituting 13.9 wt.% of the raw material. Special attention must be paid to the nitrogen content in the feedstock, as this is an important control parameter for the quality of biocrude [76, 205] due to the formation of NO_x during combustion and the demanding treatment during biocrude upgrading. However, protein-rich sludge may still be desirable because of the higher thermochemical biocrude conversion efficiencies compared to those obtained with biomass that is richer in more recalcitrant carbohydrates and lignin [120].

Table 4-1 Characterization of sewage sludge sample used in this study

Moisture (wt.%)		Ash (wt.%) ^a		Organic compositions (wt.%) ^a							
				Carbohydrates		Proteins		Lipids		Others	
78.75		35.61		27.9		34.6		13.9		23.6	
Elemental compositions (wt.%) ^a											
C		H		O ^b		N		S		HHV (MJ/kg)	
29.10		5.70		23.19		5.00		0.90		13.84	
Inorganic content (wt.%) ^a											
Al	Ca	Fe	Mg	Mn	P	Zn	Ba	Cr	K	Na	Cu
4.26	3.7	1.17	0.03	0.03	3.31	0.14	0.05	0.01	0.57	0.16	0.04

^a: dry basis

^b: calculated by difference

4.3.2 The influence of pre-treatment

It is accepted that the direct application of sludge received from the WWTP for HTL experiments may be closer to scale-up process, to avoid unnecessary pre-processing cost.

Pre-drying with processes such as freezing or oven drying is impossible in industrial applications, and crushing is quite a costly process. However, in lab-scale work, the homogenizing process is aimed at reducing the uncertainty between duplicate experiments to reach reliable results. To examine the pre-treatment's influence on the certainty of the experiments' outcomes, the biocrude obtained through HTL of raw and treated sludge are compared at 300 °C in this chapter. It is noted that the depicted values are averages of four and two experimental results for the raw sludge and treated sludge, respectively. Unsurprisingly, the uncertainty achieved in HTL of raw sewage sludge is much higher than that of treated sludge, with a value of 36 % and 2.6 %, respectively. In the latter case of HTL of treated sludge with only two sets of HTL, which is half the repetitions as compared to HTL of raw sludge, a negligible uncertainty was found. Additionally, the pre-treatment caused a drastic increase of bio-crude yields in all experiments involving pre-treatment. Before and after treatment, the bio-crude yields significantly increase from 12.98 to 18.63 wt.%. This significant difference is ascribed to the property of sewage sludge being composed of inorganic and organic compounds as stated in Chapter 1.1. And the HTL process is a self-catalytic reaction with water as reaction reagent, while ash behaves as a metal catalyst. Homogeneity is a favourable condition not only to achieve the experimental reproducibility, but also to enlarge the contact surface area of chemicals in the SS to react with homogeneous and heterogeneous additives and catalysts. Therefore, in order to minimize the uncertainty and maximize the biocrude products, the experiments below were performed with treated sludge.

4.3.3 Product yields

Mass balance

The mass balance of different phases is estimated on a dry-ash free basis. In practice, the quantity of organic matter in the water phase is difficult to assess with simple drying, because many compounds are volatile, resulting in the loss of organic content. According to literature, the aqueous phase yield is calculated by difference, closing the mass balance of the organic matter to 100 %. However, by this calculation, the aqueous phase yield also integrates the mass balance closure error. Because of hydration and dehydration reactions, the overall organic mass balance does not necessarily add up to 100 %. Therefore, the mass yield of organics is not separately reported in the aqueous phase, unlike the mass yield of the other phases, since it cannot be accurately determined. Complete closure of

mass balance was not possible due to experimental errors such as leaking a few drops of mixture while opening, residue being stuck to the vacuum filtration's funnel, crudes and solid residue remaining on the reactor walls, and biocrude volatilizing during the solvent removal. These, together with the aqueous phase and were calculated by difference, are defined as uncertainty as shown in Figure 4-1.

Around 50 wt.% of OM is turned into solid residue through HTL of SS at 250 °C, while the solid residue yields decrease with the increase of biocrude yields at rising temperatures. A strong temperature dependency was observed in the experiments as the yields of biocrude increased from 12.02 to 22.05 wt.% at 350 °C, yielding around 80 % more biocrude than the experiments conducted at 250 °C. The yields of biocrude and aqueous phases increased at the expense of the solid residue in the investigated temperature range, indicating that the organic compounds in the solid phase decompose into water-soluble chemicals. Oligomers and monomers are produced through condensation, dehydration, and decarboxylation reactions to form biocrude.

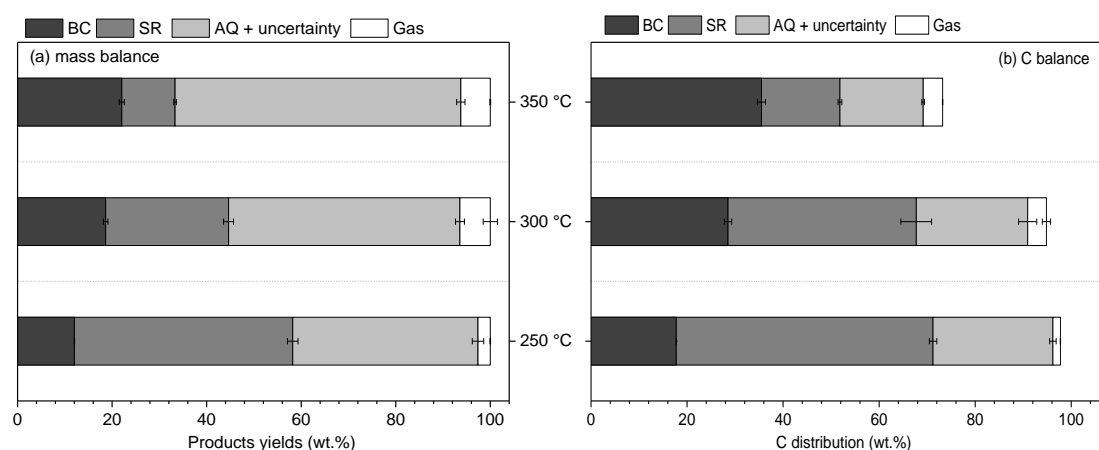


Figure 4-1 (a) mass balance and (b) carbon (C) balance of products from HTL of SS at different conditions

Unlike organic content in the aqueous phase, carbon recovery in the aqueous phase can be easily determined. Therefore, the C balance between biocrude, solid residue, aqueous and gas phases is also reported. The C balance/distribution in different phases is compared in Figure 4-1. The total C recovery ranges from 73.2 to 97.8 %. Notably, an increase of the C distribution to biocrude with a decrease to solid residue and the aqueous phase is observed with the increasing temperature. Even the smallest part of C was converted into the gas phase, an increase by nearly factor 2 is obtained at the highest temperature. At 250 °C, around half C remains in solid residue, followed by the aqueous phase, while the third part contributes to biocrude. With the decrease of C in solids and the aqueous phase,

the C divided in biocrude is higher than that in the aqueous phase at 300 °C, reaching the maximum percentage of 35.5 % at 350 °C. The measured C balance decreases with increasing temperature, indicating that the formation of volatile compounds that are evaporated during the removal of the solvent by N₂ flushing is favoured by higher temperatures.

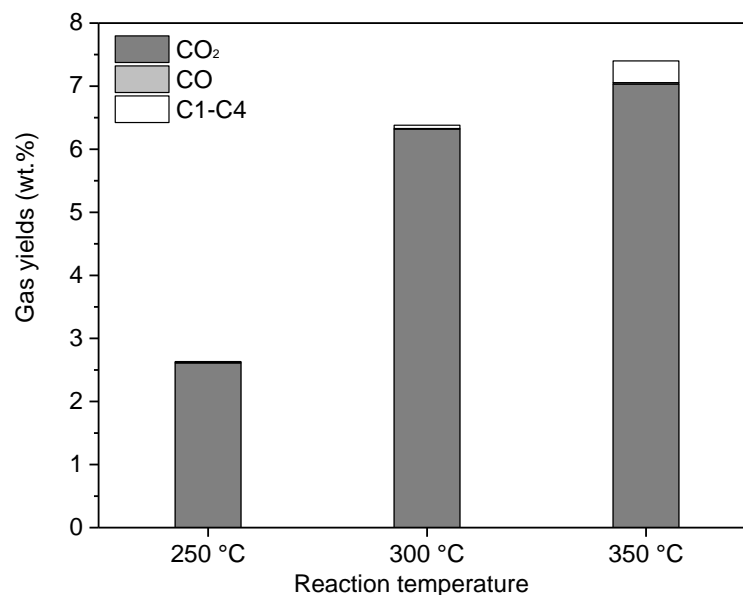


Figure 4-2 Gas yields from HTL SS at different temperatures

The gas products are displayed in

Figure 4-2, although the highest yield is less than 12 wt.%. Exploration of the composition of produced gases is important for the investigation of the HTL reaction mechanism. The gas produced by HTL of SS mainly consisted of CO₂, CO, and C1-C4 light gas, which includes methane, ethane, ethane propene, propane, i-butane, and n-butane. CO₂ is the major fraction, which significantly increased with rising temperatures, suggesting that decarboxylation occurs across HTL to release carbon dioxide, and that an increase in temperature favours CO₂ production. The generation of C1-C4 gases increases with the experienced temperature. The CO generation remained low at all temperatures with a slight general increase at 350 °C. With regard to the N-species gas, to my knowledge, only one reference is available to report the N-containing gases consist of NO₂, N₂O, HCN and NH₃ after HTL of algae, which is not quantified, and the N distribution in the gas phase was calculated by difference [193]. In other publications covering the pyrolysis of sewage sludge, HCN and NH₃ were reported as the predominant N-containing gases based on the immediate measurement of FTIR [186]. It would be

more helpful to close the N-balance and understand the removal of N in the form of gas if the N-species gas could be characterized, however, due to the limitation of the analytic technique and the lower yields of total gas at the HTL temperature investigated, it is assumed that the N-containing gases are negligible.

4.3.4 Characterization of Bio-crude

Elemental composition

The elemental compositions of the biocrude products from HTL of SS samples are compiled in Table 4-2. Compared with the SS feedstock, the recovered biocrude has significantly higher carbon and hydrogen, and lower nitrogen and oxygen contents. The carbon content in the biocrude increases from 66.5 to 72.8 wt.% with raising temperature.

Table 4-2 Elemental composition and high heating values in the obtained bio-crude

samples	C (wt.%)^a	H (wt.%)	N (wt.%)	O^b (wt.%)	S (wt.%)	HHV(MJ/kg)
250 °C	66.5	9.9	7.6	14.0	2.0	34.1
300 °C	69.2	10.0	6.8	12.4	1.7	35.5
350 °C	72.8	10.0	6.0	9.8	1.5	37.1

^a: dry organic basis

^b: calculated by difference

No significant difference can be observed regarding the H content in all the biocrude products, ranging between 9.5 – 10.2 wt.%. The N content in the biocrude decreases with the reaction temperature. A maximum reduction of about 23 % is observed at 350 °C, suggesting the deamination is facilitated by high temperatures. A significant reduction in O is observed compared with the initial content of SS feedstock, which is mainly removed in the form of H₂O and CO₂ by dehydration and decarboxylation. Furthermore, the decrease of O with the reaction temperature is in consistent with an increase of CO₂ in the gas products. The sulphur content is reduced with increasing temperature. The heating values of the biocrude products were almost tripled compared to those of the feedstock (13.84 MJ/kg vs. 37.32 MJ/kg), close to those reported for biocrude produced from sewage sludge (35 – 40 MJ/kg) [65] and paper sludge (35 – 37 MJ/kg) [191], but lower than those of petroleum crude oil (43 MJ/kg) [206].

GC-MS characterization

Nitrogen-containing compounds are another important characteristic of biocrude. Qualitative analysis of the biocrude composition is conducted with GC-MS. For each biocrude sample, approximately 80 % of the sum of GC-MS peak areas was identified. By using this technique, the biocrude obtained through HTL of sewage sludge at 300 °C

was selected to be representative in this chapter. The major GC-detectable compounds were listed in Table 4-3. These compounds were also categorized into 5 groups according to the functional groups: N-containing heterocycles, amines and amides, hydrocarbons, O-containing compounds, and others, mainly composed of unknown substances. It should be noted that some low molecular weight components may have gotten lost during the solvent evaporation process for biocrude oil recovery, while some higher molecular weight compounds might not have eluted from the GC column. Thus, not all components in biocrude can be characterized through GC-MS.

Table 4-3 Identified main components of biocrude obtained from HTL of SS at 300 °C and relative percentage in the total ion chromatogram (RT: retention time)

RT (min)	Components	Relative area (%)
6.98	Pyrazine, methyl-	1.5
8.46	pyrazine,2,5-dimethyl-	2.0
8.51	Pyrazine, ethyl-	1.4
9.62	Pyrazine, 2-ethyl-6-methyl-	0.9
9.67	Pyrazine, 2-ethyl-5-methyl-	2.6
10.5	Pyrazine, 3-ethyl-2,5-dimethyl-	1.3
10.64	2,5-Pyrrolidinedione, 1-methyl-	5.2
10.69	1,5-Dimethyl-2-pyrrolidinone	
11.18	1H-Pyrrole, 2-ethyl-3,4,5-trimethyl-	0.9
12.58	1H-Indole	1.2
13.19	2,5-Pyrrolidinedione, 1-butyl-	2.1
13.34	1H-Indole, 2-methyl-	0.9
15.19	2,3-dimethyl-1H-imidazo(1,2-A)pyrrolo(3,2-E)pyridine	1.8
17.03	3,9-diazatricyclo[7,3,0,0*3,7]dodecan-2,8-dione	2.9
17.25	9H-Pyrido[3,4-b]indole-1-methyl-	1.2
19.31	1H-Indole, 5-methyl-2-phenyl-	
	N-heterocycles	25.9
9.92	Acetamide, N-(2-methylpropyl)-	2.8
11.01	Acetamide, N-(2-methylpropyl)-	2.7
11.44	Pyrrolidine, 1-acetyl-	2.5
11.75	Piperidine, 1-acetyl-	1.4
12.31	N-[2-Hydroxyethyl]succinimide	2.3
14.22	Acetamide, N-(2-phenylethyl)-	1.9
18.15	Hexadecanamide	0.9
18.53	Butanamide, N-ethyl-	1.1
19.14	9-Octadecenamide, (Z)-	2.2
19.24	Octadecanamide	
	Amines & Amides	17.8
9.37	Phenol	2.3
10.07	2,3-dimethyl-2-cyclopenten-1-one	1
11.08	Phenol,2-ethyl-	4.8
13.9	Cyclopentanecarboxaldehyde, 2-methyl-3-methylene-	1.1
16.42	Phenol, 3,5-dimethoxy-	2
26.04	Cholestan-3-ol, (3,α,.,5,β,.)-	3.6
	O-containing compounds	15

13.98	1-Pentadecene	1.5
14.43	1-Hexadecene	1.5
17.91	1-octadecene	1.5
21.19	Tetradecane	
22.53	Cholest-3-ene, (5,α)-	1.9
22.79	Cholest-3-ene, (5,α)-	1.4
22.93	Cholest-7-ene, (5,α)-	1.3
Hydrocarbons		9.1

Up to 70 % of detectable components can be identified by GC-MS. The N-cyclic heterocycles (e.g., pyrazines, pyrrolidinediones, and indole), amines and amides (piperidines, acetamides, and hexadecanamide) are the main compounds. Heterocyclic nitrogenous compounds are mainly reactants from Maillard reactions between amino acids/NH₃ and the reducing sugars [125, 207]. Amines are mainly derived from the decarboxylation of amino acids. Acylation of amines by fatty acids is the primary process for the formation of amides in biocrude. In addition, the acylation of amine by amino acid, the dimerization of amino acid, and acylation of amines by carboxylic acids can also contribute to the formation of amides [207]. O-containing compounds (phenolic compounds and (3α, 5β)-cholestan-3-ol) is the third functional group, and these oxygenated aromatic or cyclic molecules may be ascribed to the decomposition or repolymerization of carbohydrates and lignin contained in the sludge. Hydrocarbons are the desirable compounds in any biofuel, fatty acids might further convert into aliphatic hydrocarbons and CO₂ by decarboxylation, increasing the biocrude and gas phase yields

4.3.5 Characterization of solid residue

Solid residue, also called hydro-char, which has the potential to be used as solid fuel due to the remaining carbon, can be used as fertilizer to recover nutrients like N, P and K, as well as in new materials. However, the focus of this study is the investigation of the N behaviour during catalytic HTL, hence only the elemental composition and evolution of nitrogen functionalities were determined.

Elemental composition

Elemental composition together with ash in the solid residue was listed in Table 4-4. The ash content in the solid residue increases at the expense of decomposed organic components, which is consistent with the observation in Figure 4-1. Organic matter of SR is around 40 – 50 wt.% at 250 °C, dramatically reducing to 20 wt.% at 250 °C. The C content is predominately responsible for the overall lower yields as it made up most of the SR's mass. As a matter of fact, the measured C content and H content significantly

decrease from 27.0 to 17.1 wt.% and 3.8 to 0.8 wt.%, respectively. An increase in temperature favours the hydrolysis and decomposition of organic components in the sludge, resulting in a reduction of C and H, along with the lower heating values. The measured N content was almost reduced by half, from 2.8 to 1.5 wt.%, by the temperature increase from 250 to 350 °C. This is probably due to the release of proteins at lower temperatures, undergoing deamination to release ammonia into the aqueous phase with increasing temperature. The produced water-soluble N-containing intermediates are preferred to accumulate into biocrude rather than to condensate into solid residue.

Table 4-4 Elemental composition and high heating values in the solid residue

samples	Ash (wt.%)	C (wt.%) ^a	H (wt.%)	N (wt.%)	O ^b (wt.%)	S (wt.%)	HHV (MJ/kg)
250 °C	54.8	27.0	3.5	2.8	10.9	1.0	12.2
300 °C	67.0	22.5	2.7	2.2	4.9	0.9	10.5
350 °C	81.9	11.7	0.8	1.5	3.2	1.0	4.5

^a: dry organic basis

^b: calculated by difference

Evolution of N functionalities in solid residues

different product phases during HTL of SS, the investigation of functional groups in the solid residue is important for understanding the behaviour of N. An XPS analysis was conducted to investigate the nitrogen-containing species in the solid residue, the N 1s spectra of the raw sewage sludge and the solid residue is displayed in

Figure 4-3. Regarding the resolution of standard XPS, all peaks must be broader than the intrinsic line width of the incoming beam (~0.8 eV), which means that in the high-resolution N1s peaks, all components must have a line width of at least ~1.1 eV. The composition is calculated from the peak areas after background subtraction, using the overview spectrum. Large errors are possible if the material distribution is inhomogeneous since XPS is surface sensitive. In a certain range of binding energy, any fit with more components is not reliable and can only be used as a consistency check if other information about the components is available, but it cannot be a XPS-based proof for the existence of certain components. Due to the lack of an additional technique to proof the specific fitting components, the functional groups here are merely divided into organic-N, and inorganic-N. The deconvolution results (% normalized peak intensities) of solid residue are displayed in Table 4-5. It can be observed that all solid residues exhibited two peaks representing organic protein-N and inorganic-N varying in the range of 398.6 – 400 eV and 400.7 – 403.7 eV, respectively. According to literature [72, 169,

208, 209], organic-N could include pyridine-N (398-398.5 eV), and pyrrole-N (401.4 eV), while inorganic-N contains quaternary N compounds (401.4 eV).

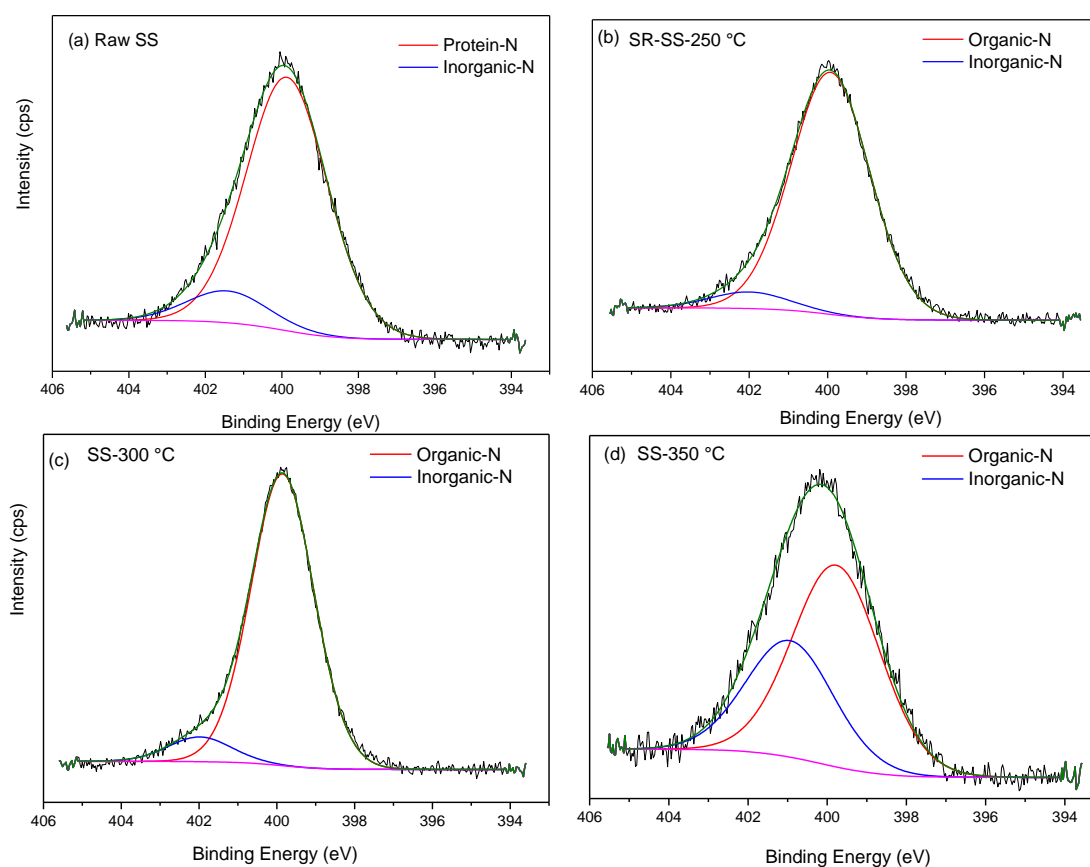


Figure 4-3 Evolution of N 1s XPS spectra for original sewage sludge and solid residue derived from HTL at different conditions

The deconvolution results show that the N in SS mainly consisted of 82.6 % organic-N and 17.4 % inorganic-N. After HTL at 250 °C, the organic-N in SR was slightly increased, but dramatically declined with rising temperatures; the inorganic-N increased accordingly. The large reduction of organic-N in the solid residue can be a clue that helps explain the loss of N content with temperature.

Table 4-5 The deconvolution results (% normalized peak intensities) of XPS for the solid residue from HTL of SS under three temperatures

	Organic-N	Inorganic-N
RSS	82.4	17.6
SS-250 °C	93.1	6.9
SS-300 °C	92.9	7.1
SS-350 °C	63.4	36.6

Peak1: position varied in the range 398.6 – 400 eV;

Peak2: position varied in the range 400.7 – 403.7 eV

4.3.6 Characterization of aqueous phase

The nitrogen found in the aqueous phases can be classified into three fractions: ammonium ($\text{NH}_4^+\text{-N}$), nitrite/nitrate ($\text{NO}_2^-/\text{NO}_3^-$), and organic nitrogen-containing compounds (org-N). Organic nitrogen was calculated as the difference of total nitrogen and the sum of nitrogen in form of ammonium nitrite and nitrate species. Figure 4-4 shows the concentration of total N, ammonium (NH_4^+), nitrite and nitrate in the aqueous phase resulting from HTL of sewage sludge at different temperatures. After HTL, the total N seems to remain constant with the reaction temperature, at around 6600 mg/L, indicating that the equilibrium of total water-soluble containing compounds occurs at temperatures below 250 °C, while the NH_4^+ fraction shows great temperature dependency. As can be seen, the concentration of $\text{NH}_4^+\text{-N}$ increased from 3982 to 5993 mg/L, around 50 % increase is obtained at 350 °C. Considering the smallest fraction of NO_2^- and NO_3^- is less than 1.2 % of total N in all the cases, it is thus reasonable to conclude that the organic N-containing compounds decline with the temperature according to the trend of constant total N and a extensive growth of NH_4^+ . Even with the presence of inorganic matter in the sewage sludge, like ammonium salts, which may not completely release or dissolve at lower temperatures, higher temperatures create a more active medium to dissolve inorganic salts, resulting in more NH_4^+ . However, taking into account the 17.6 % inorganic-N estimated by XPS in SS, which is actually not completely released from solid residue after HTL. Thus, it is acceptable that higher temperatures favour the organic-containing compounds that produce ammonia by deamination. Also, parts of polar N-containing compounds could transform into non-polar states with a subsequent accumulation in the biocrude phase.

Due to the internal fraction distribution between ammonium and organic N-containing compounds in the aqueous phase, a deep investigation of the N-species composition can help to better understand the conversion during HTL. GC-MS was again applied for qualitative analysis. Only the aqueous phase obtained with HTL of SS at 300 °C was selected as representative. However, unlike biocrude, which is condensed, the concentrations of some individual components in AQ are too low to be identified with high detected probabilities. Thus, only the top 10 compounds based on the peak-normalized volume detected across all samples were put into focus. These account for more than 50 % of the total species.

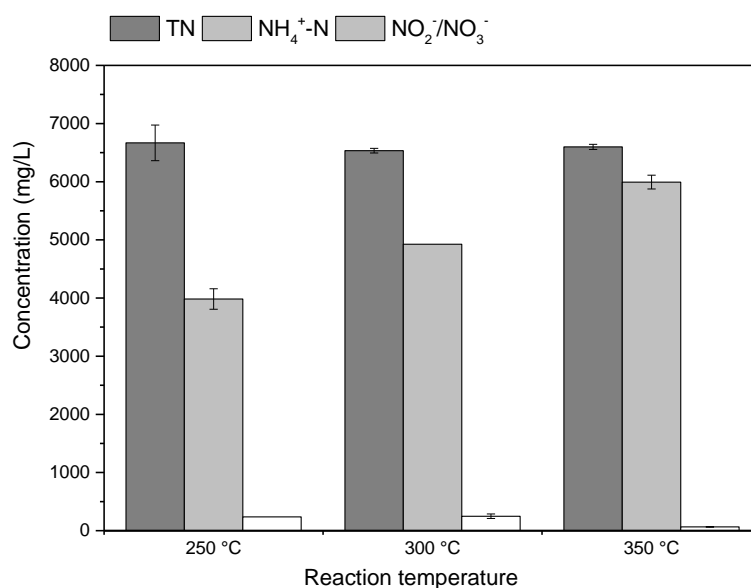


Figure 4-4 The concentration of total Nitrogen, ammonium, nitrite and nitrate in the aqueous phase from HTL at different temperatures

The most abundant products identified in the AQ were carboxylic acids, such as acetic acid, propanoic acid, butanoic acid, hexanoic acid, and pentanoic acid. Among these acids, acetic acid accounts for 30 – 40 % of the total identified components. The second major chemical is acetamide and propanamide, in the range of 17 – 24 %. Smaller amounts of N-cyclic compounds including pyrrolidinone, 2-piperidinone, pyridinole and aminopyridine, which are found in the range of 9 – 15 %. The observed fractions of different functional groups are largely limited to the polar-column used for quantification, which is very sensitive to organic acid and short-chain fatty amides, while some common O-containing compounds like phenols cannot be detected by this specific column. In addition, some less polar N-containing heterocycles may not be identified. Nonetheless, the detected amides with high amounts of organic acids may explain the high amount of ammonium in AQ, since acids can enhance the deamination to produce ammonia.

4.3.7 Nitrogen distribution

Looking at the behaviour of N in the three phase products, the overall N distribution (ND) can be concluded. The nitrogen distribution in the different phases of the various experiments is compared in Figure 4-5. The same applies to the C-balance, the N-balance was not 100 %, the “missing” N was primarily in the experimental uncertainty. The N balance is determined only for the biocrude, solid residue and the aqueous phases. In general, a noticeable trend of ND in the bio-crude significantly increases from 11.8 % to 17.4 % as the temperature rises from 250 to 350 °C. At first glance, this seems to be

contradicting the decrease of N content in the biocrude, but the reason is that the increase yields of biocrude over-compensate the decrease of N content. ND in the aqueous phase seems stable, in the range from 41.2 to 45.1 %. Correspondingly, a decrease of the ND is observed in the solid residue.

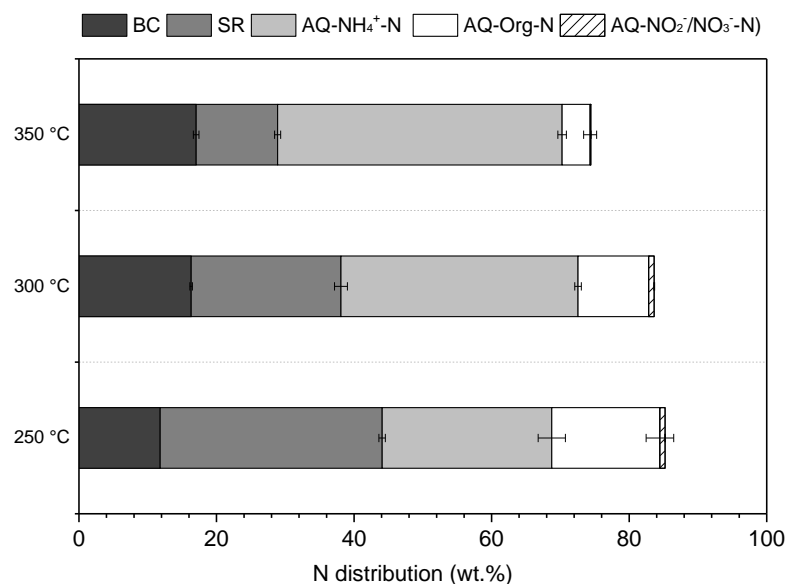


Figure 4-5 N distribution of HTL products from SS at different temperatures

4.4 Conclusion

HTL of sewage sludge has been examined at temperatures between 250 and 350 °C with 20 min residence time. Overall, the N distribution in biocrude, solid residue and the aqueous phase is in the range of 12 – 17 wt.%, 12 – 33 wt.%, and 41 – 52 wt.%, respectively. An increase in biocrude with a decrease in the solid residue is seen with rising temperature. The biocrude yields increase from 12.02 to 22.1 wt.% along with a nitrogen content decrease from 7.6 to 6.0 wt.%. It is obvious that the required improvement in HTL of sewage sludge is the reduction of nitrogen from the resulting biocrude.

The identification of organic components in the biocrude confirmed the presence of high fraction of N-containing heterocycles, which provided an incentive to investigate the reaction mechanism (Chapter 6-7).

Chapter 5 HTL of sewage sludge via continuous processing

5.1 Introduction

In the last decades, the majority of HTL process has been carried out in batch reactors, typically with a few hundred millilitres in volume at a time, due to their relative simplicity of operation and product collection.

A significant advantage is that relatively high dry matter concentrations can easily be processed as there are no complications due to the difficulties in pumping the feedstocks and plugging occurring in the pipes in continuous flow processes. The sample collection procedure in batch HTL systems often uses relatively high amounts of solvents to extract a limited amount of added-value products, which is unsuitable for practical use in industrial applications. However, the addition of a solvent (e.g. DCM) to the water phase enables the extraction of organic compounds. This eventually leads to the overestimation of high biocrude yields with different organic fractions extracted from the aqueous phase, as was demonstrated [210, 211]. Moreover, It has been reported in some of these references that instant heating rates enhance the formation of biocrude products [65]. Therefore, they enhance the bulk fragmentation of feedstock and inhibit the char formation through secondary repolymerization reactions. For this reason, the biocrude yields can be improved through instant heating rates provided by a continuous plant, which may lead to different outputs in comparison to batch processes.

Therefore, it is evident that batch HTL processing alone is of limited value for the industrial development of the process. The attention is now increasingly shifting towards scaling up HTL processes, from lab-scale to pilot-scale plants operating with continuous flow. Some research groups have developed and demonstrated bench-scale pilots as stated in Section 1.3.6. Thus far the reports regarding the fate of N have been limited to batch reactor testing, specific investigations of the behaviour of N during continuous flow processes are very rare, owing to the influence of different parameters, such as feedstock concentration, solvent extraction and heating rates.

Regarding the transaction of outputs from the batch process to a continuous system, the difference between batch and continuous is significant. Therefore, these issues provided motivated for the present study to determine the fate of N during continuous flow process

operation in a bench-scale reactor. Moreover, testing in continuous devices provides experiences with some technical issues and facts that are typical of continuous processing [212]. One of these is, for example, high pressure pumping, which will be more specifically affected by the type of feedstocks and the pre-treatment of sludge.

In order to verify that sewage sludge can be converted into biocrude with satisfactory results using a continuous process, the results of continuous HTL were compared with those of batch processing using autoclaves.

5.2 Methodology

5.2.1 Materials

Two types of sewage sludge feedstocks were primarily tested for the pumping system, and it turned out that mixed primary and secondary sludge showed better practical feasibility for pumping in the continuous process. After preliminary tests, the freshly mixed sludge could be pumped without blockage.

5.2.2 Continuous procedure

The experimental work on continuous flow HTL was carried out with a continuous plant as described in Section 3.3.2. With the preliminary tests of two different kinds of sludge, it was observed that the main issue of pumping sludge slurry is constituted by ash content in the sewage sludge, due to the fact that ash can impact the abrasion rate of the internal needle of the electro-pneumatic valve. Therefore, based on the practical feasibility of preliminary performance, mixed sludge (the mixture of primary sludge and activate sludge) was selected as feedstock, with the addition of 10 wt.% (db.) KOH, which was applied as a catalyst in continuous flow experiments to increase the fluidity of pumped slurry, and to achieve practical feasibility [182].

The flow rates were adjusted from 2 kg/h leading to residence times within the reactor of 8 min at a temperature of 350 °C. The system used to control the pressure inside the reactor in this process led to small pressure fluctuations during the reactions, but they were always lower than 1 MPa, which represented a minimum variation around the set-point 20 (MPa). It is assumed that the small fluctuations are negligible with regard to their influence on the reaction.

A slurry concentration of 10 wt.% was prepared by mixing 200 g of dried sludge with 1800 mL of distilled water. The slurry feedstock solution was processed in the continuous

flow pilot plant at 350 °C for 8 min. Following liquefaction, the product stream was collected in a 2 L separatory funnel. Since the continuous processing was implemented to study the scale-up of the process, it is believed that a solvent-free procedure is highly likely to collect products that enable industrial application. Due to its high viscosity, biocrude can be easily gravimetrically separated from the aqueous phase by decanting the aqueous phase. This alleviates the need of using solvents for the recovery of the biocrude as it is commonly practiced in batch HTL experiments [182]. This leads to a more realistic assessment of the continuous process. However, it is inevitable that some inorganics remain in the biocrude phase in this procedure, leading to problems in the subsequent analysis. Therefore, the less dangerous solvent acetone was used in order to recover the biocrude from solid residues. The aqueous phase was separated through the addition of a small volume of cyclohexane, which was used as a non-polar solvent to effectively isolate the water-soluble products from biocrude and solid residue. And the biocrude was collected using acetone.

Batch HTL was applied to the same feedstock in line with the same product separation procedure, using slurry loadings of 10 wt.%. The time at the reaction temperature (350 °C) was also kept at 8 min. It should be noted that acetone, which was used as a solvent, is miscible with water. Instead, the mixtures collected after the reactions were poured directly into a pre-weighed conical tube and centrifuged at 40000 rpm for 20 min to separate solids. The detailed procedure is described in Figure 5-1.

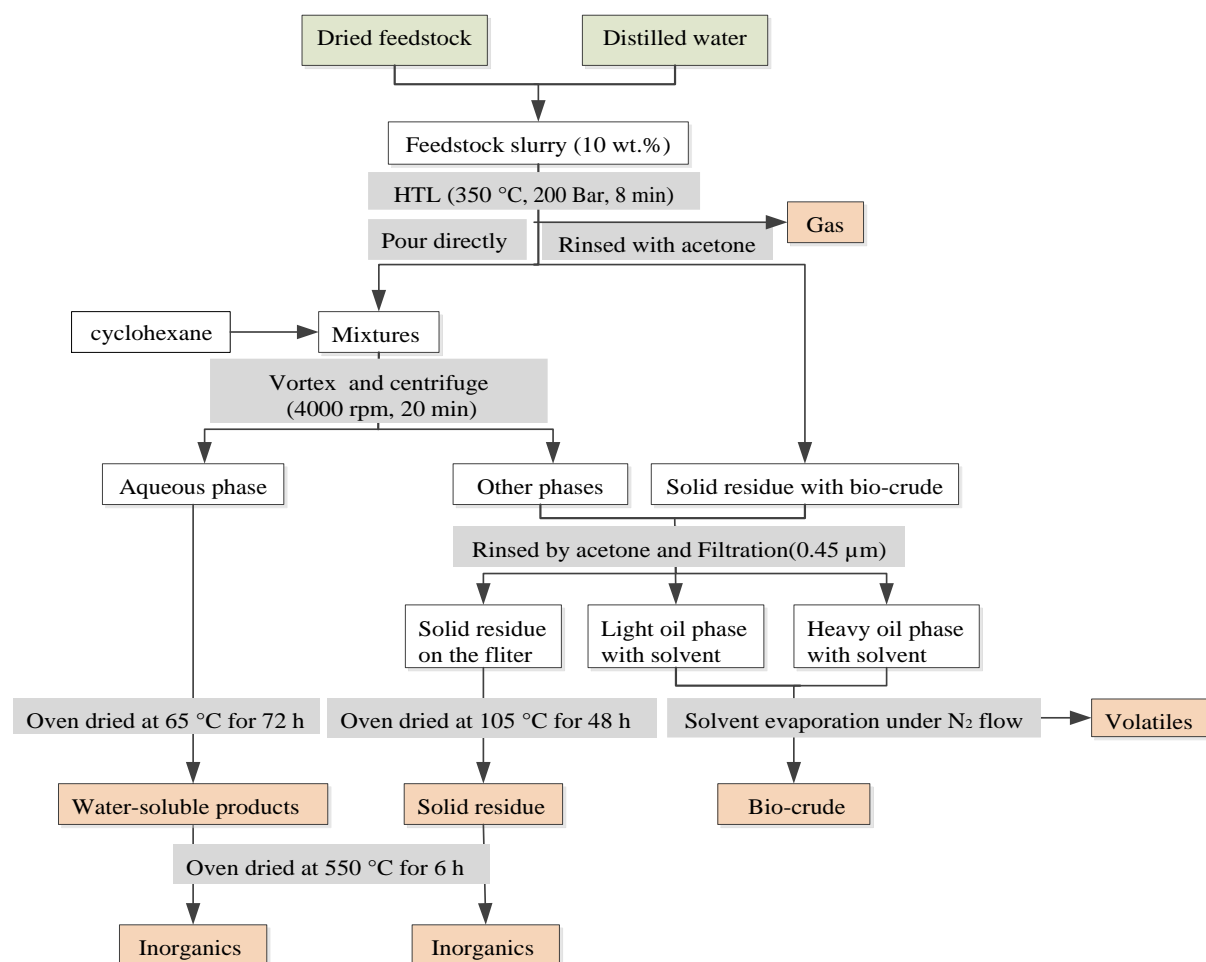


Figure 5-1 The flow chart of procedures for product separation and extraction from continuous and batch HTL process

One adapted experimental procedure with the possibility to collect volatiles during evaporation solvent was applied. This method was developed by Prestigiacomo et al. [213]. The controlled stripping process was performed at 50 °C for around 6 h under a continuous flow of N₂ (approximate flow rate of 1 L/min), condensing the produced vapours in a cold trap cooled at -10 °C by a chiller, as shown in Figure 5-2. After evaporation, the biocrude was condensed in the rounded bottom flask, the trapped liquid phase was collected in the glass-jacketed flask.



Figure 5-2 Controlled evaporation system to collect evaporated solvents with volatiles

The characterization of samples was done with the same methods described in chapter 0. It should be noted that the retention time of detected chemicals by GC-MS is longer than the previous chapter, owing to the different set-up program.

5.3 Results and discussion

5.3.1 Characterization of feedstock

The properties of mixed sludge are shown in Table 5-1. 24.66 wt.% ash content remained, which is much lower than in the digested sludge (35.61 wt.%) used in the previous chapter, but higher than in raw mixed sludge (10 wt.% in the mixture of primary sludge and activated sludge) [73]. Lower inorganics make it possible for a continuous plant to run for several hours without any problem. Relatively higher C and H contents lead to a higher HHV with a value of 17.22 MJ/kg.

Table 5-1 Characterization of sewage sludge sample used in this study

Moisture (wt.%)	Ash (wt.%) ^a	Elemental compositions (wt.%) ^a					HHV (MJ/kg)				
		C	H	O ^b	N	S					
75.42	24.66	39.11	5.83	24.51	5.29	0.6	17.22				
Inorganic content (wt.%) ^a											
Al	Ca	Fe	Mg	Mn	P	Zn	Ba	K	Na	Cu	
0.73	2.53	5.71	0.28	0.06	2.54	0.11	0.0	4	0.3	0.33	0.02

^a: dry basis

^b: calculated by difference

5.3.2 Mass balance

The results obtained from processing sewage sludge in the continuous reactor are presented in Table 5-2. In order to achieve homogeneous downstream products, the

products were collected for continuous processing of 30 min, the mass balance was based on the initial mass of pumping feedstock, calculated by the flow rate of 2 kg/h. The yields of products are based on the dry-ash free basis. It is noted that the gas yield and composition was not analysed in this work.

Table 5-2 Mass balance and the yields (wt.%) of products from continuous process at 350 °C with 8 min

HTL	Bio-crude		Solid residue		Aqueous phase		Recovery (%)	
	Y ^a	Y ^b	Y ^a	Y ^b	Y ^a	Y ^b	Y ^a	Y ^b
	2.72	30.84	1.90	5.98	77.52	17.32	81.69	54.13

^a: based on initial mass of feedstock

^b: on the dry ash-free basis

Concerning the mass balance, the recovery is higher than 80 %, with the aqueous phase as primary product accounting for 77.50 wt.%. As the fact of low slurry (10 wt.%) content in feedstock, accordingly, lowest solid residue is formed after HTL. Regarding the yields of different products, biocrude is the main product with 30.84 wt.%. This result is much lower than the findings of Itoh et al. [174], who obtained 40 – 53 wt.% of heavy oil with a continuous process. That can be explained with the employed separation procedure, as they used the same procedure as described in Chapter 4, namely DCM, which was added to the mixtures to isolate and collect biocrude. In order to determine the effects of DCM on the yields of biocrude, the extraction of DCM to the aqueous phase was additionally conducted in this study. It is observed that an average of 18.2 wt.% organic content can be extracted using DCM. If this part is added to the collected biocrude, 3.1 wt.% and more can be obtained. The yield from this work is higher than that reported by Aarhus University [182], mostly due to the lower initial slurry concentration (4 wt.%) and the solvent-free separation of biocrude used in their work. The use of organic solvents for the separation of biocrude in batch systems can result in the extraction of additional organics from the water phase and/or the solids leading to an increase in the measured biocrude yields.

However, the recovery of organic contents is observed half around. This can be explained by the uncertainty caused by missing gas, volatiles during the drying and solvent evaporation process, as well as by the remaining products stuck to the inner wall of the reactor.

A carbon and nitrogen balance/distribution between the biocrude, solid residue and aqueous phase was performed in order to shed light on the partitioning of the carbon and

nitrogen present in the feedstocks. A majority of C is transformed into the biocrude phase, reaching 42.83 wt.%, followed by the aqueous phase, and then into solid residue. The carbon loss in the form of gas was not analysed. The majority of C is desired to be converted into biocrude in order to increase its yield and the overall carbon efficiency of the process. Some unrecovered carbon leads to the relatively low (around 81.69 %) closure of the carbon balance. However, it is still comparable with others' work. Anastasakis et al. [182] only took account of the aqueous and biocrude phases, which, on average, amounted to 30.6 wt.% and 34.8 wt.% of the carbon in the original sewage sludge partitioned to the biocrude and processed water, respectively, after continuous flow HTL. Marrone et al. [140] found that during continuous flow HTL of primary and secondary sludge, approximately 60 wt.% and 40 wt.% of the carbon was present in the biocrude, respectively, while 20 wt.% and 40 wt.% of the carbon was retained in the process water. In total, a carbon balance of 94 % and 97 %, respectively, were recovered.

Table 5-3 Carbon and nitrogen distribution (CD/ND, wt.%) of products from continuous process at 350 °C with 8 min

	Bio-crude	Solid residue	Aqueous phase	Recovery (%)
CD	42.83	7.71	30.93	81.69
ND	17.13	2.94	51.34	71.42

A majority of C is transformed into the biocrude phase, reaching 42.83 wt.%, followed by the aqueous phase, then into solid residue. The carbon loss in the form of gas was not analysed. The majority of C is desired to be converted into biocrude in order to increase its yield and the overall carbon efficiency of the process. Data from the literature shows that higher carbon recovery to the biocrude can be achieved in continuous flow HTL reactors by optimizing reaction conditions. Unlike carbon distribution, the majority of N is partitioned into the aqueous phase, around half is converted into water-soluble N-containing products, almost three times higher than that divided into biocrude phase. Only 2.93 wt.% remains in the solid residue. However, the recovery of N is 10 % lower than that of C across the products. The “missing” N was probably lost in the form of volatiles during the evaporating of solvents and while drying the solid residues.

5.3.3 Characterization of products

Biocrude characterization

The biocrude produced from continuous flow HTL was 72.1 wt.% C, 9.9 wt.% H, 3.9 wt.% N, 0.8 wt.% S, and the O content, by difference, was 13.3 wt.%. The higher heating value was 36.3 MJ/kg. The reduction of the N and O content indicates that the removal of O

heteroatoms is enhanced during continuous flow HTL, mostly because of the typical reactions occurring in hydrothermal conditions such as decarboxylation, dehydration and deamination [49, 59]. The C content is very comparable to what was reported by Marrone et al. [175]. 76.5 wt.% and 72.8 wt.% were found in the bio-crude derived from primary and secondary sludge, respectively. Regarding the reported N content of 4.3 and 5.1 wt.%, the lower N content in this work is probably due to the relatively lower N content in the initial sewage sludge.

The semi-quantitative results for the molecular compositions of biocrude analysed by GC-MS are listed in Table 5-4. The chemical compounds detected can be divided into 5 functional groups.

Table 5-4 Identified main components with relative area percentage in the total ion chromatogram of biocrude obtained from continuous flow HTL of SS at 350 °C with 8 min (RT: retention time)

RT	Components	Molecular	(%)
	N-heterocycles		
29.77	1-Azetidinecarboxaldehyde, 2,2,4,4-tetramethyl-	C8H15NO	1.7
46.97	Quinoline, 4-methyl-	C10H9N	1.0
47.47	1H-Indole, 4-methyl-	C9H9N	3.2
51.10	Pyridine, 3-phenyl-	C11H9N	3.6
74.02	9H-Pyrido[3,4-b]indole, 1-methyl-	C12H10N2	1.1
74.78	1H-naphth[1,2-d]imidazole	C11H8N2	1.2
71.50	1-Cyclohexyliminomethyl-naphthalen-2-ol	C17H19NO	0.9
	Amides & amines		
32.36	2,2,6,6-Tetramethyl-4-piperidone	C9H17NO	1.4
55.02	(3-Methoxy-2-nitrophenyl)acetic acid, methyl ester	C10H11NO 5	1.2
72.59	Tetradecanamide	C14H29NO	1.1
	O-containing compounds		
13.79	3-Penten-2-one, 4-methyl-	C6H10O	3.2
16.07	2-Pentanone, 4-hydroxy-4-methyl-	C6H12O2	5.0
20.34	Butyrolactone	C4H6O2	1.5
31.29	Phenol, 4-methyl-	C7H8O	3.3
36.15	Phenol, 4-ethyl-	C8H10O	2.5
41.21	Phenol, 4-ethyl-2-methoxy-	C9H12O2	2.7
45.79	Phenol, 2-methoxy-4-propyl-	C10H14O2	2.1
49.79	Bicyclo[3.3.0]oct-2-en-8-one, 3-methyl-	C9H12O	2.2
50.12	Phenol, 2-methoxy-4-(1-propenyl)-, (E)- Eugenol	C10H12O2	2.0
50.51	3-tert-Butyl-4-hydroxyanisole	C11H16O2	2.3
55.71	1-(4-Methoxymethyl-2,6-dimethylphenyl)ethanol	C12H18O2	2.0
56.84	Benzene, 2-(1,1-dimethylethyl)-1,4-dimethoxy-	C12H18O2	1.6
58.77	Benzophenone	C13H10O	2.0

61.02	2-Pentadecanone	C15H30O	1.0
64.79	Cyclobutanecarboxylic acid, 2-methyloct-5-yn-4-yl ester	C14H22O	2.5
69.43	9-Tetradecenal, (Z)-	C14H26O	0.9
72.06	Z-7-Tetradecenoic acid	C14H26O2	1.9
75.91	Z-6-Tetradecen-1-ol acetate	C14H26	3.5
	hydrocarbons		
51.72	1-Tridecene	C13H36	1.5
53.33	Benzene, 1-methyl-2-(phenylmethyl)-	C14H14	1.9
54.66	2-Tetradecene, (E)-	C14H28	2.4
60.19	Cyclotetradecane	C14H28	2.6
60.74	Cyclopentadecane	C15H30	1.1
62.28	9H-Fluorene, 9,9-dimethyl-	C15H14	1.1
67.89	Z-1,6-Tridecadiene	C13H24	2.6
68.68	1-Hexadecene	C16H32	5.4
76.81	Cyclohexadecane, 1,2-diethyl-	C20H40	2.7

O-containing compounds formed the majority of compounds identified in the biocrude, mainly including phenolic compounds, acids and ketones. This was consistent with the high O content of biocrude. These oxygenated aromatic or cyclic molecules may be ascribed to the carbohydrates and lignin content in the sludge. As a matter of fact, six carbon-containing compounds (phenols, guaiacols and benzene) primarily originated from the degradation of lignin component under sub- and supercritical conditions. Five other carbon-containing oxygenates, including cyclopentanones, furfurals, and cyclopentenones, were derived from carbohydrates [98, 214]. Aliphatic acids like tetradecenoic acid were a product of lipid hydrolysis. Other types of compounds derived from the lipids were detected, mostly in the form of long-chain aliphatic molecules and cyclic hydrocarbons, including the major compounds in biocrude, which were hexadecane (5.4 %), cyclohexadecane (2.7 %), and cyclotetradecane (2.6 %), indicating the active decarboxylation occurred during the continuous HTL process.

Certain amounts of nitrogenous compounds in the biocrude from the continuous process were found as well. Specifically speaking, they may be derived from the decarboxylation and rearrangement of amino acids. N-containing heterocycles such as indoles and pyridines are generally generated by Maillard reactions. Long-chain saturated tetradecanamide was detected, probably originating from the reaction between lipids and proteins.

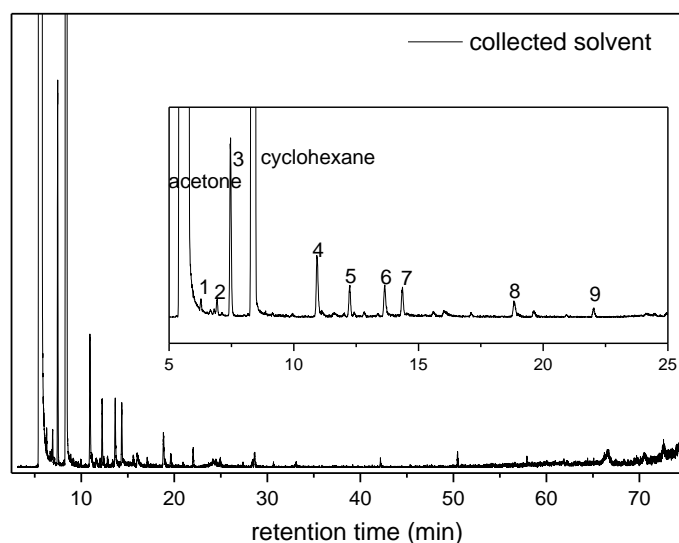


Figure 5-3 GC-MS total ion chromatograms of volatiles in the collect solvent from continuous flow HTL of sewage sludge at a concentration of 10 wt.%

Table 5-5 Identified main components with relative area percentage in the total ion chromatogram of volatiles in the collect solvent collected solvent obtained from continuous flow HTL of SS at 350 °C with 8 min (RT: retention time)

Number	RT	Chemicals	Molecular	(%)
1	6.28	3-Hexanamine	C ₆ H ₁₅ N	1.93
2	6.93	Furan, 2-methyl-	C ₅ H ₆ O	2.57
3	7.47	1-Methoxy-1-propene	C ₄ H ₈ O	30.77
4	10.93	1H-Pyrrole, 1-methyl-	C ₅ H ₇ N	13.25
5	12.24	Toluene	C ₇ H ₈	6.39
6	13.65	3-Hexen-2-one	C ₆ H ₁₀ O	6.19
7	14.36	1H-Pyrrole, 1-ethyl-	C ₆ H ₉ N	5.96
8	18.83	Bicyclo[4.2.0]octa-1,3,5-triene	C ₈ H ₈	3.94
9	22.04	1H-Pyrrole, 1-butyl-	C ₈ H ₁₃ N	2.01

The light phase in the biocrude might evaporate during solvent removal. One possible way to collect volatiles is described in Figure 5-2. The trapping of solvent was measured by GC-MS, as shown in Figure 5-3, and several peaks can be detected before the retention of 25 min. These chemicals with carbon numbers less than 8, as listed in Table 5-5, consist of 30.7 % 1-Methoxy-1-propene, and 21.2 % pyrroles.

The characterization of the aqueous phase and solid residue will be discussed and compared with the results from batch processing under the same HTL conditions in the next section.

5.3.4 Comparison between continuous and batch HTL

This section provides a comparison between the performance of batch and continuous

flow HTL. Owing to the fact that the sludge applied in previous studies was unable to be pumped for use in the continuous flow plant. Therefore, mixed primary and secondary sludge is selected as feedstock for batch processing. The batch experiments were conducted with the same conditions of continuous processing. In brief, batch HTL was conducted with the same sewage sludge and according to the same separation procedure, using the sludge loading of 10 wt.%, liquefied at 350 °C for 8 min. It must be noted that, in order to achieve a faster heating rate to approach the continuous flow HTL heating rate, a fluidized sand bath with a heating rate of 36 K/min was used to heat the micro-autoclaves in this work, instead of a GC oven.

The product yields for batch and continuous experiments are shown in Figure 5-4.

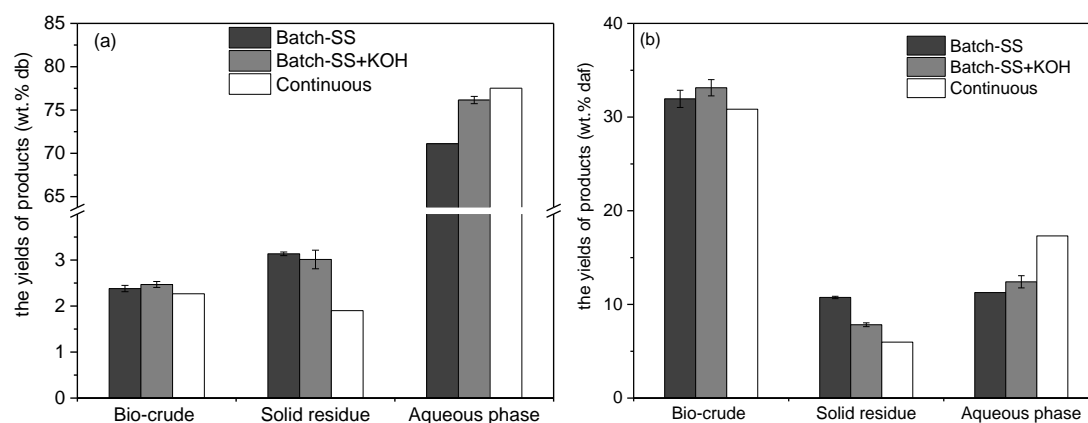


Figure 5-4 Comparison the yields of products from batch and continuous flow HTL experiments with a loading of 10 wt.% at 350 °C for 8 min, (a) on dry basis;(b) on dry ash free basis

As in continuous flow HTL, gas products are not considered in this section. The total mass balance shown in Figure 5-4 (a) displays a better mass closure obtained with continuous flow HTL, reaching 81.7 wt.% compared to 76.2 wt.% and 81.6 wt.% achieved with batch HTL of sewage sludge without and with KOH, respectively. This observation is probably due to the higher volume of feedstocks processed during continuous flow HTL, which can reduce the importance of missing balance during the collection and separation procedure. In both processes, the aqueous phase is the major product after HTL, and, owing to the initial feedstock concentration, 90 wt.% is water. Regarding the yields of products on an organic basis, as shown in Figure 5-4 (b), biocrude is the dominant product, and around 30 wt.% organics are converted into oily products. The biocrude obtained through batch processing shows higher yields than in continuous flow HTL, which is unexpected, because a faster heating rate is supposed to enhance biocrude production [59, 215]. In this case, it can possibly be explained by the different

collection procedure. One more step was applied in the batch reactor: the inter wall of the reactor was washed with solvent, leading to the collection of more sticky biocrude than continuous flow HTL. Moreover, comparable results were also reported from HTL of microalgae. Barreiro et al. [216] investigated the difference in biochemical fractions of feedstock and the orders of HTL reaction kinetics. Many molecules involved in the HTL process show a different reactivity. The repolymerization of water-soluble compounds that form biocrude or char normally exhibits reaction orders higher than one [217]. In a continuous tube reactor, the decrease of biocrude yield with an increase in water-soluble products indicates that the rate of the pathways with reaction orders higher than one was reduced. Therefore, the choice of a batch or continuous reactor will influence the concentration of the various molecules in the reaction medium, thus affecting the reaction kinetics and the final product yields of the HTL process.

In the case of catalytic batch HTL, KOH has a slight effect on the biocrude yields, which, to a great extent, is in line with others' work [66, 68, 162]. The alkali catalyst has negligible effects on the yields of biocrude from HTL of sewage sludge. However, as can be seen, the presence of KOH dramatically suppresses the formation of char leading to lower yields of solid residue, and catalyses the conversion of water-soluble organics.

Batch and continuous HTL processes also exhibit differences in the elemental composition of the biocrude (Table 5-6). In the presence of KOH, The C, H and N contents are higher in batch operation, while the O and S content are higher in the continuous process. The higher N content in batch reactions is probably caused by the higher relevance of repolymerization reactions occurring in batch systems. The pathways toward the formation of biocrude from proteins typically imply the occurrence of repolymerization reactions [217]. On the other hand, they can be ascribed to Maillard reactions, as stated in detail in Section 0.

Table 5-6 The comparison of elemental content and heating values in the biocrude obtained from batch and continuous HTL of sludge at 350 °C with 8 min

Samples	Elemental content (wt.%) ^a					HHV (MJ/kg)
	C	H	O ^b	N	S	
Batch-SS	72.24	10.04	12.32	4.76	0.64	36.71
Batch-SS+KOH	72.98	10.51	11.66	4.25	0.60	37.76
Continuous	72.10	9.90	13.30	3.90	0.80	36.28

^a: On a dry basis

^b: calculated by difference

Maillard reactions can occur between reducing sugars and active amino acids at low temperatures of about 150 °C, which means the melanoidin-like products can be

generated at lower temperatures. In the present study, even when a faster heating rate (36 K/min) than for batch processing was applied, it still took a while to reach 350 °C. The formation of Maillard reaction products is inevitable during the heating period, explaining the higher nitrogen content of the biocrude produced. A deeper investigation into the reaction pathways of Maillard reactions is determined in Chapter 7. The cooling period could also lead to the water-soluble N-containing compounds accumulated in biocrude. This requires further research.

The observation of a higher O content in the biocrude from continuous HTL is in line with the reports of fast HTL of sewage sludge [65], indicating that an increase in the heating rate inhibits the degradation of or increases the formation of oxygenates. Theoretically, either the reaction rate of decarboxylation or the dehydration is reduced. The un-measured gases (which are mostly composed of CO₂) might help explain this. The addition of KOH shows an increase in C and H with a decrease in O, N and S, therefore leading to the highest heating values.

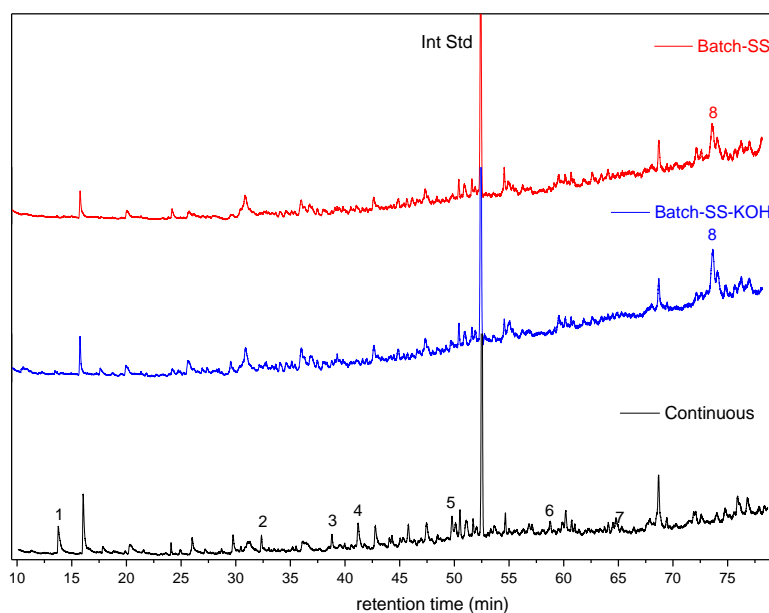


Figure 5-5 The comparison of GC-MS total ion chromatograms of biocrude from batch and continuous flow HTL of sewage sludge at 350 °C with 8 min

The organic species were detected by GC-MS, with the comparison of total ion chromatograms shown in Figure 5-5 and Figure 5-6. No significant differences were found in the type of molecules detected by GC-MS in the biocrude from batch processing in the presence or absence of KOH. It was observed that a little bit more N-containing heterocycles were produced with the addition of KOH. Compared with continuous flow

HTL, several different peaks can be observed, as marked with numbers, and listed in Table 5-7.

The various peaks observed in the total ion chromatogram evidently indicate that a faster heating rate improves the formation of oxygenates, an aligns to the higher O content found in the biocrude from continuous flow HTL.

Table 5-7 The different components identified by GC-MS of the biocrude from continuous flow HTL of SS at 350 °C with 8 min (RT: retention time)

Number	RT	Chemicals	Molecular
1	13.8	3-Penten-2-one, 4-methyl-	C ₆ H ₁₀ O
2	32.4	2,2,6,6-Tetramethyl-4-piperidone	C ₉ H ₁₇ NO
3	38.8	unknown	
4	41.2	Phenol, 4-ethyl-2-methoxy-	C ₉ H ₁₂ O ₂
5	49.8	Bicyclo[3.3.0]oct-2-en-8-one, 3-methyl-	C ₉ H ₁₂ O
6	50.1	Phenol, 2-methoxy-4-(1-propenyl)-, (E)- Cyclobutanecarboxylic acid, 2-methyloct-5-yn-4-yl	C ₁₀ H ₁₂ O ₂
7	64.8	ester	C ₁₄ H ₂₂ O

On the other hand, peak 8 marked in total ion chromatograms of biocrude from batch processing corresponds to (Z)-9-Octadecenamide, being a long-chain aliphatic amide, accounting for 10.2 and 7.5 wt.% in the bio-crude from the top 50 peaks identified, hence resulting in higher amides.

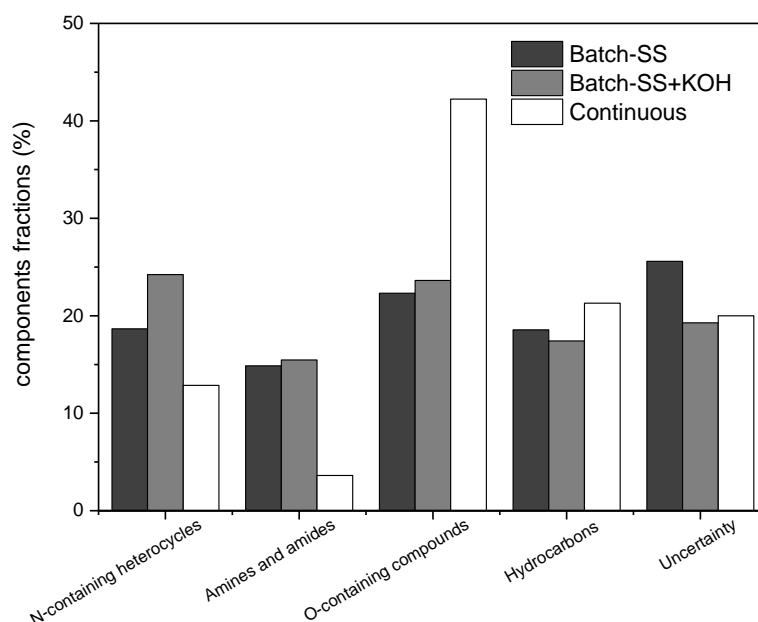


Figure 5-6 The comparison of component fractions in biocrude obtained from batch and continuous flow HTL of sewage sludge at a concentration of 10 wt.% under 350 at 350 °C with 8 min

The comparison of aqueous products obtained from batch and continuous HTL is

discussed in the following. As indicated in the literature [150, 192], organic acetic acids, mostly acetic acid, were commonly identified in the aqueous phase from HTL. In this work, acetic acid ranges from 2175 – 3429 mg/L. Despite the presence of several organic acids in the aqueous phase, it is slightly alkaline. The pH of aqueous products from batch processing of sludge without and with KOH is 8 and 8.2, respectively, and the same value of 8.2 is found in the continuous system. This is because of the relatively high ammonium content. Table 5-8 presents the recovery of several elements in the aqueous phase, compared to their concentration in the feedstock, including the application of KOH in the case of K. As a general trend, it can be said that less than one third of C is recovered in AQ, and most carbons are available in the form of organic carbons, contributing to water-soluble organic compounds. In contrast, more than half of N is obtained with a significant proportion of ammonium (27.6 – 30.9 wt.%). Only a trace amount (< 40 mg/L) of nitrate is found in the products of batch HTL of SS, the presence of other organic nitrogen-containing molecules in the aqueous product is clearly indicated by the gap between total nitrogen and nitrogen in the form of ammonium, respectively, in the range of 20.5 – 22.9 wt.%.

The monovalent ions K^+ and Na^+ led to high recovery rates of AQ in both processes, and the divalent ions Ca^{2+} and Mg^{2+} could not be recovered in the aqueous products. These were converted and remained in the solid residue from the process.

Table 5-8 The comparison of nutrients recovery (wt.%) in the aqueous phase from batch and continuous HTL of sludge at 350 °C with 8 min

	C	Org-C	N	NH ₄ ⁺ -N	Ca	Fe	K	Mg	Na	P
Batch-SS	23.7	22.8	50.5	27.6	0.6	0.1	57.4	1.3	10.2	1.9
Batch-SS+KOH	30.7	27.5	61.0	38.3	0.1	0.2	59.1	1.4	7.5	8.5
Continuous	30.9	28.0	51.3	30.9	0.2	0.3	48.5	1.6	14.0	3.1

A simple investigation of solid residue is presented in Table 5-9. With the addition of KOH, the batch experiment shows a higher ash content, which indicates that more organics were converted into bio-crude or the aqueous phase, leading to a higher HTL conversion efficiency. A big drop of C content is found in the batch process, with an increase in O content, resulting in the lowest heating values of solid residue. The lowest O content (4.63 wt.%) in the solid from continuous HTL is highly consistent with the highest O content (13.30 wt.%) of biocrude, suggesting that faster heating rates enhance

O convert into bio-crude at the expense of the contribution to solid residue. In the presence of KOH, the N content is decreased by almost half and most likely transformed into the aqueous phase in the additional base condition.

Table 5-9 characterization of solid residue from batch and continuous HTL of sludge at 350 °C with 8 min

Samples	Ash (wt.%)	Elemental content (wt.%) ^a					HHV (MJ/kg)
		C	H	O ^b	N	S	
Batch-SS	73.83	16.50	1.40	6.07	1.50	0.70	6.51
Batch-SS+KOH	77.68	12.80	0.95	7.12	0.85	0.60	4.42
Continuous	76.87	15.50	1.70	4.63	0.80	0.50	6.86

^a: On a dry basis

^b: calculated by difference

Last but not least, the overall elemental balance is compared in Table 5-10. It can be clearly seen that the major part of carbon is converted into the biocrude phase, while half of N is transformed into the aqueous phase, while less than one sixth remains in the solid residue. Batch processing leads to higher ND distribution into the biocrude, owing to the higher biocrude yields and N content. Again, this confirms that slower heating rates favour the formation of N-containing compounds during the heating period. The addition of KOH improves water-soluble products, especially the recovery of N is greatly increased from 50 to 60 wt.%. Therefore, it becomes necessary to create ways to implement water management in HTL processes. Increasing attention is paid to the recovery of organics and nutrients from the aqueous stream [153-155], as well as to energy recovery [156, 157].

Table 5-10 The comparison of Elemental distributions (wt.%) across various products from batch and continuous HTL of sludge at 350 °C with 8 min

Samples	Bio-crude		Solid residue		Aqueous phase		Recovery	
	CD	ND	CD	ND	CD	ND	CD	ND
Batch-SS	45.76	22.40	14.26	9.63	23.66	50.51	83.68	82.55
Batch-SS+KOH	47.94	20.72	11.06	5.46	30.74	61.01	89.74	87.19
Continuous	42.83	17.13	7.71	2.94	30.93	51.34	81.47	71.41

In any case, comparing batch and continuous flow HTL is a complex subject because of the difficulty in accounting for the effect of the heating and cooling periods, even though the same separation procedure is applied. The information provided in this study indicates that the results available in literature for sewage sludge HTL (carried out in batch experiments in the vast majority of cases) may vary when continuous processing is applied.

5.4 Conclusion

HTL experiments with continuous flow processing were successfully conducted for sewage sludge with the additive of KOH at 350 °C and a residence time of 8 min. The operation appears to be stable, though some problems were observed while pre-pumping sludge slurries. Without the collection of gases, 81 wt.% mass balance can be achieved, which is comparable with other reports on continuous processes. 30.8 wt.% biocrude was obtained, which is, however, slightly lower than in batch processing, probably because the repolymerization of water-soluble products to form biocrude was reduced. The type of chemical components in the bio-crude from both processes identified by GC-MS is similar. No positive influence was found in terms of the yields of biocrude from continuous flow HTL while applying instant heating rates to achieve the reaction temperature. However, more N content was found after batch processing, and it can be concluded that remarkable effects of Maillard reactions occur during the heating period.

Chapter 6 HTL of model substances: Effects of lipids

6.1 Introduction

Given the great motivation to better understand reactions occurring during HTL of sewage sludge, model substances are highly required to simplify the comprehensive feedstock. As stated above in Chapter 0, a considerable number of studies conducted so far have been focused on the HTL of various types of model substances with different objectives. The effect of reaction parameters has been investigated systematically. Maillard reactions (MRs) have been confirmed to be important interactions during HTL, leading to a decrease in the quality due to an increasing N content. Amide formation is also regarded as an undesired reaction, which adds to the N content in the bio-oil and decreases the fatty acid yields [200, 201]. So far, to the best of my knowledge, no studies have directly examined a simple ternary mixture of model amino acids, carbohydrates and lipids under hydrothermal conditions in order to determine the effects of lipids on the fate of N during HTL. Therefore, to have a full grasp of the distribution of N during HTL, it is paramount to include the presence of lipids in the mixture.

Moreover, as co-liquefaction of different organic materials is becoming more attractive (in Section 1.3.4), knowing the effects of the possible interactions between different chemical compounds could be of great future value in producing high yields of better-quality oils [122, 126, 218]. The investigation of ternary mixtures can be used to evaluate their potential biocrude production via co-liquefaction.

In the current study, a system of lactose (lac) as a model carbohydrate, lysine (lys) as a model protein, and palmitic acid (PA) as a model fatty acid is explored. Lactose was chosen because it is a strongly reducing disaccharide widely occurring in natural products. Lysine (lys) is known to be the most reactive amino acid in Maillard reactions due to the presence of two reactive amino groups [219]. In order to determine the effects of lipids on the fate of N, particularly with regard to N-containing heterocyclic compounds, lactose and lysine were selected to undergo relatively active Maillard reactions, which helps quantify the specific components in the obtained bio-crude. Palmitic acid (PA) was selected as model fatty acid as it has been widely confirmed as the major fatty acid in lipid-rich biomass [125, 220].

The specific objectives of this work are: (1) to demonstrate the effects of lipids on the fate of N during HTL; (2) to determine the possible reaction pathways based on the influence of temperature. The results of the study are expected to provide detailed information regarding N transformation of protein and lipid-derived sewage sludge under HTL conditions.

6.1 Methodology

6.1.1 Materials

The model compounds used in this study, i.e. palmitic acid, lactose, and lysine, were of analytical grade and purchased from Sigma-Aldrich. Piperidine, 2,5-dimethylpyrazine, 2,3,5-trimethylpyrazine, and palmitamide were purchased from Alfa Aesar, octahydrodipyrido[1,2-a:1',2'-d]pyrazine-6,12(2H,6aH)-dione (DKP) was bought from MolPort, and caprolactam was purchased from Sigma-Aldrich.

6.1.2 HTL procedure

HTL of model substances was conducted at 250, 300 and 350 °C for 20 min, in micro-autoclaves heated by a GC oven. Each batch was constituted by 10 wt.% of feedstock that was dissolved in distilled water and filled into the reactor. For the binary mixture tests, the feedstock was a 50:50 wt.% mixture of each model compounds, whereas for the ternary mixture, the feedstock was a 1:1:1 wt.% mixture of PA, lactose, and lysine.

Sample separation and analysis were conducted according to the procedures described in Chapter 0.

6.2 Results and discussion

6.2.1 HTL conversion of single lipid

First of all, the product distributions obtained from HTL of single palmitic acid were determined. At reaction temperatures ranging from 250 to 350 °C, no gas products can be collected to detect the CO₂ fraction. It is most likely that very weak decarboxylation happens to palmitic acid in the hot-compressed water below 350 °C, leading to the dissolution of a small amount of CO₂. Therefore, only biocrude, solid residue and the aqueous phase were collected and analysed.

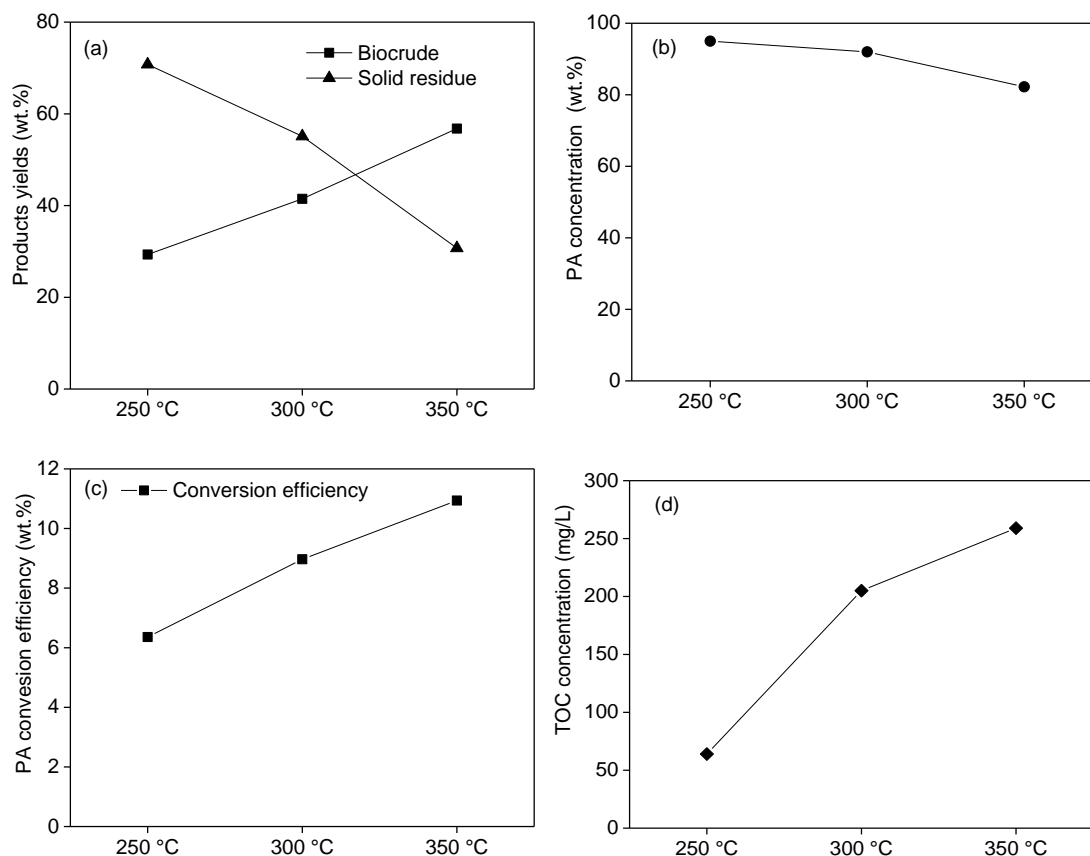


Figure 6-1 (a) products yields; (b) PA concentration in the bio-crude; (c) PA conversion efficiency; (d) TOC concentration in the aqueous phase from HTL of PA at different temperatures

Figure 6-1 (a) shows that the biocrude yields increase from 29.3 to 56.8 wt.%, and the solid residue decreases accordingly from 70.8 to 30.7 wt.%. At first glance, the significant increase of biocrude with elevated temperature seems to be in contrast to the observations in other reports [70, 220], which revealed that the long chain fatty acids are relatively stable in subcritical water. This can be explained by the solubility of palmitic acid in DCM solvent. A typical long chain fatty acid, which is always represented as fatty acids in the biocrude from real biomass, indicates that palmitic acid can be directly extracted by solvent, thus contributing to biocrude. Hence, the quantification of PA in the bio-crude is shown in Figure 6-1 (b). As can be seen, 95.1 wt.% of PA is found in the biocrude at 250 °C, then slightly reduces to 82.2 wt.% at 350 °C. As a matter of fact, more than 80 wt.% of biocrude is composed of non-reacted PA, indicating that palmitic acid has a relatively high thermal stability and can be considered stable below 350 °C, although experience shows that some degree of degradation under hydrothermal conditions produces long-chain hydrocarbons by decarboxylation. This may possibly explain the negligible changes of the element content in the bio-oil phase (Table 6-1) as compared to different

temperatures.

Table 6-1 Elemental content in the biocrude and solid residue from HTL of palmitic acid at three temperatures

Materials	Elemental content (wt.%)			HHV (MJ/kg)
	C	H	O ^a	
Palmitic acid	75	12.5	12.5	40.97
Biocrude - 250 °C	75.0	75.0	12.5	41.0
Biocrude - 300 °C	74.8	12.5	12.3	41.6
Biocrude - 350 °C	74.8	12.7	12.5	41.2
Solid residue - 250 °C	74.7	12.6	12.8	40.95
Solid residue - 300 °C	74.2	13	12.8	41.36
Solid residue - 350 °C	74.9	12.7	12.4	41.24

^a: calculated by difference

Owing to the limited amount of DCM to collect bio-crude samples, the high amount of solid residue might also originate from non-reacted PA. The elemental analysis is therefore performed to compare with feedstock PA, as listed in Table 6-1. No observable difference could be found in C, H and O content, and it can be concluded that the solid residue is considered palmitic acid, specifically the part of PA which cannot be dissolved or extracted by a limited amount of DCM. Therefore, the conversion rate of PA is calculated by the difference of the initial amount of PA and the amount of PA remaining in the solid phase and extracted into biocrude by DCM.

Figure 6-1 (c) shows that the conversion rate of PA is only 6.4 % at 250 °C and that it increases to 10.9 % at 350 °C. Accordingly, the TOC concentration in the aqueous phase is fairly low, increasing from 64 to 259 mg/L, suggesting that PA is quite resistant to decomposition below 350 °C. The main portion of the non-reacted PA remains in the solid residue, and a part of the PA is extracted by a DCM solvent to form bio-crude products. This outcome is likely due to limited amount of DCM being unable to fully dissolve all of the fatty acid, suggesting the biocrude yield highly depends on the amount of solvent and the separation procedure.

6.2.2 Biocrude products from HTL of mixture

The biocrude yield obtained from HTL of single, binary, and ternary mixtures is displayed in Figure 6-2. Regarding isolated components, PA yields the most potential bio-oil products, around 10 times more than those from isolated lysine and lactose under the same conditions. As discussed before, this is mostly due to the solubility of PA in DCM. All bio-oil yields considerably increase with rising temperature, except in the case of lactose, which shows a low dependency on the temperatures, and for which a maximum

of 7 wt.% was obtained at 350 °C. In general, the overall lower biocrude yield might be due to the high yields of solid residue formed by carbonization, and large amounts of molecules in carbohydrates breaking down to polar water-soluble organics dissolved into the aqueous phase. It is known that the carbohydrates, once hydrolysed, undergo dehydration, forming intermediates such as furfural and hydroxymethylfurfural. Those substances further polymerize and form a carbonaceous material, which is referred to as hydro-char [221].

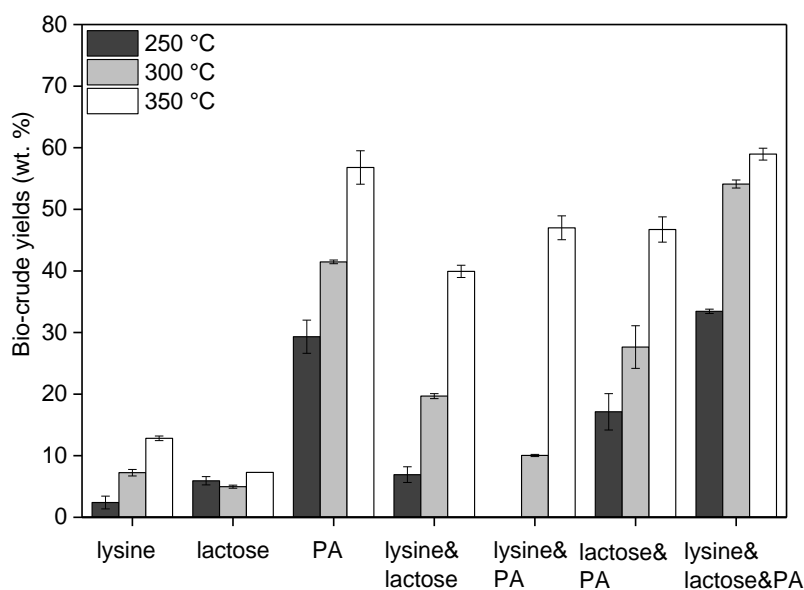


Figure 6-2 Biocrude yields from HTL of model compounds at three different temperatures (biocrude from lysine mixed with PA at 250 °C were not collected)

Regarding HTL of lysine, the bio-oil yield obtained increases from 2.4 to 12.8 wt.% as the temperature rose from 250 to 350 °C. During hydrothermal conversion, the peptide bonds in proteins quickly hydrolyse and release amino acids, which can produce alkylamines and carbonic acid by decarboxylation or deamination to form ammonia and organic acids. With increasing temperature, these products can recombine into aromatic ring structures and N-cyclic compounds [127].

In all binary mixture cases, the results show a significant increase in the bio-oil yield with temperature, although it should be noted that the bio-oil from HTL of lysine and PA at 250 °C is missing due to the difficult separation from the aqueous phase, as shown in Figure 6-3. A stable emulsion of the biocrude in the aqueous phase was formed, making it unrecoverable. When the reaction temperature increases, it becomes easier to separate and collect the biocrude. Compared to lysine mixed with PA at 300 °C, higher biocrude yields are obtained from HTL of a lactose and PA mixture. Notably, ternary mixtures

produce much more biocrude with yields increasing from 33.4 to 60 wt.% when the temperature increases from 250 to 350 °C, suggesting the strong interactions take place between different organic compositions, which can be of great benefit in producing high yields of biocrude.



Figure 6-3 Mixed samples from HTL of palmitic acid and lysine at 250 °C

6.2.3 N content in the biocrude

As mentioned in the experimental section, the initial feedstock concentration was fixed at 10 wt.%, which means that the relative lysine content in the binary and ternary mixtures are only half and one third of that in the single lysine sequence, respectively. Therefore, the initial N content is different as shown in Figure 6-4 with a square plot, starting at 19.2, 9.6, and 6.4 % for lysine, binary and ternary mixtures, respectively. In order to compare the effect of different compounds on the N transformation to biocrude, the N distribution was introduced. Seeing that, after HTL of lysine alone, the N content dramatically drops, decreasing from 16.6 to 10 wt.% with the increasing temperatures. The reduction is also enhanced by the reaction temperature, ranging from 13.5 to 47.9 %. A decrease in the N content with rising temperature is observed, owing to the fact that amino acid nitrogen compounds tend to form water-soluble components, which are partitioned into the aqueous phase.

When mixed with lactose, and as compared with single lysine, a similar trend with regard to the temperature dependency can be found. The N content in the biocrude gradually decreases with increasing temperature, but the difference in the N contents of feedstock and biocrude, which is also called reduction, is smaller than that that seen in HTL of lysine alone. At 250 °C, the N content in the biocrude is even higher than that of the initial feedstock, reaching a similar value at 300 °C before a larger drop is observed at 350 °C.

This observation suggests that the input of carbohydrates enhance the conversion of N into biocrude. Regarding the mixtures of lysine and palmitic acid, even though the results at 250 °C are missing, it seems like the N content in the bio-oil decreases with increasing temperature, with a reduction of nearly 50 % at 350 °C compared to the value at 300 °C. This might be caused by the interaction between lysine and palmitic acid, which largely decreases the production of N-containing compounds, or it could be the dilution of non-reacted palmitic acid, which will be discussed below.

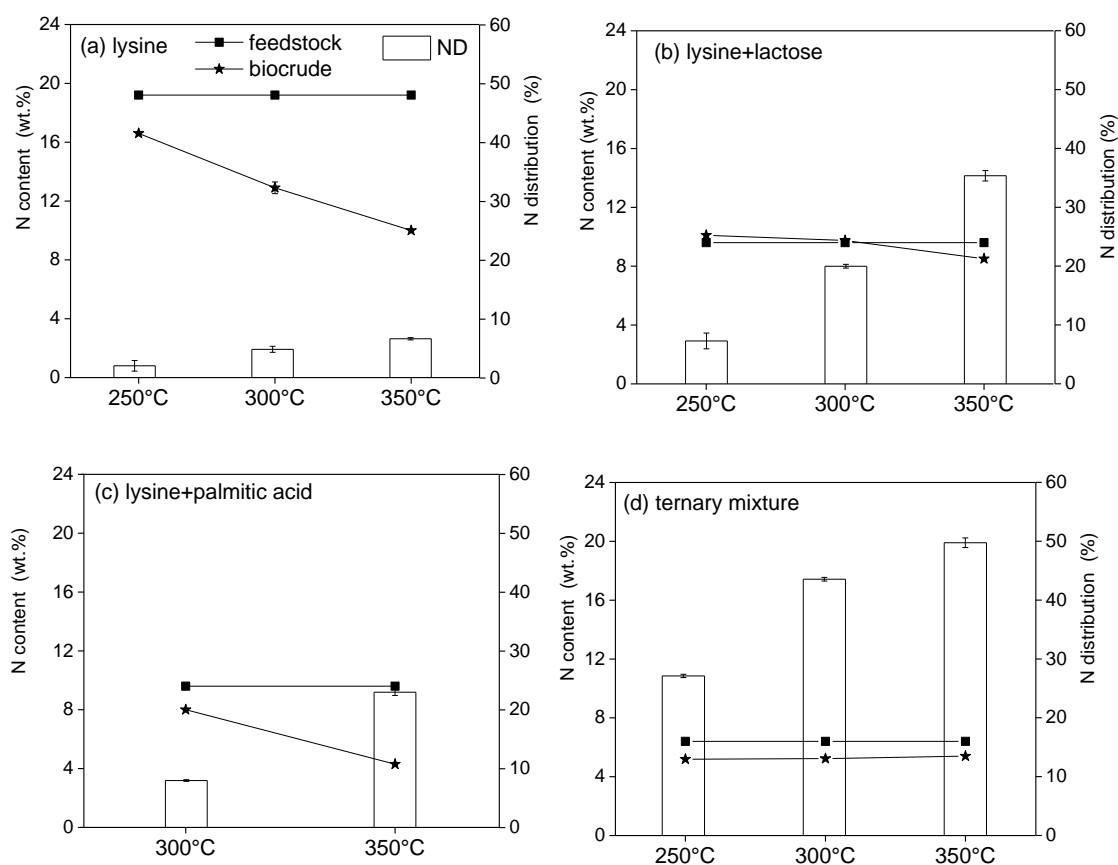


Figure 6-4 Comparison of N content (represented by data points) and N distribution (represented by bars) in the biocrude obtained from (a) lysine; (b) lysine mixed with lactose; (c) lysine mixed with palmitic acid; (d) ternary mixture at different temperatures

Figure 6-4 (d) shows that the N content in the biocrude from HTL of ternary mixtures, which is quite stable, experiences a slight increase from 5.2 to 5.4 wt.% when the temperature rises from 250 to 350 °C, with a reduction of 18 % from the initial N content in the feedstock. The N distribution significantly increases with reaction temperatures in all the cases. Under the same conditions, unlike the N content, ternary mixtures show the highest N distribution, followed by lysine and lactose mixtures, then palmitic and lysine mixtures and single lysine, despite the fact that biocrude produced from lysine contains

the highest amount of N. The contrastive trend with regard to N content can be explained with the higher yields of biocrude as shown in Figure 6-2, which compensate the decrease in N content, suggesting that the reaction rate of biocrude is faster than the deamination rate under HTL conditions.

6.2.4 Chemical compositions in the bio-crude

As mentioned before, the relatively lower N content obtained from HTL of the mixture with palmitic acid might be due to dilution effects. It is necessary to quantify the remaining PA in the non-reacted bio-crude. As shown in Figure 6-5, the yields of PA from lysine and the PA increase with the reaction temperature, nearly reaching 31.8 wt.% at 350 °C, can support that the lower N content in the bio-oil is partly owing to the dilution effect of a relatively higher fraction of PA remaining in the biocrude. Therefore, in cases of the binary mixture of lysine and PA, as well as the ternary mixture, the calculated N content in the bio-oil was defined as the total N mass divided by the remaining biocrude mass (total biocrude is excluded from the non-reacted PA). As a result, the calculated N content in bio-oil obtained from lysine mixed with PA is 11.1 and 6.4 % at 300 and 350 °C, respectively. In case of the ternary mixture, the calculated N content is increased from 6.4 to 7.8 % as the temperature rises from 250 to 350 °C. As evidence of the dilution effect of PA on the N content, it is necessary to further confirm the effects of PA on the specific N-containing compounds.

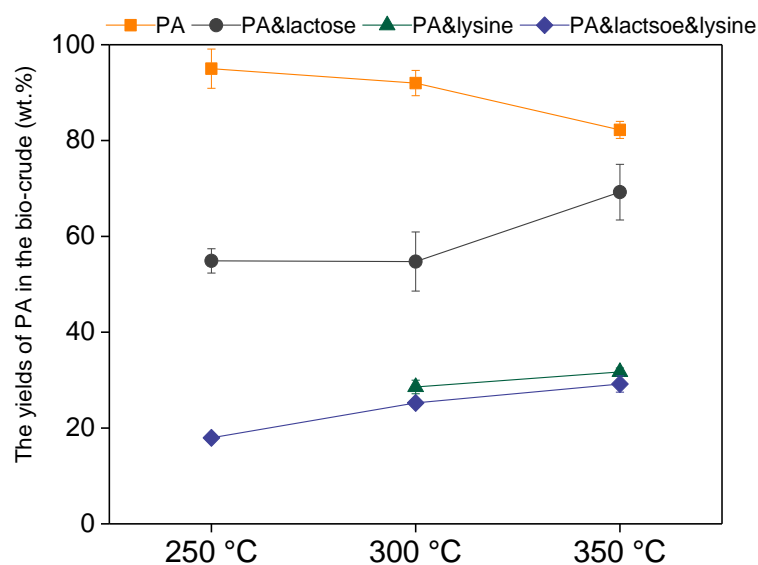


Figure 6-5 Yields of palmitic acid in the biocrude obtained from HTL of model compounds at different temperatures (biocrude from lysine mixed with PA at 250 °C were not collected)

GC–MS analysis was again used to identify the organic compounds in the biocrude. The bio-oil is a complex mixture, and hundreds of peaks were displayed in the total ion chromatograms. Here, only the representative biocrude obtained from HTL of mixtures at 300 °C were described and categorized, as listed in Table 6-2.

Table 6-2 Identified main components with relative area in the total ion chromatogram of biocrude obtained from HTL of model substances at 300 °C for 20 min

Retention time (min)	Components identified	Relative area content (%)			
		Lysine	Lysine& lactose	Lysine &PA	Lysine&lactose&P A
	N-heterocycles				
6.96	Pyrazine,methyl-		4.9		
7.05	Pyrazine, methyl-				0.1
8.45	Pyrazine,2,5-dimethyl-		9.6		0.0
8.53	Pyrazine,2,3-dimethyl-		3.22		0.1
9.67	Pyrazine, trimethyl-		7.4		0.1
10.51	Pyrazine, 2-ethyl-3,5-dimethyl-		1.1		
10.56	Octahydro-2H-quinolizine	0.8			
11.07	Pyridine, 2-ethyl-6-methyl-5,6,7,8-		3.4		
11.07	Tetrahydroindolizine				0.1
11.36	Quinoline, decahydro-, cis-	4.5		0.3	
11.54	Quinoline, decahydro-, cis-	1.7			
11.6	Quinoline, decahydro-1-methyl-,cis-	0.9		0.2	
11.73	Pyridine, 2-ethyl-4,6-dimethyl-		8.7		
12.34	Quinoline, 1,2,3,4-tetrahydro-		3.5		
12.52	2-ethyl-6-isopropylpyridine		3.9		
12.52	2-ethyl-6-isopropylpyridine		0.0		0.1
12.65	1-Propyl-2-methyl-5-vinylpyrrole		3.6		0.1
13.19	1-Methylimidazolidin-2-one		0.0	1.5	
13.34	1H-Indole, 6-methyl-		3.5		0.3
14.23	pyrazine, 1,2-dimethoxy-4-(1-propenyl)-		4.3		
14.57	Pyrazine, 3,5-diethyl-2-methyl-				0.1
14.94	2H-Indol-2-one, 1,3-dihydro-1,3,3-trimethyl-				0.1
16.38	2-ethyl-3,5,6,7-tetramethyl-pyrazolo(1,5-a)pyrimidine	0.6			
18.93	Pyrazol-5(4H)-one, 1-phenyl-3-propyl-	2.8			

20.49	Pyrrolidine, 1-(1-oxooctadecyl)-				0.8
20.85	Thiazole, 4-ethyl-2-propyl- Amines			3.25	10.2
5.68	Piperidine	14.8		3.8	0.1
7.43	Piperidine, ethyl-				0.3
7.39	Piperidine, 1-ethyl-	0.6	2.4		
11.22	1-Piperidinecarboxaldehyde	1.4	2.6	0.1	
11.78	Piperidine, 1-acethyl-	2.2	10.8		0.2
12.2	Benzenamine, 2,4,6-trimethyl-		2.6		0.1
12.9	Benzenamine, 2,6-diethyl-		1.8		0.0
13.23	Propanal, dimethylhydrazone				0.0
13.41	Benzenemethanol, 4-hydroxy-.alpha.-[1-(1-methyl)]			0.2	0.1
14.5	Piperidine, 3,5-dimethyl-				0.0
14.76	Decahydroisoquinoline				0.1
15.8	Benzaldehyde, 4-(diethylamino)-	0.9	3.0	1.5	0.1
16.38	2-ethyl-3,5,6,7-tetramethylpyrazolo(1,5-a)pyrimidine				0.1
16.63	N-Formyl-2-(2,5-dimethylphenyl)-piperidine	1.0			0.3
21.19	Butanedioic acid, 2,3-bis(1-piperidinylmethyl)-			1.8	
22.09	Butanedioic acid, 2,3-bis(1-piperidinylmethyl)- Amides			1.3	
12.27	Caprolactam	9.5	4.4	6.8	
13.48	l-Alpha-amino-epsilon-caprolactam	1.8			
17.79	Acetamide, Octahydrodipyrido[1,2-a:1',2'-d]pyrazine-6,12(2H,6aH)-dione	15.2	4.0	10.4	2.3
17.83	Octahydrodipyrido[1,2-a:1',2'-d]pyrazine-6,12(2H,6aH)-dione	22.8	5.8	15.9	2.9
18.15	hexadecanamide			3.5	5.9
18.53	N,N-Dimethyldodecanamidepropyl-				1.5
18.7	Triethylenemelamine				0.8
22.22	N-(1,3-dioxo-1H,3H-benzo[de]isoquinolin-2-yl)-2-piperidin-1-yl-acetamide O-containing compounds	2.7			

8.33	2-cyclopenten-1-one,2-methyl-		1.6	
10.07	2,3-dimethyl-2-cyclopenten-1-one		1.1	
11.81	1-oxaspiro[2.5]octane			0.5
12.82	Bicyclo[4.2.0]oct-1-ene, 7-endoethenyl	0.2		
13.41	benzene, 1,2-dimethoxy-4-(1-propenyl)-	1.8	2.8	
16.40	9-Anthracenemethanol			0.8
16.94	Hexadecanoic,acid			17.8
17.19	9-Fluorenone, 2,4-dimethyl-	2.4		59.9
17.22	5,7-Dihydroxy-4-methylcoumarin			1.8
17.46	9H-Fluorene, 9-propyl-	0.6		
17.91	2H-1-Benzopyran-2-one, 5,7-dimethoxy-	2.8		3.0
18.34	10-Methylanthracene-9-carboxaldehyde	0.7		1.2
29.59	18,19-Secolupan-3-ol, (3beta,17xi)-			2.9

To ease the discussion, the major chemical compounds in the biocrude were classified into five categories based on relevant functional groups: N-containing heterocycles (e.g. pyridines and pyrazines), amines (e.g. cyclic piperidines, and 2,4,6-trimethylbenzenamine), amides (e.g. caprolactam, DKP and palmitamide), O-containing compounds (mostly palmitic acid in case PA is involved in the feedstock), and others which represent the undetected compounds.

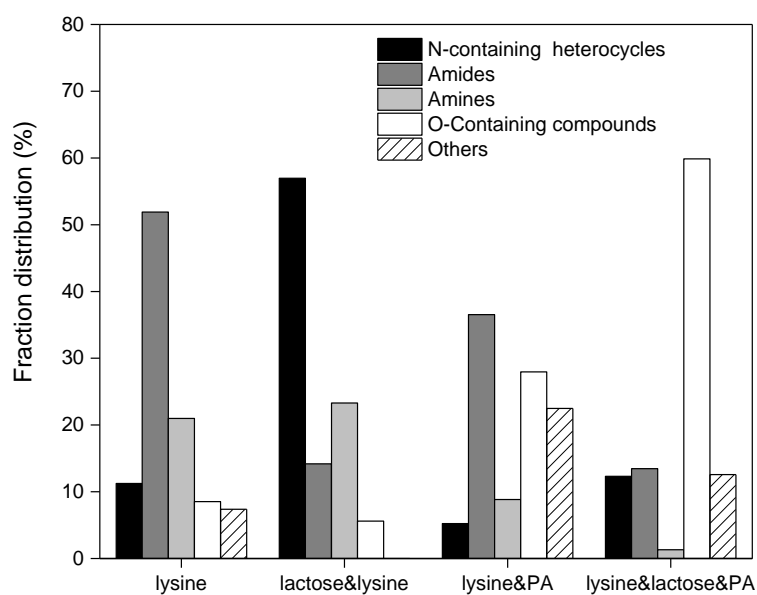


Figure 6-6 Comparison of compounds identified by GC-MS analysis of biocrude from HTL of model compounds at 300 °C (20 min) based on fraction distribution

As illustrated in Figure 6-6, the fractions identified in the bio-oil are largely dependent on the initial model substances. The lysine biocrude contains a large fraction of cyclic amides, such as caprolactam and DKP in Table 6-2. These amides are dramatically decreased (reduction of 73 %) in the biocrude obtained from the mixture with lactose, whereas N-containing heterocycles increase from around 10 % to 54 %. As can be seen in the table above, the new derivatives of pyrazines and pyridines are generated, reflecting the strong interaction between lactose and lysine and leading to N-containing heterocycles.

Considering the binary mixture of lysine and palmitic acid, the amides fraction, which is the highest relative concentration (36 %) in the biocrude, is lower compared to the crude derived from HTL of lysine alone. Except for the dominant amount of DKP, a high fraction of palmitamide (3.5 %) must be mentioned, which reflects the direct interaction between lysine and PA. Regarding the ternary mixture, 59 % of the products belong to the O-containing compounds including 57 % non-reacted palmitic acid, and similar amounts of N-cyclic heterocycles and amides, which are obtained from the ternary mixture (around 12 %).

Somehow, it seems confusing to illustrate the effects of lipids on the N-containing compounds, especially the combined lysine-derived cyclic amides and the fatty amides generated from PA mixed with lysine. It is therefore necessary to further quantify the absolute yields of typical chemicals as shown in

Figure 6-7. The yields, which can be referred to as the concentration, of specific products are defined as the mass of individual compounds based on the mass of biocrude. Piperidine, caprolactam and DKP are the three main N-containing compounds detected in the output of HTL of lysine alone, representing cyclic amine and amide. As shown in Figure 6-7(a), both compounds first dramatically increase and then decrease with increasing temperature from 250 to 350 °C, while the yields of caprolactam are nearly twice that of piperidine at the same temperature. However, when mixed with lactose (Figure 6-7(b)), new N-cyclic heterocycles (pyrazine derivatives) are present at the great expense of the piperidine and DKP. Less than 0.4 wt.% of piperidine is found in the biocrude, caprolactam is levelled off with the reaction temperature, reaching to 0.8 wt.% at 350 °C, which is 5 times less than in the product of single lysine. DKP undergoes an increase and then a decrease with increasing temperature, the maximum amount is 10 times less than that what is generated from single lysine. Pyrazines are almost linearly

reduced with increasing temperature. Considering the mixture of lysine and palmitic acid (Figure 6-7 (c)), in contrast to single lysine, higher piperidine yields of around triple that of caprolactam are found in the biocrude, and the yields of piperidine slightly increased to 7.5 wt.% at 350 °C, indicating that either intermediates generated from palmitic acid improve the cyclization of lysine, or the decomposition of caprolactam increases the piperidine yield directly. Palmitamide is identified as a new N-containing amide, increasing from 3.8 to 5.7 wt.% as the temperature rises from 300 to 350 °C. Accordingly, a decrease in caprolactam from 1.7 to 0.7 wt.% is observed. Regarding ternary mixtures (Figure 6-7 (d)), palmitamide and piperidine become the major N-containing compounds, increasing from 0.8 to 2.8 wt.% and 0.3 to 1.3 wt.%, respectively. 0.1 wt.% 2,3,5-trimethylpyrazine and 0.2 wt.% 2,5-dimethylpyrazine are obtained in the biocrude, 0.3 wt.% caprolactam is found at all temperatures.

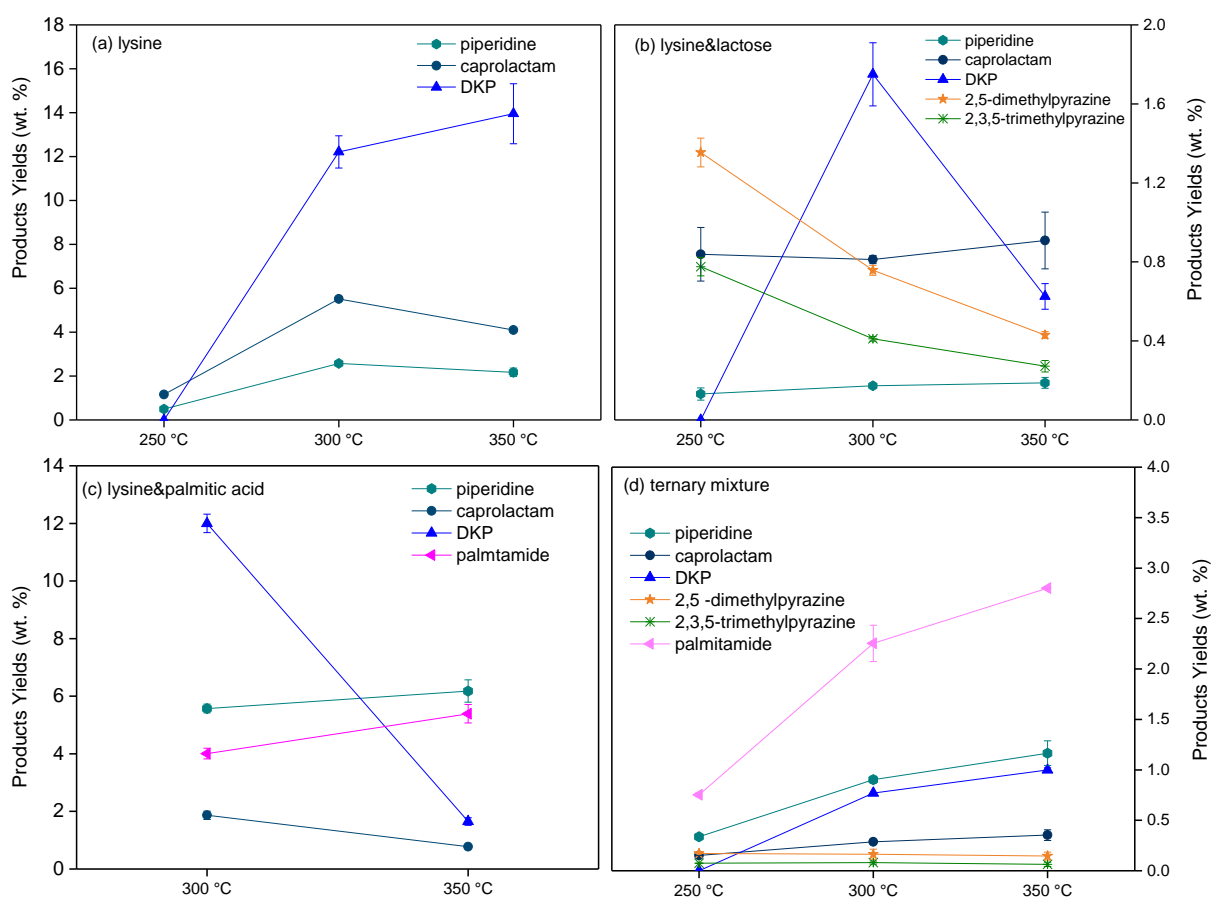


Figure 6-7 Key N-containing compounds in the biocrude obtained from HTL of model compounds (a) single lysine; (b) lysine and lactose mixtures; (c) lysine and palmitic acid; (d) ternary mixture

The only substituted long-chain aliphatic amide is found in the biocrude and increased

with reaction temperature, which is in line with findings of Chiaberge [200]. This can indicate a base reaction medium, in which the rate of amide formation or condensation is much faster than the hydrolysis rate of hexadecanamide.

With regard to pyrazines in the biocrude from ternary mixture, an extremely low yield of pyrazines is produced and remains essentially constant. Accordingly, a significant increase in amides indicates the strong competition between amidation and MRs. It has been reported that some lipid-Maillard products are produced by the interaction between lipid and Maillard precursors as evidence of long-chain heterocyclic compounds containing N or S was found when thiophene was mixed with pyrazines at 140 °C [222]. This could be one reason to explain the suppression of Maillard reactions, even though in this work, no S-containing compounds are involved. Being in the same periodic group, N and S, however, can behave similarly in this case. It is likely that fatty acids and their free-radical degradation products compete with the sugar-derived carbonyl compounds to react with active amino groups or the amines formed during the heating time to generate amides, thus interfering with the Maillard pathways, leading to an extensive suppression of pyrazines.

A possible second reason could be the occurrence of Mannich reactions between amines and formaldehyde in the presence of carbonyl functional groups [124]. During HTL, after more than a few minutes, lactose is easily converted into short-chain carboxylic acids as well as phenolic compounds, aldehydes, and ketones [219, 223]. The intermediate nitrogen-containing compounds may have reacted with formaldehyde and phenols via Mannich reactions, forming solid products. In the presence of lactose, the interactions between PA and lactose could generate short-chain carboxylic acids as intermediate products that increase the acidity of the reaction medium, which further inhibits pyrazine production. This is in agreement with Koehler's work [224], where the addition of sulfuric acid reduced pyrazine formation to practically zero in a glucose-asparagine system. The overall high $\text{NH}_4^+\text{-N}$ in the aqueous phase (seen Figure 6-9) could be proof that higher acidity promotes the deamination of amino acids or N-containing polar water-soluble organics, leading to a decrease in Maillard reaction products. According to the results and discussion above, the possible reaction pathways that encompass the fate of N within the system can be proposed based on the model compounds' reaction network and are shown in Figure 6-8.

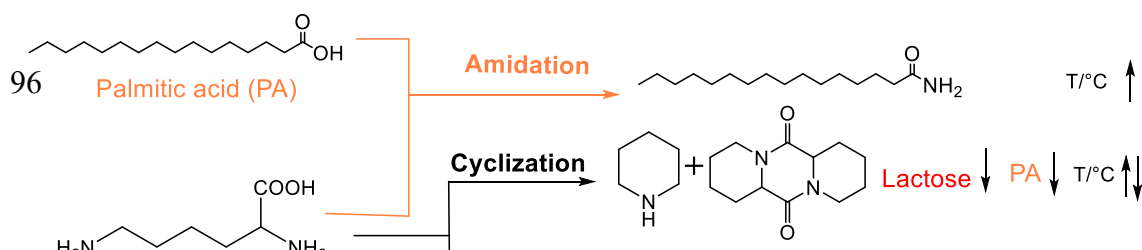


Figure 6-8 Reaction network for the N-containing compounds obtained from HTL of model substances (the up and down arrows represent the increase and decrease in efficiency, respectively)

6.2.5 Nitrogen distribution

To sum up, the nitrogen distribution (ND) in the different product phases is also illustrated in Figure 6-9.

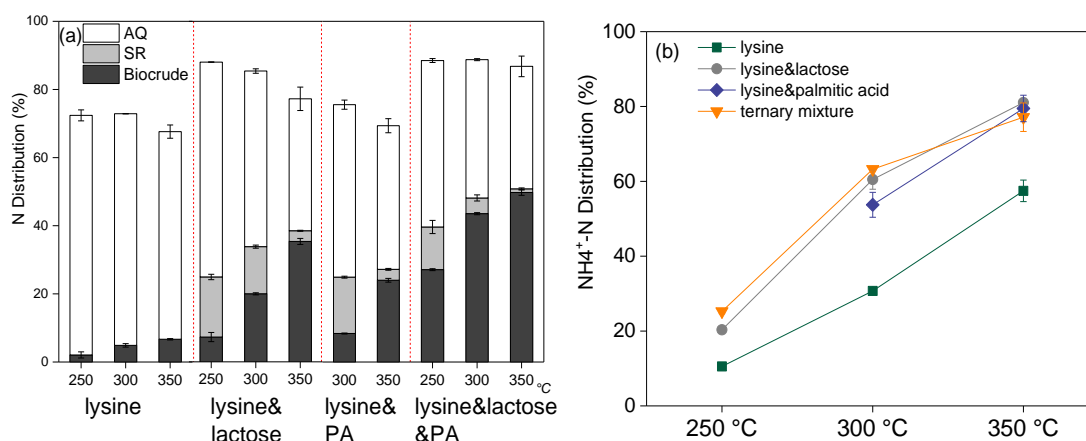


Figure 6-9 (a) N distribution to different product phases; (b) $\text{NH}_4^+\text{-N}$ distribution to aqueous phase

Compared with lysine, the ND to bio-oil is increased with the addition of lactose and palmitic acid, and significantly rises with the reaction temperature, which is not only ascribed to the increasing biocrude yields, but also the new N-containing compounds generated from the cross-linking reaction among mixed substances. Accordingly, a slight decrease in ND can be observed in the AQ, reflecting the enhanced conversion of water-soluble N-containing compounds into the biocrude phase. Considering the binary and ternary mixtures, the ND to SR and AQ are dramatically reduced with increasing temperature. In particular, the ND to SR obtained from binary and ternary mixture of

lactose decreased from 17.6 to 3.1 % and 12.5 to 1.1 %, respectively. Furthermore, it is notable to see that around 35 % (in the AQ from ternary mixture at 350 °C) to 70 % (in the AQ from lysine alone at 250 °C) are converted into the water phase. Therefore, a specific investigation of ND in AQ is displayed in Figure 6-9 (b). The N in AQ is categorized into ammonium ($\text{NH}_4^+\text{-N}$) and organic nitrogen, which is calculated by the difference between total nitrogen and ammonium. In all cases, the $\text{NH}_4^+\text{-N}$ sharply increases with increasing temperature, almost reaching 80 % in the AQ from binary and ternary mixture at 350 °C. In the presence of lactose and PA, the $\text{NH}_4^+\text{-N}$ distribution is higher than that from lysine alone.

6.3 Conclusion

The work presented here provides a fundamental understanding of the fate of N during HTL based on the comparison of biocrude samples obtained from different model substances. The dramatic difference in the chemical composition of biocrude by HTL proved that it is necessary to clarify the interaction between different organic compositions in the feedstocks. In all cases, with the addition of lipids, the N distribution in the biocrude is enhanced due to the higher biocrude yields. Amidation may explain the higher biocrude yields and composition owing to the long-chain aliphatic fatty acid amide produced. Regarding the ternary mixture, the addition of lipids largely modifies the type of N-containing species in the final biocrude, but it does not affect the nitrogen content. With increasing temperature, the strong competition between amidation and MRs significantly impacts the fate. Therefore, attention should also be paid to the Maillard reaction, particularly on the reaction mechanism of N-containing heterocycles.

Chapter 7 HTL of model substances: Maillard reactions

7.1 Introduction

As stated in Chapter 1.4.2, Maillard reactions are generally confirmed to be significant reactions during HTL of protein/carbohydrates-containing feedstock. Several studies have provided evidence that reactions induced by proteins/amino acids influence the biocrude yield and N distribution. However, this complex network of parallel and consecutive reactions that forms different polymers and co-polymers called Maillard reaction products including some nitrogen-containing compounds and nitrogenous heterocycles, is poorly understood.

To the best of my knowledge, few studies have directly examined a mixture of model compounds of proteins and carbohydrates under hydrothermal conditions to determine the reaction pathways of Maillard reactions, particularly with regard to the nitrogen impact on the main compounds in the resulting biocrude. In this study, lactose and lysine were selected as model compounds for HTL conversion. The objectives of the study were: (1) to investigate the influence of Maillard reactions on product distribution under different conditions; (2) to evaluate the N-distribution between the product phases, and (3) to identify the chemical nature of key compounds present in the bio-oil, with the goal to provide a better understanding of the reaction pathways during HTL of sewage sludge, as well as other protein-containing feedstocks with particular attention to the nitrogen-containing heterocycles.

7.2 Methodology

7.2.1 Materials

The model substances are described in Chapter 6. The analytical grade hydroxymethylfurfural (HMF) was purchased from Sigma-Aldrich.

7.2.2 Hydrothermal liquefaction procedure

In this work, batch HTL process was performed by different procedures.

The experiments aiming to investigate the effects of mixture ratio, temperatures and

catalysts were conducted using a GC oven. Specifically, in the case of mixture ratio, the initial concentration of feedstock was fixed at 10 wt.%, the mass weight ratio of carbohydrates to proteins was varied by 100/0, 80/20, 60/40, 50/50, 40/60, 20/80 and 0/100, the prepared feedstocks were loaded into micro-autoclaves and then heated at 300 °C for 20 min. The experiments related to the effects of temperature were exactly the same as in Chapter 6, where 10 wt.% feedstock was processed at 250, 300 and 350 °C for 20 min.

The batch experimental setup for examining the influence of retention time was heated to 250 and 300 °C with a fluidized sandbath. The retention times were defined as 0, 1, 5, 10, 20, 40 and 80 min.

Additional experiments with regard to the hydrothermal conversion of pure lactose and mixtures with lysine were performed according to the same procedure at 200 °C for 20 min. Moreover, another experiment was designed to investigate whether the addition of lysine would affect the conversion of HMF or not: a solution (21.5 mL) containing 2000 mg/L of HMF with or without 5 mmol of lysine was placed in a micro-autoclave and treated in the oven at 200 °C for 20 min.

The separation and analysis of products followed the same procedure as described in Chapter 3.

7.3 Results and Discussion

This chapter starts with the optimum ratio of carbohydrates to proteins with regard to the biocrude yields, followed by the effects of temperatures and heating rate on the biocrude yields and Maillard reactions products, followed by the determination of the influence of retention times.

7.3.1 The effects of carbohydrates-to-proteins ratio

This section examines the effects of the ratio between carbohydrates and proteins on the performance of Maillard reactions. HTL tests for the mixture of lactose and lysine at different ratios (100/0, 80/20, 60/40, 50/50, 40/60, 20/80 and 0/100, lactose:lysine w/w %, 100/0 and 0/100 were examined as control experiments according to the pure carbohydrates and proteins, respectively) were conducted in this work to investigate the influences of Maillard reactions on biocrude yield during HTL. All the experiments were performed at 300 °C for 20 min; 300 °C was selected as this temperature has been widely

applied in HTL of biomass.

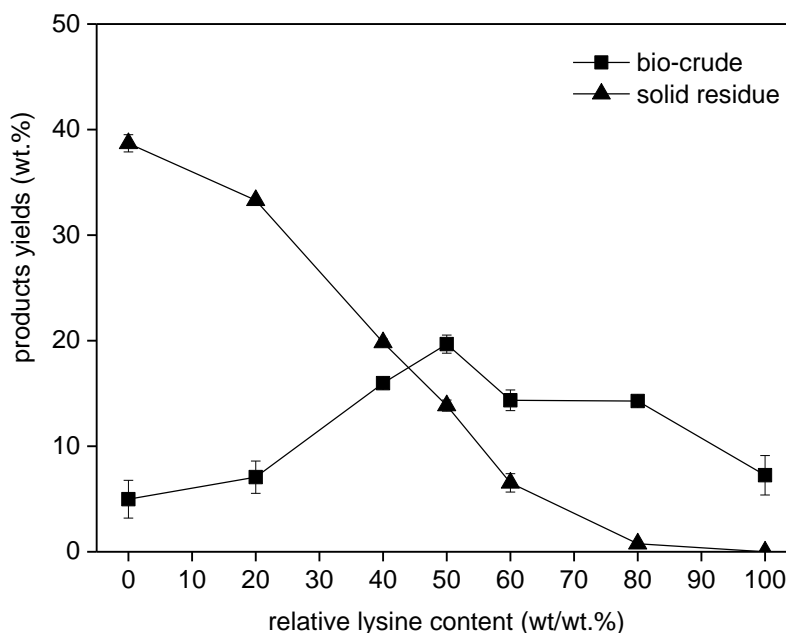


Figure 7-1 Biocrude and solid residue yields from HTL of binary mixture at 300 °C for 20 min for different initial mass ratio of lysine to mixture

The yields of biocrude and solid residue under different conditions are shown in Figure 7-1. It can be seen that 38.7 wt.% of solid residue and 5.0 wt.% biocrude are derived from HTL of lactose alone, while relatively higher yields of biocrude are obtained from single lysine. By adding lysine to lactose, the bi-crude yields increase from 7.1 to 19.7 wt.% as the relative lysine content increases from 20 to 50 wt.% and decreases to 14.3 wt.%. While the hydrochar exhibits the opposite trend to biocrude. With the increasing ratio, the hydrochar reduces significantly. As lysine could generate more biocrude than lactose during HTL, the higher content of lysine as compared to the mixture is supposed to result in higher amounts of biocrude. However, a maximum value of biocrude is obtained at 1:1 mass ratio, and an excess of lysine decreases the amount of biocrude. Compared with the production rate of biocrude, the higher amount of carbohydrates results in a faster increasing rate, and, accordingly, the higher amount of lysine is unfavourable for the biocrude products, implying reactant ratios greatly affect the amount of biocrude formed if glucose is present in excess.

The mono conversion of lactose provokes an acidification of the hydrothermal medium due to the rapid production of short-chain carboxylic acids such as lactic acid, formic acid, acetic acid and levulinic acid. The addition of lysine to the reaction buffers this acidity due to the amino acid degradation and production of NH_3 , while the addition of alkalinity to the reaction medium may catalyze further cross-linkage between all intermediates

instead of the production of hydrochars via carbonization. However, in biocrude generated using Maillard reactions, no hydrochar is observed at a 4:1 ratio of lysine to lactose. The inhibition of hydrochar formation can be explained with the fact that the ammonia formed by Maillard reactions acted as alkali catalyst to enhance decarboxylation of carbohydrates [58].

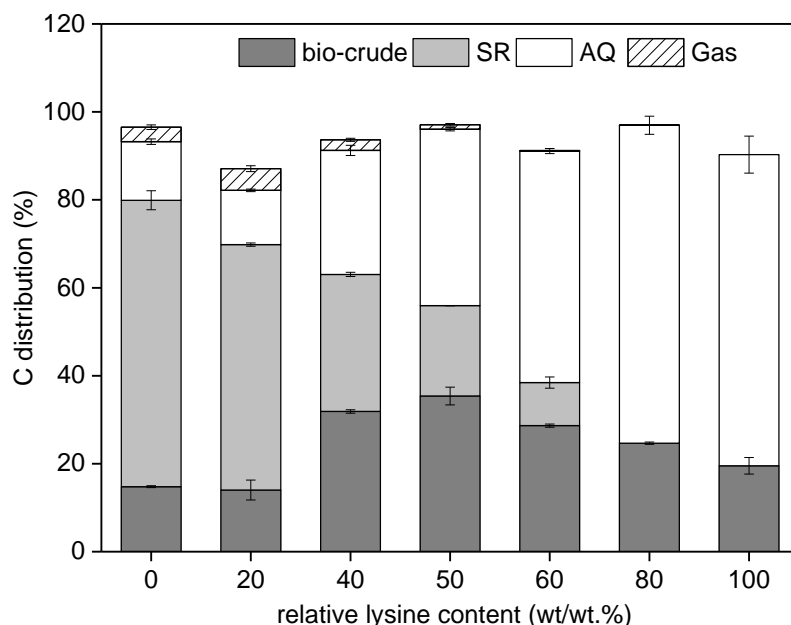


Figure 7-2 C distribution in different phases from HTL of binary mixture at 300 °C and 20 min for different initial mass ratio of lysine to mixture

As shown in Figure 7-2, about 65 % of the carbon remains in the solid residue from HTL of lactose alone, and an approximately equal amount of 14 % C was distributed to biocrude and the aqueous phase. Regarding HTL of lysine alone, no solid residue is found after HTL as the majority of carbon transforms into molecules soluble in the aqueous phase and, to a lesser extent, into biocrude. When lactose and lysine are mixed together, biocrude and the aqueous phase will contain most of the carbon, which is consistent with the increased biocrude yields obtained via HTL of the mixtures. The carbon content in the solid therefore decreases with the increasing ratio of lysine. These observations suggest that Maillard reactions suppress the carbonization of carbohydrates. Usually, carbonization occurs during hydrothermal conversion at lower temperatures (< 250 °C) via furan-based intermediates like hydroxymethylfurfural (HMF) and furfural and further polymerization to “hydro-char”, hence accumulating more carbon in the solid residue [225]. This hydrochar, once formed, is difficult to liquefy into bio-oil or aqueous phases [58]. However, when adding lysine to carbohydrates, the carbon content in the solid residue reduces, while that in biocrude and the aqueous phase increases correspondingly,

accompanied by an almost total absence of the previously discussed furan-based intermediates (see Figure 7-5 below). It has been confirmed by Titirici et al. [225] that HMF is the key intermediate, which finally condenses to “hydro-char” during HTC of hexose-based sugars. With the intention to study how exactly lysine inhibits char formation of carbohydrates, additional experiments were performed with HTL of pure lactose and HMF, as well as mixtures of both of these with lysine, at 200 °C for 20 min, aiming to investigate the effect of the amino acid on the HMF conversion.

Table 7-1 HMF concentration in the aqueous phase from HTL of model compounds at 200 °C with 20 min

Samples	Concentration (mg/L)	HMF conversion (%)
HMF	1979.3	1.3
HMF + lysine	18.2	99.1
	Concentration (mg/L)	HMF yields (wt.%)
Lactose	4930.0	4.9
Lactose + lysine	12.5	0.01

As can be observed in Table 7-1, around 99 wt.% of the added HMF has been converted in the case of added lysine. In addition, a drastic decrease of HMF formation in the lactose/lysine system is observed. Both these factors further support the theory that Maillard reactions have some inhibitory effects on the carbonization of sugars by eliminating HMF. Instead of polymerization, HMF reacts with the amino acids, reducing the formation of hydrochar. This means that more polar and less reactive compounds – in view of further polymerisation to a solid – are formed.

The N content in the biocrude for the mixture of lactose and lysine at different ratios after HTL, as well as the N content in the initial feedstock are displayed in Figure 7-3 (a). The increasing amount of lysine certainly leads to more N content in the feedstock, from 3.8 to 19.2 wt.%, however, the N content in the obtained biocrude behaves differently: initially, it increases to 11.15 wt.% as the lysine content increases from 20 to 50 wt.% and almost levels off at 10.9 wt.% as the ratio continues to increase. In order to investigate the effect of the Maillard reaction on the fate of N, the N distribution was calculated and shown in Fig. 8-3 (b). The ND in biocrude is highly in line with the biocrude yields' behaviour: initially, it significantly increases at the expense of hydrochar production, then it

remarkably decreases in the excessive presence of lysine.

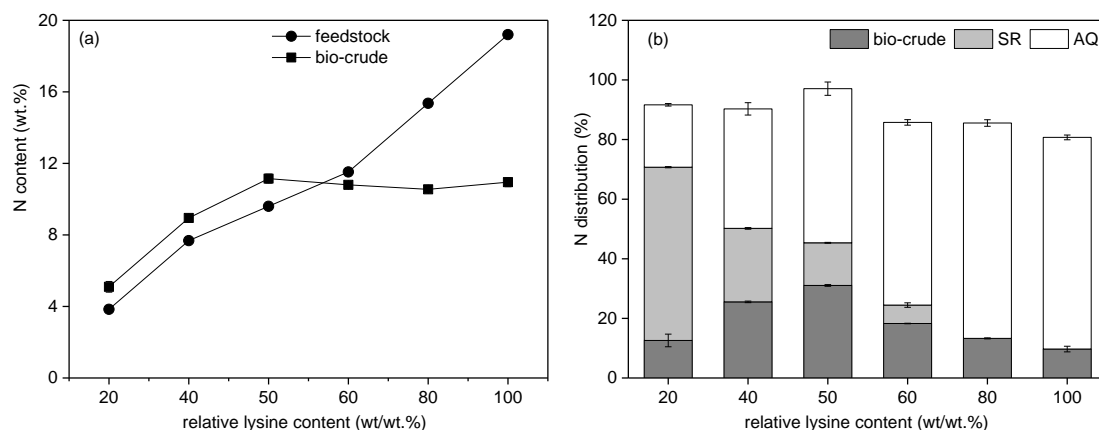


Figure 7-3 (a) N content in the biocrude and (b) N distribution in different phases from HTL of binary mixture at 300 °C and 20 min for different initial mass ratio of lysine to mixture

Having discussed the results of these mixture experiments in terms of the influence of lysine on HTL conversion of lactose, where the Maillard reactions had the main impact on carbonization, we will now examine the other side of the coin and discuss the influence of added lactose on lysine. HTL treatment of single lysine results in a considerable proportion (70.8 %) of nitrogen in the aqueous phase due to the hydrolysis of lysine under the influence of hot water. An increase in the amount of lactose enhances the N conversion into solid residue and biocrude phase, which is evidence that higher ND is found in these two phases derived from HTL of mixture as shown in Figure 7-3 (b). A possible reason for the accumulation of N in the solid residue could be the occurrence of Mannich reactions between amines and formaldehyde in the presence of carbonyl functional groups [124]. During HTL, after more than a few minutes, lactose is easily converted into short-chain carboxylic acids as well as phenolic compounds, aldehydes, and ketones [219, 223]. The intermediate N-containing compounds may have reacted with formaldehyde and phenols via Mannich reactions, forming solid products with high nitrogen contents, which is indicated by the contribution to the decrease of N in the biocrude from HTL of the binary mixture.

To prove the competition between hydrolysis and fixing of nitrogen in Maillard products as well as the temperature dependency, a more detailed review of the data is necessary. As shown in Figure 7-4, the total nitrogen (TN) concentration in the aqueous phase from HTL of single lysine conversion is rather high at approx. 16,000 mg/L. While treated together with lactose, TN dramatically decreases with an increasing lactose content. Nitrogen found in the aqueous phase can be classified into ammonia nitrogen ($\text{NH}_4^+\text{-N}$)

and organic nitrogen (Org-N), the latter being determined by the difference between TN and $\text{NH}_4^+\text{-N}$. Figure 7-4 shows the measured TN and $\text{NH}_4^+\text{-N}$ concentrations in the aqueous phase from HTL of mixture, in which the gap between two curves represents the amount of Org-N. It becomes obvious that maximum Org-N for the nitrogen contributor in the aqueous phase is produced from lysine alone, showing that lysine generates water-soluble nitrogen-containing compounds after HTL. A significant decrease with rising temperatures is observed and the ND to $\text{NH}_4^+\text{-N}$ increases correspondingly. When sugars are present, ND to $\text{NH}_4^+\text{-N}$ increases, indicating that sugars play a significant role in the final distribution of nitrogen. The reason is simply the solubility of the nitrogen compounds found.

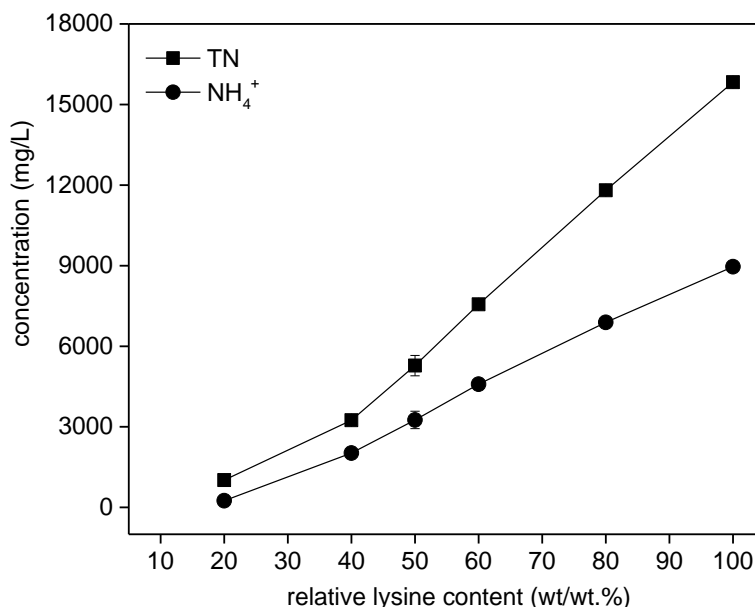


Figure 7-4 Total N concentration and ammonium in the aqueous phase from HTL of binary mixture at 300 °C and 20 min for different initial mass ratio of lysine to mixture

It is generally confirmed that carbohydrates degrade faster than proteins under equal experimental conditions, which leads to the formation of organic acid intermediates like formic acid and acetic acid, which are known to be formed during HTL [129, 226, 227]. Acids, acting as catalysts, can enhance the formation of ammonia via hydrolysis of amino acids. This means that an autocatalytic effect can additionally increase the formation of ammonia. Another possible reason could be Strecker degradation (major pathway for conversion of amino acids into structurally related aldehydes, releasing ammonia) during Maillard reactions, which increases deamination of Amadori compounds in acidic conditions [228, 229].

Key compounds in the biocrude

HTL biocrude consists of a huge number of different compounds. A complete analysis is hardly possible. Therefore, the effect of sugar / amino acid interaction is analysed using key compounds. They do not reflect every reaction pathway, but should show significant changes in the reaction network. Even though the key chemicals have been quantified in Section 0, which was focused on the investigation of the effects of lipids, less details relating to Maillard reactions occur between carbohydrates and lysine. In this section, the mechanism of Maillard reactions will be determined in detail based on the comparison of biocrudes derived from a single model compound and mixtures.

According to the total ion chromatograms of GC-MS, peaks representing different compounds are shown in Figure 7-5 and Figure 7-6. Here, only those molecules with a match quality above 80 % are considered based on the mass spectral library. It must be noted that quantitative analysis of biocrude was performed using the relative area percentage method only. FT-IR and NMR analysis of functional groups in the biocrude were carried out to supplement the results obtained by GC-MS analysis.

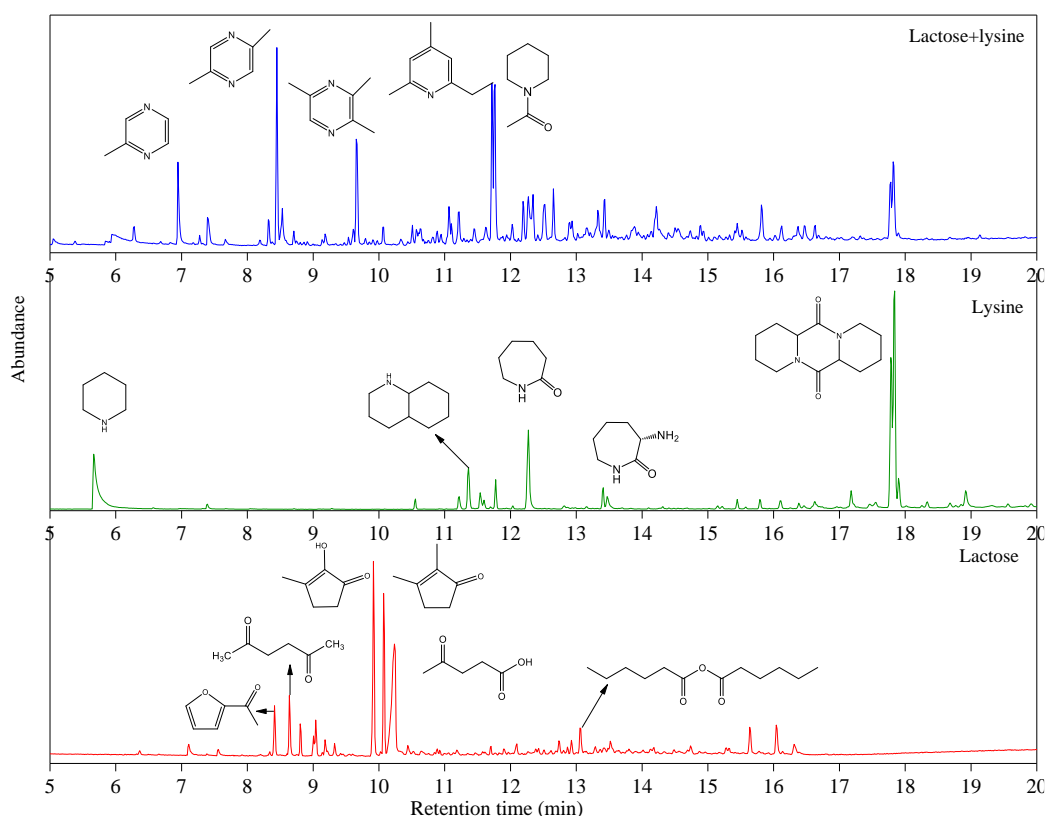


Figure 7-5 Chromatograms obtained from GCMS analysis of biocrude from HTL of model compounds under 300 °C with 20 min

Table 7-2 shows the compositions identified by GC-MS in the biocrude from HTL of lactose alone at 300 °C. The major organic component is levulinic acid, followed by

cyclopentene compounds, with their typical ring structure and carbonyl groups, as shown in Table 7-2.

Table 7-2 Identified main components of biocrude and relative percentage in the total ion chromatogram. (HTL of lactose at 300 °C for 20 min)

RT (min)	Chemicals identified	Relative content (%)
8.42	Ethanone, 1-(2-furanyl)-	1.74
8.65	2,5-Hexanedione	4.28
9.04	2(3H)-Furanone, dihydro-5-methyl-	1.15
9.19	2-Cyclopenten-1-one, 3-methyl-	1.89
9.34	phenol	1.08
9.93	2-Cyclopenten-1-one, 2-hydroxy-3-methyl-	9.7
10.08	2-Cyclopenten-1-one, 2,3-dimethyl-	8.88
10.24	levulinic acid	20.73
10.45	Phenol, 4-methyl-	0.96
12.1	2-Cyclohexen-1-one, 4-(1-methylethyl)-	1.76
12.75	1-methoxy-1,3-cyclohexadiene	2.78
13.07	Hexanoic acid, anhydride	5.08
13.32	Ethanone, 1-(2-hydroxyphenyl)-	2.62
13.43	Phenol, 2-methoxy-4-propyl-	1.66
13.53	Benzaldehyde. 2,4,6-trimethyl-	2.75
14.78	Benzene. 1-methoxy-4-methyl-	2.46

Considering the complexity of the chemical composition of biocrude from HTL, four classes of chemical compounds were considered for discussion according to the functional groups. It should be noted that, as shown in Section 0, the components of biocrude originated from lysine and binary mixture were classified including hydrocarbons due to the involvement of lipids. However, there is a specific focus on N-containing heterocycles in this section, and the different fractions of N-cyclic heterocycles have also been listed.

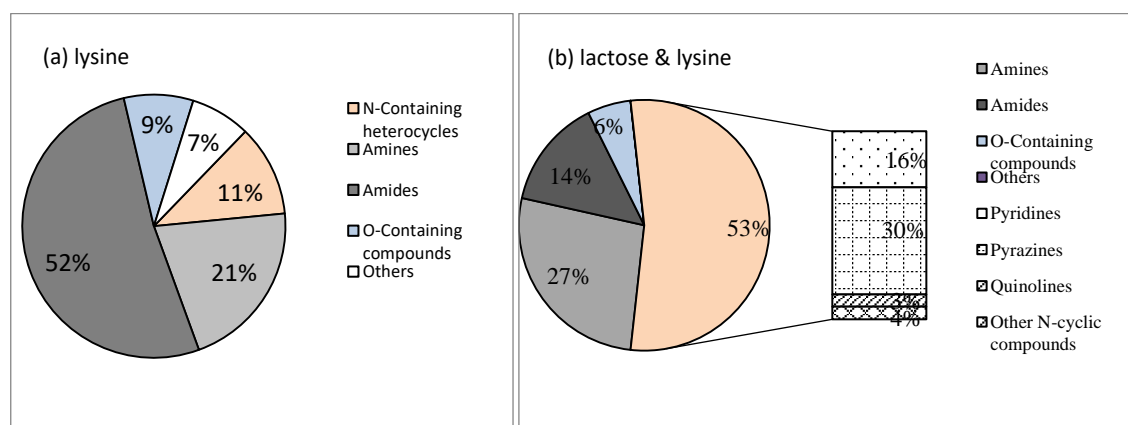


Figure 7-6 Comparison of compounds identified by GC-MS analysis of bio-oil from HTL of model compounds at 300 °C (20 min) based on fraction distribution relative peak area

Most chemicals in biocrude from HTL of lysine alone are cyclic amines and amides. They are followed by N-heterocyclic compounds like quinolines and very few O-containing compounds. When lactose is mixed with lysine, new compositions can be observed. Cyclopentenes and quinolines disappear, while nitrogen-containing heterocycles such as pyrazine and derivatives become predominant, contributing 57 % of the total heterocycles. To gain more information on the possible mechanism of the formation of key compounds, FT-IR and ¹H-NMR analysis of functional groups in the biocrude were carried out to supplement the findings obtained by GC-MS analysis. Biocrudes obtained from single or mixture compounds obtained at different temperatures show very similar FT-IR spectra as shown in Figure 7-7. Only representative spectra will be discussed in this work henceforth, i.e those of single lactose and lysine, as well as the result of their combined treatment at 300 °C. The spectra of the biocrude from lactose differ significantly from those of lysine; the strong absorption at 2952-2872 cm⁻¹ represents symmetrical and asymmetrical C-H bending stretching vibrations, indicating the presence of alkyl C-H bonds. However, the C=O bending vibration at 667 cm⁻¹ could only be found in lactose and the associated biocrudes. The C=O stretching band at 1740-1705 cm⁻¹ appears in lactose bio-oil due to the aldehydes, ketones, and carboxylic acids present, confirming the key compounds identified by GC-MS such as 2,5-hexanedione and levulinic acid. The C-N bending band at 1334-1046 cm⁻¹ and N-H bending band at 900-650 cm⁻¹ appears in lysine bio-oil, indicating the presence of amides and amines. However, both vibrations are weakened or are absent altogether in the mixture bio-oil, with an absorption band at 1660-1590 cm⁻¹ that is found in mixture bio-oil instead, insinuating the formation of aromatics including C=N and C=C groups, which is a sign of N-containing aromatic compounds identified as pyrazines and pyridines.

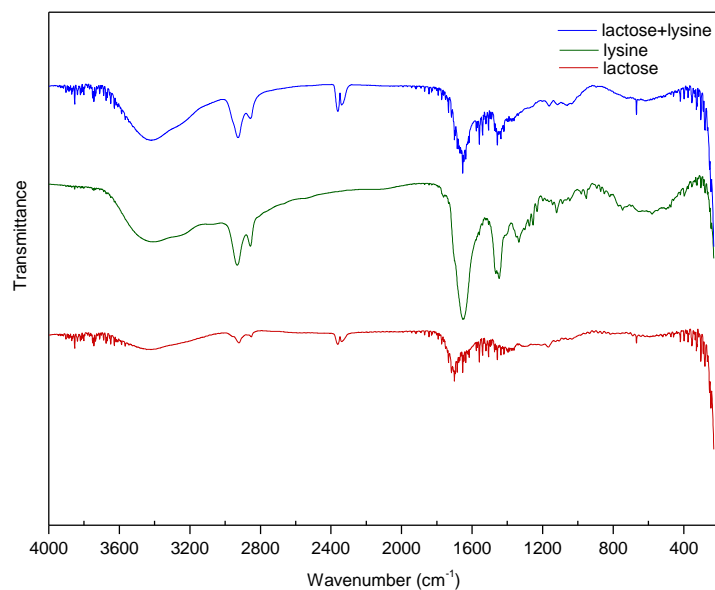


Figure 7-7 FT-IR spectra of bio-crudes from HTL of model compounds at 300 °C with 20 min

The ^1H NMR spectra of the three bio-oils discussed in the previous section are shown in Figure 7-8. The main peaks at 3.0-0.5 ppm indicate a large percentage of aliphatic functional groups in the three samples, including methylene protons ($-\text{CH}_2$) and methyl protons ($-\text{CH}_3$) obtained in the oil from lactose alone, as well as aliphatic C-NH in the oil from single lysine and mixtures. The chemical shift in the range of 8.0-6.0 ppm can be assigned to aromatic protons, that of 10.0-9.0 ppm represents carboxylic acid protons ($-\text{COOH}$) and aldehyde protons ($-\text{CHO}$). The major peaks at 3.0-2.0 ppm ($-\text{CO}-\text{CH}-$, $\text{CH}_3\text{CO}-$) appear in the bio-oil from lactose, which is in accordance with the main compounds and functional groups identified by GC-MS and FT-IR. The chemical shift of 5.0-3.7 ppm represents aromatic C-NH protons found in the bio-oils from lysine and its mixture with lactose. Apart from the aliphatic and unsaturated groups, some new significant peaks were observed in the chemical shift range of 9.0-8.0 ppm, indicating the presence of aromatic heterocycle protons in the bio-oil from the mixture, probably due to N-containing heterocycles like pyrazines identified by GC-MS. The evidence of different functional groups found in the three bio-oil samples further confirms that most N-cyclic compounds are formed by the interaction between carbonyl groups and the reactive amino groups. This will be shown in the discussion of the reaction pathways.

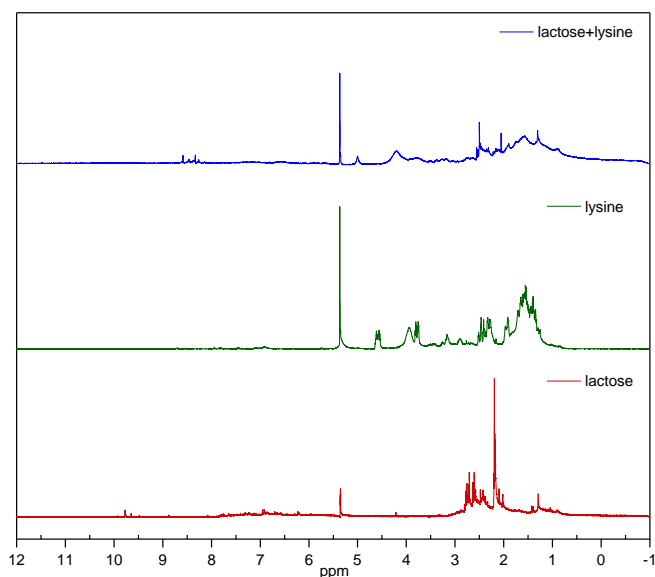


Figure 7-8 ^1H NMR spectra of bio-oils from HTL of model compounds at 300 °C with 20 min

The major N-containing compounds identified by GC-MS have been quantified as shown in Figure 7-9.

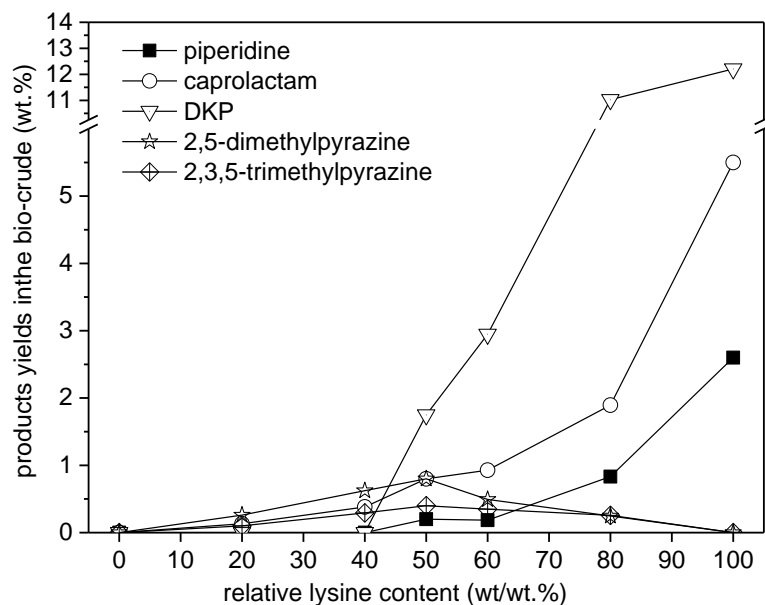


Figure 7-9 Key N-containing compounds in the biocrude from HTL of binary mixture at 300 °C and 20 min for different initial mass ratio of lysine to mixture

Notably, pyrazines can only be found in the mixture of lactose and lysine, showing an increase trend with the increasing relative content of lysine of 50 wt.%, which then significantly decreases with continued addition. This behaviour is expected because the presence of lysine would increase the initial pH of lactose conversion. The base can enhance the yields of pyrazines by increasing the reactivity of the amino groups towards

the carbonyl of glucose, increasing the rearrangement and fragmentation of sugars [224, 230]. Accordingly, piperidine caprolacam and DKP are dramatically reduced with the increased relative amount of lactose; no piperidine and DKP can be observed at 60 wt.% lactose (40 wt.% lysine), strongly indicating that Maillard reactions inhibit self-condensation of lysine to form cyclic amines and amides.

7.3.2 The effects of temperatures

It is generally accepted that temperature has a synergetic effect on the biocrude yields due to extended biomass fragmentation with increased temperature. Therefore, the aim of this section is to investigate the effects of Maillard reactions on the biocrude yields and composition in dependence of the reaction temperature.

Figure 7-10 shows biocrude yields from HTL of model compounds at 250, 300, and 350 °C, including the theoretical yields from binary mixtures, which are calculated from the sum of yields of single compounds. Filled symbols represent the measured results from model substances, the open triangle symbol shows the calculated results for mixtures based on the 50:50 wt.% ratio of single compounds. When treated individually, the biocrude yields from lysine are significantly higher than those from lactose, except at 250 °C, where lysine likely undergoes hydrolysis and fragmentation to form smaller products in the water phase at lower temperature. The biocrude yields generated from HTL of single lysine increase drastically as the temperature rises from 250 to 350 °C. While for lactose, an increase in temperature makes no significant difference regarding the biocrude products, a probable reason for this effect is the equilibrium of the two reactions in HTL involving hydrolysis and repolymerization. In the case of the mixtures, the biocrude yields always exceed those obtained from the pure compounds at all measured temperatures. The temperature dependence is more pronounced than the effect of the composition.

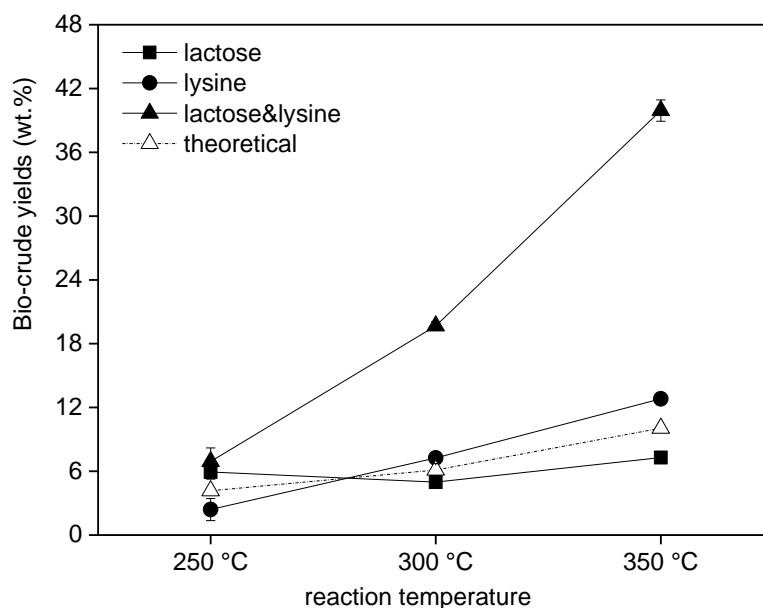


Figure 7-10 Biocrude yields obtained from HTL of the individual model compounds and their binary mixtures at different temperature

To demonstrate the effect of mixing model compounds on the biocrude yields, we compared the yields of the measured values of mixed compounds to the theoretical yields of the mixtures calculated from the sum of the single compound yields. In this comparison, the enhancement of the bio-oil yield of the mixtures becomes obvious, indicating the interactions of amino acids with carbohydrates influencing the biocrude yields derived from HTL of the mixtures; an increase in temperature thus adds a synergetic effect on the biocrude yield.

7.3.3 The effects of heating rate

Temperature and heating rate generally play a vital role in the rate of degradation and devolatilization of a given feedstock, which influences the chemical properties of the initial HTL intermediate species, from which end molecular products are formed [90]. It has to be pointed out that faster heating means shorter reaction times for the heating period below the designed temperature, which may lead to the formation of highly reactive intermediate species (e.g. radicals). Even during short residence times, these devolatilized reactive species could react with each other to generate different final products. In this study, HTL of single compounds and mixtures was carried out under various heating rates. A detailed analysis of reaction products may provide useful insights into HTL conversion, and contribute to the understanding of the effects of heating rates on Maillard reactions and N-containing compounds in the biocrude, explaining the different fate of N in the

biocrude obtained from batch and continuous processing.

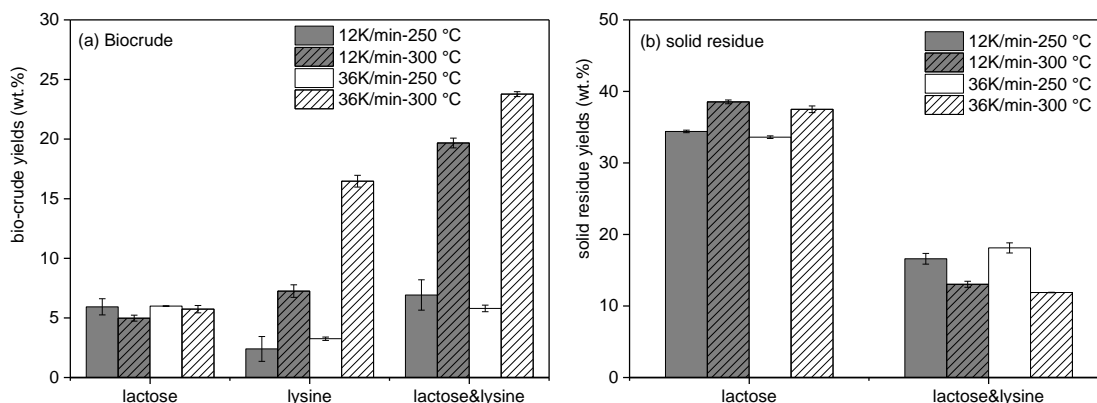


Figure 7-11 Effects of heating rate on the yields of biocrude (a) and solid residue (b) obtained from HTL of model compounds at 250 °C and 300 °C for 20 min

From Figure 7-11, it is clear that the effects of the heating rate on the biocrude highly depend on the type of model substances. The heating rates barely impact the biocrude and solid residue yielded from HTL of lactose alone, and equal yields are obtained at the same temperature, indicating that a higher heating rate does not favour hydro-char formation. Zhang et al. [231, 232] investigated the effects of heating rates on the hydrothermal conversion of grassland perennials, corn stover and wood chips, and the results suggested that hydro-char decreased as the heating rate increased. After the dissolution and stabilization of the fragmented compounds via hydrothermal processing, secondary reactions occurred for the bulk fragmentation of biomass and decreasing the heating rate could result in more solid residue [59]. High heating rates can reduce heat and mass transfer limitations and the time available for the secondary reactions of the intermediate products during HTC is also minimized. This may be explained by the potential effects of residence time. Most likely, the char formation has been stabilized before 20 min, which will be explored in the following section.

In the case of single lysine, the biocrude yields initially showed a significantly increasing trend depending on the heating rate at two temperatures: an increase from 2.4 to 7.3 wt.% and 3.3 to 16.5 wt.% with the heating rate from 12 K/min through to 36 K/min at 250 and 300 °C, respectively. As stated before, lysine mainly undergoes hydrolysis to generate water-soluble active intermediate species at lower temperatures, which can further generate non-polar compounds by cyclization and polymerization into the biocrude phase with increasing reaction temperature. Faster heating rates shorten the low temperature heating period, which may result in direct condensation of lysine to produce oily products.

Regarding the Maillard reaction system, it can be observed that the faster heating rates enhance biocrude yields at higher temperatures. This can be ascribed to the influence of temperature, since Maillard reactions are favoured at higher temperatures, while faster heating rates provide activation energies in a shorter reaction time at 300 °C. Therefore, the yields of biocrude are dramatically improved, and solid residue decreased accordingly. These results demonstrate how the combination of heating rate and temperature can be very influential for controlling the product yields from HTL.

Figure 7-12 shows the N content in the biocrude from HTL of single lysine and binary mixture at two heating rates. Faster heating rates result in a lesser amount of N in the biocrude from HTL of lysine alone, indicating that improved N removal is achieved at faster heating rates. Combined with the higher yields of biocrude, it suggests that faster heating rates can significantly improve the biocrude yields from HTL of proteins as well as their quality. While the N content remains mostly unchanged when the results of mixture HTL at heating rates of 12 K/min and 36 K/min are compared, further to confirm that the N-containing heterocycles formed by Maillard reactions are recalcitrant to be decomposed, reversely, in the form like conjugated polymers, to generate macromolecular melanoidins.

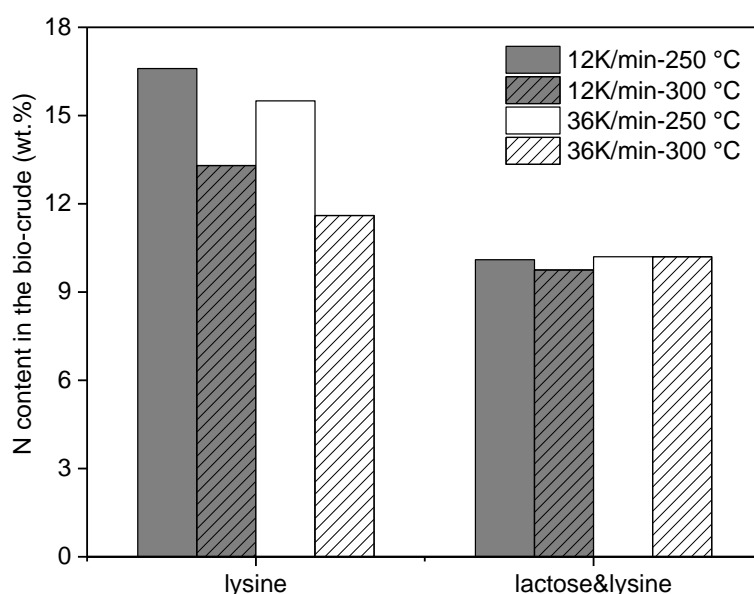


Figure 7-12 Effects of heating rate on the N content in the biocrude obtained from HTL of model compounds at 250 °C and 300 °C for 20 min

7.3.4 The effects of residence time

Regarding the observation of the heating rate on the N behaviour during HTL of sewage sludge and model mixture substances, the negligible influence could be ascribed to the

longer residence time. It could be that Maillard reactions have achieved saturation points or equilibrium conditions in less than 20 min, since such selected model substances are unstable in supercritical processes, as their rate of hydrolysis and decomposition is relatively fast. The duration of reaction times may define the overall conversion and composition of products [59]. Therefore, these assumptions motivated the author of this study to focus on the products as a function of residence time, aiming to investigate the liquefied mechanism based on the temporal variation of products.

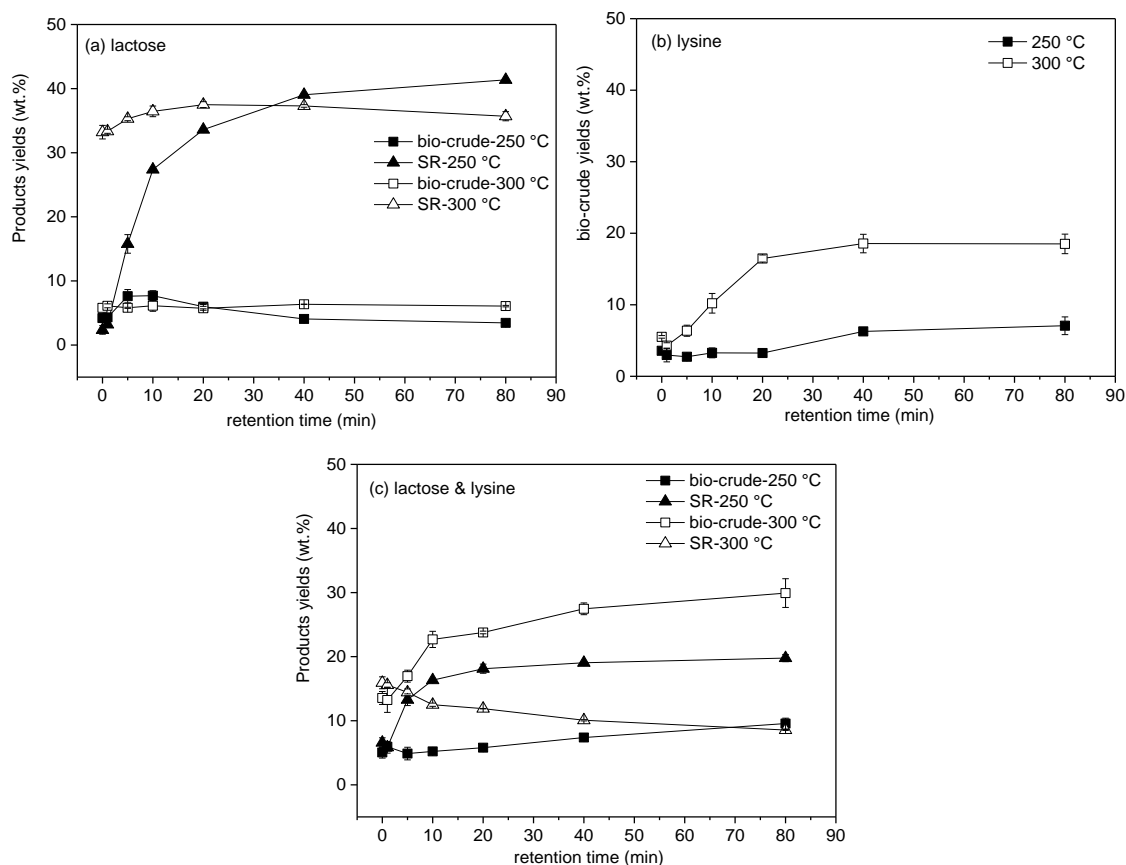


Figure 7-13 The temporal variation of biocrude and solid residue yields from HTL of model substances at 250 and 300 °C (a) lactose; (b) lysine; (c) binary mixture

Figure 7-14 The temporal variation of biocrude and solid residue yields from HTL of model substances at 250 and 300 °C: (a) lactose, (b) lysine, (c) binary mixture

Figure 7-13 (a) shows the yields of solid residue and biocrude from HTL of single lactose. It is clear that the influence of the retention time is dependent on the reaction temperature. At 250 °C for 1 min, the measured biocrude yield is equal to that of solid residue, longer reaction times significantly improve solid residue yields from 2.4 to 41 wt.%, while the biocrude yield slightly increases to 7.7 wt.% at 10 min. After that, it decreases with longer residence times. Increasing residence times at lower temperatures (250 °C) increase

biocrude yields, however, beyond a certain threshold of 10 min, any further increase in residence time has adverse results. These results mean that longer residence times enhance the repolymerization of monomers and self-condensation reactions of biocrude, resulting in the formation of char. At a temperature of 300 °C, the yield of solid residue obtained at 0 min is 33 wt.%, which is close to that of 20 min at 250 °C, slowly increasing to 37.5 wt.% at 20 min. Any further increase in the retention time leads to a slight reduction of solid residue, lower than that at 250 °C with the same time. While the reaction time does not have any significant influence on the yield of biocrude, the crude-forming reactions for lactose are essentially completed during the heating period at 300 °C.

In the case of HTL of lysine alone, no solid residue can be observed under any conditions. The biocrude yield shows a trend of an initial increase with residence time and then remains stable after exceeding the optimal reaction time (40 min). Before 40 min, the biocrude yields significantly increase from 3.5 to 6.2 wt.% and 5.5 to 18.5 wt.% at 250 °C and 300 °C, respectively. These findings suggest that the biocrude formation reaches a saturation point at 40 min; no secondary reaction occurred where the crude broke down into other by-products.

Regarding the binary mixture at 250 °C, the yields of biocrude and solid residue increased with the residence time, while the former showed a lower value than the latter, indicating that the rate of carbonization is faster than biocrude formation. While reverse results were obtained at 300 °C, as the residence time increased, biocrude yields substantially increased and solid residue yields decreased. It was observed that the biocrude yields at 300 °C were always higher than at 250 °C with the same retention time, while the solid residue yields at higher temperature less than lower temperature after 5 min. It indicates that in the Maillard reaction system, longer retention and higher temperature favour biocrude products, and secondary reactions or multiple reactions are more likely to occur to produce biocrude.

Conversion rates

The remaining sugars and lysine in the aqueous phase was determined to evaluate the conversion rate over retention time.

It should be noted that no lactose could be detected in the samples investigated at conditions with 300 °C, and only 3.4 mg/L of lactose was detected during HTL at 250 °C during the initial reaction time. The same applies to the binary mixture: less than 4 mg/L

of glucose and 95 % conversion of lysine were observed at 250 °C during the initial reaction time. It is assumed that sugars and lysine were converted almost completely.

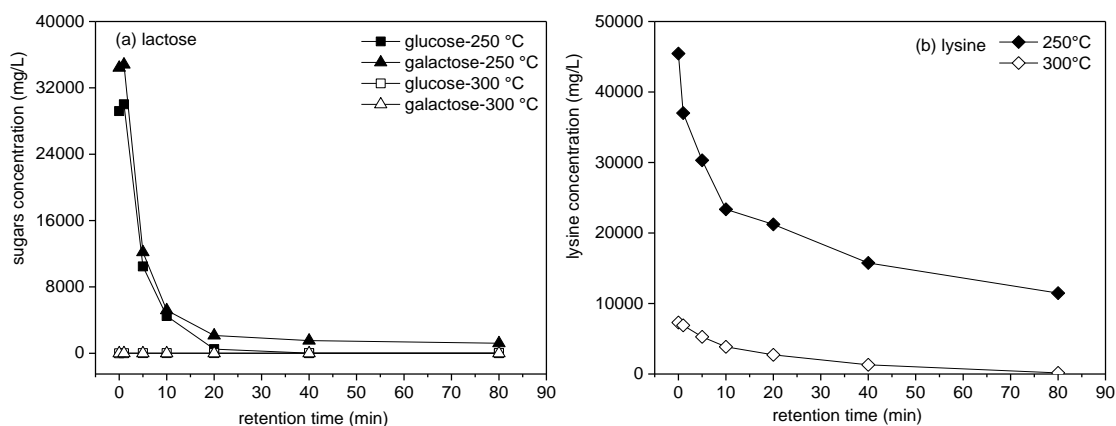


Figure 7-15 The temporal variation of sugars and lysine in the aqueous phase after HTL of model substances at 250 and 300 °C (a) lactose; (b) lysine

Theoretically, the hydrolysis of lactose should produce equal amounts of glucose and galactose, however, as shown in Figure 7-15 (a), a slightly lower content of galactose is obtained, which could be due to the fact that galactose forms carbon fragmentation units more readily than glucose. It has been noticed that at 250 °C, more than 10,000 mg/L glucose and galactose remain in the aqueous phase after 5 min, while both sugars remarkably decrease with increasing residence time. This aligns to Figure 7-13 (a), showing that less biocrude and solid residue products are generated at lower temperatures for a short retention time, indicating that the hydrolysis reactions of mono carbohydrates sustain for 5 –10 min. At 300 °C, less than 24 mg/L of sugars can be detected, suggesting that the decomposition of carbohydrates is effectively complete at this high temperature, where multiple types of reactions, such as cyclization, condensation and repolymerization, inevitably occur simultaneously and result in much more solid residue.

Lysine can be detected under all conditions as shown in Figure 7-15 (b). The concentration of lysine decreases most substantially from 0 to 80 min, the conversion rate increases accordingly from 60 to 90 % and 93 to 100 % at 250 °C and 300 °C, respectively. It is clear that lysine cannot be completely converted at 250 °C after 80 min, as 10 % lysine still remains in the aqueous phase. While higher temperatures result in a faster degradation rate of lysine, the decomposition of lysine is essentially complete at 300 °C after 20 min.

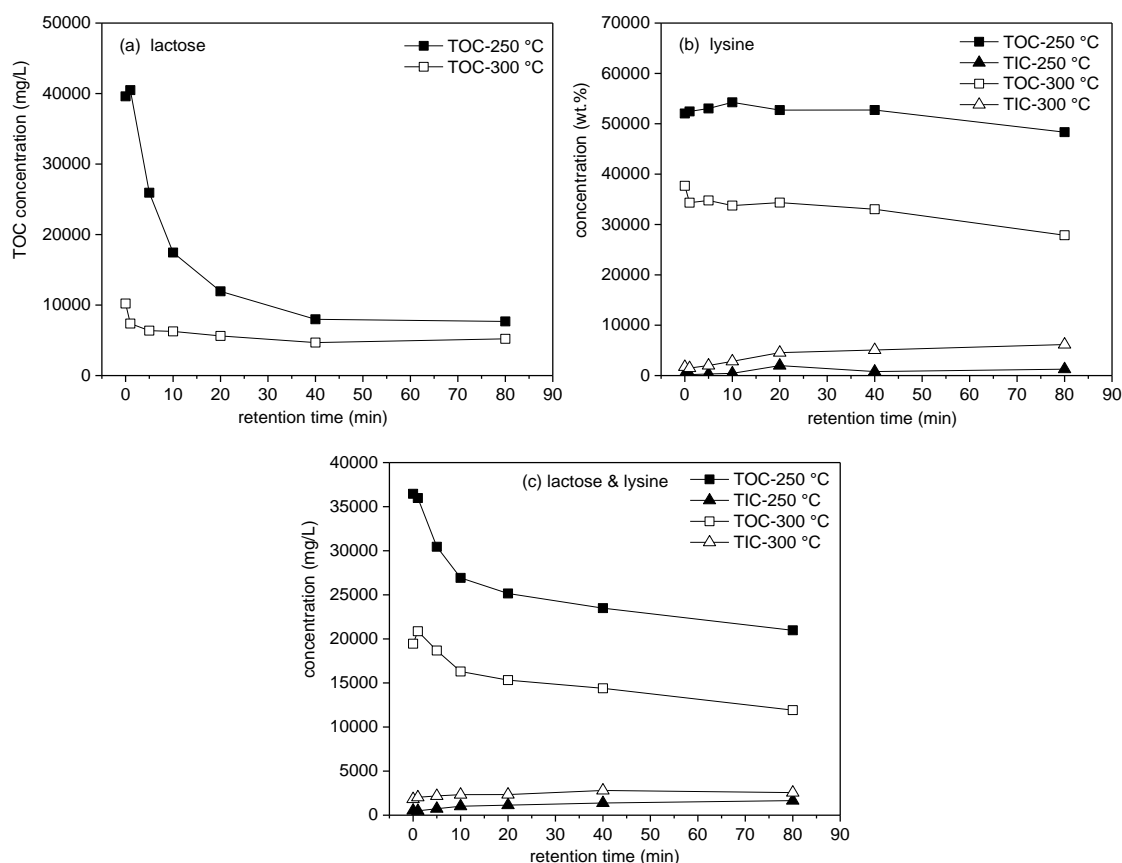


Figure 7-16 The temporal variation of total organic carbon and inorganic carbon in the aqueous phase after HTL of model substances at 250 and 300 °C (a) lactose; (b) lysine; (c) binary mixture

In all cases, the total organic carbon decreases as residence time increases at two temperatures, indicating an enhancement of the conversion of water-soluble organic compounds into biocrude or solid residue phases. Saturation of the aqueous phase could drive biocrude and solid residue formation by condensation of water-soluble intermediates. Lower temperature always leads to a higher content of organic carbon, which is highly in line with the higher sugars and lysine content detected in the aqueous phase. Notably, with residence time, an increasing amount of inorganic carbon is found in HTL of lysine alone and binary mixtures, suggesting that the decarboxylation is favoured by longer retention times. Amino acid is liable to decompose into amines and CO_2 , leading to the conversion of inorganic carbons.

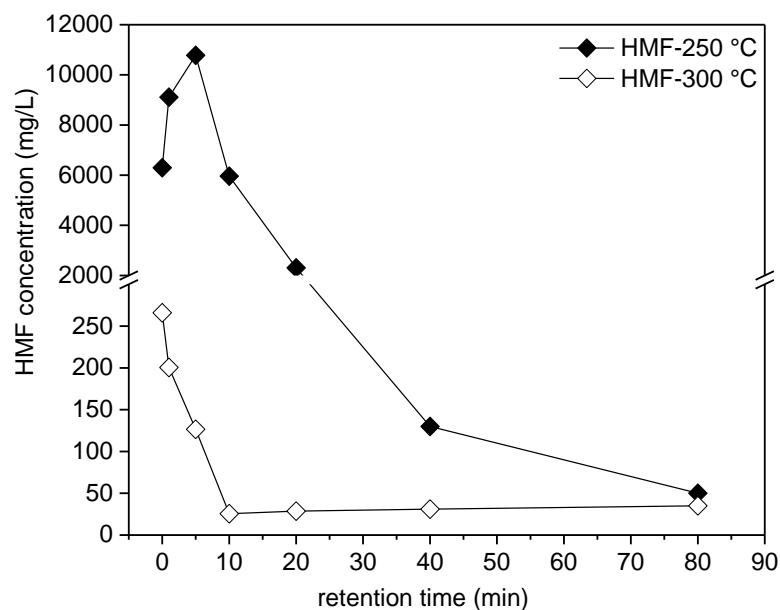


Figure 7-17 The temporal variation of HMF in the aqueous phase after HTL of model substances at 250 and 300 °C (a) lactose

As stated in Section 0, Maillard reactions inhibit carbonization mainly due to the elimination of HMF by amino acid. HMF acts as an important intermediate for end products; the change of HMF as a function of residence time is illustrated in Figure 7-17. HMF in the aqueous phase from HTL of single lactose at 250 °C shows a trend of an initial increase with reaction time, followed by a significant decrease after the optimal reaction time (10 min). This can be explained with two reaction pathways: on the one hand, HMF starts to form levulinic acid by dehydration, transferring into bio-crude; on the other hand, HMF is polymerized into hydro-char. Both reaction pathways are facilitated by high temperatures, which becomes evident due to the fact that much less HMF is found in the aqueous phase after HTL at 300 °C. In the case of binary mixtures, HMF is lower than the detected limitation, the maximum measured content was 12.5 mg/L, and it can be assumed that the addition of amino acid significantly inhibits HMF production from hydrolysis of carbohydrates or promotes its decomposition. It is difficult to ascertain whether the lysine inhibits the formation of HMF or promotes the degradation of HMF into smaller compounds such as acids. Perhaps, simply the addition of a base like lysine inhibits the acid-catalysed formation of HMF [233], or perhaps lysine enhances a reductive cleavage of HMF, which also leads to a lower HMF content. This is supported by Table 7-1, where a drastic reduction of HMF is observed in the presence of lysine in subcritical water at 200 °C. Accordingly, formic acid and acetic acids are enriched in the water phase.

N content and N-containing compounds

The N content in the biocrude varies with retention time and is shown in Figure 7-18. Regarding HTL of lysine, the N content in the biocrude obviously reduces through HTL with retention time, owing to the fact that nitrogen compounds tend to form water soluble components, which are partitioned into the aqueous phase, leading to an increase in the total nitrogen concentration. The decrease in N content could be further rationalized by compounds in the biocrude undergoing deamination, which improved with high temperatures, owing to the lower N content that was found at 300 °C.

With respect to the binary mixture, the reaction time does not have a significant influence on the N content of biocrude, with very small fluctuations around 10 wt.% observed in all the samples. This finding means that, for Maillard reactions, the competition between deamination and N-accumulation is nearly balanced. Only a small opposing trend is observed at two reaction temperatures with retention time. The N content in the bio-crude from HTL at 300 °C slightly decreases as the N content in the crude at 250 °C slowly increases: before 20 min, the former has a higher value than the latter, before they reach equal values at 20 min; then the latter constantly increases and surpasses the former. These results indicate that at lower temperatures, longer retention times favour Maillard reactions to accumulate N into biocrude.

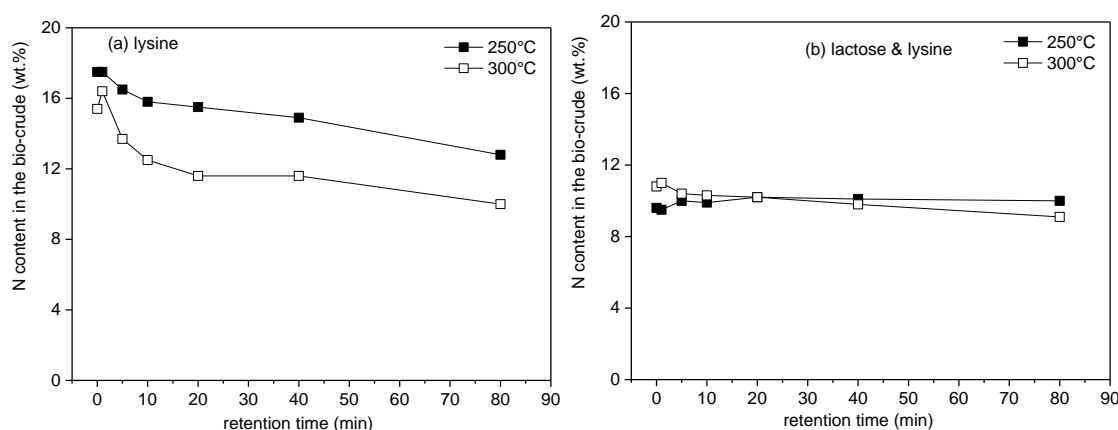


Figure 7-18 The temporal variation of N content in the biocrude after HTL of model substances at 250 and 300 °C (a) lysine; (b) binary mixture

The representative key components identified in the biocrude of lactose are furfural, levulinic acid and cyclotene as shown in Figure 7-19 (a). These are typical O-containing compounds from HTL of carbohydrates. At 250 °C, furfural and cyclotene increase greatly as the retention time increases from 0 to 20 min, before they slowly decrease with continuous residence time. Levulinic acid displays a remarkable increase trend with

retention time, which is greatly in line with the constant decrease of sugars and HMF found above, confirming that HMF is converted into levulinic acid and furfural by rehydration. At 300 °C, at the beginning of the reaction time, furfural and cyclotene show a larger value than at 250 °C, suggesting that an increase in temperature facilitates the degradation of sugars to form smaller molecular products. These compounds significantly reduce with increasing retention time, undergoing the repolymerization or condensation into macromolecular components, divided into biocrude or hydro-char. In the case of levulinic acid found at 300 °C, corresponding to the behaviour at 250 °C, a continuous increasing trend is observed with reaction time, but yields almost halve compared to 250 °C. This finding aligns with the fairly low HMF content in the aqueous phase at higher temperatures. Most likely, HMF was decomposed completely during the heating period, resulting in a less levulinic acid production. Another reason could be the improved polarity of supercritical water at high temperatures, where parts of levulinic acid can be dissolved into the water phase.

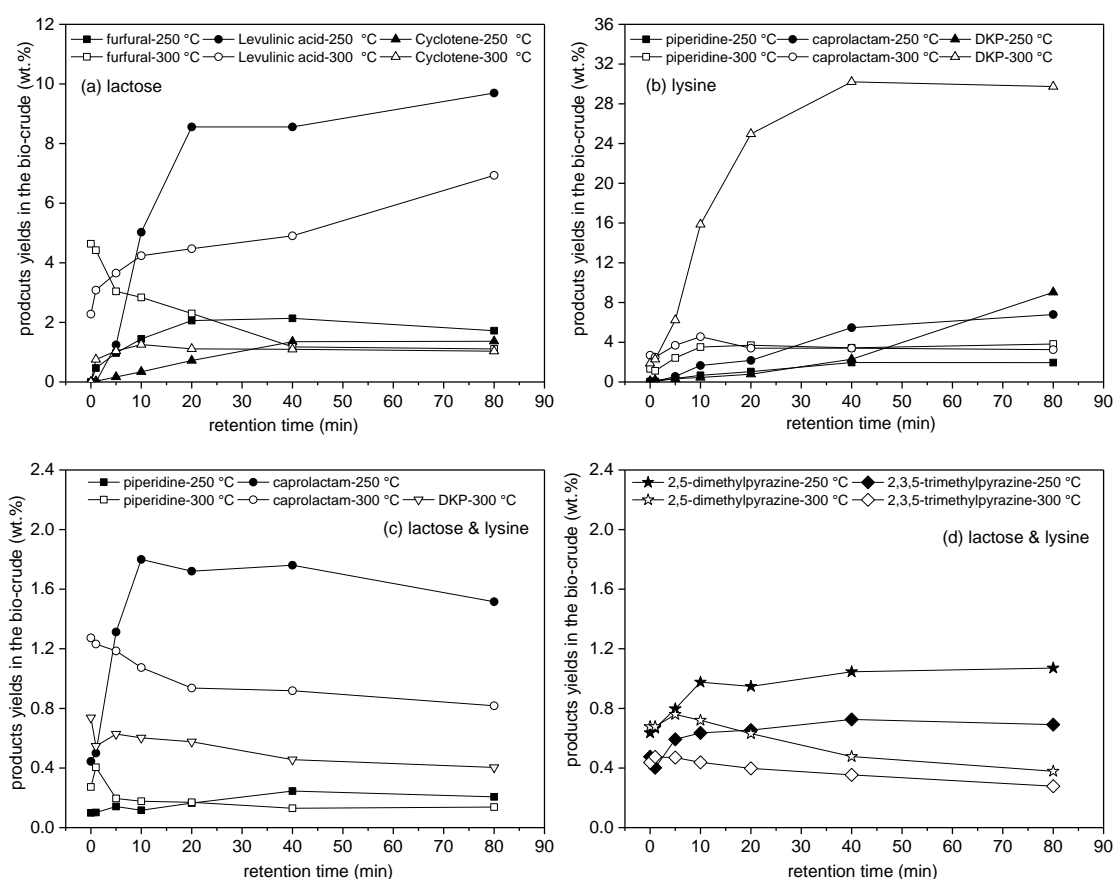


Figure 7-19 The temporal variation of key components in the biocrude after HTL of model substances at 250 and 300 °C (a) lactose; (b) lysine; (c) binary mixture; (d) binary mixture

Regarding to the main chemicals detected in the biocrude from HTL of lysine alone,

piperidine, caprolactam and DKP are quantified and displayed in Figure 7-19 (b). At lower temperatures, piperidine and caprolactam yields increase substantially between 0 and 40 min residence time before they level off, and caprolactam shows a higher yield than that of piperidine. While DKP displays the same behaviour with caprolactam at a retention time of less than 40 min, it dramatically rises to 9.0 wt.% at 80 min residence time. However, it is noticeable that DKP obtained in the biocrude processed at 300 °C shows a significant increase between 0 and 40 min, reaching a maximum value of 30.2 wt.% at 40 min, which is more than 3 times higher than that from 300 °C at 80 min. The highest yields of piperidine and caprolactam are found at 10 min, after which they remain stable with longer retention times. These results highly suggest that an increase in temperature significantly improves the conversion of lysine to biocrude by the enhancement of N-containing compounds. At longer reaction times, self-condensation reactions enhance the repolymerization of monomers to form cyclic compounds, resulting in the improved biocrude production from lysine.

Concerning the binary mixture, it can be seen that the major DKP disappears at 250 °C with any retention time, less than 1 wt.% can be found at 300 °C at the starting retention time, indicating that interactions occurring between sugars and lysine largely inhibit the formation of DKP by self-condensation of lysine. Piperidine and caprolactam decrease to 0.4 and 1.8 wt.%, respectively, much less than half compared to single lysine. This reduction clearly happens before 10 min, indicating that a strong activity of Maillard reactions occurs after a short retention time. This is evident as the identified 2,5-dimethylpyrazine and 2,3,5-trimethylpyrazine significantly increase between 0 and 10 min at 250 °C as shown in Fig. 8-21 (d), before slowly rising between 20 and 40 min, levelling off after a longer time. At longer times, the optimum retention time for MRs are shifted beforehand, i.e. 5 min, then show a constant decrease with longer retention times. At first glance, it might seem to be due to the decomposition of these two chemicals during the reaction time. However, pyrazines are well-known recalcitrant heterocycles in the bio-crude, which makes it difficult to upgrade them by denitrogenation. At a temperature of around 1000 °C, only 54 % pyrazine can be thermally destructed, and decomposition to acetylene and isomerization to pyrimidine can happen to pyrazine [234, 235]. Therefore, in this study, combining with the increase bio-crude and relatively stable N-content over the retention time, it is most likely that other N-containing heterocycles are generated from a route for the migration of aromatic ring atoms in pyrazines,

accompanied by pyrazines to polymerize melanoidins products, which are formed by the polymerization of N-containing intermediates via secondary and tertiary reactions.

A deeper investigation of the formation of N-containing heterocycles during the heating period is additionally carried out.

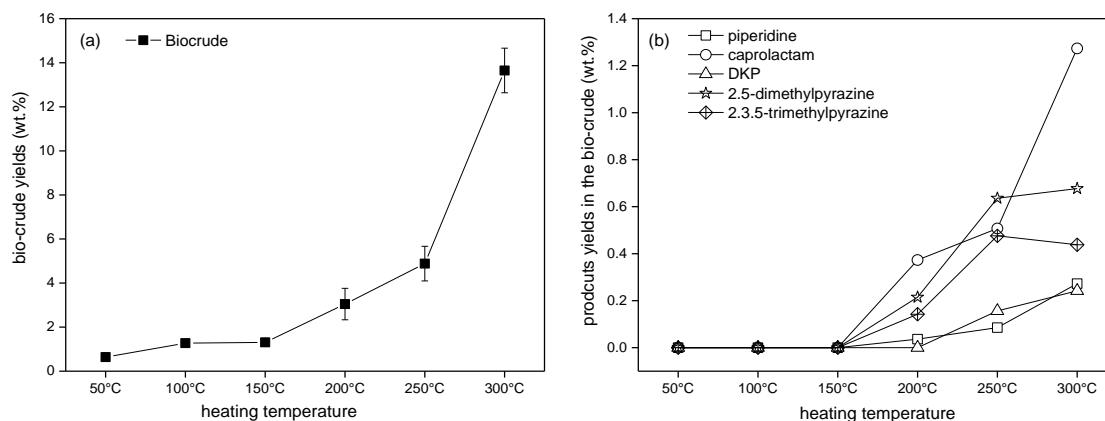


Figure 7-20 Biocrude yields (a) and key compounds in the biocrude (b) from HTL of binary mixture during heating period

In Figure 7-20, it is not surprising to see that biocrude shows a slow increase from 50 to 150 °C, due to the dominant hydrolysis of model compounds taking place. With higher reaction temperature, Maillard reactions play a more influential role in the whole process, and the biocrude presents a dramatic increase rate from 150 to 300 °C, indicating that high temperature is favourable for Maillard reactions. This can be explained with the fact that increasing the temperature could reduce the viscosity and surface tension of water, which results in an enhanced solubility of the analytes in the medium, thus increasing the reaction rate [236]. As a result, when the temperature is lower than 150 °C, the Maillard reaction products cannot be observed. All the representative components occur above 150 °C, increasing with the reaction temperature. The reaction rate of pyrazines is higher during the heating period from 150 to 250 °C. Above a reaction temperature of 250 °C, 2.5-dimethylpyrazine slightly increases and 2.3.5-trimethylpyrazine starts decreasing. These results mean that Maillard reactions occur during an earlier HTL period, indicating that the N-containing heterocycles produced in a very short time could reach the equilibrium state.

7.3.5 Reaction pathways

First of all, the mechanism of HTL of carbohydrates is set up according to the products identified by HPLC and GC-MS, combined with the results presented by Remón et al. [223] and Sinağ et al. [91, 237]. The possible reaction pathways during hydrothermal

conversion of lactose are shown in Figure 7-21. Lactose is a disaccharide consisting of the monosaccharides glucose and galactose. Hydrolysis of disaccharide theoretically yields equivalent amounts of monosaccharides and primary products. Both glucose and galactose decompose into small oxygenated compounds via retro-aldol reaction and Grob fragmentation at low reaction temperatures, while at higher temperatures and fast hydrolysis rates, furanic compounds and cyclopentenones are favoured by dehydration and decarboxylation, which can also be decomposed into oxygenated compounds like levulinic acid and formic acid [238]. Small molecular compounds can subsequently cyclize into mono-aromatic compounds, and/or further transform into polymers by oligomerization and polymerization reactions. This polymer is the carbon-rich solid found after conversion of the pure sugars.

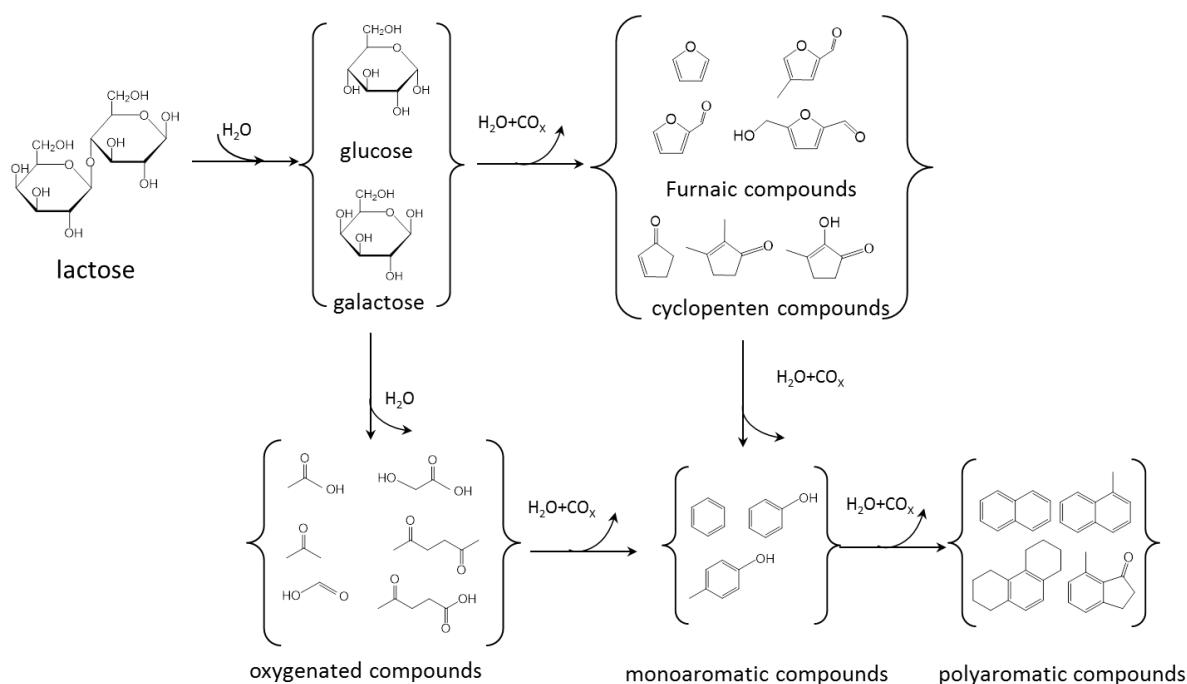
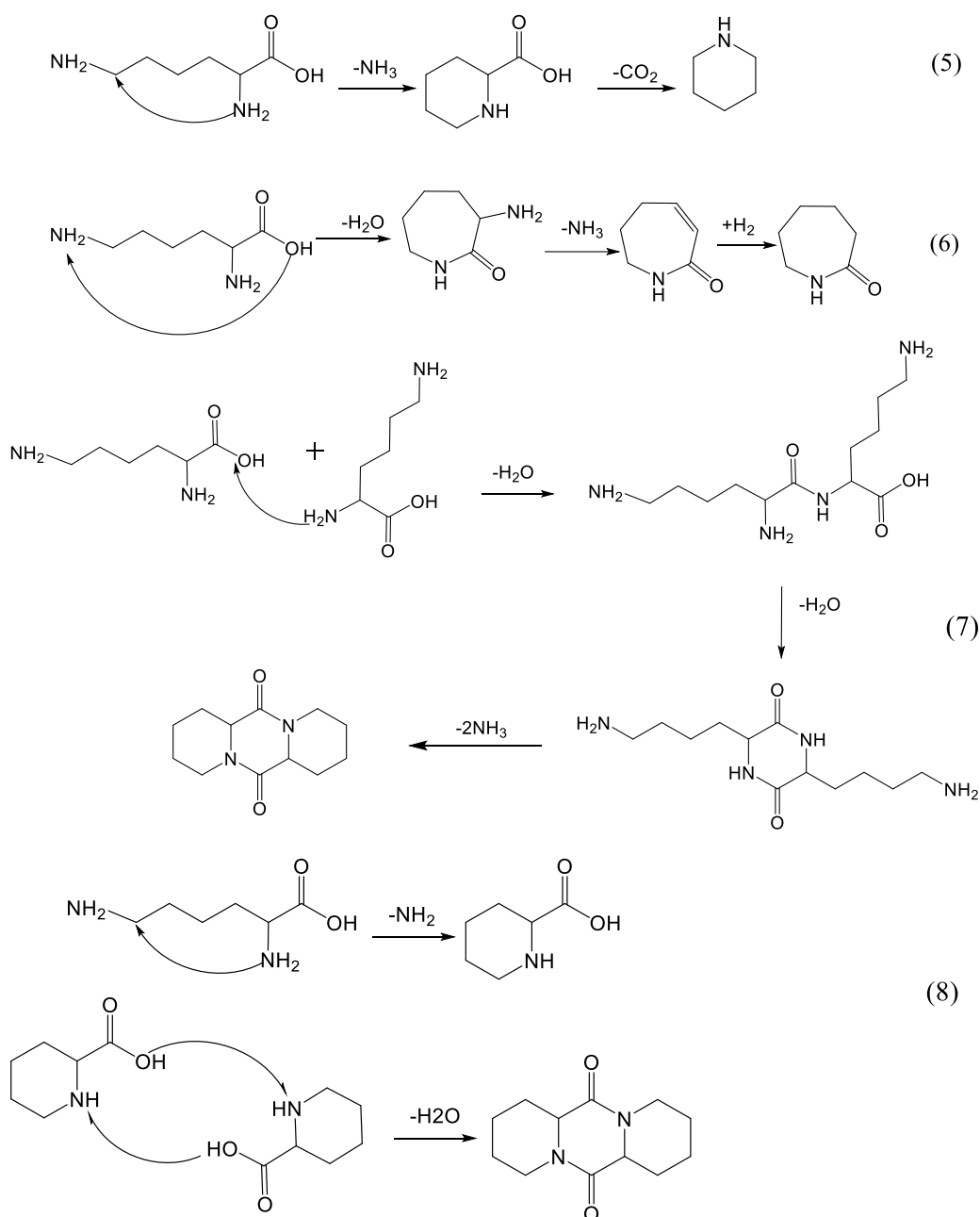


Figure 7-21 Possible reaction pathways during the HTL of lactose

In contrast to carbohydrates, only little literature is available to illustrate the reaction pathways of amino acids, peptides as well as proteins during HTL [239]. According to the experimental results of HTL of lysine, some nitrogen-containing compounds like piperidine (Eq. 5) caprolactam (Eq. 6) and DKP (Eq. 7-8) are found in the bio-crude, mainly formed through the direct cyclization reaction or internal lactamization of lysine; possible reaction pathways are revealed in the following. Concerning the formation of caprolactam via hydrogenation, due to the presence of H_2 , formed through decarboxylation of formic acid or due to water-gas shift reaction [91].



With regard to the mixtures, two possible reaction pathways are proposed based on literature results [224, 229, 230]. As shown in Figure 7-22 (a), the disaccharide first reacts with amino groups; then the formed glucosylamines rearrange to Amadori compounds as intermediates, which then undergo cyclization and cleavage to form pyrazines. In another pathway, occurring at higher temperatures, sugars may immediately undergo Grob fragmentation or retro-aldol reaction transforming into numerous smaller small oxygenated compounds like dicarbonyl and hydroxycarbonyl groups containing fragments [224]. Such fragments could then condense with nitrogen from amino acids to

form alkyl-pyrazine compounds according to the reaction pathways (b).

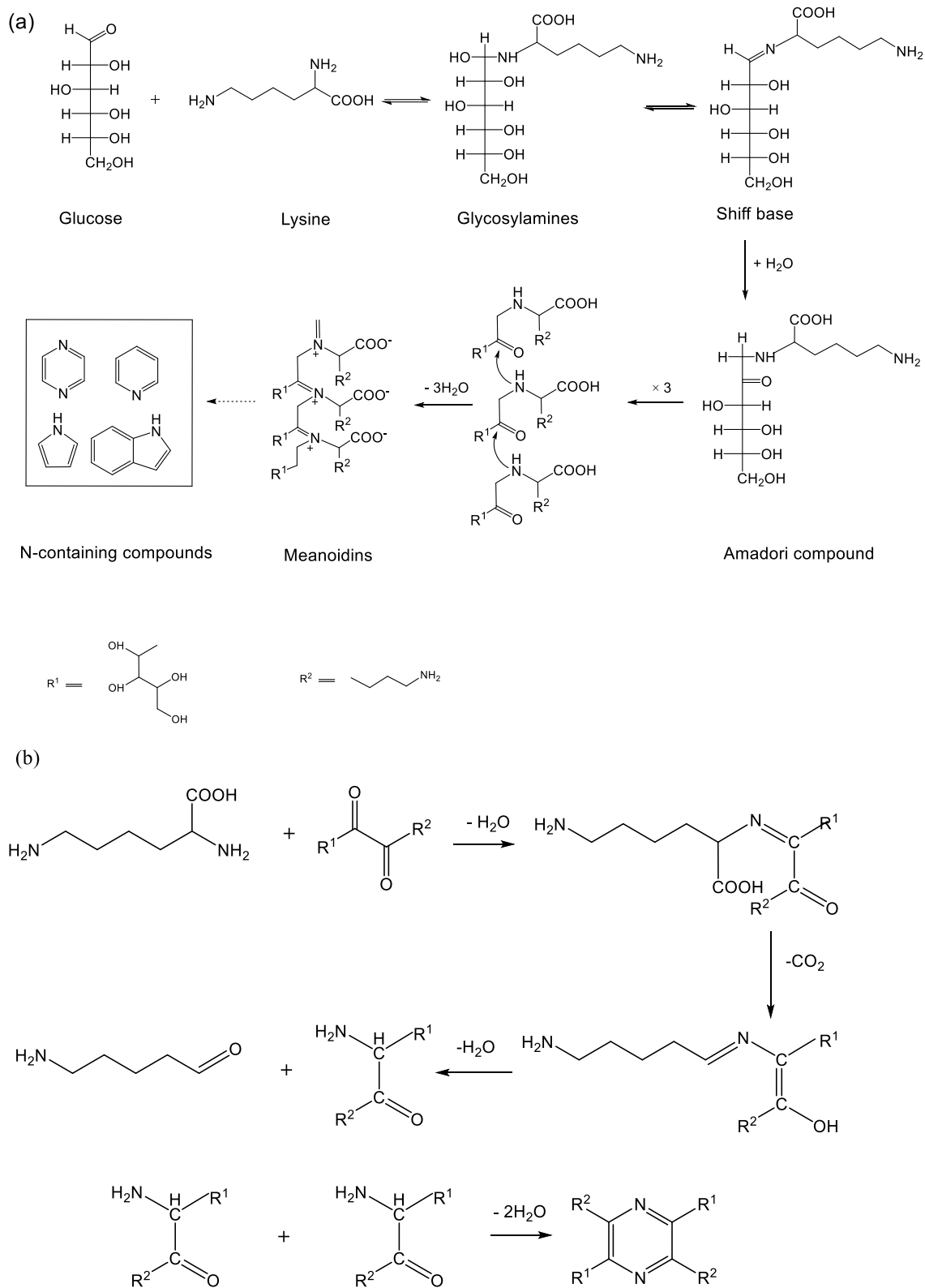


Figure 7-22 Proposed mechanisms of reaction pathways during HTL of model mixtures

7.4 Conclusion

Under the conditions studied, the influence of Maillard reactions on the fate of N during HTL of model carbohydrates and proteins have been extensively elucidated. The optimal mixing ratio of lactose and lysine for biocrude products is found at 50:50 w/w%, higher relative lysine contents decrease the biocrude yields. Maillard reactions suppress the carbonization of carbohydrates through the elimination of intermediate HMF. An increase of temperature favours the yields of bio-crude with unfavourable N. Faster heating rates increase the biocrude yields at higher temperatures through the enhancement of C content instead of N. The temporal effects on HTL conversion and the key compounds generated from HTL of model substances have been deeply investigated. Taken collectively, the hydrolysis rate of lactose is higher than that of lysine, and is accelerated by temperature. With the addition of lactose to HTL of lysine, the conversion of lysine is almost effectively complete, indicating that the rate of Maillard reactions is higher than in amino acid hydrolysis. The end products display great dependency on the temperature and feedstocks.

Regarding the dominant compounds, the chemicals resulting from self-condensation of lysine are dramatically reduced by mixing with sugars. Instead, new Maillard reaction products like pyrazines are produced in early heating periods. These chemicals occur at very short retention times (5-10 min), then level off at 250 °C, and slightly decrease at 300 °C, suggesting that Maillard reaction products subsequently polymerize or cross-link with others to produce heavier-weight molecular melanoidins during longer residence times. A reaction network based on the above observations is proposed.

Chapter 8 Energy valorization of integrating lipid extraction and hydrothermal liquefaction of lipid-extracted sewage sludge

8.1 Introduction

Chapter 6 and 7 display the mechanistic reaction pathways of N-containing compounds based on model substances, and it can be concluded that Maillard reactions play a significant role in the bio-crude products with undesirable N content during HTL at lower temperatures. Conventional reaction parameters showed a lesser impact on the reduction of N in the biocrude, upgrading seems to be the only possibility for the application of biocrude as standard fuel. It is therefore promising to consider other aspects of optimizing energy valorisation from HTL of sewage sludge. Inspired by co-liquefaction, integration of HTL with other approaches of energy valorisation from sewage sludge has been firstly investigated in this chapter.

As stated in Chapter 1.2.2, besides combustion and anaerobic digestion, biodiesel production is a promising technology to valorise renewable energy. As a matter of fact, the lipid content present in sewage sludge typically consists of free fatty acids in the range of C10 to C18 as precursors for the production of esters (typically methyl esters, FAME) [38]. Assuming an overall yield of FAMEs of 7.0 wt.% with respect to the dry sludge, Dufreche et al. [240] reached a breakeven price of $0.83 \text{ \$}\cdot\text{L}^{-1}$, for which drying the dewatered sludge (80 – 85 wt.% water) was considered the most energy- and cost-intensive step. Mandola et al. [39] reached values of $0.85 \text{ \$}\cdot\text{L}^{-1}$ for the methanolysis of dewatered sludge, assuming FAME yields of 10 wt.%, followed by liquid-liquid extraction. Pokoo-Atkins et al.[241] reported a value of $0.76 \text{ \$}\cdot\text{L}^{-1}$ by extracting the dry sludge prior to methanolysis. These values are comparable to those reported for petrodiesel and show the high potential of sewage sludge as a competitive lipid source for the production of biodiesel.

Currently, research is being focused on the extraction of lipids from wet sludge, as well as on the reuse of solvent to improve the profitability of the process. However, the residual sludge (LESS, lipid extracted sludge) must be effectively employed to achieve favourable energy balances and production costs. To the best of my knowledge, limited information

is available with regards to the integration of HTL and lipid extraction. Based on the success in using LESS as anaerobic digestion feedstock [117], and the proven feasibility of using lipid-extracted algae residue [118, 120, 121] and de-oiled yeast [242] in HTL, the integration of both processes is attractive due to the complete utilization of sewage sludge as well as the different products obtainable. When disregarding the water content, LESS is mostly comprised of proteins and carbohydrates. In particular, Maillard reactions have been previously confirmed to be important interactions in the biocrude product distribution and composition.

Therefore, the objectives of this chapter are 1) to quantify and characterize the extracted lipids from sewage sludge and to evaluate their applicability for biodiesel production; 2) to investigate the hydrothermal conversion efficiency of LESS through HTL, comparing the different products generated by HTL of SS and LESS in order to evaluate whether LESS can be a potential feedstock for the production of fuel components; 3) to estimate the coupling effect of lipid extraction and HTL of LESS in terms of the yields of fuel-like products and energetic efficiency of the process.

8.2 Methodology

8.2.1 Materials

The feedstock employed in this chapter is the same type sludge as in Chapter 4, namely digested sewage sludge. Analytical grade methanol, sodium bicarbonate, and sodium chloride were supplied by Sigma-Aldrich.

8.2.2 Lipid quantification

In-situ transesterification of SS was conducted using reactive extraction by adapting the method presented by Mondala et al. [39], which is as follows: 2 g of freeze-dried sludge was weighed into a 250 mL flask. The sludge samples were then treated at 75 °C, 5 mL (5 vol.%) H₂SO₄, and 24 mL methanol (mass ratio of methanol to dried sludge (12:1)). 25 mL of hexane was added to improve the lipid solubility in the reaction mixture. The sludge was then suspended in a solution using a magnetic stirring bar and the mixture was heated to the set temperature using a hot water bath with a retention time of 8 h. After the reaction was stopped, the mixture was allowed to cool and the flask contents were transferred into a 100 mL bottle. Then, 2.5 mL of saturated NaCl solution and 25 mL of hexane were added. The mixture was then centrifuged at 3000 rpm for three minutes and

the supernatant hexane phase was withdrawn and transferred into a 100 mL round-bottom flask. The extraction procedure was repeated three times. Afterwards, the total volume of the collected supernatant was washed with 5 ml of a 2 % (w/v) sodium bicarbonate solution and the aqueous phase was allowed to settle. The upper layer passed through a filter paper containing anhydrous sodium sulphate before being collected.

FAME content in the hexane phase was analysed using a Shimadzu GC-FID (Agilent 7890 B). A Stabilwax-DA, 30 m × 0.25 mm × 0.25 mm column was used for the analysis. The column temperature was programmed to start at 40 °C, to be maintained for 10 min, and then to be increased from 40 to 250 °C for 10 min at a rate of 8 °C/min. The sample injection volume was 1.0 µl, with a split ratio of 10:1.

8.2.3 HTL procedure

The HTL procedure conducted in this chapter is the same as in Section 0. 21.25 wt.% SS was briefly heated in a batch reactor by a GC-oven at 250 - 350 °C with a residence time of 20 min.

8.2.4 Data interpretation

The concept of ECR (Energy Consumption Ratio), was employed by Samayama et al. [243] and Minowa et al. [244] to estimate the energetic viability of the process by relating the heat demands of the process to the heating value of the feedstock. Values lower than 1 indicate a good energetic balance, saying that the energy content of the products (E_0) is higher than the energy requirement of the production process (E_L).

$$ECR = \frac{E_L}{E_0} \quad (8-1)$$

For the case of hydrothermal liquefaction, the authors propose the following formula (Eq. 8-2), for which w_i is the water content, $c_{p,w}$ is the specific heat of liquid water (4.18 kJ·kg⁻¹·K⁻¹), $c_{p,s}$ is the specific heat of dry solid (1.25 kJ·kg⁻¹·K⁻¹), ΔT is the temperature difference to ambient temperature (25 °C), Y_i is the product yield (wt.% daf), and w_0 is the organic fraction of the feedstock sludge (wt.% daf).

$$ECR_{HTL} = \frac{E_L}{E_0} = \frac{[w_i c_{p,w} \Delta T + (1-w_i) c_{p,s} \Delta T](1-r_2)}{[(1-w_i) Y_i (HHV) w_0] r_1} \quad (8-2)$$

For the complete process chain, the concept of ECR was extended to additional process steps (Eq. 8-3). considering in different process configurations : 1) HTL to produce only biocrude (ECR_{BC}), which employs Q_{HTL} and E_{BC} ; 2) HTL to produce biocrude and solid residue as energy carriers (ECR_{BC+SR}), which employs Q_{HTL} , E_{BC} and E_{SR} ; 3) considering

HTL products and lipid extraction ($ECR_{BC+SR+L}$), which employs Q_{HTL} , Q_{drying} , $Q_{extraction}$, E_{BC} , E_{SR} and E_{LIPID} ; 4) considering HTL products and FAME production from the lipids extracted ($ECR_{BC+SR+FAME}$), which employs Q_{HTL} , Q_{drying} , $Q_{extraction}$, $Q_{methanolysis}$, E_{BC} , E_{SR} and E_{FAME} ; $Q_{extraction}$ was assumed to be $60.95 \text{ MJ}\cdot\text{kg}^{-1}_{\text{lipid}}$ taken from Olkiewicz et al.[245], and a value of 934 Btu/lb ($2.17 \text{ MJ}\cdot\text{kg}^{-1}$) was obtained for the demand of the methanolysis process given by Huo et al.[246]. A value of $39.5 \text{ MJ}\cdot\text{kg}^{-1}$ was assumed as the heat of combustion of FAME (h_{FAME}) [247].

$$ECR = \frac{E_L}{E_O} = \frac{(\sum Q_{step})(1 - r_2)}{(\sum E_{product})r_1} \quad (8-3)$$

The efficiency of combustion (r_1) and the efficiency of heat recovery (r_2) can be adjusted depending on the technology employed. Samayama et al. [243], in 1999, used values for r_1 and r_2 of 0.6 and 0.5, respectively. On the other hand, more up-to-date values of 0.7 and 0.5 have been proposed by Vardon et al. [120] and an optimized hypothetical case using state-of-the-art combustion and heat recovery technology may permit reaching values of 0.9 and 0.6[248]. The latter two situations are considered during the discussion of results, and are named the case A and case B, respectively.

For the case of drying (Eq. 8-4), a final temperature of $100 \text{ }^\circ\text{C}$ was assumed with $\Delta H_{vap,w}$ as the heat of vaporization of water ($2.26 \text{ MJ}\cdot\text{kg}^{-1}$) and HHV_s as the higher heating value of the sludge.

$$Q_{drying} = [w_i(\Delta H_{vap,w} + c_{pw} \Delta T) + (1 - w)c_{ps} \Delta T] \quad (8-4)$$

The specific energy demand (ED, Eq. 8-5) serves as another indicator of the energetic efficiency of the process, in such a way that it can be compared to other values reported in the literature or to other processes. It was calculated using both FAME and biocrude as mass basis, due to being the products of main interest.

$$ED\left(\frac{\text{MJ}}{\text{kg}_{product}}\right) = \frac{(\sum Q_{step})(1 - r_2)}{m_{product}} \quad (8-5)$$

8.3 Results and discussion

8.3.1 Feedstock characterization

The properties of lipid-extracted sludge (LESS) are outlined and compared with raw sludge in Table 8-1.

Table 8-1 Characterization of sewage sludge and lipid-extracted sludge

feedstock	Biochemicals (wt.% daf) ^a				Ash	Elemental content (wt.%) ^b					HH V (MJ/kg)
	carbohydrates	proteins	lipids	others		C	H	O ^c	N	S	
SS	27.9	34.6	13.9	23.6	38. 6	25.8	4.6	26.6	3.7	0.7	10.5
LESS	31.3	38.9	-	29.8	45. 3	24.0	4.1	22.2	3.8	0.6	10.0

^a: on the ash-free basis

^b: on the dry basis

^c: calculated by difference to the total mass

It was assumed that all lipids present in the original material were extracted. The organic material was analysed for carbohydrate, protein and lipid contents, others may include lignin and fibre content. Interestingly, despite the significantly higher protein contents in the lipid-extracted sludge compared to raw sewage sludge, the N content determined from the elemental analysis was only 0.1 % greater.

Table 8-2 Summary of lipid extraction from published sources

Feedstocks	Fractions	Content wt.%(db.)	Methods (solvent)	Ref.
Primary mixed waste activated sludge	Crude fat	10.4	-	[74]
Digested sludge			Ether solvent	[66]
Raw primary sludge	Crude fat	1.9-12.2		
Waste active sludge				
Secondary SS	Lipid	8.01 (db)	-	[67]
Dewatered SS	Lipid	5.0	Soxhlet extraction	
Liquidized SS	Lipid	10.4	(Diethyl ether)	[203]
Digested sludge	Crude-lipid	<1	Ether solvent	[249]
Dewatered sludge	Lipid	2.5-10.3	Soxhlet extraction (hexane-ethanol)	[36]
		2.2-7.5	Acid hydrolysis	
		3.0-7.5	Water bath shaking	
Primary SS			Soxhlet extraction	[117]
Secondary SS	Lipid	7.7-26.2	(hexane)	
Blended sludge			Liquid-liquid Extraction (hexane)	
Raw sewage sludge	Lipid	12	Soxhlet extraction (chloroform)	[250]

-: Not mentioned

Regarding lipid extraction, many methods with different procedures can be found in publications, of which a summary is provided in Table 8-2.

8.3.2 Lipid extraction from sewage sludge

The fatty acid composition of the lipids from SS was inferred from the results of the FAMES produced by the *in-situ* transesterification of dry sludge samples. In Table 8-2, it can be seen that a significant amount of methyl esters belong to relatively short chains below C18; the cumulative amount of C16:0 and C18:1 was more than 70 %, which was similar to the value in another report [117]. The results show a predominance of palmitic acid (C16:0), stearic acid (C18:0) and oleic acid (C18:1), which is in line with previous work. Specifically, palmitic acid was the major saturated fatty acid with a value of 16.4 %, followed by stearic acid accounting for 8.9 %. Oleic acid was the major unsaturated fatty acid, followed by docosahexaenoic acid (C24:1). These fatty acids are exceptionally well-suited for the production of biodiesel [36, 38, 245].

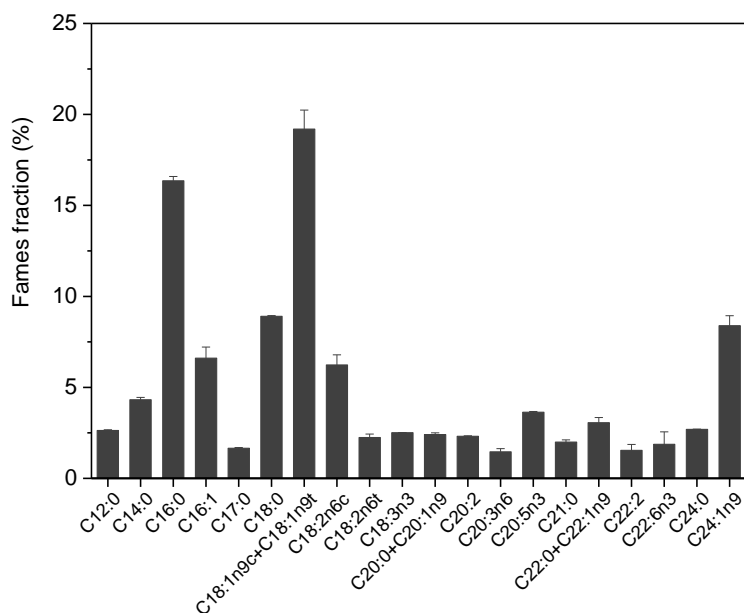


Figure 8-1 FAMES analysis of biodiesel obtained from the *in-situ* transesterification of SS

8.3.3 HTL conversion

In this chapter, raw sewage sludge is used as “reference” material to compare the hydrothermal conversion and the products obtained from the HTL of SS and LESS.

A general comparison between the HTL of SS and LESS is shown in Figure 8-2. Both HTL conversion efficiency and biocrude yield increase with the temperature of either feedstock, although HTL of SS shows higher conversion rates than HTL of LESS under the same operating conditions. Compared to results reported by other studies (average 25 wt.%) using similar operating conditions, the biocrude yields reported in this work are lower [66, 95]. At 250 °C and 300 °C, the yields of biocrude obtained from HTL of SS

and LESS are basically the same; however, a difference occurs at 350 °C, where the bio-crude yields reach values of 21.3 and 15.4 wt.% for SS and LESS, respectively. In contrast, the SR decreases with the reaction temperature. Compared to HTL of LESS, HTL of SS results in lower bio-char yields at the temperatures used. The AQ forms the dominant part of all the products, between 36.6 to 50.6 wt.% in all cases, which slightly increases with the reaction temperature.

The conversion of SS and LESS via HTL is comparable, suggesting that the residue after lipid extraction can be considered a suitable feedstock for the HTL process. A lower amount of solid residue overall is found when using raw SS, indicating that the lipids in the SS have been converted into water-soluble compounds, such as organic acids.

At lower temperatures (250 °C), the higher protein content of LESS may compensate for the absence of lipids in the feedstock. However, when the temperature increases to 350 °C, a larger amount of biocrude is produced by HTL of SS. This can be explained as follows: in one way, polar or water-soluble fatty acids in the aqueous phase further convert or condense into crude-like products. Fatty acids could undergo decarboxylation to produce alkenes or alkanes [220], as indicated by the significantly higher amounts of hydrocarbons found in the crude phase and as shown in Figure 8-4. In another way, these fatty acids get converted into biocrude constituents by cross-linking reactions like amide formation with proteins.

However, a fact to be taken into consideration is the limited solubility of lipids in DCM, which hinders their recovery and influences the estimated values of conversion. This may explain the similar yields of biocrude reported for SS and LESS at 250 °C. It has been reported that soap formation can happen at low temperatures in the base reaction medium, which hinders product separation during the extraction of lipids from sewage [39]. When the temperature increases to 350 °C, more biocrude from HTL of SS is found, which could partly originate from DCM-extracted lipids.

8.3.4 Carbon and nitrogen balance

Table 8-3 shows the elemental balance/distribution in different phases, estimated using Eq. (3-3). For both SS and LESS, the carbon content in the SR significantly decreases from 64.1 to 29.1 % and 58.2 to 38.5 % with a temperature increase from 250 to 350 °C, respectively. In the biocrude, the CD correspondingly increases from 13.5 to 34.0 % and from 12.5 to 27.6 %, respectively. The CD of the AQ seems stable, only showing a slight

tendency to decrease with the reaction temperature. When considering the gas formed while the yields are low (< 12 wt.%), the CD shows a rise by a factor of around 4 from 250 to 350 °C.

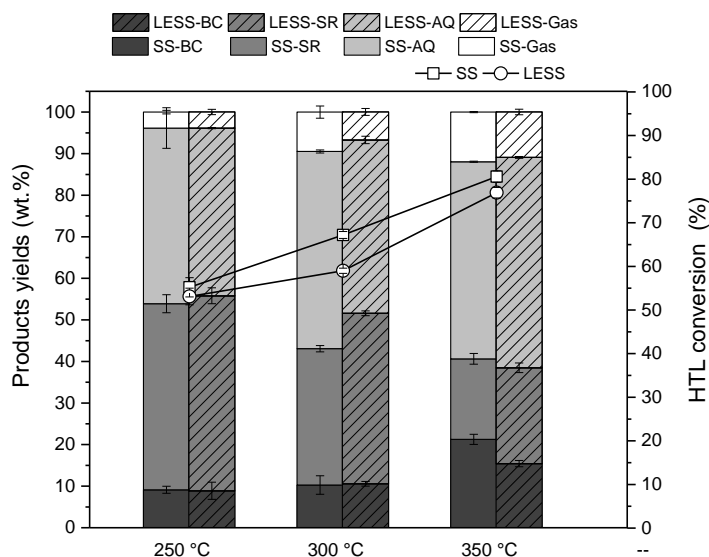


Figure 8-2 Comparison between HTL of SS and LESS at different temperatures, the yield of the aqueous phase was determined as the difference between unity and the sum of the yields of bio-crude, solid residue, and bio-gas fractions

Nitrogen has also been investigated as another important element with regard to the high protein content in both SS and LESS. In contrast to what was discussed with regard to carbon, nearly half the amount of nitrogen is recovered in the aqueous phase under all conditions. Due to this high nitrogen content, the aqueous phase has been considered as a promising medium to cultivate algae, with some success [154, 155].

Table 8-3 Elemental distribution (wt.%) of various products at various conditions.

Samples	Biocrude		Solid		Aqueous phase		Gas	Recovery	
	CD	ND	CD	ND	CD	ND	CD	CD	ND
SS-250 °C	13.5	10.3	64.1	45.5	19.6	48.8	2.5	99.8	104.6
SS-300 °C	17.1	12.1	53.6	38.0	15.6	47.1	6.2	92.6	97.2
SS-350 °C	34.0	20.8	29.1	25.6	14.8	42.2	8.2	86.2	88.7
LESS-250 °C	12.5	11.0	54.6	40.2	21.3	42.2	2.2	90.7	93.4
LESS-300 °C	17.3	11.5	49.2	35.9	15.6	45.2	4.6	86.7	92.6
LESS-350 °C	27.6	16.7	38.5	31.3	14.0	44.6	9.4	89.6	92.5

With increasing temperature, the ND in the SR of SS and LESS is significantly reduced from 37.5 to 21.1 % and 35.7 to 22.1 %, respectively. For the case of biocrude, increasing reaction temperatures seem to lead to an increased incorporation of nitrogen, as ND increases from 10.3 to 20.8 % while the temperature rises from 250 to 350 °C, affecting

the usability of this phase.

HTL resulted in a considerable proportion of dissolved organic carbon and a major proportion of N in its aqueous phase in every case. Total organic carbon (TOC) analysis was applied to determine water-soluble organic products, as shown in Figure 8-3 (a). After HTL of SS and of LESS, the TOC content significantly decreased with the temperature from 15500 to 9000 mg/L and from 14900 to 6700 mg/L, respectively. While at 250 °C, the TOC in the aqueous phase from SS and LESS are similar. At higher temperatures, the TOC observed for the aqueous phase from LESS were lower than that from SS, indicating that lipids in SS are partly converted into water-soluble products.

In ammonium (NH_4^+), as seen in Figure 8-3 (b), the opposite trend was observed. After HTL of SS and LESS, NH_4^+ concentrations steadily increased with the temperature from 4000 to 6000 mg/L and 3000 to 5000 mg/L, respectively. In addition, the NH_4^+ content present in the AQ phase after HTL of SS was higher than that of LESS under the same conditions.

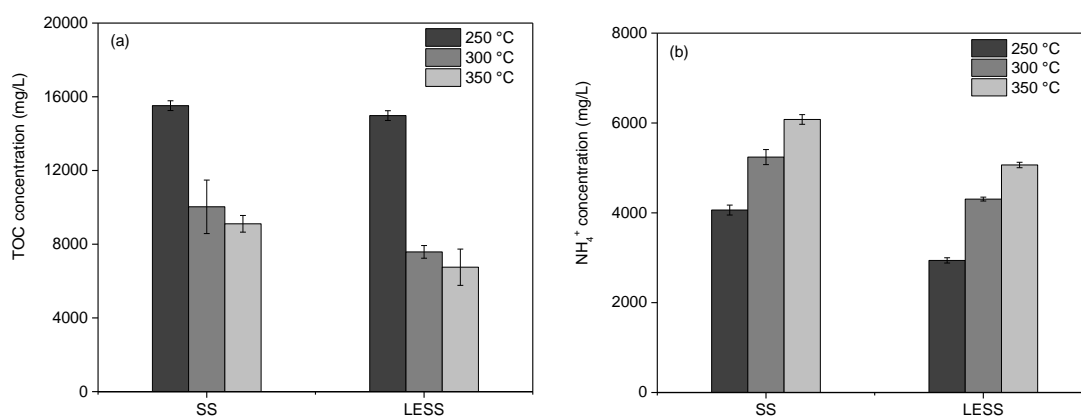


Figure 8-3 Total organic carbon concentration (a) and ammonium concentration (b) in the aqueous phase from HTL of SS and LESS

8.3.5 Energy content of the products

Table 8-4 summarizes element ratios and HHV for all biocrude and solid products. The extracted lipids exhibit HHV very similar to that of FAME (39.29 vs. 39.5 MJ/kg) [247]. When comparing the raw SS and lipid extracted LESS with the biocrude obtained, HTL shows lower H/C and O/C ratios and higher HHV. The effect of temperature is most noticeable when comparing the results at 250 °C and 300 °C, but the change between 300 °C and 350 °C is subtle and may be caused by experimental uncertainty; this trend can be observed for experiments using both SS and LESS. Regarding the solid residue, HTL treatment led to lower H/C and O/C ratios when compared to the feedstocks. The

effect of temperature seems to be similar to that found for biocrude. All heating values ranged from 28 to 40 MJ/kg, close to those reported for biocrude produced from sewage sludge (35 – 40 MJ/kg) [65] and paper sludge (35 – 37 MJ/kg) [191], but lower than that of petroleum crude oil (43 MJ/kg) [206].

Table 8-4 Elemental composition (atomic ratio), higher heating value (MJ/kg) of biocrude and solid residue

HTL	Biocrude				Solid residue			
	H/C	O/C	N/C	HHV	H/C	O/C	N/C	HHV
Raw SS					0.77	2.14	0.12	10.54
LESS					0.70	2.07	0.13	10.03
Extracted lipids	1.86	0.11	0.01	39.29				
SS - 250 °C	0.18	1.62	0.09	32.29	0.38	1.56	0.09	10.02
SS - 300 °C	0.13	1.57	0.09	34.60	0.16	1.41	0.09	10.35
SS - 350 °C	0.09	1.57	0.07	37.26	0.22	1.39	0.11	6.40
LESS - 250 °C	0.24	1.56	0.12	28.85	0.48	1.52	0.10	8.29
LESS - 300 °C	0.11	1.45	0.09	34.76	0.49	1.31	0.10	7.11
LESS - 350 °C	0.12	1.45	0.08	34.91	0.27	1.33	0.11	6.82

8.3.6 Biocrude composition

Figure 8-4 shows the groups of chemicals in the biocrudes obtained. The identification of organic compounds was achieved by comparing the spectra of sample components (limited to the top 50 compounds based on the peak-normalized volume) with those in the electronic library of NIST. The organic components were analysed using the area normalization method [201]. Detailed categories of constituents can be seen in the Supporting Information.

As shown in Figure 8-4, the identified components account for more than 56 % and 64 % of the total species in the biocrude derived from SS and LESS, respectively. The major detected compounds are N-containing heterocycles such as pyrazines, pyrrolidinones, and indoles; similar species have been described in a previous report [94]. These fractions slightly increase with the reaction temperature in the case of HTL of SS. A decrease is observed in HTL of LESS. O-containing compounds form the second largest constituent of biocrude, mainly composed of phenolic compounds. It is observed that O-containing compounds in the biocrude from HTL of SS greatly decrease with increasing temperature, whereas, conversely, a higher amount of O-containing compounds is formed in the case of HTL of LESS. The yield of hydrocarbons seems to be strongly influenced by the temperature (an increase from 1.5 to 20.1 %) for the case of SS. Here, alkenes or alkanes

are most likely produced by decarboxylation of fatty acids [220], but an almost total absence of these compounds can be observed in biocrude produced from LESS, due to the negligible lipid content.

Regarding amines and amides, the lowest fractions are produced at 250 °C, which may be too low a temperature to promote this type of reaction. Biocrude from LESS shows a higher value of those components, mostly including piperidines and acetamides. Around 1.5 % hexadecanamide could be found in biocrude from HTL of SS at 300 °C, indicating reactions between lipid and protein contents, which is strongly in agreement with the findings as reported in Chapter 6.

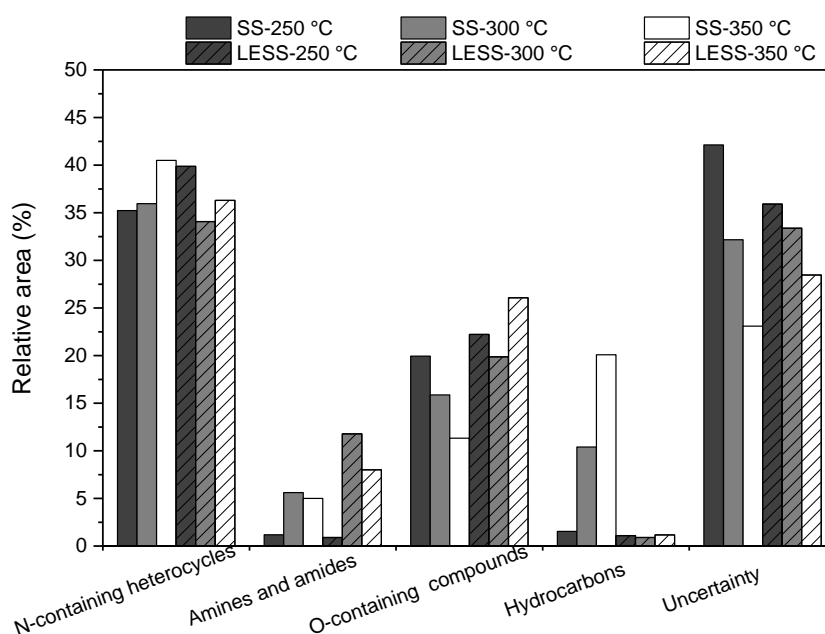


Figure 8-4 Chemical groups represented in biocrude obtained from HTL of SS and LESS under different temperatures

Table 8-5 further provides boiling point distributions which were calculated based on the weight loss during TGA measurement. Small differences in boiling point distribution trends are observed for HTL of bio-oils derived from SS and LESS. The most significant fractions correspond to compounds with volatilities similar to those of kerosene or diesel oil (200 °C to 400 °C), in agreement with results found by Liu et al. [95]. LESS biocrude contains more fractions in the gasoline range (110 – 200 °C) and less in the heavy diesel range (300 – 400 °C) when compared to SS biocrude. The amount of distilled fractions between 200 °C and 550 °C, which can generally be used in petroleum refineries [251], accounted for around 71 to 74.1 wt.% in biocrude from HTL of SS, and 67.2 to 70.9 wt.% in biocrude from HTL of LESS. Accordingly, it is worth noting that the heavy crude

fraction ($> 550\text{ }^{\circ}\text{C}$) in all biocrude is larger than 25.9 wt.%, the value reported in previous studies [95, 132], limiting the chances of direct refinery integration and requiring costly upgrading. More residues at higher boiling points ($> 800\text{ }^{\circ}\text{C}$) were obtained in the crude derived from HTL of LESS.

Table 8-5 Boiling point distribution of biocrude from HTL of SS and LESS

Distillation Range ($^{\circ}\text{C}$)	typical application ^a	Distribution (wt.%) in biocrude					
		SS			LESS		
		250 $^{\circ}\text{C}$	300 $^{\circ}\text{C}$	350 $^{\circ}\text{C}$	250 $^{\circ}\text{C}$	300 $^{\circ}\text{C}$	350 $^{\circ}\text{C}$
20-110	Bottle gas	3.3	2.6	2.8	2.3	3.8	1.6
110-200	Gasoline	12.7	11.8	13	14.7	19.7	14.7
200-300	Jet fuel/Light diesel	24.9	22.9	23.8	23.2	21.3	24.0
300-400	Heavy diesel	22	20.4	14.4	13.2	12.3	12.6
400-550	Vacuum Gas Oil	11.2	15.6	17	15.2	13.8	14.3
<550		74.1	73.3	71	68.5	70.9	67.2
550-700	Heavy Fuel Oil	3.9	2.8	5.1	3.7	6.9	4
700-800	Asphalt	1.7	1.3	3.1	2.4	5.2	2.0
>800	Residue	20.3	22.6	20.8	25.4	17	26.8

^a: Handbook of Petroleum Product Analysis [206]

8.3.7 Integration of lipid extraction and HTL of LESS

Figure 8-5 presents a block flow diagram of the processes considered in this work. The mass yields of the liquid fuels (biocrude and extracted lipid) obtained in the different process configurations of are shown in Table 8-6.

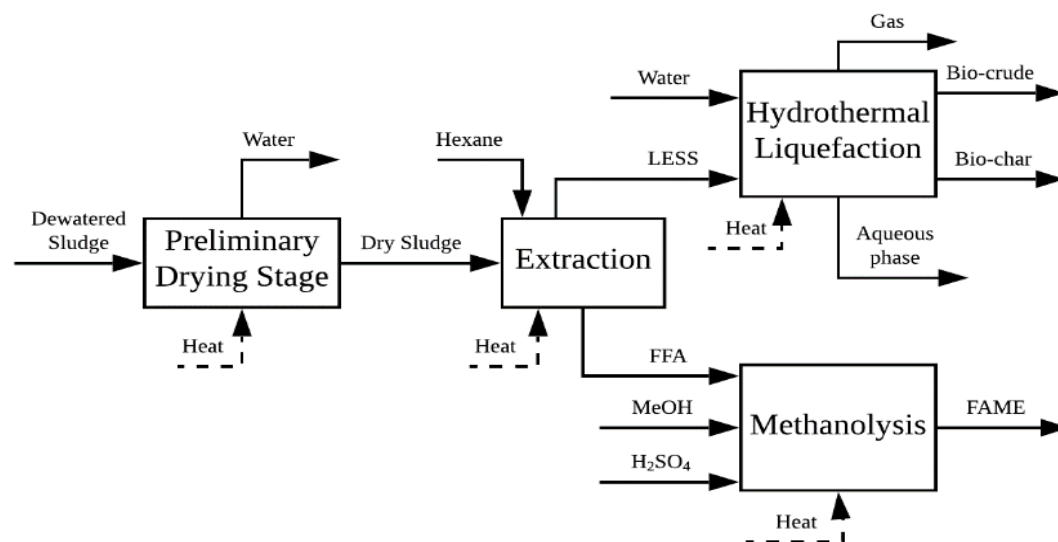


Figure 8-5 Block flow diagram of combined lipid extraction, HTL and methanolysis for FAME production

The combined yields represent the total yield of extracted lipids and biocrude produced from LESS. Accordingly, the HHV is calculated from that of both components. When

looking at the evolution of the biocrude yield without considering lipid extraction, the jump in yield is significant between 300 °C and 350 °C, while being negligible between 250 °C and 300 °C. A similar, albeit more moderate effect can be found when performing HTL of LESS. The yield of extracted lipid exceeds the yield in biocrude at 250 °C and 300 °C, leading to combined yields (HTL + extraction), which are more than double the value obtained using HTL alone. At 350 °C, the high biocrude yields diminish the effect of this coupling. Moreover, the calculated HHV is higher than that of the biocrude from HTL of SS. It appears that the greater efficiency of value-added fuel can be obtained from combining these two methods. Since lipids are commonly seen as biodiesel feedstock, which contains fewer heteroatoms in the target products, it is possible and efficient to extract lipids before conducting the HTL conversion in order to achieve a better energy valorization.

Table 8-6 Comparing the Mass yields of lipid extraction and HTL and their combination. Values in brackets correspond to the HHV of the product in (MJ/kg)

Temperature (°C)	Extraction yield (wt.%)	Liquid fuel products yields (wt.%)		
		Biocrude of SS	Biocrude of LESS	Combined Lipid extraction plus biocrude
250		9.13 (32.29)	8.86 (28.85)	22.76 (35.29)
300	13.9 (39.4)	10.27 (34.60)	10.55 (34.76)	24.45 (37.39)
350		21.26 (37.26)	15.39 (34.91)	29.29 (37.04)

However, the higher nitrogen content in the biocrude from HTL of LESS has to be kept in mind as it is not compliant with fuel standards. Post-treatments like upgrading and distillation could be applied as effective, albeit costly, processes to reduce or remove nitrogen from biocrude [144, 160]. For the latter case, lesser efforts need to be taken to reduce the acidity of the distillates owing to the extraction of fatty acids.

Table 8-7 Energy requirements (MJ/kg) for different steps of the integrated process (without considering heat recovery)

	Combined process	HTL	Drying	Extraction	Methanolysis	Total
With drying	LESS-250 °C	45.1				221.1
	LESS-300 °C	54.9	112.8	61.0	2.2	230.9
	LESS-350 °C	64.7				240.7
Without drying	LESS-250 °C	45.1				108.3
	LESS-300 °C	54.9	-	61.0	2.2	118.1
	LESS-350 °C	64.7				127.9

Table 8-7 shows the heat requirements for the combined process. Drying is a substantial part of the energy demand, contributing around half of the heat demand when employed. HTL and lipid extraction show very similar heat demands, while the energy demand of methanolysis is seemingly negligible.

In Table 8-8, estimations of energy recovery (ER, Eq. 3-5), energy consumption ratio (ECR, Eq. 8-6) and energy demand (ED) per mass of produced biocrude/FAME are shown. The estimation has been carried out based on two cases, A and B, which employ different efficiencies for combustion and heat recovery, respectively. ECR is estimated for different scenarios, considering the production of only biocrude (ECR_{BC}), both biocrude and bio-char (ECR_{BC+SR}), the former plus extracted lipid ($ECR_{BC+SR+L}$), and lipids converted into FAME ($ECR_{BC+SR+FAME}$). While conventional lipid extraction requires the drying of sludge [240, 247], the feasibility of performing extraction of non-dried sludge [117, 247] has recently been shown, thus the estimations of energy efficiency consider the process with and without a drying step.

Energy recovery ER according to Eq.5 can be found in Table 8-8. Since the effect of temperature on the HHV of the formed phases can be neglected, the energy recovery is mostly determined by the product distribution, favouring higher temperatures for biocrude formation. SS shows lower energy recovery (ER) when compared to values determined for LESS at the same temperature, due to the absence of the lipid phase, which features a high HHV. ECR values are also given in Table 8-8. Employing only HTL in case A, assuming conservative efficiencies, the calculated ECR for SS is higher than 1 at temperatures below 350 °C, suggesting that HTL is energetically inefficient, which aligns with the findings from Xu et al. [191]. However, the energy efficiency can be improved with more favourable conditions, as shown in case B, and energy breakeven can always be achieved. Table 8-8 also shows that ECR obtained for SS is lower than that obtained for LESS at the same temperature, due to the energy demand for extraction and drying processes (Table 8-7). A similar trend was reported by Vardon et al. [120], where ECR obtained from algae was lower than that from defatted algae. However, in their work, a favourable energy balance was achieved (ECR 0.44 – 0.55), probably owing to the high biocrude yields (36 – 45 wt.%) and the exclusion of energy consumption for drying and lipid extraction.

The combined process (HTL + extraction) presents higher ECRs and energy demands than the case where only HTL is considered, which can also be explained by the additional

heat requirements for drying and extraction. The minimal effect of methanolysis, aided by the slightly higher HHV of FAME, leads to a negligible difference in ECR between the lipid case and the FAME case for all temperatures. The omission of the drying step leads to a halving of the energy demand of the process. The values of the energy demand for the process with drying reported in this work are lower than those obtained by Pastore et al. [247] for methanolysis of dewatered sludge ($140\text{-}187 \text{ MJ}\cdot\text{kg}^{-1}_{\text{FAME}}$). However, when disregarding drying, the process reaches values that are comparable to the combined process presented by Pastore et al. ($44\text{-}60 \text{ MJ}\cdot\text{kg}^{-1}_{\text{FAME}}$) [247]. When including the energy demand for drying, this value increases significantly.

Table 8-8 Estimation of the Energy Recovery (ER) and Energy Consumption Ratio (ECR), as well as the Energy Demand (ED) of HTL and combined processes. Value assuming a FAME yield of 8.5 wt.% of the dry sludge.

	Process	ER	ECR _{BC}		ECR _{BC+SR}		ECR _{BC+SR+L}		ECR _{BC+SR+FAME}		Energy demand MJ/(kg BC)		Energy demand MJ/(kg FAME)	
		(%)	A	B	A	B	A	B	A	B	A	B	A	B
Only HTL	SS-250 °C	85.4	1.52	0.95	0.31	0.19	-	-	-	-	34.4	27.5	-	-
	SS-300 °C	82.1	1.54	0.96	0.78	0.48	-	-	-	-	37.2	29.7	-	-
	SS-350 °C	78.2	0.81	0.50	0.70	0.44	-	-	-	-	21.2	16.9	-	-
With drying	LESS-250 °C	98.3	1.91	1.19	0.76	0.47	1.91	1.19	1.93	1.20	185.4	147.6	110.5	88.4
	LESS-300 °C	92.3	1.69*	1.05*	0.94*	0.59*	2.02	1.26	2.03	1.26	169.7	135.1	115.4	92.4
	LESS-350 °C	96.7	1.37*	0.85*	1.06*	0.66*	2.05	1.28	2.07	1.28	121.9	97.1	120.3	96.3
Without drying	LESS-250 °C	98.3	1.91*	1.19*	0.76*	0.47*	0.93	0.58	0.94	0.59	88.9	70.4	54.1	43.3
	LESS-300 °C	92.3	1.69*	1.05*	0.94*	0.59*	1.02	0.64	1.04	0.65	85.2	67.5	59.0	47.2
	LESS-350 °C	96.7	1.37*	0.85*	1.06*	0.66*	1.08	0.67	1.10	0.68	63.7	50.5	63.9	51.1

* : only HTL of LESS is considered.

8.4 Conclusion

The study presented here has investigated the opportunity to integrate lipid extraction and hydrothermal liquefaction of the lipid-extracted sewage sludge residue. After lipid extraction, the remaining proteins and carbohydrates in the residue can be further converted into value-added products via hydrothermal liquefaction, and the lipid can be employed for the production of biodiesel (FAME). The majority of lipids in the sewage sludge cannot be converted into biocrude at lower temperatures. Maillard reactions significantly contribute to the formation of biocrude components but show high nitrogen contents. With increasing temperatures, they increasingly get converted into biocrude constituents by decarboxylation or cross-linking the reaction with other intermediate components. Regarding the energetic efficiency of the process, energy recovery of around 98 % could be achieved by the coupled process, which has a significant temperature dependency and a collective yield of up to 35 wt.% in liquid bio-fuel products. An analysis of the energy consumption ratio (ECR) of the process disfavours the coupled process due to the energetic requirements of drying and lipid extraction. The energy demand of the coupled process is, however, comparable to values obtained by other authors.

Chapter 9 Conclusion & Outlook

9.1 Conclusion

The introduction of the thesis describes the current state of development in the disposal of sewage sludge in terms of waste management and environmental issues. Instead of being marked as hazardous bio-waste, sewage sludge should be considered a maintainable feedstock for the recovery of resources and a suitable alternative feedstock for renewable biofuels production to achieve a maximum valorization. Hydrothermal liquefaction is increasingly identified as one of the most appropriate conversion technologies as it allows handling wet slurry without costly pre-drying procedures, enabling applications to obtain multiple fuel-like products with promising yields and quality. Meanwhile, the by-products, such as nutrient-rich water phase and solid residue, after appropriate treatments, can be obtained as by-products adding value to the production chain, thus achieving or improving the economic feasibility of the HTL process.

HTL of sewage sludge has received increasing attention in published literature, with considerable amounts of studies being conducted on batch reactors and, more recently, on the development of continuous flow processes. Until now, the target product of HTL is liquid biocrude; however, one of the drawbacks identified is the high problematic nitrogen content in the produced biocrude, which considerably limits the application of biocrude generated as it fails to meet existing fuel standards. Modification of different HTL parameters, the utilization of homogeneous and heterogeneous catalysts and the application of various pre-treatments have been investigated with the aim to improve the yields and quality of biocrude, but with less focus on the reduction of N content. Taken collectively, it can be concluded that N content seems to be “immune” to any external methods, as long as the sewage sludge contains proteins. Technically, the post-treatment, mostly upgrading by hydrotreatment, could achieve almost N-free (less than 0.1 wt.%) upgraded bio-oil as reported by PNNL. The promising output was tested with biocrude samples obtained with bench-scale and continuous-flow process equipment. However, the special need of sustainable H₂ resource consumption and controlling catalyst deactivation are challenges for scale-up pilot processes. In order to better apply efficient

pre-/post treatment with HTL to achieve nitrogen-reduced biocrude, the reaction mechanism in terms of N transformation during HTL is necessary. A proper understanding of its fundamentals is still missing, which motivated the present work.

HTL of sewage sludge in batch and continuous processes

Temperature plays a crucial role in HTL of sewage sludge: 12.0 to 22.1 wt.% (daf.) biocrude can be obtained with HHV from 34.1 to 37.1 MJ/kg as temperature increases from 250 to 350 °C with a retention time of 20 min. However, the reduction of N in biocrude shows to be less sensitive towards temperature: the N content in the obtained biocrude shows a slight decrease from 7.6 to 6.0 wt.% although half of the fraction (41 – 52 wt.%) of N in the sewage sludge is recovered in the aqueous phase; more N (12 – 33 wt.%) is partitioned to the biocrude instead of remaining in the solid residue (12 – 17 wt.%).

Translating HTL technology to scaled-up applications greatly depends on the selection of the type of sewage sludge and optimized parameters in terms of operational feasibility of the pilot-plant. The operation of a continuous flow HTL reactor by pumping 10 wt.% slurry was successfully performed to achieve 30.8 wt.% (daf.) biocrude with the “primary mixed with secondary” sewage sludge at 350 °C for 8 min. Unexpectedly, the heating rate showed negligible effects on the product distribution in terms of the comparable results observed between batch and continuous processes. However, in continuous processing, a slightly better reduction of the N content than in batch processing was found (4.25 vs. 3.9 wt.%), indicating that the heating rate may be useful to affect the quality of biocrude.

Fundamental research

It is well-confirmed that Maillard reactions play a crucial role in biocrude production as they contribute to higher yields and introduce undesirable N-containing compounds. The mechanism of reaction pathways are assumed as follows: Maillard reactions contribute to biocrude production while inhibiting the formation of hydro-char from carbohydrates, which has been proven by the elimination of the key HMF intermediate. Maillard reactions largely suppress the cyclization or dimerization of amino acids produced by hydrolysis of proteins or peptides. Instead of cyclic amides and amines, higher fractions of N-heterocyclic compounds such as pyrazines and indoles are generated, unfortunately reducing the quality of the biocrude. The formation of these problematic Maillard reaction products occur above 150 °C and reach nearly constant values at 250 °C with a retention time of less than 10 min. Combined with the negligible reduction of N content in the

biocrude, the decrease of Maillard reaction product yields with increasing temperature and longer retention time can be explained by the effects self-polymerization occurring among these chemicals, leading to the formation of macromolecular melanoidins, which are not detected by GC-MS. In comparison, amidation seems less competitive with Maillard reactions, owing to the fact that lipids derived from sludge are relatively difficult to convert into biocrude at low temperatures (< 300 °C). At higher temperatures, lipids can react with proteins to produce fatty amides. Thus, the competition between amidation and Maillard reaction can modify the N-containing species in the end products. An investigation of the reaction kinetics would be much more beneficial to understand the overall reaction scheme and to better optimize conditions prior to experimental performance.

Integrated approach

The results presented in this work lead to the conclusion that the undesirable N-containing compounds forming in biocrude from HTL of sewage sludge are practically impossible to be avoided or removed without post-treatment. Regarding the temperature dependency of synergistic effects of different interactions occurring among bio-chemicals in the sludge during HTL, it is promising to conduct HTL of residual sludge after lipids extraction, achieving the valorisation of energy recovery through integrated bio-diesel and biocrude production from sewage sludge. That way, a larger amount of liquid fuel-like products can be obtained with better energy recovery by the combined process. However, the energetic requirements estimated according to the energy consumption ratio turned out to be energetically inefficient at first glance. The energy breakeven can only be attained under the assumption of more favourable conditions, indicating that a deeper investigation and further development of the integrated approaches could help improve the energy valorisation of sewage sludge with possible implications in the fields of waste management and renewable energy production.

9.2 Outlook

Nitrogen removal by adsorptive denitrogenation

Plenty of studies have shown that the removal of N from biocrude can be achieved by catalytic hydrodenitrogenation to obtain energy-dense upgraded bio-oil. However, the need for H₂ consumption at high pressure is still a drawback of this technology. In the case of biocrude derived from sewage sludge, the presence of relatively higher N-heterogeneous compounds would require energy-intensive inputs owing to the frequent deactivation of catalysts. Adsorptive denitrogenation would be an alternative option for the removal of problematic N-containing compounds. The results presented in this work show that the formation of specific N-containing compounds varies depending on the temperature and feedstocks. These findings help in screening cost-effective adsorbents based on their adsorptive selectivity and capacity.

Renewable nitrogen-heterocycles production

Biocrude derived from HTL of sewage sludge contains considerable amounts of N-containing heterocycles, which are not available from conventional fuel resources. Recently, there has been increasing interest in the development of sustainable processes with simple and green approaches to access value-added heteroatom-containing chemicals. Nevertheless, the production of N-containing organic materials could also be a great opportunity for the use of biocrude. In fact, more attention has been paid to the development of sustainable processes with green approaches to produce value-added N-containing chemicals, especially N-containing heterocycles such as pyrroles, indoles, and pyrazines, which are widely used in the pharmaceutical, agrochemical and polymer industry [252, 253]. However, it should be noted that the low concentration of valuable chemicals may result in difficulties with regard to the extraction of pure functional components with high efficiency. Effective separation and purification processes should be developed to get bio-based chemicals. For example, octahydrodipyrido[1,2-a:1,2-d]pyrazine-6,12(2H,6aH)-dione, as a promising N-containing heterocycle, was isolated and identified in the biocrude obtained from the HTL of lysine.

The feasibility of integrated processes

The combination and/or integration of different processes can be considered a valorisation route to improve energy recovery. With regard to upgrading, the direct impact of N-species and inorganics on the deactivation of catalysts, as well as the design and viability

of the upgrading stage must be an additional focal point. As the implementation of industrial applications has already been started by some research groups in cooperation with industries, standards for biocrude and bio-fuel applications should be agreed as soon as possible for subsequent research and further development. The by-products must be further utilized. For additional valorisation of the HTL of the aqueous phase such as in catalytic hydrothermal gasification or anaerobic digestion, energy demands and lower environmental costs should be intensively considered. The technical strategies, such as dewatering and stabilizing, have to be effective and economically feasible for high-value applications of hydro-char. In addition, when the integrated process is considered a new approach to valorise SS into energy and other products, a comprehensive energetic evaluation of energy recovery efficiency, an economical assessment and life cycle analysis is necessary to broadly evaluate its potential in industrial applications.

Emerging technologies for waste water treatment plants

Sewage sludge, which traditionally is considered an end or downstream product from WWTP, appears to be a suitable feedstock for HTL. Once this technology is commercially applied in bio-fuel or chemical production, WWTPs will also have to undergo transitions to prepare for future challenges such as providing suitable sewage sludge with suitable biochemical properties for industrial HTL processing. Many older wastewater treatment facilities require upgrading because of increasingly strict water quality regulations and human health protection, and associated technological treatment should be also integrated with emerging technologies for downstream HTL processes.

References

1. Syed-Hassan, S.S.A., et al., *Thermochemical processing of sewage sludge to energy and fuel: Fundamentals, challenges and considerations*. Renewable and Sustainable Energy Reviews, 2017. **80**: p. 888-913.
2. Oladejo, J., et al., *A Review of Sludge-to-Energy Recovery Methods*. Energies, 2018. **12**(1): p. 60.
3. Amrullah, A., N. Paksung, and Y. Matsumura, *Cell structure destruction and its kinetics during hydrothermal treatment of sewage sludge*. Korean Journal of Chemical Engineering, 2019. **36**(3): p. 433-438.
4. Fytily, D. and A. Zabaniotou, *Utilization of sewage sludge in EU application of old and new methods—A review*. Renewable and Sustainable Energy Reviews, 2008. **12**(1): p. 116-140.
5. Seiple, T.E., A.M. Coleman, and R.L. Skaggs, *Municipal wastewater sludge as a sustainable bioresource in the United States*. J Environ Manage, 2017. **197**: p. 673-680.
6. Manara, P. and A. Zabaniotou, *Towards sewage sludge based biofuels via thermochemical conversion – A review*. Renewable and Sustainable Energy Reviews, 2012. **16**(5): p. 2566-2582.
7. Bhuta, H., *Chapter 4 - Advanced Treatment Technology and Strategy for Water and Wastewater Management*, in *Industrial Wastewater Treatment, Recycling and Reuse*, V.V. Ranade and V.M. Bhandari, Editors. 2014, Butterworth-Heinemann: Oxford. p. 193-213.
8. Peccia, J. and P. Westerhoff, *We Should Expect More out of Our Sewage Sludge*. Environ Sci Technol, 2015. **49**(14): p. 8271-6.
9. Kamizela, T. and M. Kowalczyk, *18 - Sludge dewatering: Processes for enhanced performance*, in *Industrial and Municipal Sludge*, M.N.V. Prasad, et al., Editors. 2019, Butterworth-Heinemann. p. 399-423.
10. Gong, M., et al., *Influence of sludge properties on the direct gasification of dewatered sewage sludge in supercritical water*. Renewable Energy, 2014. **66**: p. 605-611.
11. Rulkens, W., *Sewage Sludge as a Biomass Resource for the Production of Energy: Overview and Assessment of the Various Options*. Energy & Fuels, 2008. **22**(1): p. 9-15.
12. Donatello, S. and C.R. Cheeseman, *Recycling and recovery routes for incinerated sewage sludge ash (ISSA): a review*. Waste Manag, 2013. **33**(11): p. 2328-40.
13. O'Kelly, B.C., *Sewage sludge to landfill: some pertinent engineering properties*. J Air Waste Manag Assoc, 2005. **55**(6): p. 765-71.
14. Ucaroglu, S. and U. Alkan, *Composting of wastewater treatment sludge with different bulking agents*. J Air Waste Manag Assoc, 2016. **66**(3): p. 288-95.
15. Chen, Y., *Sewage Sludge Aerobic Composting Technology Research Progress*. AASRI Procedia, 2012. **1**: p. 339-343.
16. Wu, Y., et al., *Effects of bioleaching pretreatment on nitrous oxide emission related functional genes in sludge composting process*. Bioresource Technology, 2018. **266**: p. 181-188.
17. Beeckmans, J.M. and P.C. Ng, *Pyrolyzed sewage sludge: its production and*

- possible utility*. Environmental Science & Technology, 1971. **5**(1): p. 69-71.
18. Grifoni, M., et al., *26 - From waste to resource: Sorption properties of biological and industrial sludge*, in *Industrial and Municipal Sludge*, M.N.V. Prasad, et al., Editors. 2019, Butterworth-Heinemann. p. 595-621.
 19. Zhai, Y.B., X.X. Wei, and G.M. Zeng, *Effect of pyrolysis temperature and hold time on the characteristic parameters of adsorbent derived from sewage sludge*. J Environ Sci (China), 2004. **16**(4): p. 683-6.
 20. Smith, K.M., et al., *Sewage sludge-based adsorbents: a review of their production, properties and use in water treatment applications*. Water Res, 2009. **43**(10): p. 2569-94.
 21. Childers, D.L., et al., *Sustainability Challenges of Phosphorus and Food: Solutions from Closing the Human Phosphorus Cycle*. BioScience, 2011. **61**(2): p. 117-124.
 22. J.J. Schröder, D. Cordell, and A.L.S.A. Rosemarin, *Sustainable Use of Phosphorus - European Commission Tender project ENV.B.1/ETU/2009/0025*. 2010, Plant Research International, part of Wageningen UR The Netherlands,. p. 122.
 23. Gilbert, N., *Environment: The disappearing nutrient*. Nature, 2009. **461**(7265): p. 716-8.
 24. Zhou, K., et al., *Phosphorus recovery from municipal and fertilizer wastewater: China's potential and perspective*. J Environ Sci (China), 2017. **52**: p. 151-159.
 25. Römer, W. and B. Steingrobe, *Fertilizer Effect of Phosphorus Recycling Products*. Sustainability, 2018. **10**(4): p. 1166.
 26. Römer, W., *Vergleichende Untersuchungen zur Pflanzenverfügbarkeit von Phosphat aus verschiedenen P-Recycling-Produkten im Keimpflanzenversuch*. Journal of Plant Nutrition and Soil Science, 2006. **169**(6): p. 826-832.
 27. Przydatek, G. and A.K. Wota, *Analysis of the comprehensive management of sewage sludge in Poland*. Journal of Material Cycles and Waste Management: p. 9.
 28. Sever Akdağ, A., et al., *Co-combustion of sewage sludge from different treatment processes and a lignite coal in a laboratory scale combustor*. Energy, 2018. **158**: p. 417-426.
 29. Sängler, M., J. Werther, and T. Ogada, *NOx and N2O emission characteristics from fluidised bed combustion of semi-dried municipal sewage sludge*. Fuel, 2001. **80**(2): p. 167-177.
 30. Grübel, K., et al., *Microwave-assisted sustainable co-digestion of sewage sludge and rapeseed cakes*. Energy Conversion and Management, 2019. **199**: p. 112012.
 31. Luo, G., W. Wang, and I. Angelidaki, *Anaerobic Digestion for Simultaneous Sewage Sludge Treatment and CO Biomethanation: Process Performance and Microbial Ecology*. Environmental Science & Technology, 2013. **47**(18): p. 10685-10693.
 32. Guo, L., et al., *Comparison of thermophilic bacteria and alkyl polyglucose pretreatment on two-stage anaerobic digestion with waste sludge: Biogas production potential and substrate metabolism process*. Bioresource Technology, 2018. **249**: p. 694-703.
 33. Ding, H.H., S. Chang, and Y. Liu, *Biological hydrolysis pretreatment on secondary sludge: Enhancement of anaerobic digestion and mechanism study*. Bioresour Technol, 2017. **244**(Pt 1): p. 989-995.
 34. Kwon, E.E., et al., *Biodiesel Production from Sewage Sludge: New Paradigm for*

- Mining Energy from Municipal Hazardous Material*. Environmental Science & Technology, 2012. **46**(18): p. 10222-10228.
35. Zhu, F., et al., *Lipid profiling in sewage sludge*. Water Research, 2017. **116**(Can. J. Biochem. Physiol. 37 8 1959): p. 149-158.
 36. Zhu, F., et al., *Comparison of the Lipid Content and Biodiesel Production from Municipal Sludge Using Three Extraction Methods*. Energy & Fuels, 2014. **28**(8): p. 5277-5283.
 37. Demirbas, A., et al., *Biodiesel production from lipids of municipal sewage sludge by direct methanol transesterification*. Energy Sources, Part A: Recovery, Utilization, and Environmental Effects, 2017. **39**(8): p. 800-805.
 38. Siddiquee, M.N. and S. Rohani, *Lipid extraction and biodiesel production from municipal sewage sludges: A review*. Renewable and Sustainable Energy Reviews, 2011. **15**(2): p. 1067-1072.
 39. Mondala, A., et al., *Biodiesel production by in situ transesterification of municipal primary and secondary sludges*. Bioresource Technology, 2009. **100**(3): p. 1203-1210.
 40. Kruse, A. and N. Dahmen, *Hydrothermal biomass conversion: Quo vadis?* The Journal of Supercritical Fluids, 2018. **134**: p. 114-123.
 41. Czernik, S. and A.V. Bridgwater, *Overview of Applications of Biomass Fast Pyrolysis Oil*. Energy & Fuels, 2004. **18**(2): p. 590-598.
 42. Bridgwater, A.V., *Review of fast pyrolysis of biomass and product upgrading*. Biomass and Bioenergy, 2012. **38**: p. 68-94.
 43. Karaca, C., et al., *High temperature pyrolysis of sewage sludge as a sustainable process for energy recovery*. Waste Management, 2018. **78**: p. 217-226.
 44. Schmitt, N., et al., *Thermo-chemical conversion of biomass and upgrading to biofuel: The Thermo-Catalytic Reforming process - A review*. Biofuels Bioproducts & Biorefining-Biofpr, 2019. **13**(3): p. 822-837.
 45. Conti, R., et al., *Thermocatalytic Reforming of Biomass Waste Streams*. Energy Technology, 2017. **5**(1): p. 104-110.
 46. Neumann, J., Hornung, A., Apfelbacher, A., Daschner, R., *Pyrolysis of Residual Biomass via Thermo-Catalytic Reforming - Experimental Investigation of Sewage Sludge*, in *25th European Biomass Conference and Exhibition*. 2017, Florence: ETA, 2017: Stockholm, 12-15 June 2017. p. 949-951.
 47. Watson, J., et al., *Gasification of biowaste: A critical review and outlooks*. Renewable and Sustainable Energy Reviews, 2018. **83**: p. 1-17.
 48. Fan, Y.J., et al., *Catalytic gasification of dewatered sewage sludge in supercritical water: Influences of formic acid on hydrogen production*. International Journal of Hydrogen Energy, 2016. **41**(7): p. 4366-4373.
 49. Kruse, A. and N. Dahmen, *Water – A magic solvent for biomass conversion*. The Journal of Supercritical Fluids, 2015. **96**: p. 36-45.
 50. Kruse, A., et al., *Fate of Nitrogen during Hydrothermal Carbonization*. Energy & Fuels, 2016. **30**(10): p. 8037-8042.
 51. Danso-Boateng, E., et al., *Hydrothermal carbonisation of sewage sludge: Effect of process conditions on product characteristics and methane production*. Bioresource Technology, 2015. **177**: p. 318-327.
 52. Becker, G.C., et al., *Novel approach of phosphate-reclamation as struvite from sewage sludge by utilising hydrothermal carbonization*. Journal of Environmental Management, 2019. **238**: p. 119-125.
 53. Correa, C.R. and A. Kruse, *Biobased Functional Carbon Materials: Production*,

- Characterization, and Applications-A Review*. Materials (Basel, Switzerland), 2018. **11**(9): p. 1568.
54. de Caprariis, B., et al., *Hydrothermal liquefaction of biomass: Influence of temperature and biomass composition on the bio-oil production*. Fuel, 2017. **208**: p. 618-625.
55. Dimitriadis, A. and S. Bezergianni, *Hydrothermal liquefaction of various biomass and waste feedstocks for biocrude production: A state of the art review*. Renewable and Sustainable Energy Reviews, 2017. **68, Part 1**: p. 113-125.
56. Su, Y., et al., *Investigation on the decomposition of chemical compositions during hydrothermal conversion of dewatered sewage sludge*. International Journal of Hydrogen Energy, 2019. **44**(49): p. 26933-26942.
57. Wyman, C., et al., *Hydrolysis of Cellulose and Hemicellulose*. 2004.
58. Minowa, T., et al., *Hydrothermal Reaction of Glucose and Glycine as Model Compounds of Biomass*. Journal of the Japan Institute of Energy, 2004. **83**(10): p. 794-798.
59. Akhtar, J. and N.A.S. Amin, *A review on process conditions for optimum bio-oil yield in hydrothermal liquefaction of biomass*. Renewable and Sustainable Energy Reviews, 2011. **15**(3): p. 1615-1624.
60. Gollakota, A.R.K., N. Kishore, and S. Gu, *A review on hydrothermal liquefaction of biomass*. Renewable and Sustainable Energy Reviews, 2018. **81**: p. 1378-1392.
61. Xu, D., et al., *Comprehensive evaluation on product characteristics of fast hydrothermal liquefaction of sewage sludge at different temperatures*. Energy, 2018. **159**: p. 686-695.
62. He, C., et al., *Hydrothermal gasification of sewage sludge and model compounds for renewable hydrogen production: A review*. Renewable and Sustainable Energy Reviews, 2014. **39**: p. 1127-1142.
63. Lu, J.L., et al., *Research Progress of Oil Making from Sewage Sludge*. Applied Mechanics and Materials, 2016. **851**: p. 232-236.
64. Lee, S.Y., et al., *Waste to bioenergy: a review on the recent conversion technologies*. BMC Energy, 2019. **1**(1).
65. Qian, L., S. Wang, and P.E. Savage, *Hydrothermal liquefaction of sewage sludge under isothermal and fast conditions*. Bioresource Technology, 2017. **232**: p. 27-34.
66. Suzuki, A., et al., *CONVERSION OF SEWAGE SLUDGE TO HEAVY OIL BY DIRECT THERMOCHEMICAL LIQUEFACTION*. Journal of Chemical Engineering of Japan, 1988. **21**(3): p. 288-293.
67. Wang, W., et al., *Catalytic liquefaction of municipal sewage sludge over transition metal catalysts in ethanol-water co-solvent*. Bioresource Technology, 2018. **249**: p. 361-367.
68. Malins, K., et al., *Bio-oil from thermo-chemical hydro-liquefaction of wet sewage sludge*. Bioresource Technology, 2015. **187**: p. 23-29.
69. Miao, C., et al., *Hydrothermal catalytic deoxygenation of palmitic acid over nickel catalyst*. Fuel, 2016. **166**: p. 302-308.
70. Mo, N. and P.E. Savage, *Hydrothermal Catalytic Cracking of Fatty Acids with HZSM-5*. ACS Sustainable Chemistry & Engineering, 2013. **2**(1): p. 88-94.
71. Dote, Y., et al., *Thermochemical liquidization of dewatered sewage sludge*. Biomass and Bioenergy, 1993. **4**(4): p. 243-248.
72. Zhuang, X., et al., *The transformation pathways of nitrogen in sewage sludge during hydrothermal treatment*. Bioresour Technol, 2017. **245**(Pt A): p. 463-470.

73. Yokoyama, S.-y., et al., *Liquid fuel production from sewage sludge by catalytic conversion using sodium carbonate*. Fuel, 1987. **66**(8): p. 1150-1155.
74. Dote, Y., et al., *Analysis of oil derived from liquefaction of sewage sludge*. Fuel, 1992. **71**(9): p. 1071-1073.
75. Itoh, S., et al., *Production of heavy oil from sewage sludge by direct thermochemical liquefaction*. Desalination, 1994. **98**(1): p. 127-133.
76. Inoue, S., et al., *Behaviour of nitrogen during liquefaction of dewatered sewage sludge*. Biomass and Bioenergy, 1997. **12**(6): p. 473-475.
77. Toor, S.S., L. Rosendahl, and A. Rudolf, *Hydrothermal liquefaction of biomass: A review of subcritical water technologies*. Energy, 2011. **36**(5): p. 2328-2342.
78. Posmanik, R., et al., *Acid and Alkali Catalyzed Hydrothermal Liquefaction of Dairy Manure Digestate and Food Waste*. ACS Sustainable Chemistry & Engineering, 2018. **6**(2): p. 2724-2732.
79. Long, J., et al., *Comparative investigation on hydrothermal and alkali catalytic liquefaction of bagasse: Process efficiency and product properties*. Fuel, 2016. **186**: p. 685-693.
80. Zhang, B., et al., *Catalytic hydrothermal liquefaction of Euglena sp. microalgae over zeolite catalysts for the production of bio-oil*. RSC Adv., 2017. **7**(15): p. 8944-8951.
81. Yin, S. and Z. Tan, *Hydrothermal liquefaction of cellulose to bio-oil under acidic, neutral and alkaline conditions*. Applied Energy, 2012. **92**: p. 234-239.
82. Duan, P. and P.E. Savage, *Hydrothermal Liquefaction of a Microalga with Heterogeneous Catalysts*. Industrial & Engineering Chemistry Research, 2011. **50**(1): p. 52-61.
83. Zou, S., et al., *Thermochemical Catalytic Liquefaction of the Marine Microalgae Dunaliella tertiolecta and Characterization of Bio-oils*. Energy & Fuels, 2009. **23**(7): p. 3753-3758.
84. Wang, C., et al., *Influence of H₂O₂ and Ni catalysts on hydrogen production and PAHs inhibition from the supercritical water gasification of dewatered sewage sludge*. The Journal of Supercritical Fluids, 2017. **130**: p. 183-188.
85. Gong, M., et al., *Influence of NaOH and Ni catalysts on hydrogen production from the supercritical water gasification of dewatered sewage sludge*. International Journal of Hydrogen Energy, 2014. **39**(35): p. 19947-19954.
86. Jena, U., K.C. Das, and J.R. Kastner, *Comparison of the effects of Na₂CO₃, Ca₃(PO₄)₂, and NiO catalysts on the thermochemical liquefaction of microalga Spirulina platensis*. Applied Energy, 2012. **98**: p. 368-375.
87. Xu, D., et al., *Heterogeneous catalytic effects on the characteristics of water-soluble and water-insoluble biocrudes in chlorella hydrothermal liquefaction*. Applied Energy, 2019. **243**: p. 165-174.
88. Hietala, D.C., et al., *Influence of biodiversity, biochemical composition, and species identity on the quality of biomass and biocrude oil produced via hydrothermal liquefaction*. Algal Research, 2017. **26**: p. 203-214.
89. Wang, C., et al., *Char and tar formation during hydrothermal treatment of sewage sludge in subcritical and supercritical water: Effect of organic matter composition and experiments with model compounds*. Journal of Cleaner Production, 2020. **242**.
90. Efika, C.E., J.A. Onwudili, and P.T. Williams, *Influence of heating rates on the products of high-temperature pyrolysis of waste wood pellets and biomass model compounds*. Waste Management, 2018. **76**: p. 497-506.

91. Sinač, A., A. Kruse, and J. Rathert, *Influence of the Heating Rate and the Type of Catalyst on the Formation of Key Intermediates and on the Generation of Gases During Hydrolysis of Glucose in Supercritical Water in a Batch Reactor*. Industrial & Engineering Chemistry Research, 2004. **43**(2): p. 502-508.
92. Barber, W.P.F., *Thermal hydrolysis for sewage treatment: A critical review*. Water Res, 2016. **104**: p. 53-71.
93. Karl Eichnerl and M. Karel*, *Influence of water content and water activity on the sugar-amino browning reaction in model systems under various conditions*. 1972.
94. Zhai, Y., et al., *Influence of sewage sludge-based activated carbon and temperature on the liquefaction of sewage sludge: Yield and composition of bio-oil, immobilization and risk assessment of heavy metals*. Bioresource Technology, 2014. **159**: p. 72-79.
95. Liu, R., et al., *Effects of inorganic and organic acid pretreatments on the hydrothermal liquefaction of municipal secondary sludge*. Energy Conversion and Management, 2018. **174**: p. 661-667.
96. Zhang, L., P. Champagne, and C. Xu, *Bio-crude production from secondary pulp/paper-mill sludge and waste newspaper via co-liquefaction in hot-compressed water*. Energy, 2011. **36**(4): p. 2142-2150.
97. Breunig, M., et al., *Direct liquefaction of lignin and lignin rich biomasses by heterogenic catalytic hydrogenolysis*. Biomass and Bioenergy, 2018. **111**: p. 352-360.
98. Chumpoo, J. and P. Prasassarakich, *Bio-Oil from Hydro-Liquefaction of Bagasse in Supercritical Ethanol*. Energy & Fuels, 2010. **24**(3): p. 2071-2077.
99. Yuan, X., et al., *Sub- and supercritical liquefaction of rice straw in the presence of ethanol–water and 2-propanol–water mixture*. Energy, 2007. **32**(11): p. 2081-2088.
100. Baloch, H.A., et al., *Solvothermal co-liquefaction of sugarcane bagasse and polyethylene under sub-supercritical conditions: optimization of process parameters*. Process Safety and Environmental Protection, 2020.
101. Zhang, J. and Y. Zhang, *Hydrothermal Liquefaction of Microalgae in an Ethanol–Water Co-Solvent To Produce Biocrude Oil*. Energy & Fuels, 2014. **28**(8): p. 5178-5183.
102. Yang, T., et al., *Hydrothermal liquefaction of sewage sludge to produce bio-oil: Effect of co-pretreatment with subcritical water and mixed surfactants*. The Journal of Supercritical Fluids, 2019. **144**: p. 28-38.
103. Li, R., et al., *Sub-supercritical liquefaction of municipal wet sewage sludge to produce bio-oil: Effect of different organic–water mixed solvents*. The Journal of Supercritical Fluids, 2018. **138**: p. 115-123.
104. Huang, H.-j., et al., *Co-liquefaction of sewage sludge and rice straw/wood sawdust: The effect of process parameters on the yields/properties of bio-oil and biochar products*. Energy, 2019. **173**: p. 140-150.
105. Kapusta, K., *Effect of ultrasound pretreatment of municipal sewage sludge on characteristics of bio-oil from hydrothermal liquefaction process*. Waste Management, 2018. **78**: p. 183-190.
106. Chen, G., et al., *Hydrothermal Liquefaction of Sewage Sludge by Microwave Pretreatment*. Energy & Fuels, 2020. **34**(2): p. 1145-1152.
107. Chen, G.Y., et al., *Hydrothermal Liquefaction of Sewage Sludge by Microwave Pretreatment*. Energy & Fuels, 2020. **34**(2): p. 1145-1152.
108. Biller, P., C. Friedman, and A.B. Ross, *Hydrothermal microwave processing of*

- microalgae as a pre-treatment and extraction technique for bio-fuels and bio-products*. *Bioresour Technol*, 2013. **136**: p. 188-95.
109. Zheng, A., et al., *Effect of microwave-assisted organosolv fractionation on the chemical structure and decoupling pyrolysis behaviors of waste biomass*. *Journal of Analytical and Applied Pyrolysis*, 2018. **131**: p. 120-127.
110. Gao, J., et al., *Protein extraction from excess sludge by alkali-thermal hydrolysis*. *Environ Sci Pollut Res Int*, 2020. **27**(8): p. 8628-8637.
111. Gong, L., et al., *Impact of hydrothermal pre-treatment on the anaerobic digestion of different solid-liquid ratio sludges and kinetic analysis*. *RSC Advances*, 2019. **9**(33): p. 19104-19113.
112. Park, S., et al., *Effect of hydrothermal pre-treatment on physical properties and co-digestion from food waste and sewage sludge mixture*. *Waste Manag Res*, 2020: p. 734242X19897123.
113. Lerch, R.N., et al., *Sewage Sludge Proteins: I. Extraction Methodology*. *Journal of Environmental Quality*, 1993. **22**: p. 620-624.
114. Ras, M., et al., *Protein extraction from activated sludge: An analytical approach*. *Water Research*, 2008. **42**(8): p. 1867-1878.
115. Zhu, F., et al., *Preliminary Study at Lipids Extraction Technology from Municipal Sludge by Organic Solvent*. *Procedia Environmental Sciences*, 2012. **16**: p. 352-356.
116. Supaporn, P., et al., *Bio-oil production using residual sewage sludge after lipid and carbohydrate extraction*. *Environmental Engineering Research*, 2018. **24**(2): p. 202-210.
117. Olkiewicz, M., et al., *Direct liquid-liquid extraction of lipid from municipal sewage sludge for biodiesel production*. *Fuel Processing Technology*, 2014. **128**: p. 331-338.
118. Shahi, T., et al., *Bio-oil production from residual biomass of microalgae after lipid extraction: The case of Dunaliella Sp.* *Biocatalysis and Agricultural Biotechnology*, 2020. **23**: p. 101494.
119. Guo, B., *Hydrothermal liquefaction of residual microalgae biomass after pulsed electric field-assisted valuables extraction*. *Algal research*, 2019. **v. 43**: p. 2019 v.43.
120. Vardon, D.R., et al., *Thermochemical conversion of raw and defatted algal biomass via hydrothermal liquefaction and slow pyrolysis*. *Bioresour Technol*, 2012. **109**: p. 178-87.
121. Frank, E.D., et al., *Life cycle comparison of hydrothermal liquefaction and lipid extraction pathways to renewable diesel from algae*. *Mitigation and Adaptation Strategies for Global Change*, 2012. **18**(1): p. 137-158.
122. Yang, J., Q. He, and L. Yang, *A review on hydrothermal co-liquefaction of biomass*. *Applied Energy*, 2019. **250**: p. 926-945.
123. Brilman, D.W.F., N. Drabik, and M. Wądrzyk, *Hydrothermal co-liquefaction of microalgae, wood, and sugar beet pulp*. *Biomass Conversion and Biorefinery*, 2017. **7**(4): p. 445-454.
124. Chen, X., et al., *Investigation of Mannich reaction during co-liquefaction of microalgae and sweet potato waste*. *Bioresour Technol*, 2019. **284**: p. 286-292.
125. Zhang, C., et al., *Enhancing the performance of Co-hydrothermal liquefaction for mixed algae strains by the Maillard reaction*. *Green Chem.*, 2016. **18**(8): p. 2542-2553.
126. Raikova, S., et al., *Co-liquefaction of Macroalgae with Common Marine Plastic*

- Pollutants*. ACS Sustainable Chemistry & Engineering, 2019. **7**(7): p. 6769-6781.
127. Posmanik, R., et al., *Biomass conversion to bio-oil using sub-critical water: Study of model compounds for food processing waste*. The Journal of Supercritical Fluids, 2017. **119**: p. 26-35.
128. Lu, J., et al., *Synergistic and antagonistic interactions during hydrothermal liquefaction of soybean oil, soy protein, cellulose, xylose, and lignin*. ACS Sustainable Chemistry & Engineering, 2018.
129. Déniel, M., et al., *Energy valorisation of food processing residues and model compounds by hydrothermal liquefaction*. Renewable and Sustainable Energy Reviews, 2016. **54**(Supplement C): p. 1632-1652.
130. Biller, P., et al., *Primary sewage sludge filtration using biomass filter aids and subsequent hydrothermal co-liquefaction*. Water Research, 2018. **130**: p. 58-68.
131. Fox, J.T., et al., *Thermal conversion of blended food production waste and municipal sewage sludge to recoverable products*. Journal of Cleaner Production, 2019. **220**: p. 57-64.
132. Xu, D., et al., *Co-hydrothermal liquefaction of microalgae and sewage sludge in subcritical water: Ash effects on bio-oil production*. Renewable Energy, 2019. **138**: p. 1143-1151.
133. Mishra, S. and K. Mohanty, *Co-HTL of domestic sewage sludge and wastewater treatment derived microalgal biomass - An integrated biorefinery approach for sustainable biocrude production*. Energy Conversion and Management, 2020. **204**: p. 11.
134. Seljak, T., et al., *Bioliqids and their use in power generation – A technology review*. Renewable and Sustainable Energy Reviews, 2020. **129**: p. 109930.
135. Karatzos, S., J.D. McMillan, and J.N. Saddler, *The potential and challenges of drop-in biofuels*. Report for IEA Bioenergy Task, 2014. **39**.
136. Oasmaa, A. and S. Czernik, *Fuel Oil Quality of Biomass Pyrolysis Oils State of the Art for the End Users*. Energy & Fuels, 1999. **13**(4): p. 914-921.
137. Xiu, S. and A. Shahbazi, *Bio-oil production and upgrading research: A review*. Renewable and Sustainable Energy Reviews, 2012. **16**(7): p. 4406-4414.
138. Huang, H.-j., et al., *Comparative studies of thermochemical liquefaction characteristics of microalgae, lignocellulosic biomass and sewage sludge*. Energy, 2013. **56**: p. 52-60.
139. Jarvis, J.M., et al., *Assessment of Hydrotreatment for Hydrothermal Liquefaction Biocrudes from Sewage Sludge, Microalgae, and Pine Feedstocks*. Energy & Fuels, 2018. **32**(8): p. 8483-8493.
140. Marrone, P.A., et al., *Bench-Scale Evaluation of Hydrothermal Processing Technology for Conversion of Wastewater Solids to Fuels*. 2018.
141. Huber, G.W. and A. Corma, *Synergies between bio- and oil refineries for the production of fuels from biomass*. Angew Chem Int Ed Engl, 2007. **46**(38): p. 7184-201.
142. Saber, M., B. Nakhshiniev, and K. Yoshikawa, *A review of production and upgrading of algal bio-oil*. Renewable and Sustainable Energy Reviews, 2016. **58**: p. 918-930.
143. Castello, D., M.S. Haider, and L.A. Rosendahl, *Catalytic upgrading of hydrothermal liquefaction biocrudes: Different challenges for different feedstocks*. Renewable Energy, 2019. **141**: p. 420-430.
144. Ramirez, J., R. Brown, and T. Rainey, *A Review of Hydrothermal Liquefaction Bio-Crude Properties and Prospects for Upgrading to Transportation Fuels*.

- Energies, 2015. **8**(7): p. 6765-6794.
145. Liu, R., W. Fei, and C. Shen, *Influence of acetone addition on the physicochemical properties of bio-oils*. Journal of the Energy Institute, 2014. **87**(2): p. 127-133.
146. Peng, J., et al., *Upgrading of Bio-oil over Aluminum Silicate in Supercritical Ethanol*. Energy & Fuels, 2008. **22**(5): p. 3489-3492.
147. Jiang, X. and N. Ellis, *Upgrading Bio-oil through Emulsification with Biodiesel: Thermal Stability*. Energy & Fuels, 2010. **24**(4): p. 2699-2706.
148. Dahmen, N., et al. *Bioliq®-pilot plant for the preparation of synthetic fuels-operating experience*. in *European Biomass Conference and Exhibition Proceedings*. 2019.
149. Trane-Restrup, R. and A.D. Jensen, *Steam reforming of cyclic model compounds of bio-oil over Ni-based catalysts: Product distribution and carbon formation*. Applied Catalysis B: Environmental, 2015. **165**: p. 117-127.
150. Maddi, B., et al., *Quantitative Characterization of Aqueous Byproducts from Hydrothermal Liquefaction of Municipal Wastes, Food Industry Wastes, and Biomass Grown on Waste*. ACS Sustainable Chemistry & Engineering, 2017. **5**(3): p. 2205-2214.
151. Yu, G., et al., *Distributions of carbon and nitrogen in the products from hydrothermal liquefaction of low-lipid microalgae*. Energy & Environmental Science, 2011. **4**(11): p. 4587-4595.
152. Usman, M., et al., *Characterization and utilization of aqueous products from hydrothermal conversion of biomass for bio-oil and hydro-char production: a review*. Green Chemistry, 2019. **21**(7): p. 1553-1572.
153. Roberts, G.W., et al., *Promising Pathway for Algal Biofuels through Wastewater Cultivation and Hydrothermal Conversion*. Energy & Fuels, 2013. **27**(2): p. 857-867.
154. Jena, U., et al., *Evaluation of microalgae cultivation using recovered aqueous co-product from thermochemical liquefaction of algal biomass*. Bioresour Technol, 2011. **102**(3): p. 3380-7.
155. Biller, P., et al., *Nutrient recycling of aqueous phase for microalgae cultivation from the hydrothermal liquefaction process*. Algal Research, 2012. **1**(1): p. 70-76.
156. Si, B., et al., *Anaerobic conversion of the hydrothermal liquefaction aqueous phase: fate of organics and intensification with granule activated carbon/ozone pretreatment*. Green Chemistry, 2019. **21**(6): p. 1305-1318.
157. Yang, L., et al., *Integrated anaerobic digestion and algae cultivation for energy recovery and nutrient supply from post-hydrothermal liquefaction wastewater*. Bioresource Technology, 2018. **266**: p. 349-356.
158. Villamil, J.A., et al., *Anaerobic co-digestion of the aqueous phase from hydrothermally treated waste activated sludge with primary sewage sludge. A kinetic study*. Journal of Environmental Management, 2019. **231**: p. 726-733.
159. Cherad, R., et al., *Hydrogen production from the catalytic supercritical water gasification of process water generated from hydrothermal liquefaction of microalgae*. Fuel, 2016. **166**: p. 24-28.
160. Elliott, D.C., et al., *Process development for hydrothermal liquefaction of algae feedstocks in a continuous-flow reactor*. Algal Research, 2013. **2**(4): p. 445-454.
161. Elliott, D.C., et al., *Hydrothermal liquefaction of biomass: Developments from batch to continuous process*. Bioresource Technology, 2015. **178**: p. 147-156.
162. Shah, A.A., et al., *Bio-Crude Production through Aqueous Phase Recycling of Hydrothermal Liquefaction of Sewage Sludge*. Energies, 2020. **13**(2): p. 493.

163. Schuler, J., et al., *Lignin from bark as a resource for aromatics production by hydrothermal liquefaction*. GCB Bioenergy, 2018.
164. Zhou, F., C. Wang, and J. Wei, *Separation of acetic acid from monosaccharides by NF and RO membranes: Performance comparison*. Journal of Membrane Science, 2013. **429**: p. 243-251.
165. Cantero-Tubilla, B., et al., *Characterization of the solid products from hydrothermal liquefaction of waste feedstocks from food and agricultural industries*. The Journal of Supercritical Fluids, 2018. **133**: p. 665-673.
166. Herzel, H., et al., *Sewage sludge ash--A promising secondary phosphorus source for fertilizer production*. Sci Total Environ, 2016. **542**(Pt B): p. 1136-43.
167. Madsen, R.B., M.M. Jensen, and M. Glasius, *Qualitative characterization of solid residue from hydrothermal liquefaction of biomass using thermochemolysis and stepwise pyrolysis-gas chromatography-mass spectrometry*. Sustainable Energy & Fuels, 2017. **1**(10): p. 2110-2119.
168. Ovsyannikova, E., A. Kruse, and G. Becker, *Feedstock-Dependent Phosphate Recovery in a Pilot-Scale Hydrothermal Liquefaction Bio-Crude Production*. Energies, 2020. **13**(2): p. 379.
169. He, C., et al., *Effective Nitrogen Removal and Recovery from Dewatered Sewage Sludge Using a Novel Integrated System of Accelerated Hydrothermal Deamination and Air Stripping*. Environmental Science & Technology, 2015. **49**(11): p. 6872-6880.
170. Paneque, M., et al., *Hydrothermal carbonization and pyrolysis of sewage sludges: What happens to carbon and nitrogen?* Journal of Analytical and Applied Pyrolysis, 2017. **128**: p. 314-323.
171. Huang, H.J. and X.Z. Yuan, *The migration and transformation behaviors of heavy metals during the hydrothermal treatment of sewage sludge*. Bioresour Technol, 2016. **200**: p. 991-8.
172. Prestigiacomio, C., et al., *Sewage sludge as cheap alternative to microalgae as feedstock of catalytic hydrothermal liquefaction processes*. The Journal of Supercritical Fluids, 2019. **143**: p. 251-258.
173. Nartey, O.D. and B. Zhao, *Biochar Preparation, Characterization, and Adsorptive Capacity and Its Effect on Bioavailability of Contaminants: An Overview*. Advances in Materials Science and Engineering, 2014. **2014**: p. 1-12.
174. Itoh, S., et al., *Direct Thermochemical Liquefaction of Sewage Sludge by a Continuous Plant*. Water Science and Technology, 1992. **26**(5-6): p. 1175-1184.
175. Chen, Y., et al., *Hydrogen production by sewage sludge gasification in supercritical water with a fluidized bed reactor*. International Journal of Hydrogen Energy, 2013. **38**(29): p. 12991-12999.
176. Amrullah, A. and Y. Matsumura, *Supercritical water gasification of sewage sludge in continuous reactor*. Bioresour Technol, 2017. **249**: p. 276-283.
177. Jazrawi, C., et al., *Pilot plant testing of continuous hydrothermal liquefaction of microalgae*. Algal Research, 2013. **2**(3): p. 268-277.
178. He, Y., et al., *Continuous hydrothermal liquefaction of macroalgae in the presence of organic co-solvents*. Algal Research, 2016. **17**: p. 185-195.
179. Jensen, C.U., et al., *Fundamentals of Hydrofaction™: Renewable crude oil from woody biomass*. Biomass Conversion and Biorefinery, 2017. **7**(4): p. 495-509.
180. Licella. *Commercialising the Cat-HTR™ for End-of-Life Plastic in Australia*. <https://www.licella.com.au/news/licella>. 2019.
181. Marrone, P., *Genifuel Hydrothermal Processing Bench Scale Technology*

- Evaluation Project (WE&RF Report LIFT6T14)*. Water Environment & Reuse Foundation, Alexandria, VA
ISBN 9781780408408, 2016.
182. Anastasakis, K., et al., *Continuous Hydrothermal Liquefaction of Biomass in a Novel Pilot Plant with Heat Recovery and Hydraulic Oscillation*. *Energies*, 2018. **11**(10): p. 2695.
 183. *Expert workshop: Potential of Hydrothermal Liquefaction (HTL) routes for biofuel production*, in *besustainable*. 2019.
 184. Lu, J., et al., *Nitrogen Migration and Transformation during Hydrothermal Liquefaction of Livestock Manures*. *ACS Sustainable Chemistry & Engineering*, 2018.
 185. Furimsky, E. and F.E. Massoth, *Hydrodenitrogenation of Petroleum*. *Catalysis Reviews*, 2005. **47**(3): p. 297-489.
 186. Tian, K., et al., *Investigation on the Evolution of N-Containing Organic Compounds during Pyrolysis of Sewage Sludge*. *Environmental Science & Technology*, 2014. **48**(18): p. 10888-10896.
 187. Fonts, I., et al., *Assessment of the Production of Value-Added Chemical Compounds from Sewage Sludge Pyrolysis Liquids*. *Energy Technology*, 2017. **5**(1): p. 151-171.
 188. Debono, O. and A. Villot, *Nitrogen products and reaction pathway of nitrogen compounds during the pyrolysis of various organic wastes*. *Journal of Analytical and Applied Pyrolysis*, 2015. **114**: p. 222-234.
 189. Chen, W.-T., et al., *A Perspective on Hydrothermal Processing of Sewage Sludge*. *Current Opinion in Environmental Science & Health*, 2020.
 190. Dote, Y., et al., *Studies on the direct liquefaction of protein-contained biomass: The distribution of nitrogen in the products*. *Biomass and Bioenergy*, 1996. **11**(6): p. 491-498.
 191. Xu, C. and J. Lancaster, *Conversion of secondary pulp/paper sludge powder to liquid oil products for energy recovery by direct liquefaction in hot-compressed water*. *Water Research*, 2008. **42**(6): p. 1571-1582.
 192. Hu, Y., et al., *Investigation of aqueous phase recycling for improving bio-crude oil yield in hydrothermal liquefaction of algae*. *Bioresource Technology*, 2017. **239**: p. 151-159.
 193. Ross, A.B., et al., *Hydrothermal processing of microalgae using alkali and organic acids*. *Fuel*, 2010. **89**(9): p. 2234-2243.
 194. Dote, Y., et al., *Distribution of nitrogen to oil products from liquefaction of amino acids*. *Bioresource Technology*, 1998. **64**(2): p. 157-160.
 195. Teri, G., L. Luo, and P.E. Savage, *Hydrothermal Treatment of Protein, Polysaccharide, and Lipids Alone and in Mixtures*. *Energy & Fuels*, 2014. **28**(12): p. 7501-7509.
 196. Ashoor, S.H. and J.B. Zent, *Maillard Browning of Common Amino Acids and Sugars*. *Journal of Food Science*, 1984. **49**(4): p. 1206-1207.
 197. Leiva, G.E., G.B. Naranjo, and L.S. Malec, *A study of different indicators of Maillard reaction with whey proteins and different carbohydrates under adverse storage conditions*. *Food Chemistry*, 2017. **215**: p. 410-416.
 198. Inoue, S., et al., *Organic compounds formed by thermochemical degradation of glucose-glycine melanoidins using hot compressed water*. *Journal of Chemical Engineering of Japan*, 2004. **37**(7): p. 915-919.
 199. Peterson, A.A., R.P. Lachance, and J.W. Tester, *Kinetic Evidence of the Maillard*

- Reaction in Hydrothermal Biomass Processing: Glucose–Glycine Interactions in High-Temperature, High-Pressure Water*. Industrial & Engineering Chemistry Research, 2010. **49**(5): p. 2107-2117.
200. Chiaberge, S., et al., *Amides in Bio-oil by Hydrothermal Liquefaction of Organic Wastes: A Mass Spectrometric Study of the Thermochemical Reaction Products of Binary Mixtures of Amino Acids and Fatty Acids*. Energy & Fuels, 2013. **27**(9): p. 5287-5297.
201. Li, H., et al., *Conversion efficiency and oil quality of low-lipid high-protein and high-lipid low-protein microalgae via hydrothermal liquefaction*. Bioresource Technology, 2014. **154**: p. 322-329.
202. Jimenez, J., et al., *A statistical comparison of protein and carbohydrate characterisation methodology applied on sewage sludge samples*. Water Research, 2013. **47**(5): p. 1751-1762.
203. Inoue, S., et al., *Organic composition of liquidized sewage sludge*. Biomass and Bioenergy, 1996. **10**(1): p. 37-40.
204. DuBois, M., et al., *Colorimetric Method for Determination of Sugars and Related Substances*. Analytical Chemistry, 1956. **28**(3): p. 350-356.
205. Y. Fan, et al. *Formation of N-Containing Heterocycles from Hydrothermal Liquefaction of Model Compounds and Sewage Sludge*. in *26th European Biomass Conference and Exhibition*. 2018.
206. Speight, J.G., *Handbook of petroleum product analysis*. 2015: John Wiley & Sons.
207. Leng, L., et al., *Nitrogen in bio-oil produced from hydrothermal liquefaction of biomass: A review*. Chemical Engineering Journal, 2020: p. 126030.
208. Wang, T., et al., *Influence of temperature on nitrogen fate during hydrothermal carbonization of food waste*. Bioresour Technol, 2018. **247**: p. 182-189.
209. Chen, W., et al., *Transformation of Nitrogen and Evolution of N-Containing Species during Algae Pyrolysis*. Environ Sci Technol, 2017. **51**(11): p. 6570-6579.
210. López Barreiro, D., et al., *Hydrothermal liquefaction of microalgae: Effect on the product yields of the addition of an organic solvent to separate the aqueous phase and the biocrude oil*. Algal Research, 2015. **12**: p. 206-212.
211. Xu, D. and P.E. Savage, *Characterization of biocrudes recovered with and without solvent after hydrothermal liquefaction of algae*. Algal Research, 2014. **6**: p. 1-7.
212. Castello, D., T. Pedersen, and L. Rosendahl, *Continuous Hydrothermal Liquefaction of Biomass: A Critical Review*. Energies, 2018. **11**(11): p. 3165.
213. Prestigiacomio, C., et al., *Hydrothermal liquefaction of waste biomass in stirred reactors: One step forward to the integral valorization of municipal sludge*. Energy, 2020. **201**: p. 117606.
214. Carrier, M., et al., *Degradation pathways of holocellulose, lignin and α -cellulose from *Pteris vittata* fronds in sub- and super critical conditions*. Biomass and Bioenergy, 2012. **43**: p. 65-71.
215. Faeth, J.L., P.J. Valdez, and P.E. Savage, *Fast Hydrothermal Liquefaction of *Nannochloropsis* sp. To Produce Biocrude*. Energy & Fuels, 2013. **27**(3): p. 1391-1398.
216. Barreiro, D.L., et al., *Hydrothermal Liquefaction of Microalgae in a Continuous Stirred-Tank Reactor*. Energy & Fuels, 2015. **29**(10): p. 6422-6432.
217. Chuntanapum, A. and Y. Matsumura, *Formation of Tarry Material from 5-HMF in Subcritical and Supercritical Water*. Industrial & Engineering Chemistry Research, 2009. **48**(22): p. 9837-9846.
218. Wang, J., et al., *Co-liquefaction of low-lipid microalgae and starch-rich biomass*

- waste: *The interaction effect on product distribution and composition*. Journal of Analytical and Applied Pyrolysis, 2019. **139**: p. 250-257.
219. Fan, Y., et al., *Hydrothermal liquefaction of protein-containing biomass: study of model compounds for Maillard reactions*. Biomass Conversion and Biorefinery, 2018. **8**(4): p. 909-923.
220. Watanabe, M., T. Iida, and H. Inomata, *Decomposition of a long chain saturated fatty acid with some additives in hot compressed water*. Energy Conversion and Management, 2006. **47**(18-19): p. 3344-3350.
221. Jung, D., M. Zimmermann, and A. Kruse, *Hydrothermal Carbonization of Fructose: Growth Mechanism and Kinetic Model*. ACS Sustainable Chemistry & Engineering, 2018. **6**(11): p. 13877-13887.
222. Farmer, L.J., *Interactions Between Lipids and the Maillard Reaction*, in *Flavor-Food Interactions*. 1996, American Chemical Society. p. 48-58.
223. Remón, J., et al., *Hydrogen production from cheese whey by catalytic steam reforming: Preliminary study using lactose as a model compound*. Energy Conversion and Management, 2016. **114**: p. 122-141.
224. Koehler, P.E. and G.V. Odell, *Factors affecting the formation of pyrazine compounds in sugar-amine reactions*. Journal of Agricultural and Food Chemistry, 1970. **18**(5): p. 895-898.
225. Titirici, M.-M., M. Antonietti, and N. Baccile, *Hydrothermal carbon from biomass: a comparison of the local structure from poly- to monosaccharides and pentoses/hexoses*. Green Chemistry, 2008. **10**(11): p. 1204-1212.
226. Steinbach, D., A. Kruse, and J. Sauer, *Pretreatment technologies of lignocellulosic biomass in water in view of furfural and 5-hydroxymethylfurfural production- A review*. Biomass Conversion and Biorefinery, 2017. **7**(2): p. 247-274.
227. Kruse, A., P. Maniam, and F. Spieler, *Influence of proteins on the hydrothermal gasification and liquefaction of biomass. 2. Model compounds*. Industrial & Engineering Chemistry Research, 2007. **46**(1): p. 87-96.
228. Yaylayan, V.A., *Recent Advances in the Chemistry of Strecker Degradation and Amadori Rearrangement: Implications to Aroma and Color Formation*. Food Science and Technology Research, 2003. **9**(1): p. 1-6.
229. Van Lancker, F., A. Adams, and N. De Kimpe, *Formation of Pyrazines in Maillard Model Systems of Lysine-Containing Dipeptides*. Journal of Agricultural and Food Chemistry, 2010. **58**(4): p. 2470-2478.
230. Hwang, H.-I., et al., *Formation of Pyrazines from the Maillard Reaction of Glucose and Lysine-.alpha.-amine-15N*. Journal of Agricultural and Food Chemistry, 1994. **42**(4): p. 1000-1004.
231. Zhang, B., M. von Keitz, and K. Valentas, *Thermochemical liquefaction of high-diversity grassland perennials*. Journal of Analytical and Applied Pyrolysis, 2009. **84**(1): p. 18-24.
232. Zhang, B., M. von Keitz, and K. Valentas, *Thermal Effects on Hydrothermal Biomass Liquefaction*. Applied Biochemistry and Biotechnology, 2008. **147**(1): p. 143-150.
233. Antal, M.J., W.S.L. Mok, and G.N. Richards, *Mechanism of formation of 5-(hydroxymethyl)-2-furaldehyde from d-fructose and sucrose*. Carbohydrate Research, 1990. **199**(1): p. 91-109.
234. Doughty, A., J.C. Mackie, and J.M. Palmer, *Kinetics of the thermal decomposition and isomerisation of pyrazine (1,4 diazine)*. Symposium (International) on Combustion, 1994. **25**(1): p. 893-900.

235. Crow, W.D. and C. Wentrup, *Reactions of excited molecules v. Thermal decomposition of pyrazine*. Tetrahedron Letters, 1968. **9**(27): p. 3115-3118.
236. Ramos, L., E.M. Kristenson, and U.A.T. Brinkman, *Current use of pressurised liquid extraction and subcritical water extraction in environmental analysis*. Journal of Chromatography A, 2002. **975**(1): p. 3-29.
237. Sinađ, A., A. Kruse, and V. Schwarzkopf, *Key Compounds of the Hydrolysis of Glucose in Supercritical Water in the Presence of K₂CO₃*. Industrial & Engineering Chemistry Research, 2003. **42**(15): p. 3516-3521.
238. Ren, D., et al., *Production of 2,5-hexanedione and 3-methyl-2-cyclopenten-1-one from 5-hydroxymethylfurfural*. Green Chem., 2016. **18**(10): p. 3075-3081.
239. Sheehan, J.D. and P.E. Savage, *Molecular and Lumped Products from Hydrothermal Liquefaction of Bovine Serum Albumin*. ACS Sustainable Chemistry & Engineering, 2017. **5**(11): p. 10967-10975.
240. Dufreche, S., et al., *Extraction of Lipids from Municipal Wastewater Plant Microorganisms for Production of Biodiesel*. Journal of the American Oil Chemists' Society, 2007. **84**(2): p. 181-187.
241. Pokoo-Aikins, G., et al., *A multi-criteria approach to screening alternatives for converting sewage sludge to biodiesel*. Journal of Loss Prevention in the Process Industries, 2010. **23**(3): p. 412-420.
242. Chopra, J., et al., *Performance enhancement of hydrothermal liquefaction for strategic and sustainable valorization of de-oiled yeast biomass into green bio-crude*. Journal of Cleaner Production, 2019. **227**: p. 292-301.
243. Sawayama, S., T. Minowa, and S.Y. Yokoyama, *Possibility of renewable energy production and CO₂ mitigation by thermochemical liquefaction of microalgae*. Biomass and Bioenergy, 1999. **17**(1): p. 33-39.
244. Minowa, T., T. Kondo, and S.T. Sudirjo, *Thermochemical liquefaction of indonesian biomass residues*. Biomass and Bioenergy, 1998. **14**(5): p. 517-524.
245. Olkiewicz, M., et al., *Evaluation of Different Sludges from WWTP as a Potential Source for Biodiesel Production*. Procedia Engineering, 2012. **42**(Supplement C): p. 634-643.
246. Huo, H., et al., *Life-Cycle Assessment of Energy Use and Greenhouse Gas Emissions of Soybean-Derived Biodiesel and Renewable Fuels*. Environmental Science & Technology, 2009. **43**(3): p. 750-756.
247. Pastore, C., et al., *Biodiesel from dewatered wastewater sludge: a two-step process for a more advantageous production*. Chemosphere, 2013. **92**(6): p. 667-73.
248. Demirbas, A., *Combustion Efficiency Impacts of Biofuels*. Energy Sources, Part A: Recovery, Utilization, and Environmental Effects, 2009. **31**(7): p. 602-609.
249. Vardon, D.R., et al., *Chemical properties of biocrude oil from the hydrothermal liquefaction of Spirulina algae, swine manure, and digested anaerobic sludge*. Bioresource Technology, 2011. **102**(17): p. 8295-8303.
250. Boocock, D.G.B., et al., *Fuels and chemicals from sewage sludge: 1. The solvent extraction and composition of a lipid from a raw sewage sludge*. Fuel, 1992. **71**(11): p. 1283-1289.
251. Huang, Y., et al., *Bio-oil production from hydrothermal liquefaction of high-protein high-ash microalgae including wild Cyanobacteria sp. and cultivated Bacillariophyta sp.* Fuel, 2016. **183**: p. 9-19.
252. Xu, L., et al., *Renewable N-Heterocycles Production by Thermocatalytic Conversion and Ammonization of Biomass over ZSM-5*. ACS Sustainable

- Chemistry & Engineering, 2015. **3**(11): p. 2890-2899.
253. Li, H., et al., *Cycloamination strategies for renewable N-heterocycles*. Green Chemistry, 2020. **22**(3): p. 582-611.

Appendix

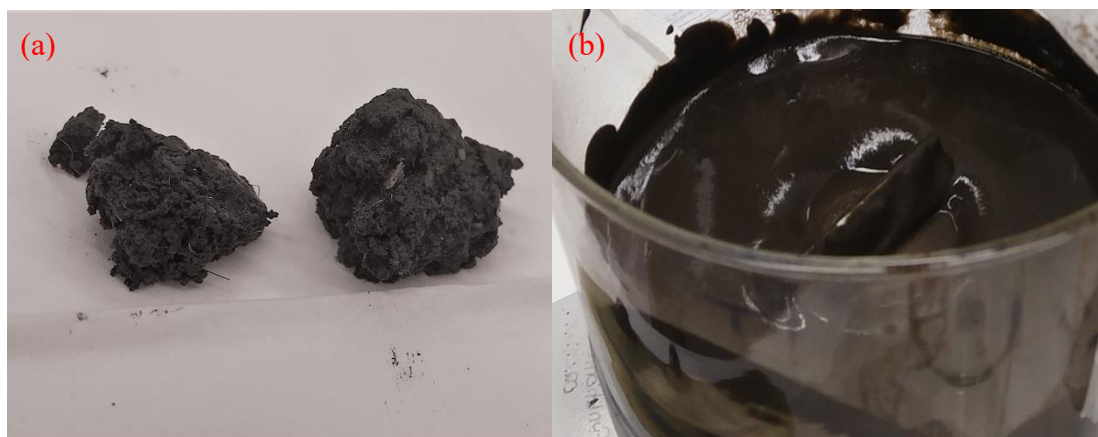


Figure A-1 Raw sewage sludge (a) and pre-treated sewage sludge (b)

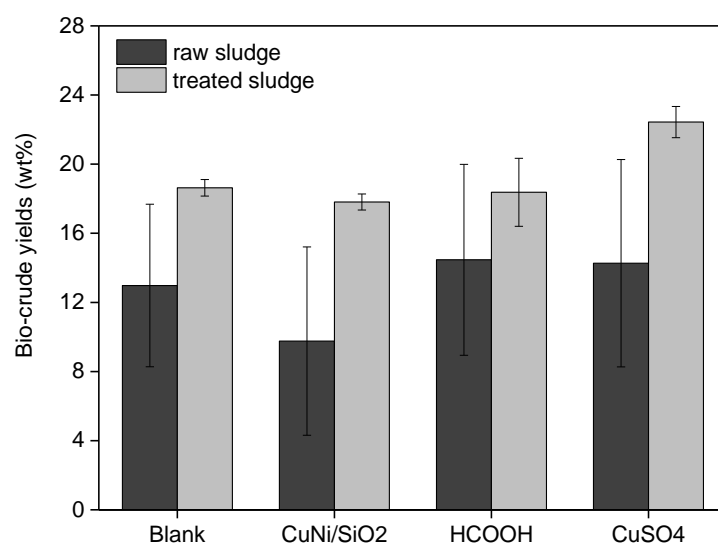


Figure A-2 The yields of biocrude obtained from catalytic HTL of raw sludge and treated sludge at 300 °C

XPS spectra of raw sludge and solid residue

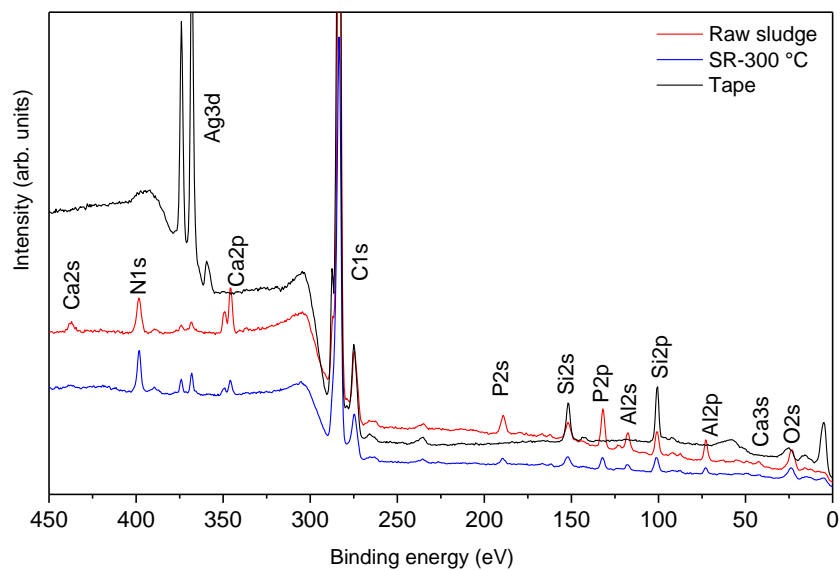


Figure A-3 Overview XPS spectra, the Auger peaks and the most intense peaks of the silver tape (zoom in region with low binding energies)

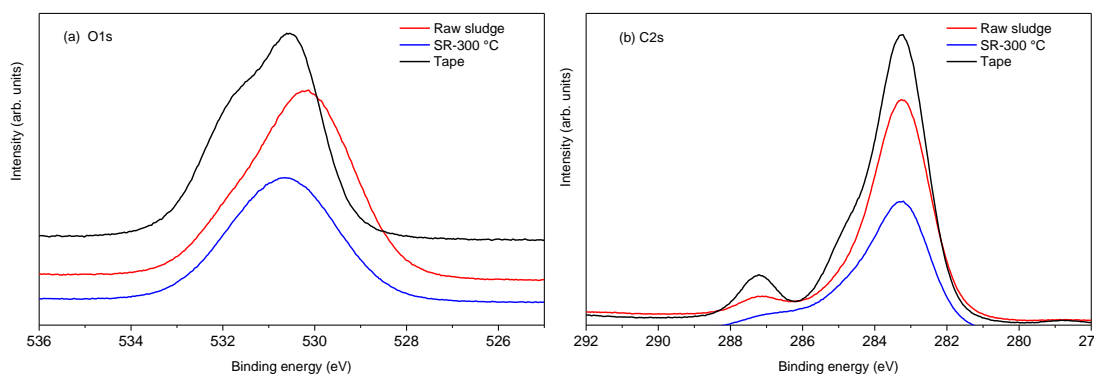


Figure A-4 Evolution of O 1s (a) and C 2s (b) XPS spectra for raw sludge and solid residue derived from HTL at 300 °C

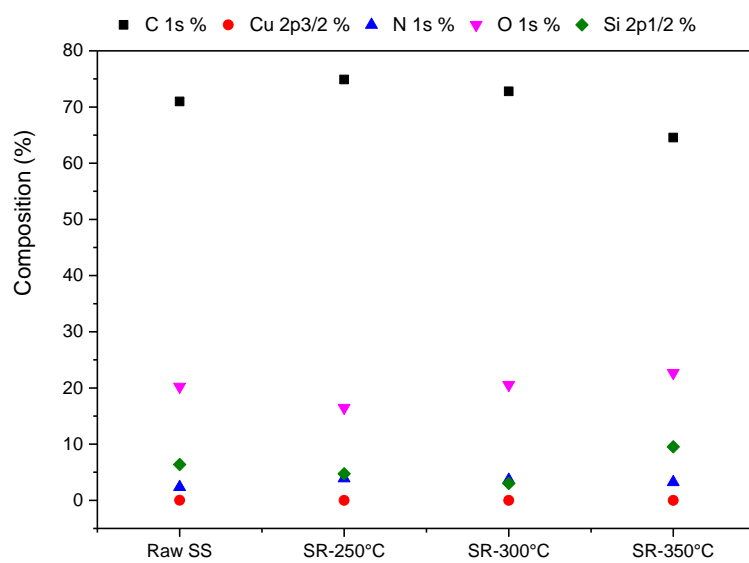
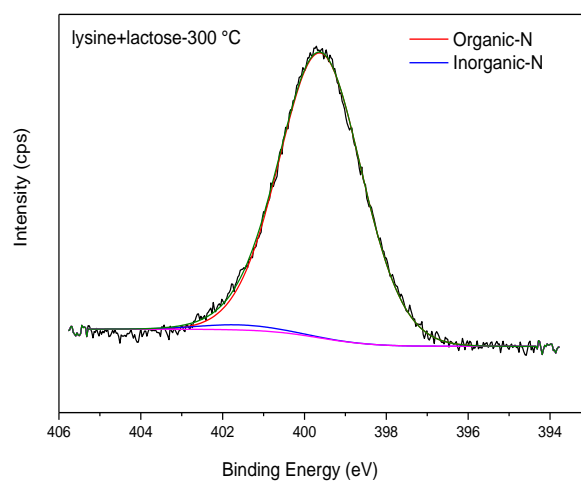
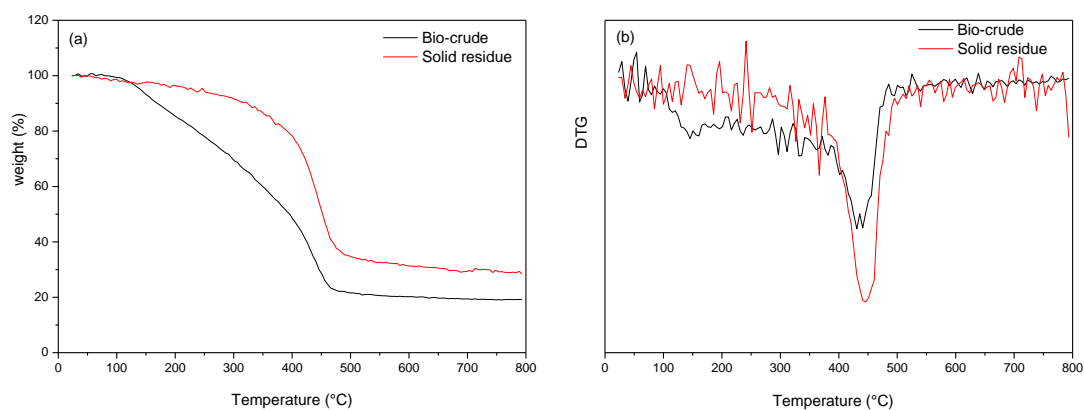


Figure A-5 Surface elemental composition (%) evaluated by XPS for raw sludge sample and solid residue from HTL of sewage sludge at different temperatures

Supporting results of products from HTL of lysine and lactose mixture

**Figure A-6 N 1s XPS spectra for solid residue derived from HTL of model system****Figure A-7 TGA (a) and DTG (b) curve of analysis of products from HTL of lysine and lactose mixture at 300 °C**

Supporting results from HTL of SS and LESS

Table A-0-1 Identified main components of biocrude and relative percentage in the total ion chromatogram

Retention time	Components identified	Relative areas (%)					
		SS-250 °C	SS-300 °C	SS-350 °C	LESS-250 °C	LESS-300 °C	LESS-350 °C
N-containing heterocycles							
6.97	Pyrazine,methyl-	4.6	1.2	1.2	2.4		
8.46	Pyrazine,2,5-dimethyl-	4.5	1.8	1.2	3.5	1.2	
8.52	Pyrazine,ethyl-	2.9		1.5	2.0	0.9	
9.67	Pyrazine, trimethyl-	4.4	1.9	2.2	3.5	1.3	1.0
10.08	2-Pyrrolidinone, 1-Methyl-		1.3	6.2		1.6	8.5
10.51	Pyrazine, 3-ethyl-2,5-dimethyl-	1.5	1.2	10.4	1.3	1.5	
10.64	2,5-Pyrrolidinedione, 1-methyl-	7.5	4.6		5.1	4.9	4.0
10.80	1-Ethyl-2-pyrrolidinone	1.8	3.2	3.7	1.6	6.6	6.9
11.44	Pyrrolidine, 1-acetyl-		2.2			2.3	0.7
12.08	3-Piperidinone, 1-ethyl-6-methyl-						1.6
12.58	1H-indole	1.4	2.0	1.7	1.3	2.4	2.8
13.34	1H-Indole, 2-methyl-		1.9	4.1		2.6	2.9
14.58	1H-Indole, 5,6,7-trimethyl-			1.9		2.1	2.3
15.12	1H-Indole, 1,2,3-trimethyl-	1.7	1.2	1.0			
15.39	3H-Indole,2-ethyl-3,3-dimethyl-			1.0			1.5
16.93	2,5-piperazinedione,3,6-bis(2-methylpropyl)	2.1	1.6		16.3		
17.05	Diazatricyclo 7.3.0.0(3 7) dodecan-2 8-dione		7.7	2.4		4.8	2.4
17.24	9H-Pyrido[3,4-b]indole, 1-methyl-	2.7	3.1				
19.23	Pyrrolo[1,2-a]pyrazine-1,4-dione,hexahydro-3-(phenylmethyl)-		1.1	2.0	2.8	1.8	1.6
Amines and Amides							
9.90	Acetamide,N-(2-methylpropyl-)		2.2	1.1		3.1	
10.99	Acetamide,N-butyl-		1.9		0.9	3.0	0.8
12.98	Piperidine, 1-methyl-			2.1			5.0
14.05	Benzenamine,N-(1-methyl-2-propynyl)-			1.9		1.8	2.2
14.22	acetamide,N-(2-phenylethyl)					2.9	
18.15	Hexadecanamide	1.2	1.5			0.9	
O-containing compounds							
8.33	2-cyclopenten-1-one,2-methyl-	1.0			1.4		
9.18	2-cyclopenten-1-one,3-methyl-						0.7
9.36	Phenol	1.8	3.6	3.4	1.0	5.4	4.7
10.33	Cyclopent-2-ene-1-one,						1.0

RT	2,3,4-trimethyl- Chemicals	SS-250 °C	SS-300 °C	SS-350 °C	LESS-250 °C	LESS-300 °C	LESS-350 °C
10.49	Phenol,4-methyl-		2.4			3.9	7.1
11.08	Phenol,2-ethyl-	0.8	3.0	1.1	1.0	4.5	2.0
11.22	Phenol, 3,4-dimethyl-	1.0	1.2	2.7	1.0	1.6	2.3
11.39	Phenol,3-ethyl-	1.1	1.3	3.1	1.0	2.4	4.0
11.93	Phenol, 2-ethyl-4-methyl-			1.1			4.1
12.38	Phenol,4-ethyl-2- methoxy-	1.5			1.1		
13.09	Pphenol, 2-methoxy-4- Propyl-	2.1	1.3		1.1		
16.42	Phenol, 3,5-dimethoxy-	10.7	3.0		14.8	2.0	
	Hydrocarbons						
14.43	1-Hexandecene	1.5	1.6	1.2	1.1	0.9	1.2
14.49	Cyclododecane			1.2			
21.12	21-Nor-5 alpha,cholest- 24-ene			3.8			
22.55	Cholest-3-ene, (5.alpha.)-		4.4	6.5			
22.66	Cholest-14-ene, (5.alpha.)-			1.7			
22.81	Cholest-3-ene, (5.alpha.)-		2.2	4.4			
22.97	Cholest-7-ene, (5.alpha.)-		2.2	1.4			

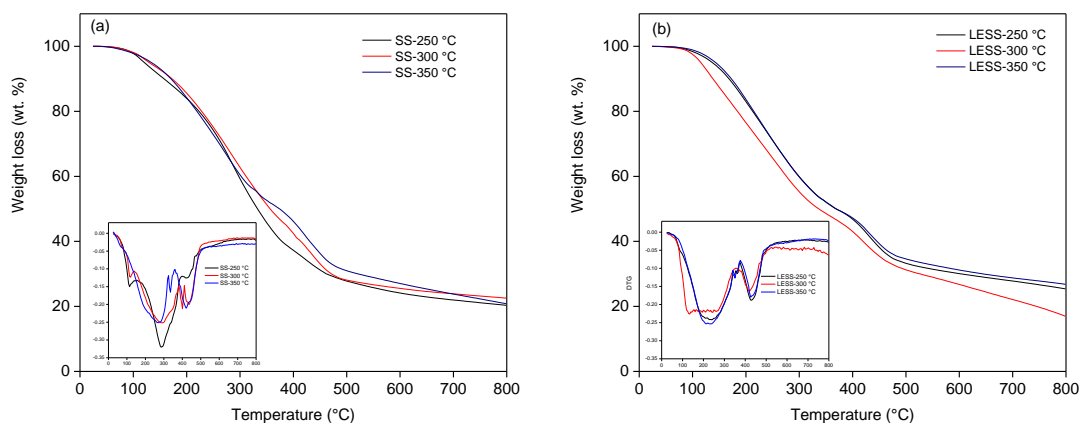


Figure A-8 TGA and DTG curves of biocrude from HTL of (a) SS and (b) LESS at different temperatures

Table A-0-2 Ash compositions (wt.%) of solid residue from HTL of SS and LESS at different temperatures

Solid samples	Al	Ca	P	Fe	Mg	Mn	Zn	Cu
Raw SS	4.26	3.70	3.31	1.17	0.03	0.03	0.14	0.04
SS-250 °C	4.60	5.00	5.00	1.60	0.55	0.04	0.16	0.74
SS - 300 °C	7.80	6.00	5.80	1.90	1.10	0.05	0.18	0.65
SS - 350 °C	9.25	7.30	6.80	2.10	1.20	0.05	0.20	0.32
LESS	4.37	3.83	3.25	1.14	0.65	<0.045	0.12	<0.46
LESS-250 °C	6.16	5.31	4.64	1.63	0.91	<0.065	0.16	<0.65
LESS-300 °C	8.40	6.40	6.25	2.00	1.20	0.05	0.20	0.45
LESS-350 °C	7.96	6.63	5.96	2.10	1.13	<0.045	0.19	<0.44

Resume

Personal details

Name: Yujie Fan

Date of Birth: 05/1990

Nationality: China

E-mail: yjfan56@gmail.com



Education

- 10.2016-present Degree as Diplom-Ingenieur in Chemical and Process Engineering
Karlsruhe Institute of Technology
- 09.2013-06.2016 Master in Environmental Science and Engineering
Hohai University
- 09.2009-07.2013 Bachelor in Environmental Engineering
Henan Institute of Engineering

Work experiences

- 01.2015-07.2016 Manager Assistant
National engineering research center of water resources efficient utilization and engineering safety
- 01.2014-10.2015 Scientific Assistant
Hydrogen production from supercritical water gasification of waste biomass(sewage sludge) (BK2011025)
A project supported Science and technology project of Jiangsu Province,China
- 01.2014-09.2015 Editor Assistant
Journal editorial department of *Water Resources Protection*
- 09.2013-12.2014 Scientific Assistant
The impact carbon-hydrogen-oxygen ratio of dewatered sludge have on gasification in supercritical water reaction(E080404)
A project supported National Natural Science Foundation of China

